A characterization of the controls of the nitrogen and oxygen isotope ratios of biologically-produced nitrous oxide and nitrate in soils.

by
David M. Snider

A thesis
presented to the University of Waterloo
in fulfilment of the
thesis requirement for the degree of

Doctor of Philosophy
in
Earth Sciences

Waterloo, Ontario, Canada, 2011

© David M. Snider 2011

AUTHOR'S DECLARATION

I hereby declare that I am the sole author of this thesis. This is a true copy of the thesis, including any required final revisions, as accepted by my examiners.

I understand that my thesis may be made electronically available to the public.

ABSTRACT

Nitrous oxide (N_2O) is a potent greenhouse gas, an important driver of climate change, and its concentration in the atmosphere is rising at an unprecedented rate. Agriculture is the leading contributor of all the anthropogenic N_2O sources, and the vast majority of agricultural N_2O emissions originate from soil. Of all the natural N_2O emissions, two-thirds originate from soil and temperate forests contribute approximately one-sixth of the natural soil emissions. Consequently, there is great interest in understanding the soil nitrogen processes responsible for N_2O production so that effective policies and management practises can be implemented to successfully mitigate climate change.

The stable isotopes of nitrogen (N) and oxygen (O) in soil N_2O emissions are hypothesized to be useful indicators of the biogeochemical processes that produce and consume N_2O, and they may be used to apportion different environmental sources. The primary objective of this thesis was to assess the utility of $\delta^{15}N$ and $\delta^{18}O$ values to differentiate N_2O produced by nitrification and denitrification.

Most of the previous research on N_2O isotopes has utilized microbial cultures of single organisms; yet natural systems contain a consortium of N-metabolizing microorganisms so the relevance of this early work to natural environments is uncertain. This thesis presents the results of experimental incubations of soil from an agricultural site and a temperate forest located within Ontario, Canada. Two well-drained soils (upland), two poorly-drained soils (wetland), and one stream sediment were incubated under varying conditions (temperature, moisture, and N-availability) to achieve a wide range in the rate of N_2O production. The $\delta^{15}N$ and $\delta^{18}O$ values of N_2O produced from the different experiments were characterized and the isotope effects (ε) of N_2O production were calculated. Experiments were conducted in aerobic or anoxic atmospheres to stimulate N_2O formation by nitrification and denitrification, respectively.

The $\delta^{15}N$-N_2O produced by denitrification in all soils was 7–35‰ lower than the $\delta^{15}N$-nitrate (NO_3^-). The $\delta^{15}N$-N_2O produced by nitrification in the upland forest soil and the agricultural soils was 28–54‰ lower than the $\delta^{15}N$-ammonium. Nitrification in the forested wetland soil yielded higher $\delta^{15}N$-N_2O values ($\Delta = -16$‰), which was likely caused by an increase in the $\delta^{15}N$-substrate. With the exception of the latter soil, there was clear ^{15}N-separation between the nitrification- and denitrification-derived N_2O in all soils. Consequently, $\delta^{15}N$ values can be used to apportion different environmental sources of N_2O on a site-by-site basis, provided that the rates of N metabolism are known and the isotopic endmembers are well-characterized.

A novel approach was employed in this thesis to help unravel the key controls of $\delta^{18}O$-N_2O and $\delta^{18}O$-NO_3^- formation. Different ^{18}O-labelled soil waters were used to demonstrate that the abiotic exchange of oxygen atoms between water and nitrite (in equilibrium) is an important control of the $\delta^{18}O$-N_2O formed by nitrifier-denitrification and the $\delta^{18}O$-NO_3^- formed by nitrification. O-exchange in these incubations was highly variable between soils (37–88%) and it appeared to be rate-related. Furthermore, the $\delta^{18}O$ value of microbial NO_3^- is partially controlled by $^{18}O/^{16}O$ fractionation that

occurs during O-exchange (equilibrium fractionation) and the uptake of molecular oxygen (O_2) and water (H_2O) (kinetic fractionation). This research showed that the $\delta^{18}O$ value of microbially-produced NO_3^- cannot be successfully predicted in soils based upon the commonly used 'one third, two-thirds rule', which only takes into account the $\delta^{18}O$ values of O_2 and H_2O. Successful predictions of $\delta^{18}O$-NO_3^- using this rule appear to be fortuitous and are because of the range of $\delta^{18}O$-H_2O at natural abundance and the magnitude of the isotope effects involved.

Enzyme-catalyzed (biotic) O-exchange between water and nitrite/nitric oxide in denitrification was also quantified for the first time in soils. O-exchange during denitrification was significant and variable (39–95%), but uniquely confined to narrow ranges for each soil type. Almost complete O-exchange occurred in the well-drained agricultural and forested soils (86–95%); less O-exchange occurred in the agricultural and forested wetland soils (63–70%); and even less O-exchange occurred in the agricultural stream sediment (39–51%). The magnitude of O-exchange during denitrification was independent of soil temperature and moisture for a given soil, and it was not related to the rate of N_2O production. This implies that the amount of O-exchange that occurs during soil denitrification is controlled by the dominant microbial community.

For the first time, estimates of the net O isotope effect were determined for N_2O production by soil denitrifiers that accounted for the complicating effects of O-exchange. The net ^{18}O-discrimination (N_2O–NO_3^-) ranged between +32‰ and +60‰, with the exception of one treatment that was cooled (ε = +17‰). The O isotope separation (Δ) that is actually observed in natural systems is often much lower, and in some cases negative. This is because the atomic O-exchange between water and nitrite/nitric oxide effectively diminishes the net ^{18}O separation between NO_3^- and N_2O because $\delta^{18}O$ values of environmental water are usually lower than the $\delta^{18}O$ values of N_2O-precursors.

The determinants of $\delta^{18}O$-N_2O produced by nitrification pathways are complex and there is no holistic explanation of the O isotope dynamics in the literature. This thesis provides the first systematic model to describe $\delta^{18}O$-N_2O formation by aerobic pathways. In addition to O-exchange between water and nitrite (at equilibrium), $\delta^{18}O$-N_2O is controlled by $^{18}O/^{16}O$ fractionation that results from this O-exchange mechanism, and from fractionation that occurs during ammonia-oxidation and nitrite-reduction. Although explaining $\delta^{18}O$-N_2O values produced by nitrification is complex, reports of nitrifier-derived $\delta^{18}O$-N_2O in the literature and this thesis are narrowly confined between +13‰ and +31‰ (rel. VSMOW). This is distinct from much of the denitrifier-produced $\delta^{18}O$-N_2O, which is often ^{18}O-enriched and higher than +33‰.

In three out of the five different soils investigated in this thesis, $\delta^{18}O$-N_2O could be used to separate N_2O formed by nitrification and denitrification. There was poor $\delta^{18}O$ separation between nitrifier- and denitrifier-derived N_2O in the well-drained soils because high amounts of biotic O-exchange and reduced O isotope separations yielded lower (predicted) estimates of denitrifier-produced $\delta^{18}O$-N_2O. On the other hand, $\delta^{15}N$ values could be used to apportion nitrifier- and denitrifier-derived N_2O sources in these soils. Thus, stable isotope ratios of N_2O are a valuable and promising tool that may help differentiate nitrifier-N_2O from denitrifier-N_2O in natural soil environments.

ACKNOWLEDGMENTS

Numerous individuals assisted me with this venture and I cannot properly express my gratitude to them within the bounds of this simple acknowledgment.

Sherry Schiff provided scientific direction and generous financial support for this research. She planted the big-picture ideas in my head and gave me the opportunity to freely discover my newfound love of nitrogen. Her encouragement to follow through with the 'mental gymnastics' is the reason this thesis contains a fifth, sixth, and seventh chapter. Thank you for taking a chance on me six years ago, and thank you for showing me how to conduct good science.

John Spoelstra was an excellent mentor and role-model from the very beginning. He taught me many basic (and not-so-basic) field and lab skills that I haven't yet forgotten. He helped me to design my experiments, extract nuggets of information, and has tirelessly read this thesis. Thank you for your guidance and collaboration.

To my remaining committee members—Ramon Aravena, Michael English, William Taylor, and Bernhard Mayer—thank you for your time and comments, and for ensuring that this thesis is a scientifically sound body of work.

Richard Elgood is the reason our lab functions. He works very hard with little thanks, and this research would not have transpired without his help. So, thanks for disposing of that funny blue liquid I accidentally cryogenically trapped. And I'm sorry I blew up your freeze-drier – I owe you one. And sorry about that...

I bounced so many ideas off of Jason Venkiteswaran that I may have permanently bruised him. Without Jason's computational assistance, the algebra and modelling in Chapters 3–5 would have buried me long ago. Thank you to all the other graduate and undergraduate students who helped unravel the mysteries of N_2O isotopes and/or helped with lab and field work. Maddy Rosamond, Krista Chomicki, Marlin Rempel, Simon Thuss, Helen Baulch, and Terra Jamieson were great friends and provided a wealth of knowledge from which I drew on frequently.

I thank William Mark, Richard Heemskerk, and others of the Environmental Isotope Lab for helping me to improve and troubleshoot the mass spectrometer on numerous occasions.

Susan Fisher and Lorraine Albrecht provided helpful administrative support and guided me through the mysterious workings of university/departmental life.

Financial support for this research was provided by the Natural Sciences and Engineering Research Council of Canada (NSERC) in the form of Strategic and Discovery Grants to Dr. Schiff and a Postgraduate Scholarship to the author. This research was also financially supported by the Canadian Foundation for Climate and Atmospheric Sciences (CFCAS), and by Environment Canada's Science Horizons Youth Internship Program. The author also received numerous forms of financial support from the University of Waterloo.

Many individuals outside of the University helped me to keep going. My immediate and extended families have continuously been an enormous support. I thank them for being patient, and I remind them that they were the ones who encouraged me to go back to school in the first place. A special thank you to my sister, Heather, who generously provided her editing services. I have yet to receive an invoice.

Finally, to Bill, Bob, and all the friends you have introduced me to. Thank you for showing me how to happily trudge along. All that is good in my life today is because of you.

For my wife, Andrea

Thanks for picking me up when I fell down,
and for reeling me in when I drifted off to science-land.



And to my daughter, Olivia,
and the one on the way...

CONTENTS

AUTHOR'S DECLARATION ii
ABSTRACT iii
ACKNOWLEDGMENTS v
DEDICATION vii
TABLE OF CONTENTS viii
LIST OF TABLES xiv
LIST OF FIGURES xvi

1. INTRODUCTION

1.1. THE NITROGEN DILEMMA 1
1.2. N_2O PRODUCTION AND CONSUMPTION: THE MICROBIAL PLAYERS 3
1.2.1. Chemolithoautotrophic Nitrification 4
1.2.2. Nitrite Oxidation 4
1.2.3. Heterotrophic Nitrification 5
1.2.4. Methanotrophic Nitrification 5
1.2.5. 'New' Ammonia-Oxidizers: Anammox and the Archaeal Nitrifiers 5
1.2.6. Denitrification 7
1.2.6.1. Heterotrophic Denitrification 7
1.2.6.2. Chemolithoautotrophic Denitrification 8
1.3. THE BIOLOGICAL PRODUCTION AND CONSUMPTION OF N_2O IN SOILS 8
1.3.1. N_2O Produced by Nitrification: Nitrifier-Denitrification 8
1.3.2. N_2O Produced by Nitrification: Hydroxylamine Oxidation 10
1.3.3. Denitrification: N_2O Production and Consumption 11
1.3.4. The Environmental Controls of N_2O Production 11
1.4. STABLE ISOTOPE THEORY 12
1.4.1. The Stable Isotopes of Nitrogen and Oxygen 13
1.4.2. Alphas (α), Epsilons (ε), and Deltas (Δ) 14
1.4.3. Kinetic Isotope Effects 16

1.5. THE USE OF $\delta^{15}N$ AND $\delta^{18}O$-N_2O TO APPORTION N_2O SOURCES AND PATHWAYS 17
1.5.1. $\delta^{15}N$-N_2O from Denitrification 17
1.5.2. $\delta^{15}N$-N_2O from Nitrification 18
1.5.3. $\delta^{18}O$-N_2O from Denitrification 20
1.5.4. $\delta^{18}O$-N_2O from Nitrification 22
1.5.5. N_2O Isotopomers: A Promising Tool to Track N_2O Production and Consumption 23
1.6. THESIS OUTLINE 24

2. $^{15}N/^{14}N$ AND $^{18}O/^{16}O$ STABLE ISOTOPE RATIOS OF NITROUS OXIDE PRODUCED DURING DENITRIFICATION IN TEMPERATE FOREST SOILS.

OVERVIEW 34
2.1. INTRODUCTION 35
2.2. MATERIALS AND METHODS 38
2.2.1. Soil Collection and Processing 38
2.2.2. Geochemical Characterization of Soils 39
2.2.3. Soil Moisture Content 39
2.2.4. Preparation and Measurement of $\delta^{18}O$-H_2O of the Incubation Waters 40
2.2.5. Incubation Design and Protocol 41
2.2.6. N_2O Concentration and Mass Spectrometric Analysis 42
2.3. RESULTS 44
2.3.1. Soil Parameters 44
2.3.2. Net N_2O Production Rates 44
2.3.3. Stable Isotope Abundances of the Emitted N_2O 44
2.4. DISCUSSION 45
2.4.1. The Rates of N_2O Production 45
2.4.2. $\delta^{15}N$-N_2O Values and ^{15}N Isotope Effects 46
2.4.3. $\delta^{18}O$-N_2O Values and Oxygen Exchange 48
2.4.4. The net ^{18}O Isotope Effect 49
2.5. SUMMARY AND IMPLICATIONS 50

3. THE $\delta^{15}N$ AND $\delta^{18}O$ OF NITROUS OXIDE PRODUCED DURING DENITRIFICATION IN AGRICULTURAL SOILS AND STREAM SEDIMENT

OVERVIEW 63

3.1. INTRODUCTION 64

3.2. MATERIALS AND METHODS 66

3.2.1. Soil Collection 66

3.2.2. Soil Processing, Geochemical Characterization and Incubation Protocols 67

3.2.3. Determination of Oxygen Isotope Exchange and Fractionation (Method I) 69

3.2.4. Determination of Oxygen Isotope Exchange and Fractionation (Method II) 69

3.3. RESULTS AND DISCUSSION 73

3.3.1. Soil Parameters 73

3.3.2. Net N_2O Production Rates 73

3.3.3. $\delta^{15}N$-N_2O and ^{15}N isotope effects (ε) 75

3.3.4. $\delta^{18}O$-N_2O and Oxygen Isotope Exchange (Method I) 76

3.3.5. $\delta^{18}O$-N_2O and Oxygen Isotope Fractionation (Method I) 77

3.3.6. Evidence of N_2O Reduction 78

3.3.7. Predicting N_2O Isotope Ratios in Open and Closed Systems 79

3.3.8. Oxygen Isotope Exchange (Method II) 81

3.3.9. Oxygen Isotope Fractionation (Method II) 82

3.4. CONCLUSIONS 83

4. STABLE OXYGEN ISOTOPE RATIOS OF NITRATE PRODUCED FROM NITRIFICATION: ^{18}O-LABELED WATER INCUBATIONS OF AGRICULTURAL AND TEMPERATE FOREST SOILS

OVERVIEW 97

4.1. INTRODUCTION 98

4.2. MATERIALS AND METHODS 100

4.2.1. Soil Collection, Processing, and Characterization 100

4.2.2. Incubations 101

4.2.3. Nitrate Isotope Analysis 102

4.3. RESULTS AND DISCUSSION 103
4.3.1. Nitrite Accumulation in High OM Agricultural Soil 103
4.3.2. Nitrogen Mineralization 104
4.3.3. Sources of ^{18}O in Microbial Nitrate 106
4.3.4. Implications of O-exchange and ^{18}O Fractionation on Estimations of $\delta^{18}O\text{-}NO_3^-$ 108

5. DECIPHERING THE OXYGEN ISOTOPE COMPOSITION OF NITROUS OXIDE PRODUCED BY NITRIFICATION

OVERVIEW 115
5.1. INTRODUCTION 116
5.2. MATERIALS AND METHODS 118
5.2.1. Experimental 118
5.2.2. Model Development 121
5.3. RESULTS 129
5.3.1. Experimental 129
5.3.2. Monte Carlo Simulations 131
5.4. DISCUSSION 131
5.4.1. Soil Incubation Experiments 131
5.4.2. Monte Carlo Simulations 133
5.4.3. The Modelled range of $\delta^{18}O\text{-}N_2O$ formed by nitrification in soils 136

6. THE $\delta^{15}N$ OF NITROUS OXIDE AND NITRATE PRODUCED BY NITRIFICATION IN AGRICULTURAL AND TEMPERATE FOREST SOILS

OVERVIEW 155
6.1. INTRODUCTION 156
6.2. MATERIALS AND METHODS 159
6.2.1. Soil Collection, Processing, and Geochemical Characterization 159
6.2.2. Soil Incubation Protocol 160

6.3. RESULTS AND DISCUSSION 161
6.3.1. Ammonification, Nitrification and N_2O Production (Treatments 1–2) 161
6.3.2. Ammonification, Nitrification and N2O Production (Treatments 3–6) 162
6.3.3. N_2O Production (Treatment 7) 164
6.3.4. The End-Product Ratios (NO_3^-:N_2O) of Nitrification 165
6.3.5. The δ^{15}N-NO_3^- Values of Treatments 1–3 166
6.3.6. The δ^{15}N-N_2O and Isotopic Separation (Δ) of the Agricultural Soils 168
6.3.7. The δ^{15}N-N_2O Values and N Isotope Effects of the Upland Forested Soils 170
6.3.8. The δ^{15}N-N_2O and Isotopic Separation (Δ) of the Forested Wetland 171
6.4. CONCLUSIONS 172

7. CONCLUSIONS AND IMPLICATIONS OF THIS RESEARCH, RELEVANCE TO IN-SITU NITROUS OXIDE DATA, AND RECOMMENDATIONS FOR FUTURE STUDIES

7.1. CONCLUSIONS AND IMPLICATIONS OF THIS RESEARCH 184
7.1.1. The Use of δ^{15}N Measurements to Separate Nitrifier and Denitrifier-Produced N_2O 185
7.1.2. The Use of δ^{18}O Measurements to Separate Nitrifier and Denitrifier-Produced N_2O 186
7.1.3. Defining the Range of Soil-Derived δ^{15}N-N_2O and δ^{18}O-N_2O in this Thesis 186
7.2. GENERAL OBSERVATIONS OF δ^{15}N-N_2O AND δ^{18}O-N_2O FIELD MEASUREMENTS 187
7.2.1. N_2O from the Turkey Lakes Watershed 188
7.2.2. N_2O from the Strawberry Creek Watershed 189
7.2.3. Soil-Derived N_2O 191
7.2.4. Aquatic N_2O from Oceans, Rivers, and Streams 191
7.2.5. Groundwater N_2O 192
7.2.6. A Statistical Description of the *In Situ* Data 193
7.3. KEY CONTROLS OF THE ISOTOPIC RANGE OF IN-SITU N_2O 194
7.3.1. The Isotopic Variation of N_2O Substrates 194
7.3.2. Variable Fractionation and Oxygen Exchange 196
7.3.3. The Effect of N_2O Consumption on the Isotope Ratios of N_2O 197
7.3.4. The Effect of Diffusion on δ^{15}N-N_2O and δ^{18}O-N_2O 198
7.3.5. N_2O Gas Exchange with the Troposphere 200
7.4. RECOMMENDATIONS FOR FUTURE STUDIES 201

PERMISSIONS

UC PRESS AUTHORIZATION AGREEMENT (CHAPTER 1) 226

ELSEVIER LICENSE TERMS AND CONDITIONS (CHAPTER 2) 228
COAUTHOR'S AUTHORIZATION OF USE FORM (CHAPTER 2) 230

AMERICAN CHEMICAL SOCIETY LICENSE TERMS AND CONDITIONS (CHAPTER 4) 231
COAUTHOR'S AUTHORIZATION OF USE FORM (CHAPTER 4) 234

REFERENCES 235

LIST OF TABLES

Table 1.1. A compilation of literature estimates of nitrogen and oxygen isotope fractionation associated with processes that produce and consume N_2O. 27

Table 1.2. The % oxygen exchange measured from various denitrifying organisms during the reductions of nitrite and nitric oxide ($N^{16}O_x + H_2{}^{18}O \rightleftharpoons N^{18}O_x + H_2{}^{16}O$). 29

Table 2.1. Literature estimates of isotope effects for ^{15}N and ^{18}O-N_2O produced from NO_3^- and N_2O reduction. 52

Table 2.2. Soil water content and $\delta^{18}O$-N_2O. 53

Table 2.3. Geochemical analysis of field-collected soils. 54

Table 2.4. N_2O production rates, $\delta^{15}N$-N_2O, N isotope effects, the measured oxygen exchange, and O isotope effects. 55

Table 3.1. The geochemical characteristics of the agricultural soils incubated in this study, the mean N_2O production rate, $\delta^{15}N$-N_2O, ^{15}N isotope effect, $\delta^{18}O$-H_2O, $\delta^{18}O$-N_2O, and the corresponding results of simple linear regression (Model I) of $\delta^{18}O$-N_2O versus $\delta^{18}O$-H_2O for treatments 1–5. 85

Table 3.2. The slope (m) of the linear regression of $\delta^{18}O$-N_2O $_{(rel.\ VSMOW)}$ versus $\delta^{18}O$-H_2O $_{(rel.\ VSMOW)}$ is a minimum estimate of O-exchange during denitrification. This table demonstrates the difference between the approximated O-exchange and the true O-exchange across the range of O-exchange measured in this study (0.40–0.94) when $f_{exch.\text{-}nir} \approx f_{exch.\text{-}nor}$; $f_{exch.\text{-}nir} \neq f_{exch.\text{-}nor}$; $f_{N2O\ red.} = 0$; and $f_{N2O\ red.} > 0$. 86

Table 4.1. Soil characteristics. 110

Table 4.2. The net production of NO_3^- and NH_4^+, and the $\delta^{18}O$ values of soil H_2O and measured NO_3^-. 111

LIST OF TABLES

Table 5.1. The experimental conditions and the mean rates of N_2O produced by nitrification in this study, and the linear regression analyses of mean production-weighted $\delta^{18}O$-N_2O versus $\delta^{18}O$-H_2O. 139

Table 5.2. Input parameters for Monte Carlo simulations of Equations 5.1–5.11. 140

Table 5.3. Hypothetical $\delta^{18}O$ values of N_2O produced by nitrification in natural environments, and a sensitivity analysis of the input parameters in Equations 5.1–5.11. 141

Table 6.1. The experimental conditions and geochemical parameters measured in this study. 174

Table 6.2. An account of select N species after 25 days and 37 days of incubation (agricultural soils) and at the end of the experiments (all soils). 175

Table 6.3. The isotope effects (ε) or isotopic separations (Δ) measured in this study for the nitrification of NH_4^+ to NO_3^- (treatments 1–3) and NH_4^+ to N_2O (treatments 1–7). 177

Table 7.1. A summary of selected results from the denitrification experiments conducted in Chapters 2–3. 205

Table 7.2. A summary of selected results from the nitrification experiments conducted in Chapters 5–6. 206

LIST OF FIGURES

Figure 1.1. A recent, 30-year record of the mean monthly concentrations of tropospheric N_2O at five locations throughout the northern and southern hemispheres. 30

Figure 1.2. The tropospheric concentrations of N_2O from the late Quaternary Period (top) and the last Millennium (bottom) inferred from polar ice cores. 31

Figure 1.3. The biogeochemical reaction pathways that produce and consume N_2O. 32

Figure 1.4. The denitrification pathway and the location of enzymes in Gram-negative bacteria 33

Figure 2.1. Proposed systematics of oxygen isotope enrichment and exchange during the denitrification of NO_3^- to N_2. 56

Figure 2.2. *a–f.* N_2O production, $\delta^{15}N$-N_2O, and $\delta^{18}O$-N_2O versus time for upland and wetland soils incubated under different moisture and temperature conditions. 57

Figure 2.3. *a–e.* The fraction of oxygen exchange between H_2O and N_2O precursors during dissimilatory reduction of NO_3^- to N_2O. 60

Figure 3.1. *a.* Approximate location of the Strawberry Creek Watershed in South-Central Ontario, Canada. 87

b. Aerial map of the upper portion of the Strawberry Creek Watershed from the headwaters to Maryhill Road. The approximate positions of the intensive study plots and the locations where soils were collected for this study are shown. 88

Figure 3.2. Proposed systematics of oxygen isotope enrichment and exchange during denitrification. 89

Figure 3.3. *a–e.* N_2O production, $\delta^{15}N$-N_2O, and $\delta^{18}O$-N_2O versus time for flooded and non-flooded anaerobic incubations of agricultural soil and stream sediment. 90

Figure 3.4. The relationship between the ^{15}N isotope effect and the ^{18}O isotope effect and the rate of N_2O production by denitrification. 93

Figure 3.5. A simple linear regression of the net ^{18}O isotope effect versus O-exchange. 94

Figure 3.6. The relationship between the oxygen and nitrogen isotope effects of the agricultural soils and the temperate forest soils. The ratio of the oxygen and nitrogen isotope effects for N_2O reduction is approximately 2½ to 1. 95

Figure 3.7 *a–c.* Predicting the $\delta^{18}O$-$N_2O_{red.}$ value in open and closed systems. 96

LIST OF FIGURES

Figure 4.1. Field observations of $\delta^{18}O\text{-}NO_3^-$ produced from nitrification in groundwater and surface water. Also shown are experimental measurements of microbial NO_3^- in a temperate hardwood forest and laboratory incubations of soil. This data is compared to the theoretical $\delta^{18}O\text{-}NO_3^-$ values that would be formed by nitrification if the oxygen was derived from H_2O and O_2 in a 2:1 ratio, respectively. 112

Figure 4.2. $\delta^{18}O\text{-}NO_3^-$ produced from nitrification of temperate forest and agricultural soils incubated with waters of varying $\delta^{18}O\text{-}H_2O$. 113

Figure 4.3. A schematic representation of bacterial nitrification describing the controls of $\delta^{18}O\text{-}NO_3^-$ ($\delta^{18}O\text{-}O_2$, $\delta^{18}O\text{-}H_2O$, abiotic oxygen exchange, and kinetic and equilibrium isotope effects). 114

Figure 5.1. A schematic representation of the biogeochemical processes that form N_2O in aerobic environments. 142

Figure 5.2. *a.* Literature reports of $\delta^{18}O\text{-}N_2O$ values produced during ammonium oxidation by single organism cultures, and the microbial consortia found in wastewater and soils. 143

b. $\delta^{18}O\text{-}N_2O$ values collected from this study (with $\delta^{18}O\text{-}H_2O$ at natural abundance) is plotted for comparison with the literature data. 143

Figure 5.3. *a–f.* $\delta^{18}O\text{-}N_2O$ and N_2O production rates measured with time for treatments 1–6. 144

Figure 5.4. Histograms of model parameters predicted using Monte Carlo simulations. 147

SUPPLEMENTARY FIGURES

Figure S5.1. Monte Carlo simulation results for Experiments 1–3 (*scenario b*) with variable fractions of N_2O produced by nitrifier-denitrification (0.75–1) and via NH_2OH oxidation (0–0.25). 148

Figure S5.2. Monte Carlo simulation results for Experiment 1 (*scenarios a–d*). 149

Figure S5.3. Monte Carlo simulation results for Experiment 2 (*scenarios a–d*). 151

Figure S5.4. Monte Carlo simulation results for Experiment 3 (*scenarios a–d*). 153

Figure 6.1. A schematic representation of NO_3^- and N_2O production by nitrification. 178

Figure 6.2. *a–g.* $\delta^{15}N\text{-}N_2O$ values and the N_2O production rates versus time for Treatments 1-7. 179

Figure 6.3. $\delta^{15}N\text{-}N_2O$ values versus the rate of N_2O production for Treatments 1-7. 183

LIST OF FIGURES

Figure 7.1. A compilation of the N isotope effects or separations measured between N_2O and NO_3^- (denitrification) and between N_2O and NH_4^+ or organic-N (nitrification).

a. All the ^{15}N data measured in this thesis is shown. 207

b. Only the ^{15}N data that was used to calculate estimates of ε and Δ reported throughout Chapters 2–3 and Chapter 6 are shown. 208

Figure 7.2. A comparison of the measured $\delta^{18}O$-N_2O data from nitrification experiments and the modelled $\delta^{18}O$-N_2O ranges from denitrification. 209

Figure 7.3. The range of $\delta^{18}O$-N_2O and $\delta^{15}N$-N_2O produced by denitrification in this thesis. 210

Figure 7.4. The range of $\delta^{18}O$-N_2O and $\delta^{15}N$-N_2O produced by nitrification in this thesis. 211

Figure 7.5. In-situ $\delta^{15}N$-N_2O and $\delta^{18}O$-N_2O data collected from soils, streams and groundwater at the Turkey Lakes Watershed. This field data is shown alongside the isotopic N_2O endmembers determined in this thesis through incubations of TLW soils. 212

Figure 7.6. In-situ $\delta^{15}N$-N_2O and $\delta^{18}O$-N_2O collected from the Strawberry Creek agricultural catchment. This field data is shown alongside the range of N_2O isotope endmembers determined in this thesis using soil incubations. 213

Figure 7.7. A hypothetical 'process plot' showing how N_2O diffusion and the consumption of NO_3^- and N_2O can influence the measured values of $\delta^{15}N$-N_2O and $\delta^{18}O$-N_2O. 214

Figure 7.8. Unpublished $\delta^{15}N$ and $\delta^{18}O$ values of N_2O collected from multiple field sites by affiliates of the Environmental Geochemistry Laboratory, University of Waterloo.

a. Site map of field locations throughout Ontario, Canada. 215

b. Soil pore gas and flux collection chambers. 216

c. Dissolved N_2O from creeks, streams, rivers, and agricultural drainage tiles. 217

d. Dissolved N_2O from groundwaters and agricultural drainage tiles. 218

Figure 7.9. *a–b.* The global in-situ N_2O isotope results that have been published in peer-reviewed journals (up to February 2011). 219

Figure 7.10. *a–d.* Compilations of published and unpublished $\delta^{15}N$-N_2O and $\delta^{18}O$-N_2O data with descriptive statistics, and the flux-weighted average soil N_2O sources. 221

Figure 7.11. *a–b.* The control of gas exchange on N_2O isotopes is illustrated with plots of $\delta^{18}O$-N_2O versus N_2O saturation (%) in a surface water (gas exchange occurs) and a groundwater (gas exchange does not occur). 225

1 Introduction

1.1. *The Nitrogen Dilemma*

The World population has multiplied five-fold in the last 150 years (UN Population Division 1999). At the same time, human activities have profoundly altered the global nitrogen (N) cycle. In pre-industrial times, the creation of biologically-available reactive N (Nr) was almost exclusively dominated by natural biological N fixers. Nr production has subsequently risen dramatically because of increased combustion of fossil-fuels, clearing of land for agriculture, and industrial production of N fertilizers. By 2005, the rate of Nr fixed via the Haber-Bosch process (121 Tg N yr^{-1}) equalled the natural rate of N fixation in all the world's oceans (121 Tg N yr^{-1}) and exceeded the natural rate of N fixation in all terrestrial ecosystems (107 Tg N yr^{-1}) (Galloway *et al.* 2004, 2008). Past and present trends of Nr production and usage suggest that before the year 2050, the total amount of anthropogenically created Nr will surpass the amount formed by all natural fixation processes (Galloway *et al.* 2004).

If it weren't for the historical fixation of synthetic Nr, it is doubtful that the World's developed nations could have achieved their current states of population and prosperity. Indeed, many developing areas of the world still suffer from extreme hunger and poverty because existing agricultural productivities and other barriers prevent basic food requirements from being met (UNEP and WHRC 2007). However, much of the Nr that is created is inefficiently used, and today we are left with a myriad of N-related environmental problems. Herein lies the great anthropocentric N dilemma; how do we feed an exponentially-expanding population while simultaneously minimize our footprint on the natural environment which supports us?

There is perhaps no better synopsis of this overarching problem than the following description provided by some of the world's most prominent global N biogeochemists (Galloway *et al.* 2003):

> "Human production of food and energy is the dominant continental process that breaks the triple bond in molecular nitrogen (N_2) and creates reactive nitrogen (Nr) species. Circulation of anthropogenic Nr in Earth's atmosphere, hydrosphere, and biosphere has a wide variety of consequences, which are magnified with time as Nr moves along its biogeochemical pathway. The same atom of Nr can cause multiple effects in the atmosphere, in terrestrial ecosystems, in freshwater and marine systems, and on human health. We call this sequence of effects the nitrogen cascade. As the cascade progresses, the origin of Nr becomes unimportant. Reactive nitrogen does not cascade at the same rate through all environmental systems; some systems have the ability to accumulate Nr, which leads to lag times in the continuation of the cascade. These lags slow the cascade and result in Nr accumulation in certain reservoirs, which in turn can enhance the effects of Nr on that environment. The only way to eliminate Nr accumulation and stop the cascade is to convert Nr back to nonreactive N_2."
>
> James N. Galloway, John D. Aber, Jan Willem Erisman, Sybil P. Seitzinger, Robert W. Howarth, Ellis B. Cowling, and B. Jack Cosby. The Nitrogen Cascade. *BioScience*, Vol. 53, no. 4 (April 2003), pp. 341–356.
>
> © 2003 by The American Institute of Biological Sciences. Published by the University of California Press.

The increased environmental loading of Nr has numerous ripple effects that have been reviewed by Vitousek *et al.* (1997) and Galloway *et al.* (2003). Examples of these impacts include the global eutrophication of freshwater and marine environments and the N-saturation of forests worldwide. The latter leads to increased soil acidification and water stress, and losses of biodiversity, soil nutrients, and frost tolerance (Aber *et al.* 1989, 1998).

Another consequence of increased Nr loading is the widespread nitrate (NO_3^-) contamination of our drinking water resources. NO_3^- is the most ubiquitous contaminant of groundwaters worldwide (Spalding and Exner 1993). In the United States, approximately one-quarter of the private, domestic water supply wells in rural areas currently exceed the maximum contaminant level (10 mg nitrate-N/L) set by the U.S. Environmental Protection Agency. Of the groundwaters in Europe for which data were available, approximately one-third have similarly elevated concentrations of NO_3^- (Ward *et al.* 2005).

An additional result of rising Nr fixation is that the atmospheric concentration of nitrous oxide (N_2O) is growing at an unprecedented rate (Figure 1.1–1.2) (Denman *et al.* 2007). N_2O is a potent greenhouse gas and it continues to have an important role in the depletion of stratospheric ozone (O_3) and the delay of its recovery (Chipperfield 2009). This ever-growing N_2O problem is the chief driver of this thesis research. Soils are the largest single source of N_2O worldwide, representing approximately one-half of the total natural and anthropogenic N_2O sources (Denman *et al.* 2007). Although there is great uncertainty in the estimated

strength of individual sources, soils under agriculture emit 2.8 (1.7–4.8) Tg N_2O-N yr^{-1} and soils under natural vegetation emit 6.6 (3.3–9.0) Tg N_2O-N yr^{-1}. Regardless of the uncertainty in these estimates, it is apparent that relative to the sum of all sources [17.7 (8.5–27.7) Tg N_2O-N yr^{-1}], soils under agriculture and natural vegetation represent a large fraction of the total N_2O emissions[1]. Thus, significant progress in mitigating rising atmospheric concentrations of N_2O can potentially be made in soil environments.

N_2O is produced in soils by nitrifying and denitrifying microorganisms found ubiquitously throughout nature. The successful mitigation of rising concentrations of atmospheric N_2O requires a much better understanding of the controls responsible for its production. The stable isotope ratios of N_2O ($\delta^{15}N$ and $\delta^{18}O$) offer a promising tool to assist with apportioning different microbial N_2O sources. Therefore, the primary objectives of this thesis are to investigate the controls of the isotope ratios of N_2O and NO_3^- in soils, and characterize the $\delta^{15}N$ and $\delta^{18}O$ values and the isotope effects (ε) of N_2O and NO_3^- formed by nitrification and denitrification in temperate forest and agricultural soils.

1.2. *N_2O Production and Consumption: The Microbial Players*

A comprehensive discussion of nitrification and denitrification and its role in producing N_2O in soils is far beyond the scope of this chapter. The breadth and content of the literature on these subjects is vast and rapidly evolving. As a starting point, the reader is referred to the following nitrification-related reviews: Bédard and Knowles (1989); Bothe *et al.* (2000); De Boer and Kowalchuk (2001); Kowalchuk and Stephen (2001); Arp *et al.* (2002); Arp and Stein (2003); Hayatsu *et al.* (2008), and the following denitrification-related reviews: Knowles (1982); Firestone and Davidson (1989); Zumft (1997); Bothe *et al.* (2000); Li *et al.* (2000); Stein and Yung (2003); Chapuis-Lardy *et al.* (2006); Seitzinger *et al.* (2006); Hayatsu *et al.* (2008).

[1] Estimates and the range of uncertainty in parentheses are reported in the 4th Assessment Report (AR) of the Intergovernmental Panel on Climate Change (IPCC) (Denman *et al.* 2007). The uncertainty ranges were derived from the 3rd AR and several other primary research articles.

1.2.1. *Chemolithoautotrophic Nitrification*

Nitrification by the chemolithoautotrophs is a ubiquitous and well-characterized process whereby ammonia[2] (NH_3) is oxidized to nitrite (NO_2^-) via hydroxylamine (NH_2OH) (Figure 1.3). The chemolithoautotrophic ammonia-oxidizers (the '*Nitroso*' bacteria such as species of *Nitrosomonas*, *Nitrosococcus*, *Nitrosospira*, *Nitrosolobus*, and *Nitrosovibrio*) are the best known group of nitrifying organisms. They generate metabolic energy from N oxidation (Equations 1.1–1.2) and use it to fix carbon dioxide (CO_2) into cellular-C (biosynthesis). This dissimilatory process is catalyzed by ammonia monooxygenase (*amo*) and hydroxylamine oxidoreductase (*hao*), and requires sufficiently high levels of molecular oxygen (O_2) to be sustained. Acetylene (C_2H_2) is an effective inhibitor of *amo* in chemolithoautotrophs and is often used in experiments to block nitrifier-derived N_2O (at partial pressure ≈ 10 Pa).

$$NH_3 + O_2 + 2H^+ + 2e^- \rightarrow NH_2OH + H_2O \quad [1.1]$$

*2 of the 4 electrons are shuttled back to *amo* (Bothe *et al.* 2000)

$$NH_2OH + H_2O \rightarrow NO_2^- + 5H^+ + 4e^- \quad [1.2]$$

1.2.2. *Nitrite Oxidation*

The final oxidation step of nitrification (NO_2^- to NO_3^-; Figure 1.3) is carried out by the nitrite-oxidizers, which commonly belong to the bacterial genus *Nitrobacter* or *Nitrococcus*. This dissimilatory chemolithoautotrophic process is catalyzed by nitrite oxidoreductase (*noxr*) (Equation 1.3).

$$NO_2^- + H_2O \rightarrow NO_3^- + 2H^+ + 2e^- \quad [1.3]$$

[2] NH_3 and NH_4^+ are related by: $NH_3 + H^+ \rightleftharpoons NH_4^+$, where the pKa = 9.25. During nitrification, NH_3 is the species that is oxidized to hydroxylamine. Organisms can actively assimilate NH_4^+ when they are N limited; otherwise NH_3 diffuses across the cell membrane (Fogel and Cifuentes 1993).

1.2.3. *Heterotrophic Nitrification*

The heterotrophic ammonia-oxidizers metabolize organic carbon for their primary energy source. This diverse group of bacteria and fungi do not gain energy by oxidizing NH_3 to NO_2^-. Akin to the chemolithoautotrophs, the heterotrophic nitrifiers have an *amo* enzyme that catalyzes the first step of this reaction (Moir et al. 1996). A hydroxylamine oxidoreductase catalyzes the second step of heterotrophic nitrification; however, this enzyme is distinctly different from those isolated from the chemolithoautotrophs (Wehrfritz et al. 1993; Moir et al. 1996; Zumft 1997).

Interestingly, these organisms are not inhibited by acetylene even at the high concentrations used to block N_2O reduction (10 kPa; De Boer and Kowalchuk 2001). Therefore, the acetylene-block technique, which is commonly used to quantify rates of N_2O production, cannot distinguish between denitrifier-derived N_2O and heterotrophic nitrifier-derived N_2O. However, using acetylene may be an easy and useful means to differentiate rates of chemolithoautotrophic nitrification from heterotrophic nitrification.

1.2.4. *Methanotrophic Nitrification*

Nitrification is also facilitated by methanotrophic bacteria, which oxidize CH_4 to cellular-C (via CH_3OH) and gain energy for metabolism (Mandernack *et al.* 2009). The oxidation of NH_3 to NO_2^- occurs concomitantly with CH_4 oxidation, and, similar to the heterotrophs, no metabolic energy is gained from the oxidations. These reactions are catalyzed by methane monooxygenase and a hydroxylamine oxidoreductase that may resemble the enzyme found in the chemolithoautotrophs (Bédard and Knowles 1989).

1.2.5. *'New' Ammonia-Oxidizers: Anammox and the Archaeal Nitrifiers*

Since the first chemolithoautotrophic bacterial nitrifier was discovered over 120 years ago (Winogradsky 1890), great discoveries in the N cycle have been made. However, recently our understanding of the N cycle has been fundamentally altered (twice) in a very short amount of time.

First, the discovery of anaerobic ammonia oxidizing bacteria (anammox) in wastewater reactors in 1992 spawned a flurry of exciting science around the globe (reviewed by Kuenen 2008). Only a mere nine years ago, we obtained the first conclusive proof that these organisms are active in natural habitats (Thamdrup and Dalsgaard 2002). Since then, it has become clear that anammox bacteria have an important role in the global N cycle, and may be responsible for 30–50% of the total reactive N loss in the World's oceans (Francis *et al.* 2007; Kuenen 2008, and references therein) (Equation 1.4).

$$NH_4^+ + NO_2^- \rightarrow N_2 + 2H_2O \qquad [1.4]$$

There is currently no evidence to support that N_2O is an intermediate compound of the anammox metabolism. All investigations into N_2O production by anammox bacteria in waste water reactors have measured small N_2O yields (<2% of the N load) (e.g., Kampschreur *et al.* 2008). These small amounts of N_2O are often attributed to production by nitrifiers or denitrifiers in the reactors. Kartal *et al.* (2007) used labelled ^{15}N tracers to delineate the NO_3^- and NO_2^- reductions of anammox and discovered very little label in the N_2O pool. The authors proposed that the small amounts of N_2O formed by anammox bacteria are a result of a NO detoxification mechanism (NO is one of the proposed intermediates).

More recently, it was discovered that *Crenarchaeota* are capable of aerobic ammonia oxidation [reviewed by Francis *et al.* (2007) and Prosser and Nicol (2008)]. For many years the archaea remained unculturable, so their role in the N cycle was a mystery. But in the last 7 years metagenomic studies of uncultivated *Crenarchaeota* have revealed *amo*-like genes in samples of seawater (Venter *et al.* 2004) and soil (Treusch *et al.* 2005); the first ammonia-oxidizing archaea was finally cultured (*Nitrosopumilus maritimus*; Könneke *et al.* 2005); and it now appears that archaeal nitrifiers may be responsible for a large portion of the total NH_3 that is oxidized in a wide variety of soil and marine environments.

1.2.6. *Denitrification*

The stepwise reduction of NO_3^- → NO_2^- → nitric oxide (NO) → N_2O → dinitrogen (N_2) (Figure 1.3) is carried out by a diverse group of bacteria and fungi that span many bacterial and archaeal genera. Many ecological niches have representative denitrifying organisms, which even include the diazotrophs (N_2-fixing organisms) and the phototrophs (photosynthetic bacteria). Although there are exceptions, denitrification is generally an anaerobic, dissimilatory process that is performed by microorganisms who have adapted to conditions of O_2 limitation or even complete anoxia. Most denitrifiers are facultative, meaning that they can use O_2 as the terminal electron acceptor in respiratory processes, but when O_2 is limited, they can utilize NO_3^- as the terminal electron acceptor. As such, many of the organisms that can denitrify are also classified as nitrifiers.

1.2.6.1. *Heterotrophic Denitrification*

The majority of denitrifiers are organotrophic, meaning that organic carbon (R–CH_2O) is the electron donor that is associated with the reduction sequence. Metabolic energy is gained by coupling the reduction of nitrogen oxides to electron transport phosphorylation (ETP), which generates proton gradients that are used in oxidative phosphorylation to generate ATP. The overall reaction for total denitrification by heterotrophs is summarized in Equation 1.5, and the individual half-reactions are given in Equations 1.6–1.9:

$$4NO_3^- + 5CH_2O + 4H^+ \rightarrow 2N_2 + 7H_2O + 5CO_2 \quad [1.5]$$

$$NO_3^- + 2H^+ + 2e^- \rightarrow NO_2^- + H_2O \quad [1.6]$$

$$NO_2^- + 2H^+ + e^- \rightarrow NO + H_2O \quad [1.7]$$

$$2NO + 2H^+ + 2e^- \rightarrow N_2O + H_2O \quad [1.8]$$

$$N_2O + 2H^+ + 2e^- \rightarrow N_2 + H_2O \quad [1.9]$$

The vast majority of NO_3^- reduction that occurs in nature is carried out by organotrophic denitrifiers. Under appropriate conditions, most of these organisms can carry out the entire sequence outlined in Equations 1.6–1.9 (Tiedje 1988).

1.2.6.2. *Chemolithoautotrophic Denitrification*

Autotrophic denitrifiers fix CO_2 for biosynthesis and reduce N-oxides using inorganic substrates [such as NH_3, ammonium (NH_4^+), sulphur compounds, and H_2] for electron donors (Zumft 1997). Example reactions are shown in Equations 1.10 to 1.13. Because the energy is gained through the oxidation of the inorganic substrates (S, H, Fe), this form of denitrification is non-respiratory.

$$8NO_3^- + 5S_2O_3^{2-} + H_2O \rightarrow 4N_2 + 10SO_4^{2-} + 2H^+ \quad [1.10]$$

$$14NO_3^- + 5FeS_2 + 4H^+ \rightarrow 7N_2 + 10SO_4^{2-} + 5Fe^{2+} + 2H_2O \quad [1.11]$$

$$2NO_3^- + 5H_2 \rightarrow N_2 + 4H_2O + 2OH^- \quad [1.12]$$

$$2NO_3^- + 10FeCO_3 + 24H_2O \rightarrow N_2 + 10Fe(OH)_3 + 10HCO_3^- + 8H^+ \quad [1.13]$$

Chemolithoautotrophic denitrification is a dissimilatory process and it tends to emit much greater proportions of N_2O than N_2 (Tiedje 1988, Robertson and Groffman 2006). NO_2^- and NO are toxic and metabolically unstable compounds, so they are reduced to N_2O by these microorganisms as a detoxification mechanism. These organisms gain no ecological benefit from reducing N_2O, however, because N_2O is biologically inert and no energy is generated. A wide variety of obligate or facultative anaerobic bacteria, fungi, and yeast can perform this type of denitrification (Bremner 1997). Interestingly, chemolithoautotrophic denitrification may occur in aerobic environments and they are also known as 'aerobic denitrifiers' (Zumft 1997). As a result, some of the N_2O that was previously thought to be derived solely from nitrification may actually be a mixture of the two processes (Robertson and Groffman 2006).

1.3. *The Biological Production and Consumption of N_2O in Soils*

1.3.1. *N_2O Produced by Nitrification: Nitrifier-Denitrification*

In the early 1970's, it was discovered that *Nitrosomonas europaea* (an autotrophic nitrifier; Section 1.2.1) was capable of yielding N_2O from the oxidation of NH_4^+ via NO_2^- (Yoshida and

Alexander 1970; Ritchie and Nicholas 1972). Following this, many studies using aerobic and anaerobic batch cultures investigated NO_2^- reduction by autotrophic nitrifiers, and it was shown that many of these organisms can produce NO and N_2O under oxygen-limited conditions (Figure 1.3). Methanotrophic nitrifiers (Section 1.2.4) can also reduce NO_2^- to N_2O; however our understanding of this metabolism is poorly known (Stein and Yung, 2003).

Many heterotrophic ammonia-oxidizers (Section 1.2.3) have been shown to reduce N-oxides (Yoshida and Alexander 1970), and this can occur over a wide range of O_2 concentrations including fully aerobic conditions (Wehrfritz *et al.* 1993). This group of 'aerobic denitrifiers' is thought to have developed this mechanism as way of managing excess reductant (Zumft 1997). The enzymes purified from the heterotrophic nitrifiers capable of denitrification are identical to those found in traditional facultative anaerobic denitrifiers (Zumft 1997). Robertson *et al.* (1995) confirmed that N_2 is produced by the heterotrophic bacteria *Paracoccus denitrificans* GB17 (formerly *Thiosphaera pantotropha*) under well-mixed aerobic conditions.

Although these organisms can denitrify under variable O_2 conditions, there must be sufficient O_2 to facilitate the oxidations of NH_3 and NH_2OH; otherwise, the substrate (NO_2^-) will quickly disappear. Consequently, in the natural environment this coupled nitrification-denitrification will only subsist in places where anaerobic microsites or biofilms occur (e.g., soil clods and sediment-stream interfaces).

When communities of ammonia-oxidizers and nitrite-oxidizers are established, NO_3^- is the major end-product of nitrification. The N_2O yields [N_2O/NO_2^-] of fully aerated cultures of chemolithoautotrophic nitrifiers are usually very low (0.05–3.3%; Colliver and Stephenson 2000). Under oxygen limitation the relative amounts of N_2O produced can increase (0.8–11%), however, NO_3^- remains the chief nitrification end-product.

Finally, in much of the scientific literature, this overall oxidation-reduction sequence ($NH_4^+ \rightarrow NO_2^- \rightarrow N_2O$) is broadly termed 'nitrifier-denitrification' without regard to the organisms involved. This is especially true in many publications that investigate the stable isotope ratios of N_2O (e.g., Wrage *et al.* 2001; Chapters 5–6 of this thesis). Using a generalized

term for this N_2O production pathway should not be problematic as long as it is understood that different groups of organisms can perform these reactions under (potentially) very different environmental conditions.

1.3.2. *N_2O Produced by Nitrification: Hydroxylamine Oxidation*

N_2O can also be a by-product of the classic nitrification reactions (Figure 1.3), whereby NH_2OH is directly oxidized to N_2O in a single step, or it is formed via one or more intermediate(s) compounds such as NO (Stein and Yung 2003). Otte *et al.* (1999) demonstrated that the heterotrophic ammonia-oxidizer *Alcaligenes faecalis* could produce N_2O by this pathway, and Sutka *et al.* (2003, 2004, 2006) confirmed this with cultures of chemolithoautotrophs (*N. europaea* and N. *multiformis*) and methanotrophs (*Methylococcus capsulatus* Bath and *Methylosinus trichosporium*). Thus, all three groups of bacterial nitrifiers can form N_2O by this pathway.

Very little is known about this side-reaction, including whether or not it is enzymatically-catalyzed. Hydroxylamine oxidoreductase may be involved, or it may well be an example of an abiotic N_2O production mechanism (Stein and Yung 2003)[3]. Its ecological and biogeochemical triggers are unknown, and whether it occurs in nature at rates that are comparable to nitrifier-denitrification remains a key question. Indeed, there is not even a consensus as to what we should name this reaction mechanism. For this thesis, the least ambiguous nomenclature was chosen and the terminology 'N_2O by nitrification' is avoided. Instead, N_2O via NH_2OH oxidation describes this pathway, and nitrifier-denitrification is reserved for N_2O formed by nitrifiers via NO_2^- reduction (Figure 1.3).

[3] During this thesis research an unreported, peripheral experiment was conducted to synthesize a working standard of N_2O gas that was isotopically distinct from commercially-available N_2O sources. When hydroxylamine hydrochloride was added to a solution of excess ferric chloride (a mild oxidizing agent) at laboratory temperature and pressure, N_2O was rapidly formed according to the following postulated abiotic reaction:

$$4FeCl_{3(aq)} + 2NH_2OH{\cdot}HCl_{(aq)} \rightarrow 4Fe^{2+} + N_2O + H_2O + 6H^+ + 14Cl^-$$

1.3.3. *Denitrification: N_2O Production and Consumption*

N_2O is an obligate intermediate of total denitrification and most denitrifiers are capable of performing the entire reduction sequence ($NO_3^- \rightarrow NO_x \rightarrow N_2$). However, not all denitrifiers possess N_2O reductase (*nos*), the enzyme responsible for the catalysis of N_2O reduction, and N_2O is the terminal end-product of denitrification in these organisms ($NO_3^- \rightarrow NO_x \rightarrow N_2O$). Additionally, *nos* is very sensitive to O_2, and very small amounts can inhibit N_2O reduction (Knowles 1982). Other controls of the N_2O yield [the N_2O:N_2 ratio] are poorly understood and they are briefly summarized below in Section 1.3.4.

Some denitrifiers are capable of assimilating extracellular N_2O from their environment and reducing it to N_2 for metabolic energy. Along with the N_2O/N_2 yield described above, this process of N_2O consumption is the main determinant of the net N_2O production rate (or flux) measured in a soil environment. N_2O consumption is dependent upon several factors, which include redox conditions, the rate of diffusion, soil moisture, soil pH, and soil texture (Chapuis-Lardy *et al.* 2006).

1.3.4. *The Environmental Controls of N_2O Production*

Many researchers have attempted to constrain and characterize the environmental parameters that directly and/or indirectly control N_2O emissions from soils. There are several reviews of the ecological, microbiological, and biochemical drivers of N_2O production in soils [Firestone *et al.* 1980; Tiedje *et al.* 1982; Tiedje 1988; Firestone and Davidson 1989; Davidson 1993; Ye *et al.* 1994; Bremner 1997; Zumft 1997; Colliver and Stephenson 2000; Li *et al.* 2000; Megonigal *et al.* 2003; Smith *et al.* 2003; Stein and Yung 2003; Chapuis-Lardy *et al.* 2006].

Although the factors controlling N_2O emissions are complex, generalizations can be made about the conditions that are optimal and sub-optimal for nitrifiers and denitrifiers. Oxygen is a primary control of the activity of nitrifiers and denitrifiers, and consequently O_2 is a master regulator of N_2O production. For example, O_2 inhibits the series of denitrifying enzymes that catalyze the reductions of N-oxides, and their sensitivity increases along the reduction sequence. As such, it is believed that N_2O consumption (or total denitrification) will

only occur under very anoxic conditions. Dissolved oxygen (DO) concentrations as low as 0.5 mg/L can inhibit the activity of denitrification enzymes and nitrous oxide reductase can be suppressed by less than 0.2 mg/L of DO (Maier et al. 2009; Tiedje 1988).

Soil water content, temperature, substrate availability, and pH all play a role in the activity of soil microorganisms; however, their influence on N_2O production is less clear. For example, the water content of natural soils often limits the diffusion of O_2, and thereby partially controls the redox conditions. In general, nitrification is stimulated in drier soils and denitrification predominates at higher soil moisture contents (Smith *et al.* 2003). However, the direct, intrinsic role of soil water content on the rate of N_2O production is unclear.

Soil temperature is positively correlated with the biological activity of nitrifiers and denitrifiers (Stein and Yung 2003). Yet significant rates of biological N_2O production have been observed in contrasting climates ranging from tropical soils (Perez *et al.* 2000) to snow-covered soils (Maljanen *et al.* 2003). Additionally, some environmental parameters may have a combined effect on N_2O production as Blackmer and Bremner (1977) and Firestone *et al.* (1980) have shown that high concentrations of NO_3^- and low soil pH inhibit N_2O consumption.

1.4. *Stable Isotope Theory*

The stable isotope ratios of N_2O ($^{15}N/^{14}N$ and $^{18}O/^{16}O$) can be used in conjunction with traditional geochemical tools to trace N transformations throughout the environment. They provide a non-invasive means to determine N_2O formation pathways in environments where multiple, simultaneous sources exist. There are several references on the use of stable isotopes in biogeochemical and ecological research where the reader can obtain more background information. These include: Mariotti *et al.* (1981, 1982); Hübner (1986); Fogel and Cifuentes (1993); Clark and Fritz (1997); Högberg (1997); Kendall (1998); Kendall and Caldwell (1998); Mook (2000); Bedard-Haughn *et al.* (2003); Kendall and Doctor (2003); Fry (2006); Sharp (2007);

Aravena and Mayer (2010). There are one book chapter (Pérez 2005) and one article (Kool *et al.* 2007) that review the subject matter specific to the stable isotopes of N_2O.

1.4.1. *The Stable Isotopes of Nitrogen and Oxygen*

Isotopes are atoms of the same element that have an equal number of protons but differ in their number of neutrons. The variation in the number of neutrons leads to slightly different masses, and this yields subtle differences in the physical and chemical properties of isotopes of the same element. The translational, vibrational, and rotational energies at the nuclear level are different, and this causes heavier isotopes to have lower mean velocities, collision frequencies and zero-point energies (Kaiser 2002). As a consequence, this translates into subtle (but measurable) differences in many processes such as chemical reaction rates (k), equilibrium phase changes, diffusion, and photolysis (Kaiser 2002).

Isotopic compositions are measured on a mass spectrometer and their values, denoted as deltas (δ), are expressed as a per mill (‰) deviation from an international standard. For nitrogen and oxygen, the $\delta^{15}N$ and $\delta^{18}O$ is calculated according to Equations 1.14 and 1.15, respectively.

$$\delta^{15}N_{sample} = {}^{15}N/{}^{14}N_{sample} \div {}^{15}N/{}^{14}N_{atmospheric\ N_2} - 1 \quad [1.14]$$

$$\delta^{18}O_{sample} = {}^{18}O/{}^{16}O_{sample} \div {}^{18}O/{}^{16}O_{\ VSMOW} - 1 \quad [1.15]$$

By convention, a factor of one-thousand ($\times$ 1000) is omitted from Equations 1.14–1.15, because δ values are expressed in units of ‰.

There are 16 known isotopes of nitrogen but only two are stable (^{14}N and ^{15}N). The longest living radioactive N isotope (^{13}N) has a half-life (t½) of 9.965 minutes. Atmospheric air (N_2) is the primary reference material for nitrogen isotope measurements because it is a large, homogenous, and easily accessible N source at the surface of the Earth. The mole frac-

tions of ^{14}N and ^{15}N in air (N_2) are 0.996337 and 0.003663, respectively (Coplen *et al.* 2002). By definition, the $\delta^{15}N$ value of atmospheric N_2 is 0‰.

There are seventeen known isotopes of oxygen and three are stable (^{16}O, ^{17}O and ^{18}O). The remaining radioactive isotopes all have a t½ of <2 minutes. The recommended international reference for oxygen isotope ratios of N_2O is Vienna Standard Mean Ocean Water (VSMOW), although oxygen isotope ratios of N_2O are sometimes related to atmospheric oxygen (O_2) in the literature. The mole fractions of ^{16}O, ^{17}O, and ^{18}O in VSMOW are 0.9976206, 0.0003790, and 0.0020004, respectively (Coplen *et al.* 2002). By definition, the $\delta^{18}O$ value of VSMOW is 0‰. To convert $\delta^{18}O$ values reported against atmospheric O_2 to VSMOW, Kim and Craig (1990) suggested the following conversion provided in Equation 1.16.

$$\delta^{18}O_{VSMOW} = (\delta^{18}O_{\text{atmospheric } O_2} + 23) \times 1.0235 \quad [1.16]$$

Changes in the relative distribution of isotopes are very small and difficult to measure in absolute terms. Therefore, the isotopic composition of a substance is always measured as a ratio of the heavy (or rare) isotope relative to the light (or common) isotope. In turn, this ratio is always compared to an international standard that has an absolute composition that has been agreed upon by the international community.

1.4.2. *Alphas* (α), *Epsilons* (ε) *and Deltas* (Δ)

Changes in the isotopic abundance of a geochemical pool can be quantified with a fractionation factor (α). Physical processes such as diffusion or adsorption can cause measureable isotopic fractionation. A reversible (equilibrium), chemical exchange reaction can be fractionating and the magnitude is temperature-dependent. The fractionation factor for these processes ($X \rightleftharpoons Y$) is given by Equation 1.17, where R is the ratio of the heavy isotope to the light isotope (e.g., $^{15}N/^{14}N$) of X and Y, respectively.

$$\alpha = R_X \div R_Y \quad [1.17]$$

NH_3 volatilization can significantly increase the $\delta^{15}N$ of the nitrification endmember in high pH environments (pH $>$ 8), because the α factor for volatilization can be as high as 1.030 (Fogel and Cifuentes 1993). There is an important equilibrium oxygen isotope exchange reaction between NO_2^- and H_2O (Casciotti *et al.* 2010). Exchange occurs rapidly, and at room temperature the $\alpha \approx 1.014$ (Casciotti *et al.* 2007). This is an important control on the $\delta^{18}O$ values of NO_3^- and N_2O formed by nitrification (Chapters 4–5). Finally, under non-steady-state conditions, the diffusion of N_2O in soils can be a fractionating process if a diffusional gradient exists (Well and Flessa 2008). This is further described in Chapter 7 (Section 7.3.4).

Kinetic isotopic fractionations associated with biochemical reactions are typically larger than fractionations associated with physical processes. Isotopic discrimination occurs because of differences in the reaction rates of the heavy and light isotopes. Normally, as the reaction proceeds, the heavy isotopes accumulate in the substrate and the light isotopes accumulate in the product. The fractionation factor (α) for a unidirectional, kinetic reaction (product−substrate) is given by Equation 1.18. In the literature, kinetic fractionations are often defined as the inverse of Equation 1.18 ($R_{substrate} \div R_{product}$). Regardless of how α is calculated, it is important to clarify its definition so that readers do not erroneously interpret published results.

$$\alpha = R_{product} \div R_{substrate} \quad [1.18]$$

Fractionation can be conveniently expressed as an enrichment factor (ε) with a per mill (‰) unit, which is defined according to Equation 1.19.

$$\varepsilon = (\alpha - 1) \quad [1.19]$$

This is an instantaneous enrichment factor, which is only valid when the size of the substrate pool is considered infinitely large. When fractionation is small and the size of the substrate pool is large, the enrichment factor can be approximated by the isotopic separation (sometimes called 'del') (Δ), which is given by Equation 1.20.

$$\varepsilon \approx \Delta = \delta_{\text{product}} - \delta_{\text{substrate}} \quad [1.20]$$

For situations where the substrate is limiting Equations 1.19–1.20 do not apply. Instead, if a system is closed (with respect to the substrate), well-mixed, and the product is constantly removed, then fractionation can be modelled using a Rayleigh distillation (Equation 1.21, Mariotti *et al.* 1981). This relation describes the partitioning of isotopes among a substrate pool and a product pool, where the substrate is finite and decreasing, and f is equal to the fraction of substrate remaining.

$$R_{\text{product}} = R_{\text{substrate}} \times f^{(\alpha - 1)} \quad [1.21]$$

In practise, Equation 1.21 is often used to model systems that do not strictly satisfy the above definition because computationally the situations are very similar (Kendall 1998). For example, the denitrification of NO_3^- to N_2 in groundwater is often modelled using the Rayleigh equation despite the system being open to newly-produced NO_3^-. The size of the substrate reservoir is not infinitely large, and the instantaneous product (N_2) does not re-equilibrate with the substrate (NO_3^-).

1.4.3. *Kinetic Isotope Effects*

All biological reactions have an intrinsic isotope effect that is a result of different reaction kinetics between isotopes at the molecular level (Bedard-Haughn *et al.* 2003). In most cases, the light isotope reacts faster than the heavy isotope (i.e., $k_{\text{light}} > k_{\text{heavy}}$). There are numerous kinetic isotope fractionations within the nitrogen cycle (Table 1.1) and the magnitude that is observed is often a reduced estimate of the intrinsic isotope effect. This is because the measured net isotope effect is dependent upon the size of the substrate pool, its relative turnover rate, and the number of rate-limiting steps in the reaction.

Larger fractionations are often observed in laboratory studies with cultures of single organisms because experimental conditions provide substrate concentrations that are usually

non-limiting (Table 1.1). These studies are extremely useful as they provide the first lines of evidence of what might be observed in nature. The net isotope effects measured in soil incubation studies are not always equal to those measured from culture studies because soils contain a consortium of microorganisms, and the reaction rates and isotope effects may differ from one species to the next. Additionally, soils measurements of fractionation may incorporate physical isotope effects (such as diffusion or sorption/desorption) in addition to the kinetic isotope effects.

1.5. *The Use of $\delta^{15}N$ and $\delta^{18}O$-N_2O to Apportion N_2O Sources/Pathways*

Only a brief review of others' findings is presented here. A more thorough discussion of the relevant literature is found in the introduction of each research chapter contained in this thesis. The inclusion of Table 1.1 is a noteworthy contribution to this thesis as it summarizes the vast majority of the measured ^{15}N and ^{18}O isotope effects (ε) or separations (Δ) measured for N_2O formed from denitrification and nitrification. This quick-reference table accompanies Figure 1.3, and, at a glance, can be used to look up information on specific pathways.

1.5.1. *$\delta^{15}N$-N_2O from Denitrification*

Most $\delta^{15}N$-N_2O formed by denitrification is approximately 10–45‰ lower than the $\delta^{15}N$ of the NO_3^- substrate. This wide range of estimates in Table 1.1 is probably a result of different experimental conditions across studies. For example, some researchers found an inverse exponential relationship between the denitrification rate and ε (Mariotti *et al.* 1982; Perez *et al.* 2006; Vieten *et al.* 2007), while others found no such relationship (Well and Flessa 2009a). Additionally, not all studies used the same methods to calculate ε. In some of the incubation studies NO_3^- was limiting whereas in others there was an abundant NO_3^- supply. Finally, the fraction of N_2O consumption in each study was not the same. The consumption of N_2O in the soil environment causes the remaining pool to become ^{15}N-enriched (ε = +2‰ to +9‰ in

soils; Table 1.1), and the magnitude of fractionation depends on whether or not the system is open/closed with respect to newly-formed N_2O substrate.

1.5.2. $\delta^{15}N$-N_2O *from Nitrification*

Some of the first evidence to indicate that N_2O from nitrifier-denitrification is highly ^{15}N-depleted was provided by Mariotti *et al.* (1981) and Yoshida (1988). Using cultures of *N. europaea* they observed large negative ^{15}N-enrichments for the oxidation of NH_4^+ to NO_2^- ($\varepsilon = -37‰$ to $-32‰$, Mariotti *et al.* 1981; $\varepsilon = -32‰$ to $-25‰$, Yoshida 1988). Yoshida (1988) also measured the ^{15}N fractionation for the reduction of NO_2^- to N_2O using the same organism, and reported an enrichment factor of about $-35‰$. Sutka *et al.* (2003, 2004) confirmed this estimate with *N. europaea* and found a similar enrichment of $-38‰$ to $-32‰$ for NO_2^- reduction.

These large ^{15}N isotope effects measured (*separately*) for the oxidation and reduction portions of nitrifier-denitrification have led some researchers to conclude that the overall ^{15}N isotope effect for N_2O produced by nitrifier-denitrification ought to be approximately $-75‰$ to $-60‰$ (e.g., Perez *et al.* 2000, 2001, 2006). This conclusion may be erroneous, however, because the separately measured isotope effects (Figure 1.3, pathways b,c + j,k) can only be summed to derive an overall ε (N_2O–NH_4^+) when NH_4^+ and NO_2^- exist as two separate, non-limiting pools of N.

It is generally agreed that the initial oxidation of NH_4^+ to NH_2OH is the rate-limiting step of nitrification (Kendall 1998; Schmidt *et al.* 2004), and therefore is the site of ^{15}N fractionation for most N-cycle processes that originate from NH_4^+ (e.g., nitrifier-derived NO_3^-, N_2O by NH_2OH oxidation). Aside from studies that have examined highly impacted environments, there is little evidence to indicate that NO_2^- persists in nature. Finally, it was explained in Section 1.3.1 that NO_3^- is the major end-product of nitrification and that N_2O comprises a small fraction of the total NH_3 that is oxidized. 'Normally' ammonia-oxidizing bacteria (AOB) produce NO_2^- and then excrete it to the extracellular environment where it is rapidly assimilated by nitrite-oxidizing bacteria (NOB) that perform the final oxidation to

NO_3^-. When N_2O is made by nitrifier-denitrifiers, it is unclear if they reduce extracellular NO_2^- (e.g., $NO_2^-{}_{\text{outside cell}} \leftrightsquigarrow NO_2^-{}_{\text{inside cell}} \rightarrow NO \rightarrow N_2O$), or if the NO_2^- is an intermediate in the redox chain whereby N compounds are shuttled from one enzyme to the next (e.g., $NH_4^+{}_{\text{outside cell}} \leftrightsquigarrow NH_4^+/NH_3{}_{\text{inside cell}} \rightarrow NH_2OH \rightarrow NO_2^- \rightarrow NO \rightarrow N_2O$). The latter hypothesis is the most plausible because N_2O production by nitrifier-denitrifiers is likely caused by environmental cues (such as O_2-limitation), and once signalled, nitrite reductase is activated and N_2O becomes the main end-product. Under this scenario, a build-up of NO_2^- is unlikely, and the ^{15}N fractionation associated with $NO_2^- \rightarrow N_2O$ is not expressed because there is quantitative conversion of NO_2^-.

Relative to the number of studies that have examined $\delta^{15}N\text{-}N_2O$ produced by denitrification in soils, very few studies have measured nitrifier-derived $\delta^{15}N\text{-}N_2O$ and fewer have reported ^{15}N isotope effects ($N_2O{-}NH_4^+$). Perez *et al.* (2006) modelled the ε of nitrifier-denitrification in tropical soils by approximating the contributions of nitrifier- and denitrifier-derived N_2O using acetylated and non-acetylated incubations. Using 'Keeling plots' ($\delta^{15}N\text{-}N_2O$ versus $[N_2O]^{-1}$) they calculate a massive isotope effect of $-112‰$ to $-102‰$. Well *et al.* (2008) conducted incubations of NH_4^+-fertilized soils and they reported Δ values of $-56‰$ to $-12‰$ for early-time differences between $\delta^{15}N\text{-}N_2O$ and $\delta^{15}N\text{-}NH_4^+$. The fertilizer applied to these soils was rapidly consumed, and the $\delta^{15}N\text{-}NH_4^+$ increased shortly after the onset of incubation giving rise to the reduced isotopic separation. Finally, studies using cultures of single organisms have found the isotope effect ($N_2O{-}NH_4^+$) to be $-47‰$ (*N. europaea*; Sutka *et al.* 2006) and $-55‰$ to $-48‰$ (methanotrophs; Mandernack *et al.* 2009). To date, there is no direct evidence that confirms $\delta^{15}N\text{-}N_2O$ produced by nitrifier-denitrification is $>60‰$ lower than $\delta^{15}N\text{-}NH_4^+$.

Only a few studies have measured the ^{15}N isotope effect for N_2O formed by NH_2OH oxidation (Figure 1.3, pathway i) because it is very difficult to measure this independently from nitrifier-denitrification (although concurrent measurements of N_2O isotopomers may provide a means to estimate this). It appears that little to no ^{15}N-fractionation occurs during $NH_2OH \rightarrow N_2O$ (Table 1.1, Sutka *et al.* 2003, 2004, 2006). One notable measurement of ε for

this pathway by *N. europaea* was large ($\varepsilon = -32‰$ to $-20‰$; Sutka *et al.* 2003, 2004), but another experiment with the same organism revealed a lower estimate ($\varepsilon = -3‰$ to $+7‰$; Sutka *et al.* 2006). This discrepancy was not addressed in Sutka *et al.* 2006.

In natural soils, NH_2OH oxidation to N_2O may not be a site of ^{15}N-fractionation because NH_2OH does not accumulate. Instead, the $\delta^{15}N$-N_2O formed by NH_2OH oxidation is likely controlled by fractionation at the rate-limiting $NH_3 \rightarrow NH_2OH$ step (Kendall 1998; Schmidt *et al.* 2004).

Given all the available evidence, the expected ^{15}N ε of nitrifier-denitrification and NH_2OH oxidation is not absolutely clear. The $\delta^{15}N$ values of N_2O produced by nitrification may not be as highly ^{15}N-depleted as some of the earlier estimates would suggest. However, the use of $\delta^{15}N$ to separate nitrifer-N_2O from denitrifier-N_2O remains promising because the available measurements of ^{15}N ε for nitrifier-denitrification are more negative than the ε values reported for denitrifier-derived N_2O (Table 1.1).

1.5.3. *$\delta^{18}O$-N_2O from Denitrification*

Oxygen isotope fractionation occurs at several points within the denitrification pathway. There is a kinetic isotope effect associated with the reduction of NO_3^- to NO_2^- because the rate of $N^{16}O^{16}O^{16}O$ reduction occurs faster than the rate of $N^{18}O^{16}O^{16}O$ reduction. This gives rise to a negative ^{18}O isotope effect whereby the residual $\delta^{18}O$-NO_3^- increases (e.g., $\varepsilon = -8‰$; Böttcher *et al.* 1990). This $^{18}O/^{16}O$ fractionation is commonly used along with $^{15}N/^{14}N$ fractionation as evidence of denitrification in the environment (such as studies of N-contaminated groundwater). Once NO_2^- is produced it is immediately shuttled to nitrite reductase (*nir*), and the NO product is shuttled to nitric oxide reductase (*nor*), and so on (Figure 1.4). If any other denitrification intermediates accumulate and are released to the extracellular environment, then this could be another site of intermolecular isotope fractionation.

Fractionation also occurs several times during denitrification as O from NO_x is removed and incorporated into H_2O. Because the rate of $N\cdots^{16}O$ bond breakage is faster than the rate of $N\cdots^{18}O$ breakage, ^{18}O accumulates in the denitrification intermediates and ^{16}O ac-

cumulates in the H_2O by-product. For every one molecule of N_2O that is formed, five N···O bonds are severed (Equation 1.22). Therefore, even with the small, negative ε associated with NO_3^- reduction (intermolecular fractionation), the $\delta^{18}O$ value of N_2O ought to be much higher than the $\delta^{18}O$-NO_3^-, and the net ^{18}O isotope effect ($N_2O - NO_3^-$) should be large and positive.

$$2NO_3^- + 10H^+ + 8e^- \rightarrow N_2O + 5H_2O \qquad [1.22]$$

Finally, $^{18}O/^{16}O$ fractionation can also occur when extracellular N_2O is taken up by denitrifiers and reduced to N_2. This process of N_2O consumption leaves the residual pool of environmental N_2O enriched in ^{18}O (ε = +5‰ to +26‰; Mandernack *et al.* 2000 and Vieten *et al.* 2007, respectively). Wahlen and Yoshinari (1985) measured an even stronger ^{18}O isotope effect with cultures of *Psuedomonas aeruginosa* (ε = +42‰).

To be clear, the reduction of the N_2O intermediate (along the reduction chain $NO_3^- \rightarrow NO_2^- \rightarrow NO \rightarrow N_2O \rightarrow N_2$) is not a fractionating process unless N_2O accumulates in the intracellular environment and some 'leaks' out (Figure 1.4). If at any point (within a single organism) a portion of the newly-produced N_2O is reduced to N_2, and a portion diffuses out of the cell, then the remaining fraction of N_2O ought to be further ^{18}O-enriched. The likelihood that a single, denitrifying organism is partially 'leaky' is unclear (Firestone and Davidson 1989).

Despite our expectations, reports of the net ^{18}O isotope effect (ε_{net}) for denitrification (N_2O—NO_3^-) in the literature vary widely from almost zero (Toyoda *et al.* 2005) to values that are highly negative (ε = −54‰ to −34‰; Menyailo and Hungate 2006) and highly positive (ε ≈ +40‰; Casciotti *et al.* 2002). Such disparate reports of the ε value may be due to variable expressions of atomic oxygen exchange (O-exchange) with H_2O, which occurs during the reductions of NO_2^- and NO in some denitrifying organisms (Table 1.2). The mechanism of exchange is poorly-understood, but it may be a result of reversible reactions of the N-reductase···O intermediate complex and H_2O (Kool *et al.* 2007). Ye *et al.* (1991) measured the

fraction of O-exchange that occurred during NO_2^- and NO reduction to N_2O, and found that it was highly variable, ranging from 4–94% during NO_2^- reduction and 4–84% during NO reduction (Table 1.2). The amount of O-exchange was not well-correlated to the type of *nir* an organism possessed (cytochrome cd_1 *nir* or copper-type *nir*).

Oxygen exchange with H_2O would lower the $\delta^{18}O$ value of the denitrification intermediates because $\delta^{18}O$-H_2O is usually several per mill lower than NO_x compounds. Large amounts of O-exchange would effectively erase the ^{18}O signal that was imparted on the NO_x compound prior to its exchange with H_2O. Whether or not O-exchange actually occurs in soils remains to be seen. Soils contain a consortium of denitrifying microorganisms, and preliminary evidence from controlled laboratory experiments suggest O-exchange is highly variable (Table 1.2). If it is a significant control of $\delta^{18}O$-N_2O in soils, however, it would help explain the enormous variation in ^{18}O ε that has been measured for denitrification in soils (Table 1.1).

1.5.4. *$\delta^{18}O$-N_2O from Nitrification*

Our current understanding of $\delta^{18}O$-N_2O produced by NH_2OH oxidation and nitrifier-denitrification is weak. There are very little in- and ex-situ data available in the published literature (Chapter 5, Figure 1.2a) and no complete, systematic interpretations of nitrification-derived $\delta^{18}O$-N_2O exist. The data that are available are thoroughly discussed in Chapter 5, which provides the first comprehensive understanding of the ^{18}O dynamics involved in the formation of $\delta^{18}O$-N_2O.

Molecular O_2 is the source of oxygen in NH_2OH (Hollocher *et al.* 1981; Andersson and Hooper 1983). Therefore, N_2O derived from NH_2OH oxidation ought to reflect the $\delta^{18}O$ of atmospheric O_2 (+23.5‰; Kroopnick and Craig 1972) and any kinetic ^{18}O fractionations associated with this formation pathway. The sources of O in NO_2^- are NH_2OH (i.e., O_2) and H_2O (Andersson and Hooper 1983). Therefore, N_2O derived by nitrifier-denitrification ought to reflect the $\delta^{18}O$-NO_2^- (an average of $\delta^{18}O$-O_2 and $\delta^{18}O$-H_2O) plus any kinetic ^{18}O fractionations associated with the oxidation and reduction portions of this pathway.

The first measurements of $^{18}O/^{16}O$ fractionation in these pathways were published within the last year and a half (Mandernack *et al.* 2009; Casciotti *et al.* 2010). Using cultures of various methanotrophs and marine chemolithoautotrophs, these authors measured the ^{18}O isotope effects for O_2 and H_2O uptake during NH_3 and NH_2OH oxidation, respectively (Table 1.1). Even more recently, Frame and Casciotti (2010) measured the net ^{18}O isotope effects for NH_2OH oxidation (almost zero) and for the reductive portion of nitrifier-denitrification (NO_2^- $\rightarrow$ N_2O) (Table 1.1). This subject matter is thoroughly reviewed, discussed and expanded upon in Chapter 5.

1.5.5. *N_2O Isotopomers: A Promising Tool to Track N_2O Production and Consumption*

Many recent investigations of N_2O isotope biogeochemistry have included N isotopomer measurements in conjunction with the traditional isotopologues ($\delta^{15}N_{bulk}$, $\delta^{18}O$). Isotopomeric N_2O measurements were not conducted in this thesis. As such, only a brief review of this technique and its potential to aid N_2O source apportionment is provided here. More information about this technique can be found in the references cited below.

Measurement of the intra-molecular distribution of ^{15}N in the linear N_2O molecule ($N^{\beta}=N^{\alpha}=O$) was first introduced by Toyoda and Yoshida (1999) and Yoshida and Toyoda (2000). This technique relies on the fragmentation of N_2O^+ to NO^+ within the ion source of a mass spectrometer, which allows for the determination of $\delta^{15}N^{\alpha}$. Experimentally determined correction measures must be made to account for rearrangement of NO^+ within the ion source, and the correction differs from one IRMS to the next. The difference in the isotopic composition of the peripheral N atom (N^{β}) and the central N atom (N^{α}) is the intra-molecular site preference (SP: $\delta^{15}N^{\alpha} - \delta^{15}N^{\beta}$). Similar to $\delta^{15}N_{bulk}$ measurements, the SP can be used to identify N_2O production pathways; however, the apparent advantage of N_2O isotopomeric measurements over $\delta^{15}N_{bulk}$ is that the SP is independent of the substrate $\delta^{15}N$.

Sutka *et al.* (2006, 2008) have shown that the average SP of N_2O produced by denitrification and nitrifier-denitrification is close to 0‰, whereas the SP of N_2O produced by NH_2OH oxidation and fungal denitrification is between +33‰ and +37‰. Thus, SP can be

used to separate N_2O formed by the two known aerobic (nitrifier) pathways, but it cannot be used to distinguish N_2O produced by denitrification and nitrifier-denitrification. The consumption of N_2O increases the SP of the residual N_2O pool, and this can be used as evidence of N_2O reduction in field studies (Ostrom *et al.* 2007; Yamagishi *et al.* 2007; Well and Flessa 2009).

Frame and Casciotti (2010) showed that correlations between the $\delta^{18}O$-N_2O and SP (cross-plots) can be used in conjunction with modelling to quantify the contributions of N_2O derived from nitrifier-denitrification and NH_2OH oxidation. This is a powerful approach that may prove very useful in future studies. As we learn more about SP and $\delta^{18}O$-N_2O we may be able to combine measurements of SP, $\delta^{15}N$-N_2O, and $\delta^{18}O$-N_2O (in three dimensions) to differentiate N_2O that is produced by denitrification, nitrifier-denitrification, and NH_2OH oxidation. In many cases, the $\delta^{18}O$ of denitrifier-derived N_2O is several per mill higher than nitrifier-denitrifier-derived N_2O but the site-preferences are similar. Further, N_2O formed by nitrifier-denitrification and NH_2OH oxidation may have similar $\delta^{18}O$-N_2O values, but their site-preferences are unique.

1.6. *Thesis Outline*

Despite all the progress in our understanding of the controls of $\delta^{15}N$-N_2O and $\delta^{18}O$-N_2O produced by denitrification and nitrification pathways, many uncertainties remain. The ultimate objective of this thesis is to acquire an improved understanding of the dynamic controls of N_2O and NO_3^- isotopes in soils. This thesis places a special emphasis on gaining a better understanding of the controls of $\delta^{18}O$ values, and evaluates the usefulness of $\delta^{18}O$-N_2O to apportion different environmental N_2O sources.

This thesis contains an introductory chapter, five research chapters (Chapters 2–6), and a concluding chapter (Chapter 7). The work contained in the following chapters has already been published (Chapters 2 and 4), submitted for publication (Chapter 5), or it will be submitted to peer-reviewed journals for publication in the near-future (Chapters 3 and 6).

David M. Snider is the first-author of all the research chapters (Chapters 2–6). Dr. Sherry L. Schiff (Supervisor) and Dr. John Spoelstra (Advisory Committee Member) are co-authors of Chapters 2–6. Dr. Jason J. Venkiteswaran (Post-Doctoral Fellow) is a co-author of Chapters 3–5. His expert knowledge of MATLAB® facilitated the numerical modelling that is presented in these chapters.

Chapter 2 (Snider *et al.* 2009) was published in *Geochimica et Cosmochimica Acta*. In this chapter, experiments were conducted with temperate forest soils to quantify the ^{15}N and ^{18}O isotope effects of N_2O formed by denitrification. This is the first published study to quantify O-exchange between water and N_2O-precursors in soils and to report estimates of soil-derived $^{18}O/^{16}O$ fractionation that are not masked by the effects of O-exchange.

Chapter 3 builds upon the knowledge gained from Chapter 2, and investigates O-exchange and N_2O isotope fractionation during denitrification in agricultural soils and sediment. In addition to broadening the measured range of O-exchange and $^{18}O/^{16}O$ fractionation, this research examines the effects of soil flooding and introduces a N_2O consumption component to this thesis that was absent from Chapter 2. A mathematical approach to quantifying O-exchange and the ^{18}O-isotope effect is also evaluated in this chapter.

Chapter 4 (Snider *et al.* 2010) was published in *Environmental Science & Technology*. The research documented in this chapter utilized different ^{18}O-labelled soil waters to examine the isotope composition of microbially-derived NO_3^-. The $\delta^{18}O\text{-}NO_3^-$ data that were generated allowed us to comment on the validity of a widely-used approach to estimate the $\delta^{18}O$ value of microbial NO_3^- (the 'two-thirds, one-third rule'). It was concluded in this chapter that $\delta^{18}O\text{-}NO_3^-$ derived from nitrification cannot be successfully predicted because variable and significantly high amounts of abiotic O-exchange occur between NO_2^- and H_2O.

Chapter 5 has been submitted to *Global Change Biology*. It presents work conducted with agricultural and temperate forest soils to better understand $\delta^{18}O\text{-}N_2O$ produced by nitrification. Conceptual and mathematical models are developed, and a series of Monte Carlo simulations are done to explain experimental data obtained from aerobic soil incubations with ^{18}O-labelled water. This chapter presents the first holistic interpretation of $\delta^{18}O\text{-}N_2O$ gener-

ated by nitrifier-denitrification and NH_2OH oxidation, and concludes that N_2O formed in aerobic environments is confined to a narrow range of $\delta^{18}O$ values.

Chapter 6 describes the $\delta^{15}N$ values of N_2O and NO_3^- produced by nitrification in agricultural and temperate forest soils. For the sake of brevity, these data were not included in Chapters 4 and 5 because these chapters emphasize the $\delta^{18}O$ values of NO_3^- and N_2O, respectively. The nitrogen isotope effects (ε) and separations (Δ) of NO_3^- and N_2O produced by NH_4^+ oxidation are reported and the $^{15}N/^{14}N$ dynamics of soil nitrification are discussed.

Chapter 7 summarizes the important conclusions derived from this thesis as they relate to the use of $\delta^{15}N$ and $\delta^{18}O$-N_2O to apportion different environmental N_2O sources. The expected ranges of $\delta^{15}N$-N_2O and $\delta^{18}O$-N_2O from nitrification and denitrification are defined and related to *in situ* N_2O data. A large compilation of published and unpublished N_2O isotope data are presented in Chapter 7, which can be used in future research efforts to help explain N_2O production/consumption processes in different environments. This chapter is the first attempt to merge the theoretical, lab-based information gained from this thesis (and other's work) with the *in situ* data collected from field sites across Canada by University of Waterloo researchers.

Table 1.1. A compilation of literature estimates of nitrogen and oxygen isotope fractionation associated with processes that produce and consume N_2O. This table accompanies Figure 1.3.

Pathway(s) [Figure 1.3]	**isotope effect (ε) or separation (Δ) [product−substrate] (‰)**		**Organism(s) or Community**	**Reference**
	^{15}N	**^{18}O**		
assimilation ⇌ mineralization (ammonification)				
a	−2 to +1	n.d.	soils	Hübner 1986
nitrification and nitrifier-denitrification				
b	n.d.	−23 to −12[i]	methanotrophic bacteria	Mandernack *et al.* 2009
b,c	n.d.	−38 to −18[ii]	several '*Nitroso*' bacteria	Casciotti *et al.* 2010
b,c	−38 to −14	n.d.	several '*Nitroso*' bacteria	Casciotti *et al.* 2003
b,c	−36 to −18	n.d.	*Nitrosomonas europaea*	Delwiche & Steyn 1970
b,c	−37 to −32	n.d.	*N. europaea*	Mariotti *et al.* 1981
b,c	−32 to −25	n.d.	*N. europaea*	Yoshida 1988
j,k	−36 to −35	n.d.	*N. europaea*	Yoshida 1988
j,k	−38 to −32	n.d.	*N. europaea*	Sutka *et al.* 2003, 2004
j,k	−25 to −24	n.d.	*N. multiformis*	Sutka *et al.* 2006
j,k	−61 to −53	+7 to +10	*Nitrosomonas marina* C-113a	Frame & Casciotti 2010
b,c,j,k	−47	n.d.	*N. europaea*	Sutka *et al.* 2006
b,c,j,k	−55 to −48	n.d.	methanotrophic bacteria	Mandernack *et al.* 2009
b,c,j,k	−112 to −102[iii]	n.d.	soil nitrifiers	Perez *et al.* 2006
b,c,j,k	−56 to −12[iv]	n.d.	soil nitrifiers	Well et al. 2008
b,c,j,k	**−54 to −15**	**n.d.**	**soil nitrifiers**	**this study (Chapter 6)**
b,c,d	−29 to −12	n.d.	soil nitrifiers	Kendall 1998; Hübner 1986
d	+13	n.d.	*Nitrococcus mobilis*	Casciotti *et al.* 2009
d	+8 to +24	+1 to +10	several '*Nitro*' bacteria	Buchwald & Casciotti 2010
d	n.d.	−25 to −9[v]	several '*Nitro*' bacteria	Buchwald & Casciotti 2010
hydroxylamine oxidation				
b,i	n.d.	−4 to −2	*Nitrosomonas marina* C-113a	Frame & Casciotti 2010
i	−3 to 0	n.d.	*Methylococcus capsulatus*	Sutka et al. 2003, 2004
i	+4 to +8	n.d.	*Methylosinus trichosporium*	Sutka et al. 2006
i	−32 to −20	n.d.	*N. europaea*	Sutka et al. 2003, 2004
i	−3 to +7	n.d.	*N. europaea*	Sutka et al. 2006
i	−1 to +5	n.d.	*N. multiformis*	Sutka et al. 2006

[i] Mandernack *et al.* 2009 measured the ^{18}O isotope effect for O_2 uptake during NH_4^+ oxidation to N_2O by methanotrophic bacteria.

[ii] Casciotti *et al.* 2010 measured the combined ^{18}O isotope effect for the uptake of O_2 ($2NH_3 + O_2 \rightarrow 2NH_2OH$) and H_2O ($NH_2OH + H_2O \rightarrow NO_2^- + 5H^+$) during ammonium oxidation.

[iii] modelled values estimated from 'Keeling Plots' derived from $\delta^{15}N$-N_2O measurements of acetylated and non-acetylated soil incubations.

[iv] Δ values (NH_4^+−N_2O) of early-time $\delta^{15}N$-N_2O measurements from fertilized soils. The fertilizer quickly became ^{15}N-enriched as the NH_4^+ was consumed. These authors find that "$\delta^{15}N^{bulk}$ is a poor indicator of NH_4^+-induced N_2O fluxes from autotrophic nitrification in soils."

[v] Buchwald and Casciotti 2010 measured the ^{18}O isotope effect for the uptake of H_2O ($NO_2^- + H_2O \rightarrow NO_3^- + 2H^+$) during nitrite oxidation.

n.d. – not determined

Table 1.1 continued.

Pathway(s) [Figure 1.3]	isotope effect (ε) or separation (Δ) [product−substrate] (‰)		Organism(s) or Community	Reference
	^{15}N	^{18}O		
denitrification				
e,f,g	−22 to −10	+4 to +23[vi]	*Paracoccus denitrificans*	Toyoda et al. 2005
e,f,g	−33 to −24	n.d.	*P. denitrificans*	Barford et al. 1999
e,f,g	−37	n.d.	*Psuedomonas aureofaciens*	Sutka et al. 2006
e,f,g	n.d.	+40	*P. aureofaciens*	Casciotti et al. 2002
e,f,g	−13	n.d.	*Psuedomonas chlororaphis*	Sutka *et al.* 2006
e,f,g	−39 to −17	−1 to +32[vi]	*Psuedomonas fluorescens*	Toyoda *et al.* 2005
e,f,g	−37 to −33	n.d.	*P. fluorescens*	Yoshida 1984
e,f,g	−32 to −24	n.d.	soil denitrifiers	Mariotti *et al.* 1981
e,f,g	−35 to −24	n.d.	soil denitrifiers	Mariotti *et al.* 1982
e,f,g	−16	−8	soil denitrifiers	Schmidt & Voerkelius 1989
e,f,g	−27	n.d.	soil denitrifiers	Wada *et al.* 1991
e,f,g	−29 to −24	−54 to −34[vi]	soil denitrifiers	Menyailo & Hungate 2006
e,f,g	−45 to −10[iii]	n.d.	soil denitrifiers	Perez *et al.* 2006
e,f,g	−55 to −45	−11 to +8[vi]	soil denitrifiers	Well and Flessa 2009a
e,f,g	−42 to −27	n.d.	soil denitrifiers	Meijide *et al.* 2010
f,g	−37 to −9	n.d.	soil denitrifiers	Mariotti *et al.* 1982
e,f,g,h	−23 to −14	n.d.	soil denitrifiers	Blackmer & Bremner 1977
e,f,g,h	−43 to −32	n.d.	soil denitrifiers	Tilsner *et al.* 2003
e,f,g,h	**−29 to −20**	**+17 to +43**	**soil denitrifiers**	**this study (Chapter 2)**
e,f,g,h	**−31 to −7**	**+32 to +60**	**soil denitrifiers**	**this study (Chapter 3)**
N_2O consumption [final−initial, so that the remaining N_2O is ^{15}N- and ^{18}O-enriched]				
h	−27 to −1	n.d.	*Paracoccus denitrificans*	Yoshida 1984
h	−19 to −7	n.d.	*P. denitrificans*	Barford *et al.* 1999
h	n.d.	−42 to −37	*Psuedomonas aeruginosa*	Wahlen & Yoshinari 1985
h	−4	−11	*Pseudomonas stutzeri*	Ostrom *et al.* 2007
h	−7	−15	*Pseudomonas denitrificans*	Ostrom *et al.* 2007
h	−9 to −2	−25 to −5	soil denitrifiers	Ostrom *et al.* 2007
h	−4	−11	soil denitrifiers	Schmidt & Voerkelius 1989
h	−2	−5	soil denitrifiers	Mandernack *et al.* 2000
h	−10 to −6	−25 to −13	soil denitrifiers	Menyailo & Hungate 2006
h	−9	−26	soil denitrifiers	Vieten *et al.* 2007
h	−8 to −3	−20 to −9	soil denitrifiers	Jinuntuya-Nortman *et al.* 2008
h	−11 to −5	−25 to −11	soil denitrifiers	Well & Flessa 2009b
h	−13 to −11	−34 to −27	Eastern Tropical N. Pacific	Yamagishi *et al.* 2007

[iii] modelled values estimated from 'Keeling Plots' derived from δ^{15}N-N_2O measurements of acetylated and non-acetylated soil incubations.

[vi] Δ values (NO_3^-−N_2O) of δ^{18}O-N_2O measurements do not account for O-exchange with H_2O.

n.d. – not determined

Table 1.2. The % oxygen exchange measured from various denitrifying organisms during the reductions of nitrite and nitric oxide ($N^{16}O_x + H_2{}^{18}O \rightleftharpoons N^{18}O_x + H_2{}^{16}O$).

Organism	**Oxygen Exchange**		**Type of nitrite reductase (*nir*)**[1]	**Reference**
	$NO_2^- \rightarrow NO$	**$NO \rightarrow N_2O$**		
Achromobacter cycloclastes	4% ± 2	30% ± 7	copper-type *nir*	Ye et al. (1991)
Alcaligenes entrophus	94% ± 5	84% ± 6		
Rhodopseudomonas sphaeroides	90% ± 15	61% ± 19		
Pseudomonas aureofaciens	6%	37% ± 14		
P. aureofaciens	under 10%, frequently less than 3%			Casciotti et al. (2002)[2]
Corynebacterium nephridii	30%			
Pseudomonas chloraphis	61–78%		cytochrome cd_1 *nir*	
Pseudomonas stutzeri	5%			Shearer and Kohl (1988)[2]
P. stutzeri	58% ± 14	4% ± 1		Ye et al. (1991)
Pseudomonas aeruginosa	76% ±6	19%		
Pseudomonas fluorescens	39% ± 1	15% ± 1		
Paracoccus denitrificans	59% ± 5	11% ± 1		

[1] As described in Ye *et al.* (1991, 1993)

[2] An overall estimate of O-exchange for NO_2^- reduction to N_2O was measured.

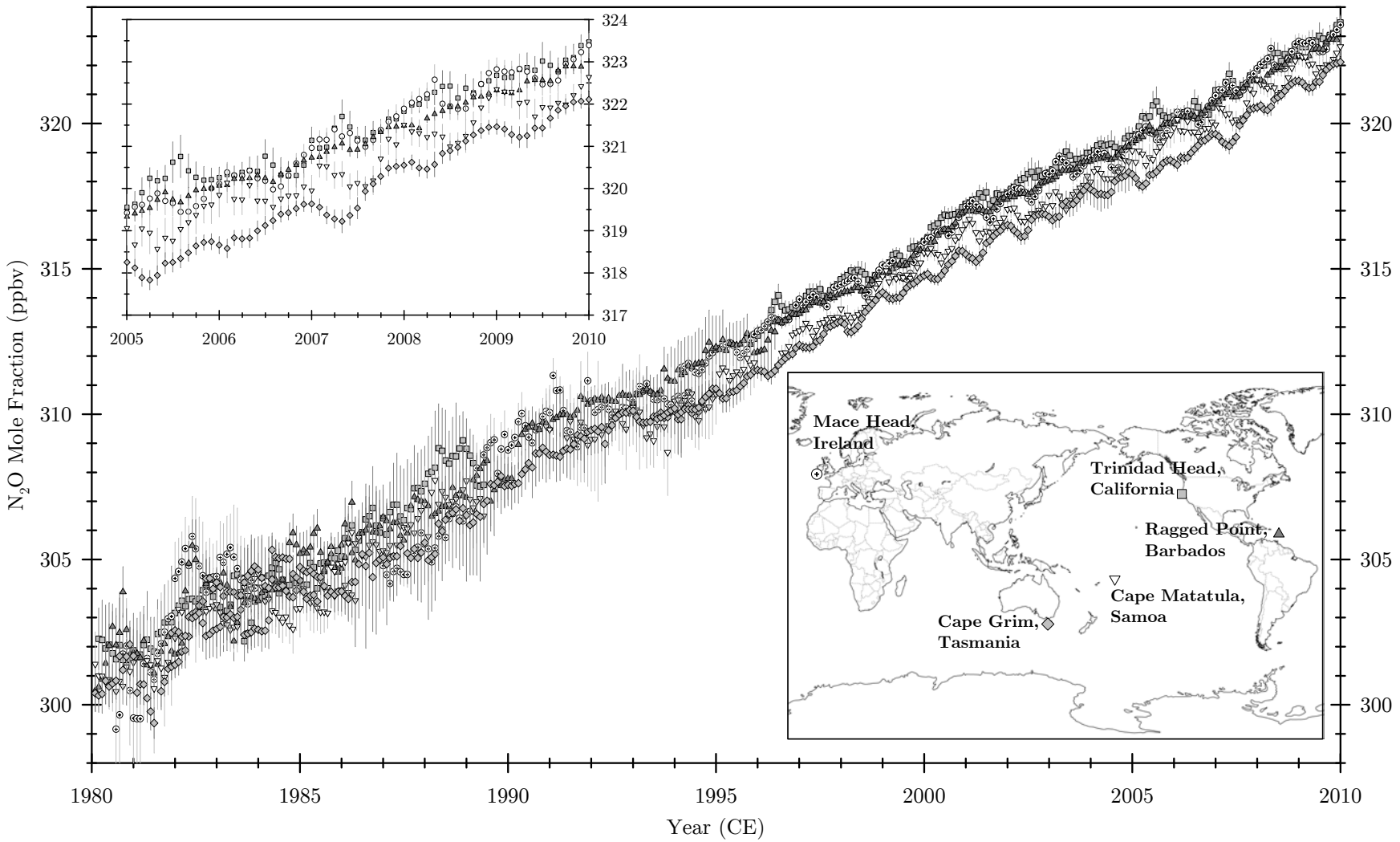


Figure 1.1. A recent, 30-year record of the mean ($\pm$ 1σ) monthly concentrations of tropospheric N_2O at five locations throughout the northern and southern hemispheres. Data is provided courtesy of the ALE/GAGE/AGAGE global network program (see Prinn *et al.* 1990, 2000 for further details). Linear trendlines through the data of each sampling location show that since 1980, the tropospheric N_2O concentration has increased at a rate of 0.70–0.75 ppbv/year ($r^2 = 0.978$–0.996). The top-left inset (years 2005–2010) demonstrates the high resolution of the data and the annual, temporal variation in N_2O concentrations. The bottom-right inset shows the global location of each sampling site.

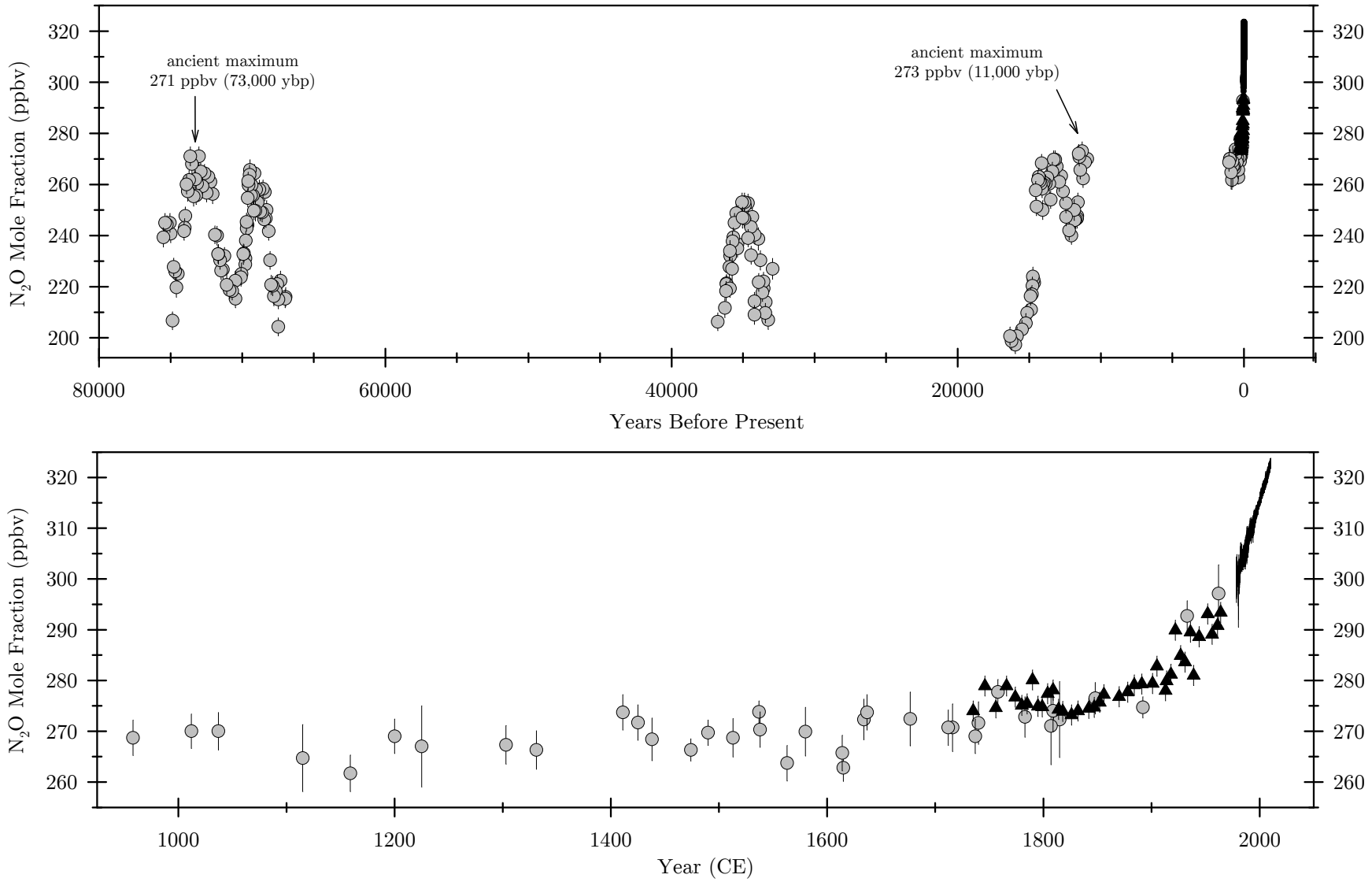


Figure 1.2. The tropospheric concentrations of N_2O from the late Quaternary Period (top) and the last Millennium (bottom) inferred from polar ice cores. Data is provided courtesy of Flückiger *et al.* 1999a, 1999b, 2004a, 2004b [grey circles] and Machida *et al.* 1995 [black triangles]. Recent data from the ALE/GAGE/AGAGE global network program (Prinn *et al.* 1990, 2000) is also shown.

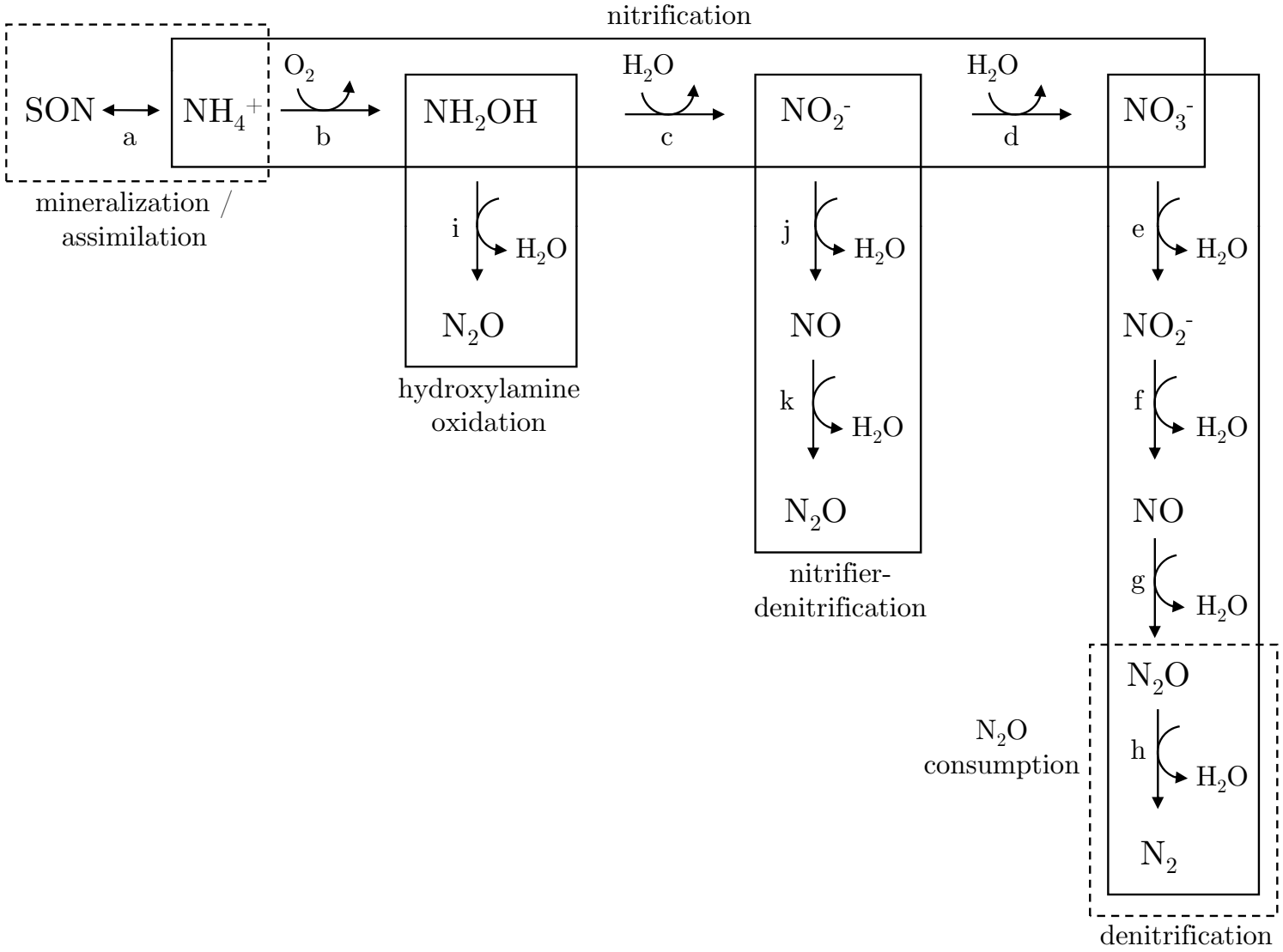


Figure 1.3. The biogeochemical reaction pathways that produce and consume N_2O. The ^{15}N and ^{18}O isotope effects (ε) or separations (Δ) reported for each step (denoted by letters a–k) are listed in Table 1.1.

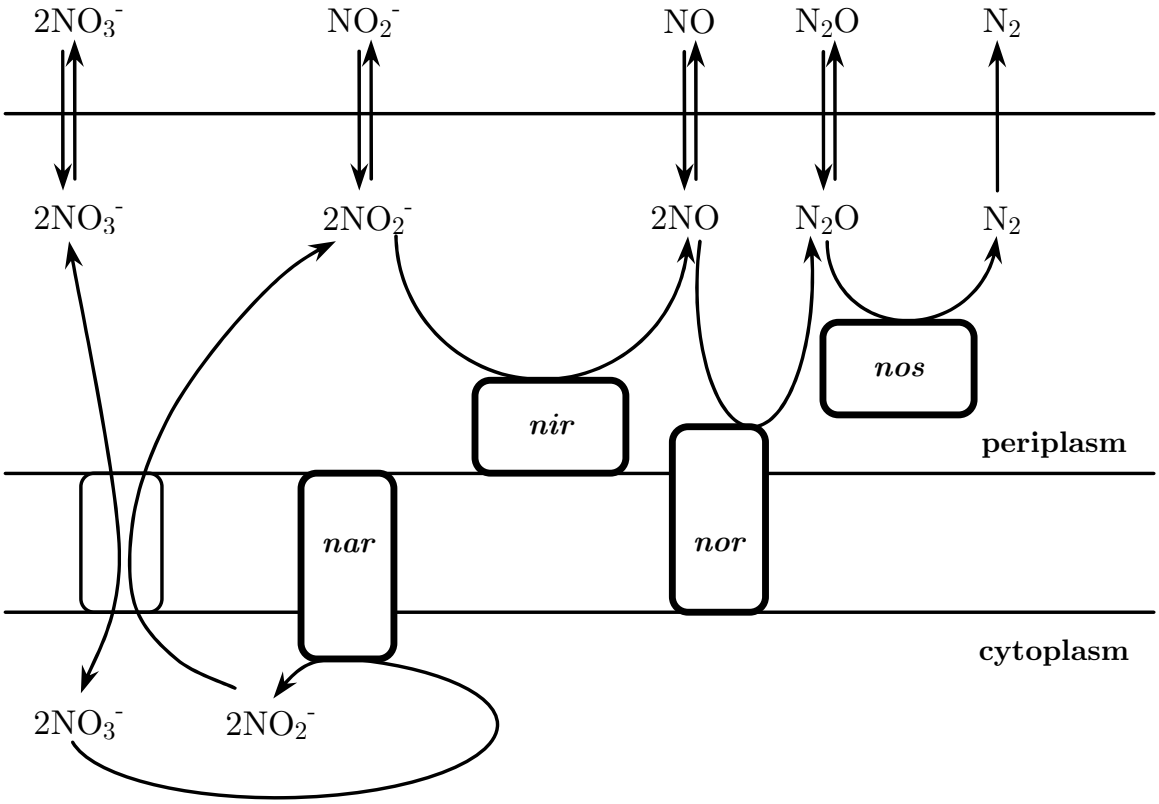


Figure 1.4. The denitrification pathway and the location of enzymes in Gram-negative bacteria [nitrate reductase (*nar*); nitrite reductase (*nir*); nitric oxide reductase (*nor*); nitrous oxide reductase (*nos*)]. [Modified after Averill (1996)].

Reproduced with permission from:

Snider DM, Schiff SL, Spoelstra J (2009) $^{15}N/^{14}N$ and $^{18}O/^{16}O$ stable isotope ratios of nitrous oxide produced during denitrification in temperate forest soils. *Geochimica et Cosmochimica Acta*, **73(4)**, 877–888. doi:10.1016/j.gca.2008.11.004

© 2008 Elsevier Ltd.

2 $^{15}N/^{14}N$ and $^{18}O/^{16}O$ stable isotope ratios of nitrous oxide produced during denitrification in temperate forest soils

Overview

Anaerobic incubations of upland and wetland temperate forest soils from the same watershed were conducted under different moisture and temperature conditions. Rates of nitrous oxide (N_2O) production by denitrification of nitrate (NO_3^-) and the stable isotopic composition of the N_2O ($\delta^{15}N$, $\delta^{18}O$) were measured. In all soils, N_2O production increased with elevated temperature and soil moisture. At each temperature and moisture level, the rate of N_2O production in the wetland soil was greater than in the upland soil. The ^{15}N isotope effect ($\varepsilon_{product-substrate}$) ranged from $-29‰$ to $-20‰$. These results are consistent with other published estimates of ^{15}N fractionation from both single species culture experiments and soil incubation studies from different ecosystems.

A series of incubations were conducted with ^{18}O-enriched water (H_2O) to determine if significant oxygen exchange (O-exchange) occurred between H_2O and N_2O precursors during denitrification. The exchange of H_2O-O with nitrite (NO_2^-) and/or nitric oxide (NO) oxygen has been documented in single organism culture studies but has not been demonstrated in soils prior to this study. The fraction of N_2O-O derived from H_2O-O was confined to a strikingly narrow range that differed between soil types. H_2O-O incorporation into N_2O produced from upland and wetland soils was 86–94% and 64–70%, respectively. Neither the temperature, soil moisture, nor the rate of N_2O production influenced the magnitude of O-exchange.

With the exception of one treatment, the net ^{18}O isotope effect (ε_{net}) (product-substrate) ranged from +37‰ to +43‰.

Most previous studies that have reported ^{18}O isotope effects for denitrification of NO_3^- to N_2O have failed to account for the effect of oxygen exchange with H_2O. When high amounts of O-exchange occur after fractionation during reductive O-loss, the ^{18}O-enrichment is effectively lost or diminished and $\delta^{18}O$-N_2O values will be largely dictated by $\delta^{18}O$-H_2O values and subsequent fractionation. The process and extent of O-exchange, combined with the magnitude of oxygen isotope fractionation at each reduction step, appear to be the dominant controls on the observed oxygen isotope effect. In these experiments, significant oxygen isotope fractionation was observed to occur after the majority of water O-exchange. Due to the importance of O-exchange, the net oxygen isotope effect for N_2O production in soils can only be determined using $\delta^{18}O$-H_2O addition experiments with $\delta^{18}O$-H_2O close to natural abundance.

The results of this study support the continued use of $\delta^{15}N$-N_2O analysis to fingerprint N_2O produced from the denitrification of NO_3^-. The utilization of $^{18}O/^{16}O$ ratios of N_2O to study N_2O production pathways in soil environments is complicated by oxygen exchange with water, which is not usually quantified in field studies. The oxygen isotope fractionation observed in this study was confined to a narrow range, and there was a clear difference in water O-exchange between soil types regardless of temperature, soil moisture, and N_2O production rate. This suggests that $^{18}O/^{16}O$ ratios of N_2O may be useful in characterizing the actively denitrifying microbial community.

2.1. *Introduction*

Nitrous oxide (N_2O) is a powerful greenhouse gas (GHG) with a global warming potential ~300 times stronger than carbon dioxide (CO_2) over a 100-year time period (IPCC 2007). N_2O has an atmospheric lifetime of ~114 years and accounts for ~5% of the total GHG radiative-forcing of global temperatures (Rodhe 1990). The only known stratospheric sinks of N_2O

are oxidative and photo-degradation mechanisms that are linked to the destruction of the ozone layer. The current mixing ratio in the mid-latitude northern hemisphere is 320 ppb (v/v), and this has increased in the last quarter-century at a rate of 0.25% yr^{-1} (data provided by ALE/GAGE/AGAGE investigators; see Prinn *et al.* 1990, 2000).

Soils represent approximately two-thirds of the total natural sources of N_2O, and emissions from temperate forests make up approximately one-sixth of all natural soil emissions (IPCC 2001). Enormous efforts have been made to constrain the global budget of N_2O and to enhance our ability to apportion its sources in different environments. N_2O is formed as an intermediate within nitrifier-denitrification and dissimilatory denitrification. These enzyme-mediated metabolic processes are ubiquitous in marine, freshwater, and terrestrial environments. N_2O production via hydroxylamine (NH_2OH) oxidation has also been shown to occur in laboratory cultures (Lees 1952; Otte *et al.* 1999; Sutka *et al.* 2003, 2006); however, the importance of this pathway in the natural environment is currently unknown.

Stable isotope methods have been used to differentiate nitrifier-denitrification and denitrifier-derived N_2O with varying degrees of success and certainty (e.g., Tilsner *et al.* 2003; Wrage *et al.* 2005; Perez *et al.* 2006). These non-intrusive methods exploit measurable changes (fractionations) in the stable isotopologue (^{15}N–^{14}N–^{16}O and ^{14}N–^{14}N–^{18}O) and isotopomer ($^{15}N^{\beta}$–$^{15}N^{\alpha}$–O) compositions that occur at various points along the reaction pathways (e.g., Sutka *et al.* 2003, 2006; Toyoda *et al.* 2005). Many studies have been carried out with single organism cultures in controlled laboratory environments and have provided a basis for the interpretation of field data (e.g., Yoshida 1988; Barford *et al.* 1999). These studies are extremely useful because they show the magnitude of fractionation that might occur from different phylogenetic groups of microorganisms under specific biogeochemical conditions. However, the isotope effects associated with N_2O production in real soils are currently unknown (Perez *et al.* 2006).

Isotope effects within the dissimilatory denitrification pathway are dependent upon: (a) substrate availability; (b) kinetics of bond formation and destruction; (c) relative reaction rates within the pathway; and (d) physical isotope effects (e.g., diffusion). In general, the rate

limiting step(s) will govern where isotopic fractionation occurs. If a build-up and loss of intermediate product occurs at any point within the reaction pathway, opportunities exist for the subsequent selective reduction of isotopologues. Preferential reduction of ^{14}N-NO_x results in N_2O that is depleted in ^{15}N relative to its precursor. Estimates of the N isotope effect ($\varepsilon_{product-substrate}$) for NO_3^- reduction to N_2O vary from −45 to −10‰ (Table 2.1).

Several researchers have reported isotope effects associated with N_2O consumption (Yoshida 1984; Wahlen and Yoshinari 1985; Schmidt and Voerkelius 1989; Barford *et al.* 1999; Mandernack *et al.* 2000; Ostrom *et al.* 2007; Vieten *et al.* 2007). When an extracellular supply of N_2O is available to denitrifying organisms, the uptake and reduction to N_2 increases the $\delta^{15}N$ and $\delta^{18}O$ values of the remaining external pool of N_2O by +1‰ to +27‰ and +5‰ to +42‰, respectively (Table 2.1). The magnitude of this fractionation is dependent upon the isotope effect (ε) and the fraction of substrate remaining.

Current understanding of oxygen isotope systematics during denitrification is poor compared to comprehension of nitrogen (N) isotope effects. As NO_3^-, nitrite (NO_2^-), and nitric oxide (NO) are progressively reduced, oxygen atoms are cleaved and combine with hydrogen (H^+) to form water (H_2O) molecules. Reaction kinetics energetically favour the breaking of an N–^{16}O bond. Theoretically, this should result in N_2O that is significantly enriched in ^{18}O relative to its precursors, because for every one N_2O molecule that is formed from two NO_3^- molecules, five N–O bonds are severed (Figure 2.1). There are, however, no reports of large oxygen isotope effects from laboratory or field studies. Very few published values of oxygen isotope effects exist in the literature (Table 2.1). Available data suggests that $\delta^{18}O$ values of N_2O can differ by −8‰ to approximately +40‰ compared to the $\delta^{18}O$ values of the NO_3^- from which it is produced (Schmidt and Voerkelius 1989; Casciotti *et al.* 2002).

Isotopic exchange of oxygen (O-exchange) can occur with H_2O during NO_2^- and NO reduction (Shearer and Kohl 1988; Ye *et al.* 1991; Casciotti *et al.* 2002; Kool *et al.* 2007). The amounts of O-exchange are highly variable among different organisms, ranging from ~2% to almost complete loss of the original NO_x oxygen atoms (Kool *et al.* 2007). Varying amounts of O-exchange between H_2O and NO_x species could have large implications for the use of $\delta^{18}O$-

N_2O values to apportion different sources of N_2O (e.g., nitrifier-denitrification vs. denitrification). The insertion of water-oxygen into a precursor of N_2O effectively erases or diminishes the $\delta^{18}O$ signal from the source NO_3^-. What remains unclear is whether or not O-exchange occurs appreciably in natural settings (where microbial diversity is great), or if it is restricted to laboratory cultures of single organisms.

The primary objectives of our study were to: (a) characterize the $\delta^{15}N$ and $\delta^{18}O$ values of N_2O emitted from pristine upland and wetland temperate forest soils from a single watershed under denitrifying conditions; (b) determine if significant O-exchange with water occurred; and (c) determine if temperature and soil moisture affect isotopic fractionation and O-exchange during denitrification. As the majority of the previously estimated isotope effects for denitrification of NO_3^- to N_2O have been derived from single culture experiments, this study investigates isotopic fractionation in soil environments where the microbial diversity is more representative of natural forested systems.

2.2. *Materials and Methods*

2.2.1. *Soil Collection and Processing*

Soils were collected from the Turkey Lakes Watershed (TLW; www.tlws.ca), located in Central Ontario (47°03'N, 84°25'W), Canada, approximately 50 km north of Sault Ste. Marie. The watershed has been the focus of extensive nitrogen cycling research due to high turnover rates of inorganic and organic N and unusually low N-retention (Nicolson 1988; Foster *et al.* 1989; Mitchell *et al.* 1992). The TLW forest is mixed sugar maple (*Acer Saccharum* Marsh.) and yellow birch (*Betula alleghaniensis* Britt.) with Humo-Ferric and Ferro-Humic podzol soils (Canada Soil Survey Committee, Sub-Committee on Soil Classification 1978; Cowell and Wickware 1983).

Two batches of highly humified, organic-rich, Oh-horizon (H – FAO equivalent; Oa – U.S. equivalent) soil were collected from the same plot within an upland site (hereafter referred to as *upland 2005* or *upland 2006*). In addition to upland soils, a highly decomposed

peat with significant amounts of wood debris and living root mass was collected from a forested swamp (hereafter referred to as *wetland 2006*). All soils were refrigerated at 4 °C in resealable freezer bags. Soils were spread out on covered trays within 3–12 days of collection, air-dried for 9–12 days at room temperature, homogenized, and sieved to 2 mm. Soils were then stored in resealable freezer bags in a dark cabinet at room temperature.

2.2.2. *Geochemical Characterization of Soils*

In preparation for analysis of %N, δ^{15}N-Total Nitrogen, %C, and δ^{13}C-Total Carbon, representative subsamples of each soil were freeze-dried to remove water and homogenized using a ball mill. Replicate analyses of each sample were performed on an elemental analyzer (EA) in line with a Micromass IsoChrom isotope ratio mass spectrometer (IRMS) at the Environmental Isotope Laboratory (EIL), University of Waterloo, Waterloo, ON. C:N ratios are reported on a molar basis.

Organic matter contents were measured by loss on ignition (LOI). After being oven-dried to a constant weight at 105 °C, three replicate samples of each soil (1–2 g) were placed in a muffle furnace at 550 °C for 4 hours.

Soils were extracted with 2M potassium chloride (KCl) and Nanopure deionized water (DI) (Barnstead International, Dubuque, IA) for determination of extractable NH_4^+ and NO_3^-, respectively. The extracts were analyzed for NH_4^+ by UV spectrophotometry (Berthelot reaction) and for NO_3^- by ion chromatography.

2.2.3. *Soil Moisture Content*

The gravimetric water content of each air-dried soil was determined by drying a known weight of moist soil in an oven at 105 °C until a constant weight was obtained. The water holding capacity (WHC; Equation 2.1) was determined by saturating soils with DI under a vacuum, and then gravimetrically measuring the water retained after a 24-hour drainage period.

$$\% \text{ WHC} = 100 \times [\text{mass } H_2O \text{ (g)} + \text{mass soil}_{\text{oven-dried}} \text{ (g)}] \div \text{mass soil}_{\text{field capacity}} \text{ (g)} \quad [2.1]$$

To assess the effects of soil moisture on the isotopic composition of N_2O, soils were incubated at different moisture levels (qualitatively defined as *moist* and *wet* – see Table 2.2).

2.2.4. *Preparation and Measurement of $\delta^{18}O$-H_2O of the Incubation Waters*

In each experiment, DI water was added to the air-dried soil to achieve the desired moisture content. The same water stock (30 L of Nanopure DI) was used in all incubations. A water sub-sample was analyzed for $\delta^{18}O$-H_2O by CO_2 equilibration (Epstein and Mayeda 1953) on a VG MM 903 (EIL, University of Waterloo, Waterloo, ON). The $\delta^{18}O$-H_2O value of the Nanopure DI was $-10.8‰$. Hereafter, this water will be referred to as *bulk Nanopure DI*.

In order to gain a better understanding of the oxygen isotope dynamics of N_2O, a series of experiments were conducted using ^{18}O-enriched waters. These were prepared by diluting a 1.6 atom% standard (Bio-Rad Laboratories, Hercules, CA) with bulk Nanopure DI. Two 850 mL ^{18}O-enriched water stock solutions were prepared with $\delta^{18}O$-H_2O values of $+118.3‰$ (hereafter denoted *level 1 water*) and $+76.2‰$ (hereafter denoted *level 2 water*).

Air-drying of soils does not remove 100% of the soil water. Depending on the rate of evaporation and the ambient humidity, the remaining soil water may become enriched in ^{18}O. Each soil contained different amounts of residual soil water after air-drying. In order to properly interpret $\delta^{18}O$-N_2O data, it was necessary to characterize the $\delta^{18}O$-H_2O of the soil water remaining in the air-dried soils (Table 2.2). Azeotropic distillation of soils with toluene (Revesz and Woods 1990) was used to extract any residual soil water that was not bound within the particle matrices of the air-dried soils. The isolated water, which is assumed to be microbially-available, was subsequently analyzed for $\delta^{18}O$-H_2O by CO_2 equilibration. Each of the three air-dried soils was submitted for analysis. In addition, wetland soil moistened with the level 1 water was analyzed to check: (a) that the overall soil water was a simple mixture of two different isotopic pools (residual soil water plus DI), and (b) that the water extracted in the toluene distillation was available to mix fully with the added water. The results of the mixed sample agreed with this simple model of pore water mixing (results not shown).

2.2.5. *Incubation Design and Protocol*

Static incubation chambers were designed using 500 mL borosilicate glass jars (Wheaton GL 45's, Wheaton Science Products, Inc., Millville, N.J.) The chambers were stoppered with halo-butyl rubber, 43 mm, 2-leg lyophilization stoppers (Wheaton Science Products Inc., Millville, N.J.) and an additional 42 mm, silicon septa (Chromatographic Specialties, Brockville, ON). The two closures were secured using an open-topped screw cap (Wheaton Science Products Inc., Millville, N.J.). Tests of the apparatus demonstrated that it was gas-tight and that none of the materials were a source of N_2O. Soils were suspended in the jars in rigid, porous sacs made from nylon screening (Morgans Screening and Filters, Ltd., Pickering, ON) that was secured to the legs of the lyophilization stoppers using stainless steel wire. The chamber design promoted homogenous mixing of gases and reduced the likelihood of significant N_2O consumption.

At the onset of incubation, a known amount of air-dry soil (17.63 g oven-dry weight [dw] equivalent) was moistened by slowly applying 80% of the required water. Jars were stoppered and flushed with ultra-high purity (UHP) helium (He) for 25 minutes at 600 mL/min to establish anoxic conditions. Jars were then pre-incubated in the dark, either in a cabinet (21–23 °C, hereafter referred to as *warm*) or in a custom-built incubation chamber (8.5–9.5 °C, hereafter referred to as *cool*). All incubations were subjected to a pre-incubation period of 5–7 days during which N_2O production was monitored and the headspace was periodically flushed with UHP He. The pre-incubation period was necessary to establish microbial populations and remove the endogenous soil NO_3^- so that it did not contribute to the overall isotopic composition of the substrate pool.

At the beginning of each experiment, upland or wetland soils were fertilized with potassium nitrate (KNO_3) (1.47 mg N/g-soil$_{dw}$, $\delta^{15}N = +13.8 \pm 0.3‰$ and $\delta^{18}O = +28.0 \pm 0.8‰$) dissolved in the remaining 20% of the water required to achieve the desired moisture level (moist or wet). Anaerobic conditions were maintained during fertilization. Following NO_3^- addition, jars were purged with He, and left for 1–2 hours for NO_3^- reduction to occur. After 1–2 hours, each replicate jar was analyzed for N_2O concentration and then immediately

sub-sampled for isotopic analysis of N_2O ($\delta^{15}N$ and $\delta^{18}O$). Isotope samples were stored in evacuated (10^{-1} torr) serum bottles (Wheaton Science Products, Inc., Millville, N.J.) stoppered with 20 mm butyl-blue rubber stoppers (Bellco Glass, Inc., Vineland, NJ) and aluminum crimp seals (Chromatographic Specialties, Brockville, ON). Following sampling, the head-space of the incubation jars was purged with He, and then jars were left undisturbed until the next sampling interval.

Denitrification experiments were short (~8 hours), with the exception of the final sampling of Treatment A, which occurred after a 16-hour (overnight) incubation period. The short incubation periods minimized ^{15}N and ^{18}O-enrichment of the substrate pool (NO_3^-). Flushing with He after each sampling prevented unnecessary accumulations of N_2O in the headspace, which might have induced feedback effects on microbial activity and the isotopic composition of N_2O. With respect to $\delta^{15}N$-N_2O and N_2O production rates, each treatment was replicated 9 times (Level 1 × 3 jars; Level 2 × 3 jars; bulk Nanopure DI × 3 jars). Each jar was sampled 5 times over the course of an experiment (approximately 1.5 hours apart), and sampling was non-destructive.

A control experiment with sterilized soils was carried out to assess the degree of abiotic N_2O production. Three replicate jars (17.63 g dw upland 2005 soil, moist water level) were pre-incubated for 7 days. After fertilization (1.47 mg N/g-$soil_{dw}$), jars were placed inside a pressure cooker and were sterilized for 1 hour at 110 °C. Soils were incubated for 3 days at 21–23 °C, and headspace N_2O concentrations were monitored.

2.2.6. *N_2O Concentration and Mass Spectrometric Analysis*

The headspace concentration of N_2O was analyzed with an Electron Capture Detector (ECD) on a Varian CP 3800 greenhouse gas analyzer (Varian Canada, Inc.) A range of commercial certified standards (0.1, 1.0, 10.0, and 100.0 ppm N_2O (v/v); Matheson Tri-Gas, Inc.; Praxair Canada, Inc.) were injected daily to calibrate the sample data. The lower detection limit for N_2O analysis was 100 ppb, well below concentrations measured during the incubations.

Analyses of δ^{15}N-N_2O and δ^{18}O-N_2O were conducted on a continuous flow-isotope ratio mass spectrometer (CF-IRMS) in-line with a TraceGas pre-concentrator system (GV instruments, Thermo Electron Corp., Manchester, UK). Samples (and working standards) were injected through a septum port, and they passed through magnesium perchlorate, Ascarite, and a Nafion membrane (Perma Pure LLC, Toms River, NJ) to remove CO_2 and moisture. N_2O was concentrated and cryo-focused in liquid N_2 before passing through a PoroPLOT Q, 30m GC column to separate residual CO_2 from N_2O. N_2O subsequently passed on to the ion source where m/z 44: $^{14}N^{14}N^{16}O$; m/z 45: $^{15}N^{14}N^{16}O$; and m/z 46: $^{14}N^{14}N^{18}O$ were compared to monitoring tanks of commercial N_2O (purity: 99.9% and 99.5%, Praxair Canada, Inc.).

In the absence of any internationally recognized reference materials for N_2O isotope ratios, our monitoring tanks and working standards were calibrated against a local source of tropospheric N_2O. Kaiser *et al.* (2003) recently characterized the isotopic composition of tropospheric N_2O with extreme precision and found little variability throughout the northern hemisphere. For calibration purposes, the local tropospheric N_2O was assigned a value of 6.72‰ (δ^{15}N) relative to (rel.) AIR and 44.62‰ (δ^{18}O) rel. VSMOW (Kaiser *et al.* 2003). The $^{15}N/^{14}N$ and $^{18}O/^{16}O$ isotope ratios of N_2O were calculated and results reported in delta (δ) notation, where R is the ratio of the heavy isotope to the light isotope (Equation 2.2).

$$\delta = (R_{sample} \div R_{standard} - 1) \times 1000‰ \quad [2.2]$$

All data is reported relative to the international standards for N [atmospheric N_2 – AIR; $^{15}N/^{14}N = 0.0036765$ (Coplen *et al.* 2002)] or O [Vienna Standard Mean Ocean Water – VSMOW; $^{18}O/^{16}O = 0.0020052$ (Coplen *et al.* 2002)]. Typical precisions (1σ) for δ^{15}N-N_2O and δ^{18}O-N_2O were 0.2‰ and 0.4‰, respectively. Analysis of one sample run in triplicate yielded precisions (1σ) of 0.16‰ and 0.09‰ for δ^{15}N-N_2O and δ^{18}O-N_2O, respectively. Repeat analysis of one sample that had been run six months prior generated precisions (1σ) of 0.02‰ (δ^{15}N) and 0.38‰ (δ^{18}O) ($n = 2$). $^{15}N/^{14}N$ and $^{18}O/^{16}O$ isotope ratios were corrected for iso-

topologues that contribute to mass 45 ($^{14}N^{14}N^{17}O$) and mass 46 ($^{14}N^{15}N^{17}O$, $^{15}N^{14}N^{17}O$, and $^{15}N^{15}N^{16}O$), followed by daily corrections for linearity and drift.

2.3. *Results*

2.3.1. *Soil Parameters*

The upland and wetland soils contained high amounts of total carbon (19.1% to 45.2%) and nitrogen (1.2% to 2.6%; Table 2.3). Although the extractable inorganic nitrogen contents of all soils were high, the NO_3^- and NH_4^+ levels in Wetland 2006 (39.6 μg NO_3^--N/g-$soil_{dw}$ and 21.8 μg NH_4^+-N/g-$soil_{dw}$) were greater than those in Upland 2005 and Upland 2006 (mean values: 18.2 μg NO_3^--N/g-$soil_{dw}$ and 13.6 μg NH_4^+-N/g-$soil_{dw}$).

2.3.2. *Net N_2O Production Rates*

N_2O production occurred in all treatments (1.5 to 38.6 nmol N_2O/hr/g-$soil_{dw}$; Table 2.4; Figure 2.2) except for the control experiment (sterilized soils), which formed a negligible amount (18 pmol) of N_2O over the entire 70-hour incubation. In most cases, the variation between treatments was larger than the variation within treatments, indicating that different environmental conditions had a measurable effect on the magnitude of N_2O production. N_2O production increased with temperature in wetland soils. Soils incubated at 21–23 °C under wet conditions (Treatments E and F) produced more N_2O than soils at the moist water level (Treatments C and D). In most treatments, N_2O production increased with time, and the largest increases occurred during the beginning of the incubations. Production rates were most constant in the final two sampling periods of each experiment (Figure 2.2).

2.3.3. *Stable Isotope Abundances of the Emitted N_2O*

All treatments exhibited relatively similar mean $\delta^{15}N$-N_2O values (−13.0‰ to −5.9‰; Figure 2.2; Table 2.4), and with the exception of Treatment A (Figure 2.2a), the variation throughout each experiment was small. At the onset of Treatment A, very little difference in $\delta^{15}N$

values was observed between the substrate NO_3^- ($\delta^{15}N = +13.8 \pm 0.3‰$) and the N_2O produced (Figure 2.2). At the end of the incubations, however, ^{15}N-depleted N_2O was produced. The mean $\delta^{15}N$-N_2O values of all treatments at the fourth and fifth samplings ranged from $-15.3‰$ to $-6.5‰$ (Figure 2.2; Table 2.4).

The $\delta^{18}O$ values of N_2O produced in incubations with three different ^{18}O-H_2O enrichments fell into three distinctly different ^{18}O ranges (Figure 2.2a–e). For all soil water ^{18}O-enrichment levels, the temporal variation of the $\delta^{18}O$-N_2O values was relatively small in all treatments and reached minimum values towards the end of each experiment.

2.4. *Discussion*

2.4.1. *The Rates of N_2O Production*

The high rates of N_2O production observed from these soils suggest that N_2O was formed by soil denitrifiers. Concurrent aerobic incubations of the same soils had N_2O formation rates that were more than two orders of magnitude lower than those observed in the current study (results to be published separately; Chapters 5–6). The control experiment with sterilized soils indicated that negligible amounts of N_2O were produced by abiotic means.

The rate of N_2O production increased as soil conditions became warmer and wetter. For example, a 7-fold increase in the N_2O production rates occurred between Treatment B (cool and moist) and Treatment F (warm and wet) (Table 2.4). Reported Q_{10} values of N_2O emissions in the literature range up to 10 or greater (e.g., Brumme 1995). Smith *et al.* (2003) explained that a simultaneous increase in the anaerobic soil fraction occurs as the temperature increases due to increased O_2 consumption via respiration. On a per unit anaerobic volume basis, the Q_{10} is approximately 2 (Smith *et al.* 2003). In this study, the soil atmosphere remained anaerobic throughout the experiment and the calculated Q_{10} value for the wetland soils was 2.3 (Treatment D vs. B). As soil moisture was increased from moist to wet at constant temperature (Treatment C vs. E and D vs. F), a 3-fold increase in the production rates

was observed in both the upland and wetland soils. N_2O production rates have been shown to increase exponentially with soil moisture (Barton *et al.* 1999).

Under the same treatment conditions (i.e., Treatments A vs. B; C vs. D; and E vs. F), the wetland soil produced more N_2O than the upland soils (on a dry soil weight basis). However, there was twice as much organic carbon in the wetland soil than in the upland soils, and on an organic carbon basis, the difference in the rate of N_2O production between soil types was less (Table 2.4). The microbial population density of the wetland soil may have been greater than the upland soils given the higher organic carbon content. If this was the case, variation in N_2O production rates between soil types need not be an effect of higher rates of individual microbial activities or different microbial consortia, but could also be due to different population densities.

2.4.2. *$\delta^{15}N$-N_2O Values and ^{15}N Isotope Effects*

A comparison of the N_2O produced from the initial sampling periods versus the later sampling periods suggests that a quasi steady state was reached towards the end of the experiments. The rate of N_2O production and the $\delta^{15}N$ and $\delta^{18}O$ values were most variable immediately following the NO_3^- application. This is most evident in the $\delta^{15}N$-N_2O of Treatment A (Figure 2.2a) and the $\delta^{18}O$-N_2O values of Treatments E and F (Figure 2.2e–f). Non-steady state behaviour of soil data is typical in incubation studies (e.g., Perez *et al.* 2006), and may be explained by disturbance effects or uneven distribution of substrate within the soil clod. As time progressed, however, N_2O production rates and isotope values tended towards steady state. Therefore, all further discussion and analysis of the datasets (e.g., isotope effects or O-exchange) will only include data from the fourth and fifth samplings of an experiment.

Overall, soil organisms were not NO_3^- limited during the course of the incubations. Post-incubation extractions of Treatment C revealed that the amount of NO_3^- reduced was less than 5% of the total NO_3^- applied at the onset of incubation. With the exception of Treatment A, the duration of the experiments was short (7 hours) to ensure only a small portion of the NO_3^- pool was consumed. Minimal substrate loss ensured that no significant

Rayleigh distillation occurred. Instantaneous ^{15}N isotope effects (ε) represent a net isotope effect for N_2O production via denitrification in temperate forest soils, and were calculated using Equations 2.3 and 2.4 (Mariotti *et al.* 1981).

$$\varepsilon = (\alpha - 1) \quad [2.3]$$

$$\text{where, } \alpha = R_{\text{15N-nitrous oxide}} \div R_{\text{15N-nitrate}} \quad [2.4]$$

Although acetylene was not used in this study to inhibit N_2O reductase, significant N_2O reduction was minimized by avoiding large accumulations of N_2O in the soil atmosphere. Incubation periods were kept short (<2 hours), the surface area of soil clods was maximized, and the headspace was completely flushed between samplings. Additionally, the large quantity of NO_3^- in the soil likely acted to suppress N_2O reduction because soil denitrifiers preferentially use NO_3^- as an electron acceptor (Firestone *et al.* 1980). If a significant reduction of the extracellular N_2O did occur in these experiments, it would have been accompanied by a concurrent increase in both the $\delta^{15}N$ and $\delta^{18}O$-N_2O values. This was not observed in our dataset (Figure 2.2).

The range of ^{15}N isotope effects observed in this study ($-29‰$ to $-20‰$; Table 2.4) is in accordance with estimates for soil denitrifiers from other ecosystems (Table 2.1). Despite differences in soil type and possible differences in the soil microbial community composition (based on O-exchange, see below), the range of ^{15}N isotope effects observed in this study was narrow. Although the rates of N_2O production among the different treatments varied by more than an order of magnitude, and soils were exposed to different temperature and moisture conditions, the maximum difference in mean $\delta^{15}N$-N_2O was only $9‰$. This further supports the use of $\delta^{15}N$ values to differentiate N_2O production pathways under field conditions, which are often spatially and temporally diverse.

2.4.3. $\delta^{18}O$-N_2O Values and Oxygen Exchange

In this study, the high level of incorporation of elevated ^{18}O indicates that most of the oxygen atoms in the N_2O were derived from soil water. In order to quantify O-exchange and net isotope effects, data was normalized to the $^{18}O/^{16}O$ ratio of the added NO_3^- (R = 0.0020613) according to Equation 2.5a–b. Normalization removes one of the two independent variables ($\delta^{18}O$-NO_3^-) so that the contribution of $\delta^{18}O$-H_2O to $\delta^{18}O$-N_2O can be easily compared. When

$$\delta^{18}O\text{-}N_2O \text{ (rel. } \delta^{18}O\text{-}NO_3^-) = R_{\text{nitrous oxide}} \div R_{\text{nitrate}} - 1 \quad [2.5a]$$

$$\delta^{18}O\text{-}H_2O \text{ (rel. } \delta^{18}O\text{-}NO_3^-) = R_{\text{water}} \div R_{\text{nitrate}} - 1 \quad [2.5b]$$

$\delta^{18}O$-H_2O (rel. $\delta^{18}O$-NO_3^-) is plotted versus the $\delta^{18}O$-N_2O (rel. $\delta^{18}O$-NO_3^-) (Figure 2.3), the slope of the linear regression line is the mean fraction of N_2O-O that originated from soil water (i.e., fraction of O-exchange), and the y-intercept is the net difference between $\delta^{18}O$-N_2O and $\delta^{18}O$-NO_3^-. In each treatment there was a strong linear relationship with the slope not equal to zero or one (Figure 2.3). This confirms that the $\delta^{18}O$-N_2O measured in this study was dictated by a combination of the $^{18}O/^{16}O$ ratio of N_2O precursors (e.g., NO_3^-), the $^{18}O/^{16}O$ ratio of soil water, and the oxygen isotope fractionation that is associated with denitrification.

The degree of O-exchange observed for the wetland soil was distinctly different from that observed for the upland soils. Treatments A, C, and E (upland soils) exhibited a narrow range of O-exchange from 87–91%, whereas O-exchange in Treatments B and D (wetland soils) was 65–70% (Table 2.4). Neither temperature nor soil moisture (and, hence, production rates) affected the large degree of exchange in either soil type. Examinations of different denitrifying bacteria have shown that O-exchange is highly variable (Kool *et al.* 2007). Interestingly, although these soils are from the same forested watershed, they exhibited very different amounts of O-exchange. This might be due to different active microbial communities present in these two soils.

2.4.4. *The net ^{18}O Isotope Effect*

The observed net oxygen isotope fractionation (ε_{net}) for denitrification is highly dependent upon: (a) the magnitude of the individual fractionating steps for N_2O production (ε_1, ε_2, and ε_3, Figure 2.1); (b) isotope effects associated with consumption of the external, residual pool of N_2O (ε_4, Figure 2.1); (c) the extent and location of O-exchange processes; and (d) isotopic fractionation associated with the incorporation of H_2O-O into NO_x (ε_{H2O}, Figure 2.1). The oxygen isotope effect (ε) for N_2O produced from NO_3^- is equivalent to the sum of the individual isotope effects (Equation 2.6).

$$\varepsilon = \varepsilon_1 + \varepsilon_2 + \varepsilon_3 + \varepsilon_4 \quad [2.6]$$

If no O-exchange occurs, ε_{net} is equal to ε (Equation 2.6) and the $\delta^{18}O$-N_2O will be significantly higher than the $\delta^{18}O$-NO_3^- because ε_1, ε_2, ε_3, and ε_4 are all greater than zero. If O-exchange does occur, ε_{net} is an integration of: (a) the isotope effect(s) that occurs before O-exchange (e.g., ε_1) and the expression of this isotope effect(s) in the $\delta^{18}O$-N_2O; (b) isotopic discrimination that occurs during the exchange of H_2O-O with NO_x-O (ε_{H2O}); and (c) isotope effects that occur after O-exchange (e.g., ε_4). When O-exchange is significant, isotope effects that occurred before the exchange are diminished and only a small fraction of the original isotope effect(s) is expressed in the N_2O. In this case, ε_{net} is predominantly comprised of an isotope effect associated with O-exchange (ε_{H2O}), which is likely a minor constituent of ε_{net}, and isotope effects that occur after O-exchange.

In this study, ε_{net} is the y-intercept of the linear regressions in Figure 2.3. Treatments B through E exhibited a very narrow range of ε_{net} (+38‰ to +43‰, Table 2.4). This is very similar to the oxygen isotope effect for denitrification with *Pseudomonas aureofaciens* (approximately +40‰), a species reported to have very low amounts of O-exchange (Casciotti *et al.* 2002). The mean ε_{net} for Treatments B–E (+40.3‰) has a remarkably narrow deviation [± 2.3‰ (1σ)], despite the significantly different ranges of O-exchange that occurred between soil types. This would indicate that significant fractionation occurred after the majority of O-exchange.

Variations in soil moisture, temperature, and N_2O production rates did not have significant effects on oxygen isotope discrimination for Treatments B–E. Only Treatment A exhibited a significantly different and smaller oxygen isotope discrimination (+17‰, Table 2.4). The amount of O-exchange in Treatment A, however, did not vary significantly from other incubations of upland soil (Treatments C and E). This suggests that the isotope effects that occurred after O-exchange in Treatment A were diminished compared to Treatments B–E.

The influence of water O-exchange on $\delta^{18}O$-N_2O values is likely not limited to temperate forest soils. The use of $\delta^{18}O$-N_2O analysis as a tool to apportion N_2O produced from the denitrification of NO_3^- may be severely limited by water O-exchange. In most field situations, the $\delta^{18}O$ of soil water will be lower than the $\delta^{18}O$ values of soil NO_3^-. The oxygen isotopic effects of the actual fractionation between NO_3^- and N_2O will be reduced or erased if significant O-exchange with H_2O occurs. The extent of O-exchange may be highly variable from one environment to another (e.g., saturated vs. unsaturated environments), and localized differences may exist within the same study site given the large differences in O-exchange reported for individual organisms (Kool *et al.* 2007). The results of this study suggest that a rigorous determination of the extent of O-exchange is required for all denitrification investigations that attempt to interpret N_2O stable oxygen isotope ratios. However, the observed range of O-exchange was very narrow and clearly different between the soil types. Additionally, the magnitude of O-exchange was unaffected by temperature, soil moisture, and production rate. This suggests that $\delta^{18}O$-N_2O values may provide a means to differentiate between active microbial consortia.

2.5. *Summary and Implications*

Anaerobic incubations of upland and wetland temperate forest soils under different moisture and temperature regimes had greater rates of N_2O production (2–59 nmol N_2O/hr/g-soil$_{dw}$) as conditions became warmer and wetter. Wetland soil exhibited consistently larger N_2O production rates (on a dry soil weight basis) compared to upland soils under the same treatment,

yet ^{15}N fractionation did not vary significantly with soil type. The overall mean ($\pm$ 1σ) ^{15}N isotope effect measured in this study for N_2O produced through the denitrification of NO_3^- was $-23.7 \pm 4.5‰$ ($n = 96$), and is consistent with other estimates reported in the literature from both soil and single organism culture incubations.

Most of the N_2O measured in these experiments contained oxygen atoms that originated from soil water. Prior to this study, the exchange of water-oxygen with NO_2^- and/or NO had only been documented in single bacterial culture studies. This is the first investigation to conclusively demonstrate that O-exchange occurs in a soil environment, where a diverse number of microbes are capable of denitrification. The large amounts of O-exchange that occurred in wetland (65–70%) and upland (87–91%) soils were surprisingly well constrained. Neither soil moisture, temperature, nor the rate of N_2O production had an effect on the magnitude of O-exchange. Different amounts of O-exchange between soil types may indicate different active microbial communities present in the soils.

This research presents the first estimates of ^{18}O fractionation for N_2O produced by soil denitrifiers that account for the important effects of O-exchange. The overall mean ($\pm$ 1σ) net oxygen isotope effect for Treatments B to E was 40.3‰ ($\pm$ 2.3‰). Oxygen fractionation was not influenced by soil type, moisture, temperature, or N_2O production rate. This estimate is consistent with the findings of Casciotti *et al.* (2002), who reported a +40‰ fractionation associated with *P. aureofaciens*.

This study provides new insights and valuable information about the dynamics of oxygen isotopes during NO_3^- metabolism. Our results warrant a rigorous examination of the systematics of oxygen isotope fractionation and exchange in other environments. If $\delta^{18}O$-N_2O values are to be successfully used to help constrain the global N_2O budget, we must gain a better understanding of O-exchange, and determine its extent in aerobic and anaerobic environments. Although O-exchange complicates the usefulness of $\delta^{18}O$-N_2O data, results of this study suggest that O-exchange may be tightly constrained for each soil and may be an important indicator of some aspect of the microbial function.

Table 2.1. Literature estimates of isotope effects for ^{15}N and ^{18}O-N_2O produced from NO_3^- and N_2O reduction.

Organism	ε or Δ (product−substrate)[a]		Reference
	^{15}N (‰)	^{18}O(‰)	
$NO_3^- \rightarrow N_2O$			
Paracoccus denitrificans	−22 to −10	+4 to +23	Toyoda *et al.* 2005
Paracoccus denitrificans	−33 to −24	nd	Barford *et al.* 1999[b]
Pseudomonas aureofaciens	−37	nd	Sutka *et al.* 2006
Pseudomonas aureofaciens	nd	~+40	Casciotti *et al.* 2002
Pseudomonas chlororaphis	−13	n.d.	Sutka *et al.* 2006
Pseudomonas fluorescens	−39 to −17	−1 to +32	Toyoda *et al.* 2005
Pseudomonas fluorescens	−37 to −33	nd	Yoshida 1984[c]
Soil denitrifiers	−45 to −10	nd	Perez *et al.* 2006
	−27	nd	Wada *et al.* 1991
	−16	−8	Schmidt and Voerkelius 1989
	−32 to −24, −11	nd	Mariotti *et al.* 1981, 1982[d]
$N_2O \rightarrow N_2$			
Paracoccus denitrificans	−19 to −7	nd	Barford *et al.* 1999[b]
Paracoccus denitrificans	−27 to −1	nd	Yoshida 1984[c]
Pseudomonas aeruginosa	nd	−42 to −37	Wahlen and Yoshinari 1985
Pseudomonas stutzeri	−4	−11	Ostrom *et al.* 2007
Pseudomonas denitrificans	−7	−15	Ostrom *et al.* 2007
Soil denitrifiers	−9 to −2	−25 to −5	Ostrom *et al.* 2007
	−9	−26	Vieten *et al.* 2007
	−2	−5	Mandernack *et al.* 2000
	−4	−11	Schmidt and Voerkelius 1989
$NO_3^- \rightarrow N_2$			
Soil denitrifiers	−35 to −19	+17 to +43	*This study*
	−38	nd	Tilsner *et al.* 2003

[a] $\varepsilon = (\alpha - 1) \times 1000$; $\varepsilon = -(1000 \times \ln\alpha)/\ln f$; where, α = Rproduct ÷ Rsubstrate, and f = fraction of substrate remaining; Δ = δproduct−δsubstrate.

[b] ranges are calculated from the reported means [± standard error, $n = 5$]: −28.6 [1.9] ($NO_3^- \rightarrow N_2O$); −12.9 [5.8] ($N_2O \rightarrow N_2$).

[c] Ph.D. thesis findings as reported and referenced in Wada and Ueda (1996).

[d] the smaller fractionation was associated with faster rates of N_2O production.

nd – not determined.

Table 2.2. Soil water content and $\delta^{18}O\text{-}N_2O$.

Condition	% Water Holding Capacity	Gravimetric Water Content (g H_2O / g-soil dw)	$\delta^{18}O\text{-}H_2O$ rel. VSMOW (‰)[a] (bulk Nanopure DI, level 2, level 1)
Upland 2005 (Treatments C and E)			
Dried storage moisture	7.3	0.15	-6.8
Moist	75.2	1.55	-10.4, 68.0, 106.0
Wet	100	2.14	-10.5, 70.3, 109.4
Upland 2006 (Treatment A)			
Dried storage moisture	22.5	0.51	2.6
Moist	68.3	1.55	-6.4, 51.9, 80.1
Wetland 2006 (Treatment B, D and F)			
Dried storage moisture	8.8	0.40	-0.9
Moist	58.6	2.67	-9.3, 64.7, 100.5
Wet	83.5	3.80	-9.7, 68.1, 105.8

[a] $\delta^{18}O\text{-}H_2O$ of the soil water corrected for the contribution of the residual water in the dried soils. Soils were moistened with bulk Nanopure DI ($\delta^{18}O\text{-}H_2O = -10.8‰$), level 2 water ($\delta^{18}O\text{-}H_2O = +76.2‰$), or level 1 water ($\delta^{18}O\text{-}H_2O = +118.3‰$), respectively.

Table 2.3. Geochemical analysis of field-collected soils.

Parameter	**Upland 2005**	**Upland 2006**	**Wetland 2006**
NH_4^+ (μg N/g-soil$_{dw}$)	10.4	16.8	21.8
NO_3^- (μg N/g-soil$_{dw}$)	17.3	19.1	39.6
Total Nitrogen (%)	1.2	1.7	2.6
δ^{15}N-Total Nitrogen (‰ rel. AIR)	5.6	7.3	2.9
Total Carbon (%)	19.1	25.4	45.2
δ^{13}C-Total Carbon (‰ rel. VPBD)	−25.8	−25.3	−26.9
C:N (mol:mol)	18.4	17.7	20.3
Loss on Ignition (%)	36.0	46.4	79.3

Table 2.4. N_2O production rates, $\delta^{15}N\text{-}N_2O$, N isotope effects, the measured oxygen exchange, and O isotope effects.

	Samplings one through five			*Samplings four and five only*				
	Mean N_2O Production Rate		**Mean $\delta^{15}N\text{-}N_2O$ (‰) [1σ, *n*]**	**Mean N_2O Production Rate (nmol N_2O/hr/g-soil dw) [1σ, *n*]**	**Mean $\delta^{15}N\text{-}N_2O$ (‰) [1σ, *n*]**	**Mean N isotope effect (ε) (‰) [1σ, *n*][a]**	**Percent $H_2{}^{18}O$ incorporation into $N_2{}^{18}O$ (%) [1σ][b]**	**Mean net O isotope effect (εnet) (‰) [1σ][b]**
	(nmol N_2O/hr/g-soil dw) [1σ, *n*]	**(nmol N_2O/hr/g-carbon) [1σ, *n*]**						
Treatment A upland, moist[c] and cool[d]	1.5 [0.5, 45]	5.9 [1.5, 45]	−5.9 [11.3, 45]	1.7 [0.5, 18]	−15.3 [6.4, 18]	−28.7 [6.3, 18]	90.2 [4.1]	+17.2 [0.4]
Treatment B wetland, moist[c] and cool[d]	5.7 [2.3, 45]	12.7 [3.8, 45]	−13.0 [2.6, 45]	7.4 [2.2, 18]	−14.0 [1.9, 18]	−27.4 [1.9, 18]	64.8 [1.1]	+42.7 [0.4]
Treatment C upland, moist[c] and warm[d]	8.8 [3.5, 45]	44.7 [8.3, 45]	−10.3 [1.8, 45]	9.7 [3.6, 18]	−9.0 [0.8, 18]	−22.5 [0.8, 18]	86.6 [0.4]	+38.4 [0.2]
Treatment D wetland, moist[c] and warm[d]	17.0 [5.6, 45]	37.7 [11.1, 45]	−8.0 [1.5, 45]	21.1 [4.6, 18]	−7.0 [0.8, 18]	−20.5 [0.8, 18]	69.8 [0.0]	+41.9 [0.2]
Treatment E upland, wet[c] and warm[d]	24.2 [9.8, 45]	122.8 [45.4, 45]	−8.0 [1.8, 45]	26.4 [7.9, 18]	−6.5 [0.9, 18]	−20.0 [0.9, 18]	91.1 [1.5]	+38.3 [1.5]
Treatment F wetland, wet[c] and warm[d]	38.6 [20.0, 15]	85.5 [45.7, 15]	−10.2 [1.8, 15]	59.1 [9.6, 6]	−8.6 [1.2, 6]	−22.1 [1.2, 6]	nd	nd

[a] $\varepsilon = (\alpha - 1) \times 1000$; where, α = Rproduct ÷ Rsubstrate, and R = $^{15}N/^{14}N$.

[b] refer to Figure 2.1, Figure 2.3, and Section 2.4.4 for an explanation of εnet.

[c] refer to Table 2.2 for the soil moisture contents of each treatment.

[d] cool (8.5–9.5 °C); warm (21–23 °C).

nd – not determined. Treatment F was not incubated with multiple waters of varying $\delta^{18}O\text{-}H_2O$.

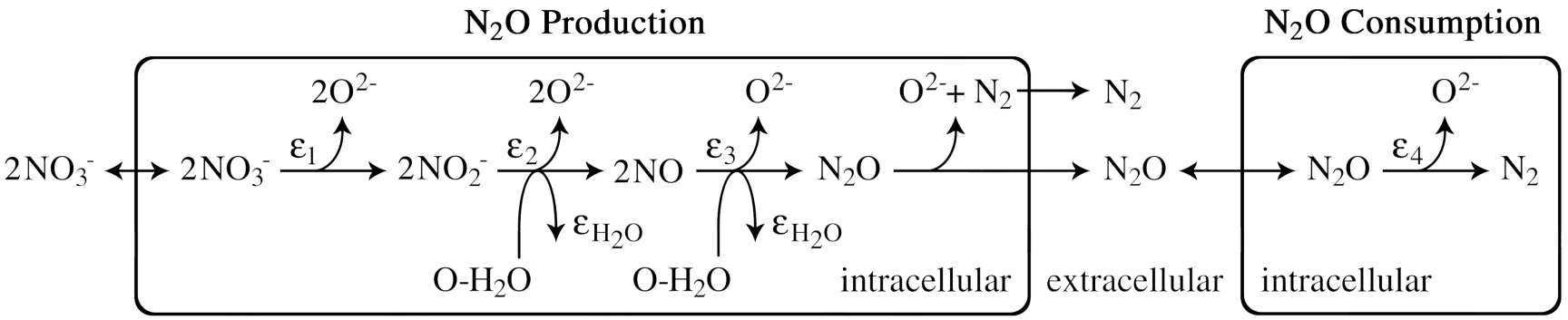


Figure 2.1. Proposed systematics of oxygen isotope enrichment (ε_1—ε_4; ε_{H2O}) and exchange during the denitrification of NO_3^- to N_2. As each N—O bond is severed there is an associated fractionation. Cumulatively, this should produce N_2O with highly enriched δ^{18}O-N_2O relative to δ^{18}O-NO_3^-. The insertion of water oxygen (O—H_2O) into N_2O precursors will effectively diminish the observed net isotope effect (ε_{net}) between N_2O and NO_3^-.

Figure 2.2a. Treatment A - upland soil, moist and cool

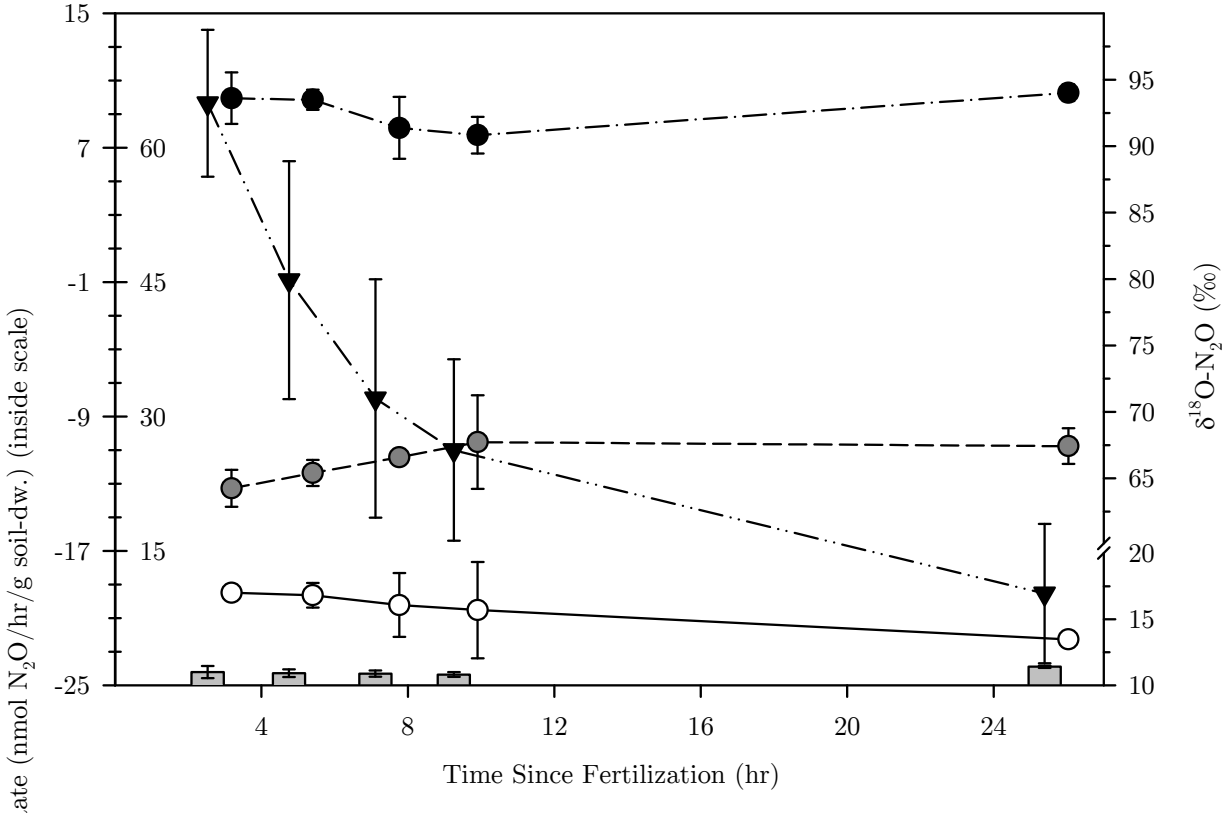


Figure 2.2b. Treatment B - wetland soil, moist and cool

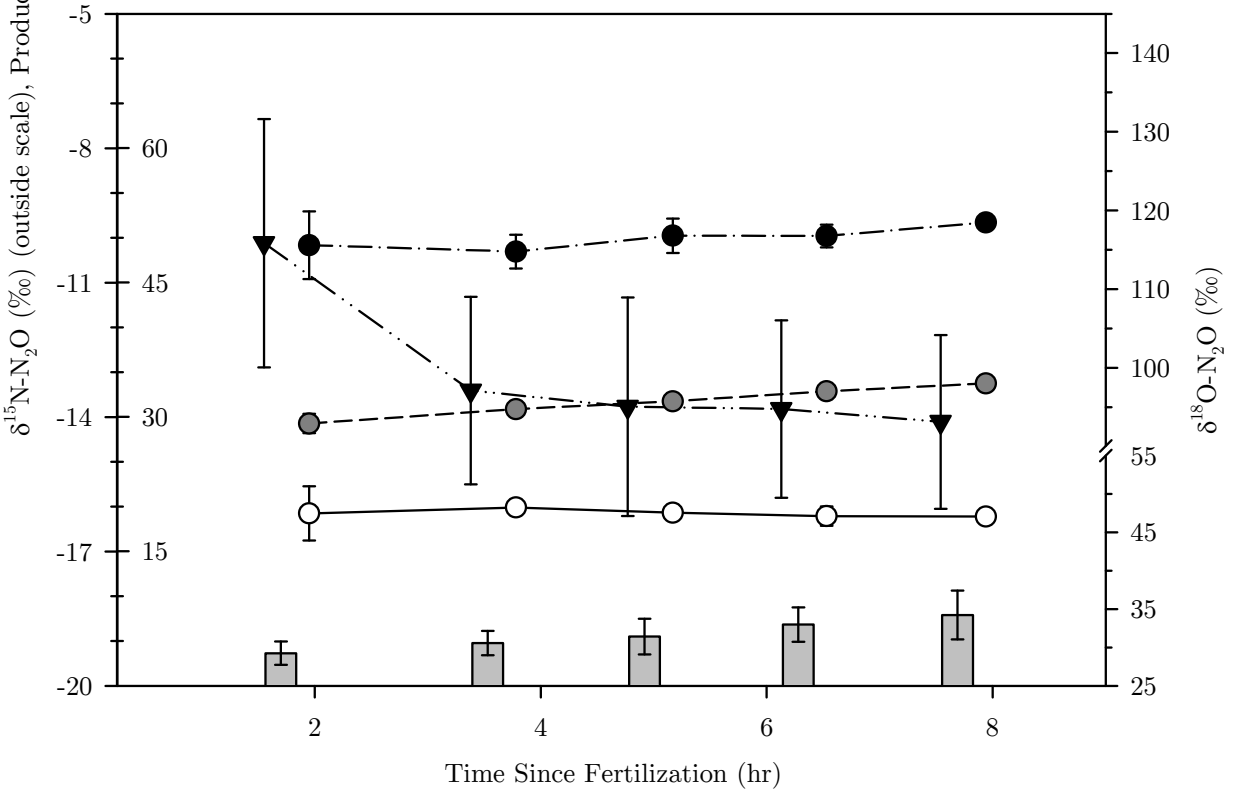


Figure 2.2c. Treatment C - upland soil, moist and warm

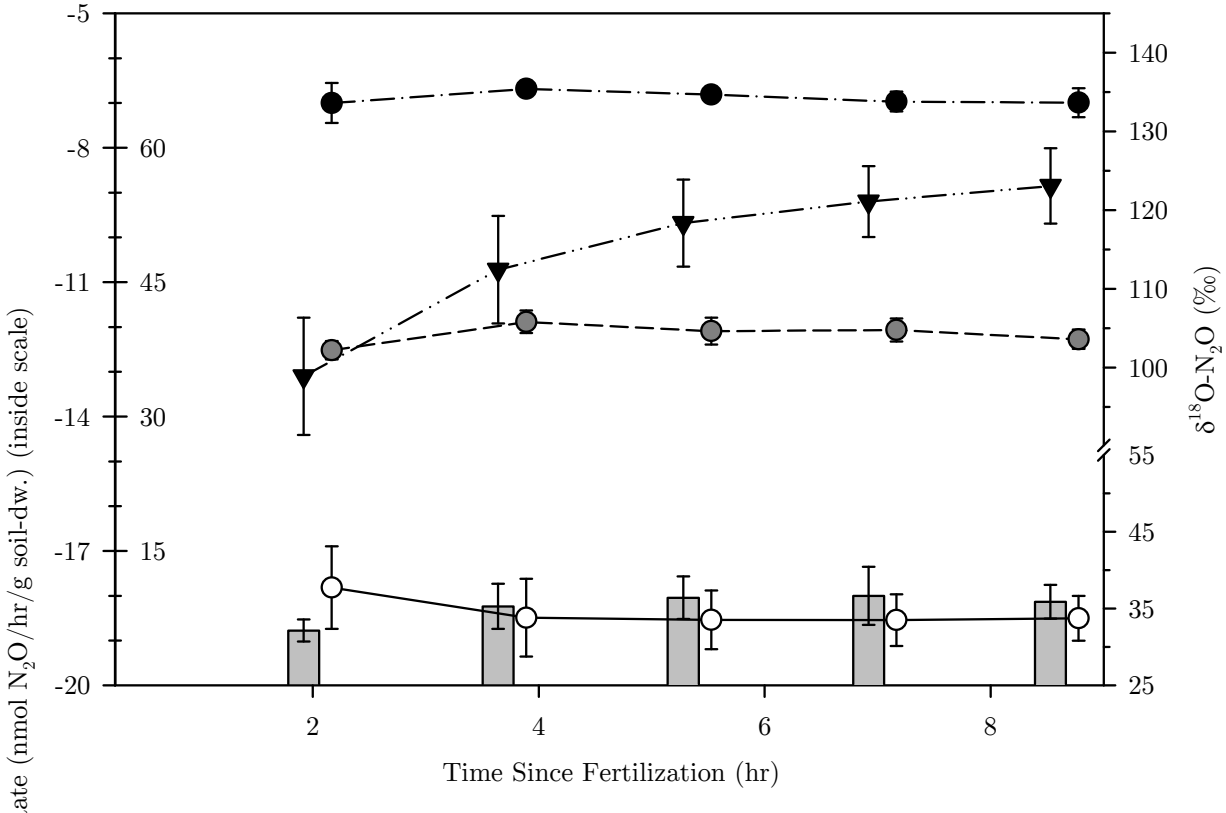


Figure 2.2d. Treatment D - wetland soil, moist and warm

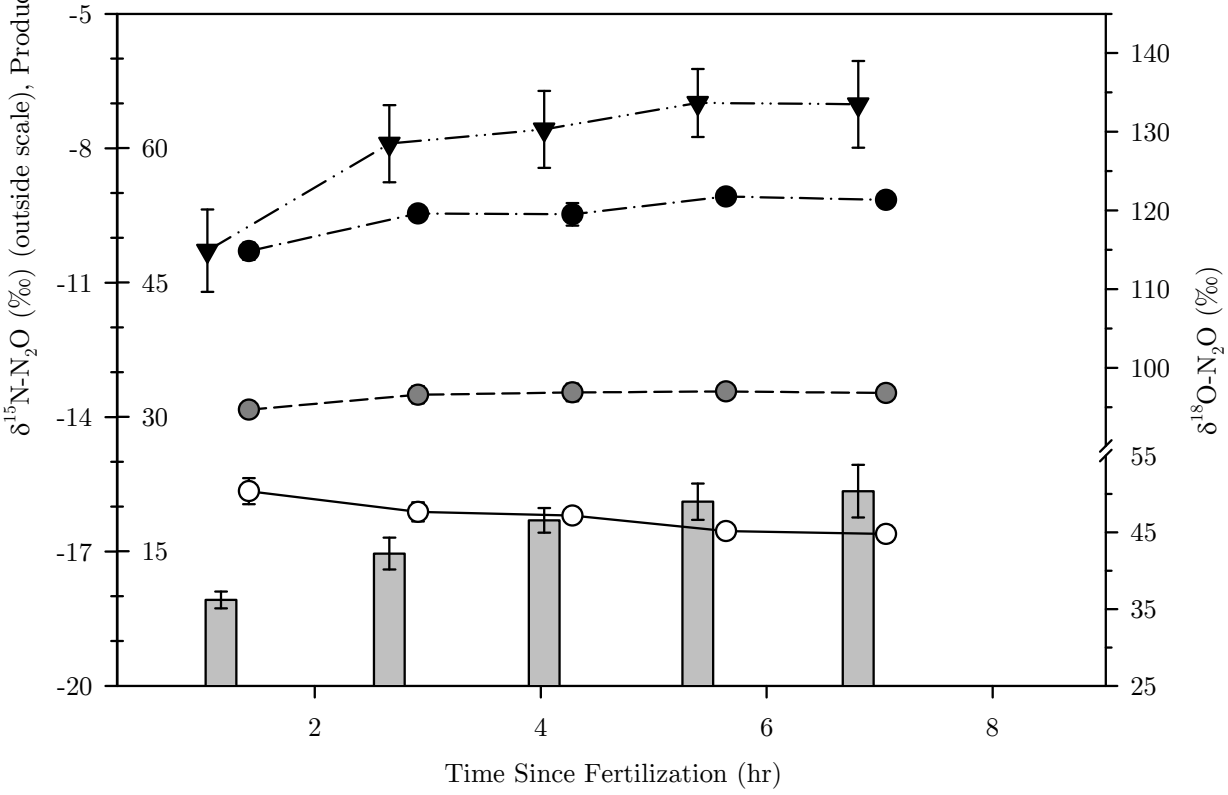


Figure 2.2e. Treatment E - upland soil, wet and warm

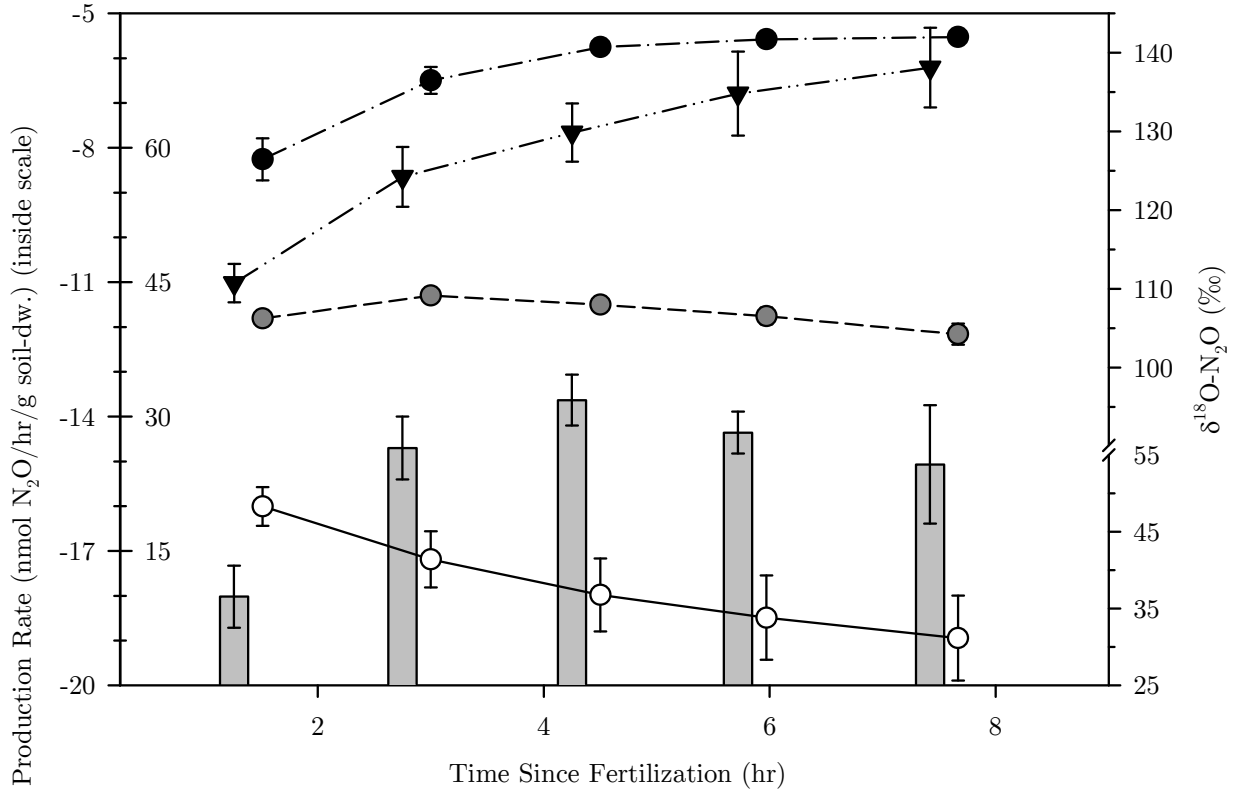


Figure 2.2f. Treatment F - wetland soil, wet and warm

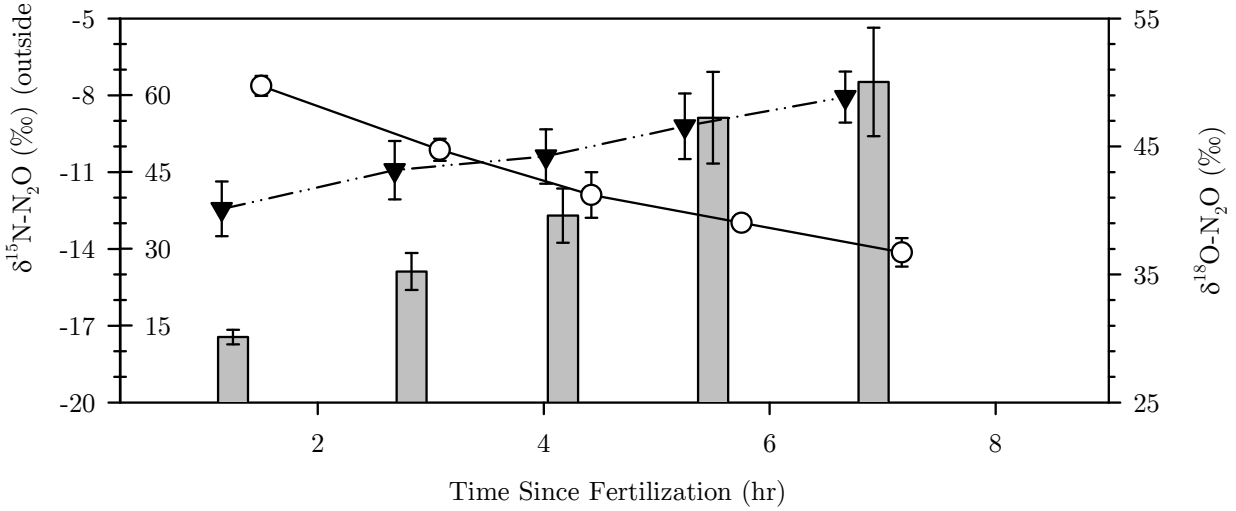


Figure 2.2a-f. N_2O production, δ^{15}N-N_2O rel. AIR, and δ^{18}O-N_2O rel. VSMOW versus time for upland and wetland soils incubated under different moisture and temperature conditions. Error bars represent 1σ from the mean, and, where they are absent, the error is smaller than the size of the symbol. Individual N_2O production rates (bar plots) and δ^{15}N-N_2O symbols (triangles) represent mean values with $n = 9$. δ^{18}O-N_2O symbols (circles) represent mean values ($n = 3$), and correspond to treatments incubated with bulk Nanopure DI (white), level 2 (grey), and level 1 (black). N.B. the axes in Fig. 2.2a and Fig. Fig. 2.2f are different (in scale and size) to those in Fig. 2.2b-e.

Figure 2.3a. Treatment A - upland soil, moist and cool

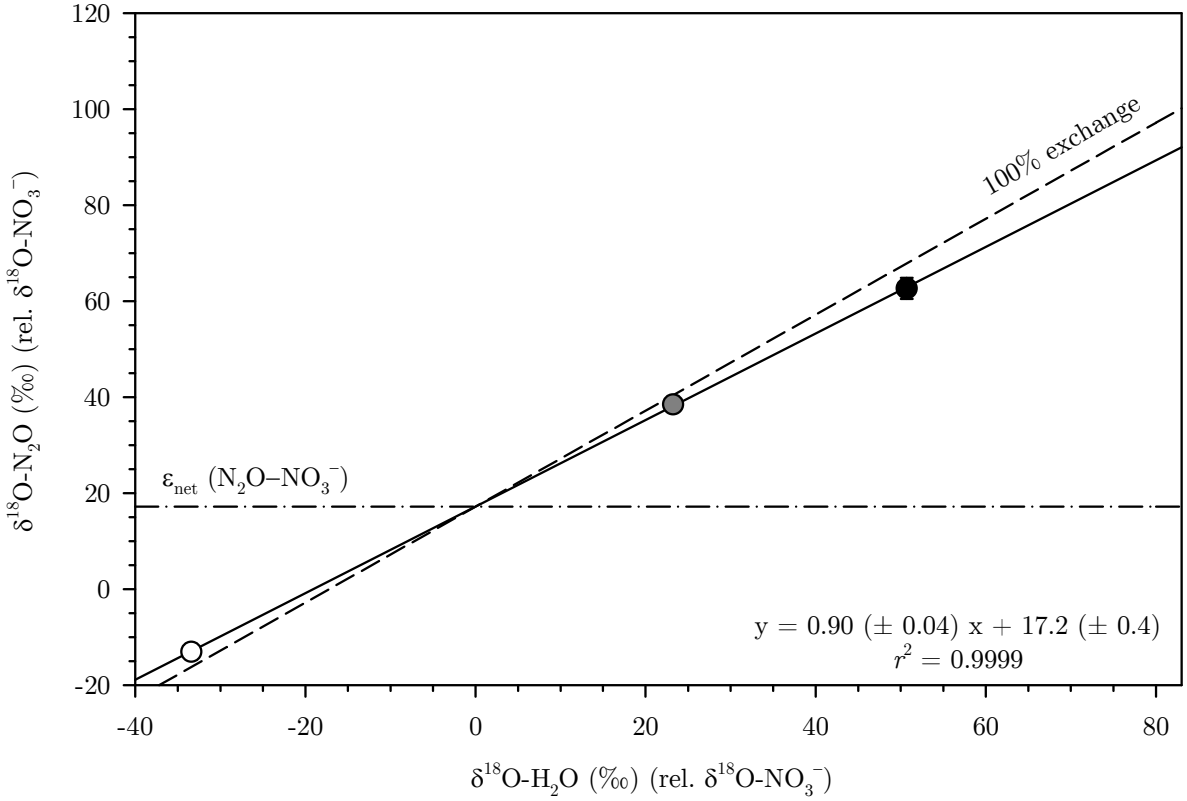


Figure 2.3b. Treatment B - wetland soil, moist and cool

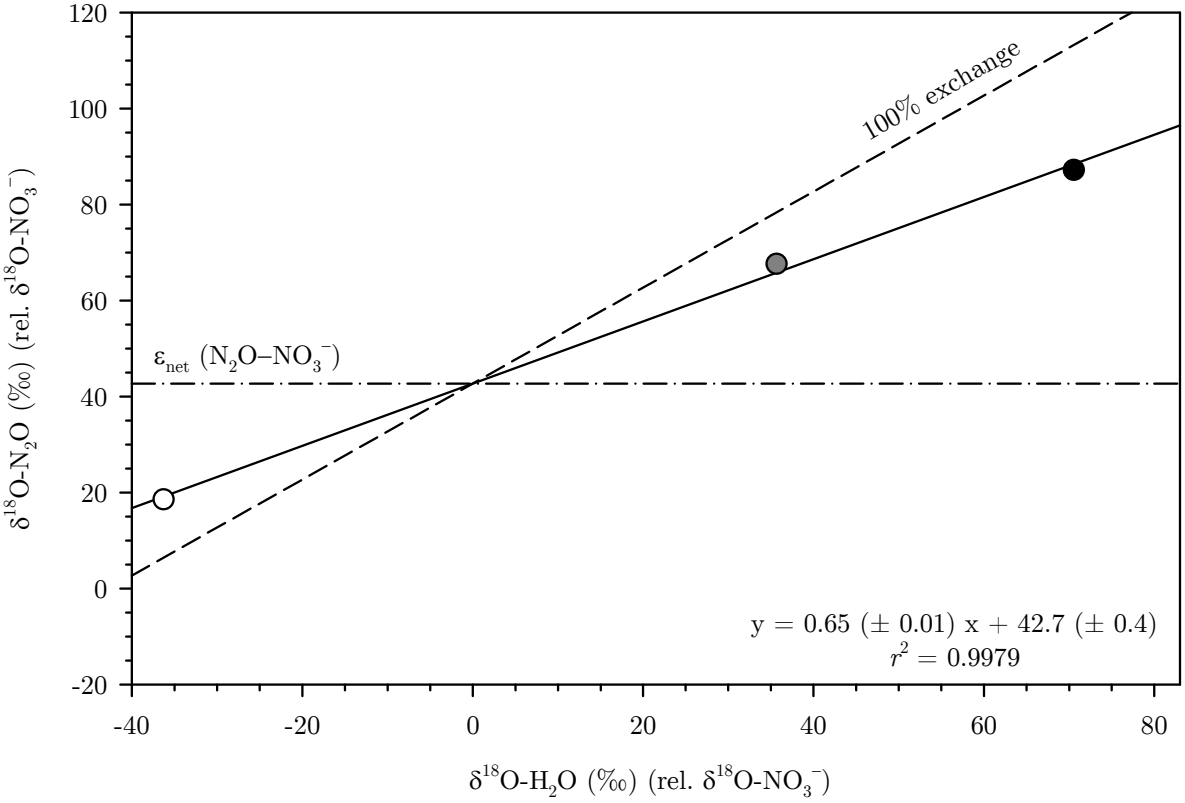


Figure 2.3c. Treatment C - upland soil, moist and warm

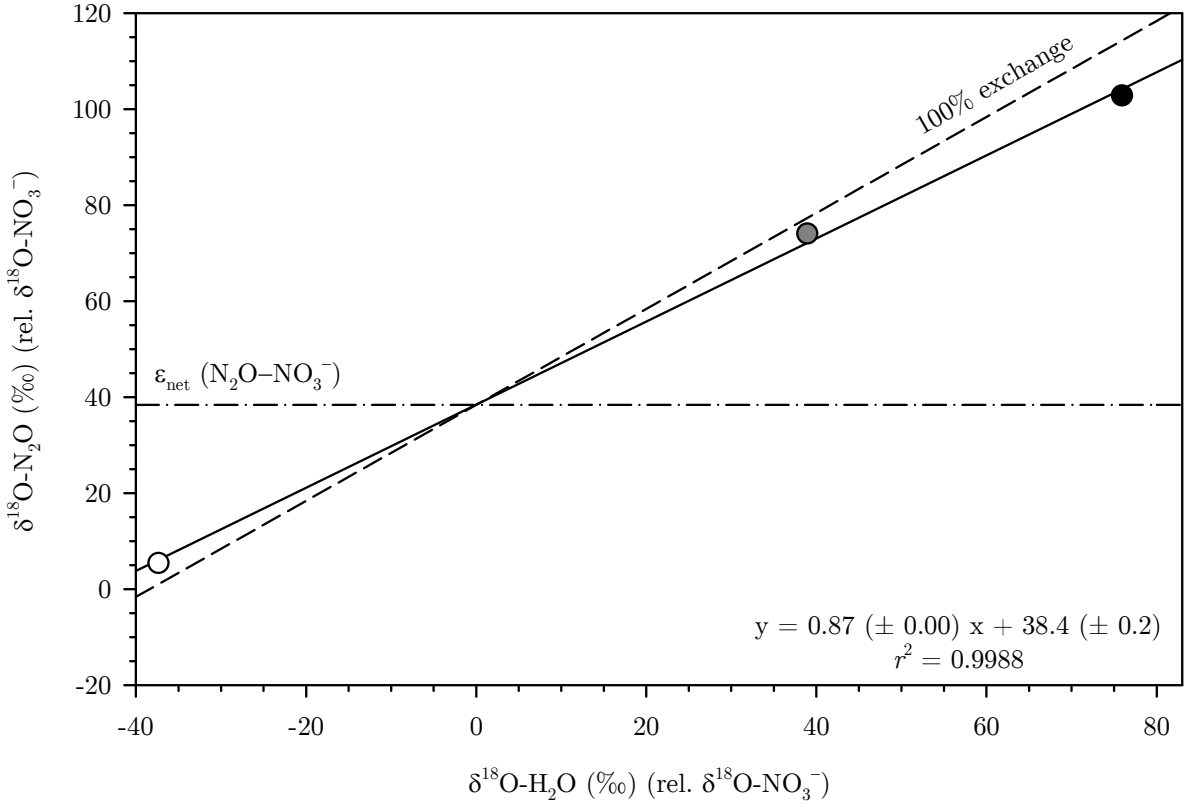


Figure 2.3d. Treatment D - wetland soil, moist and warm

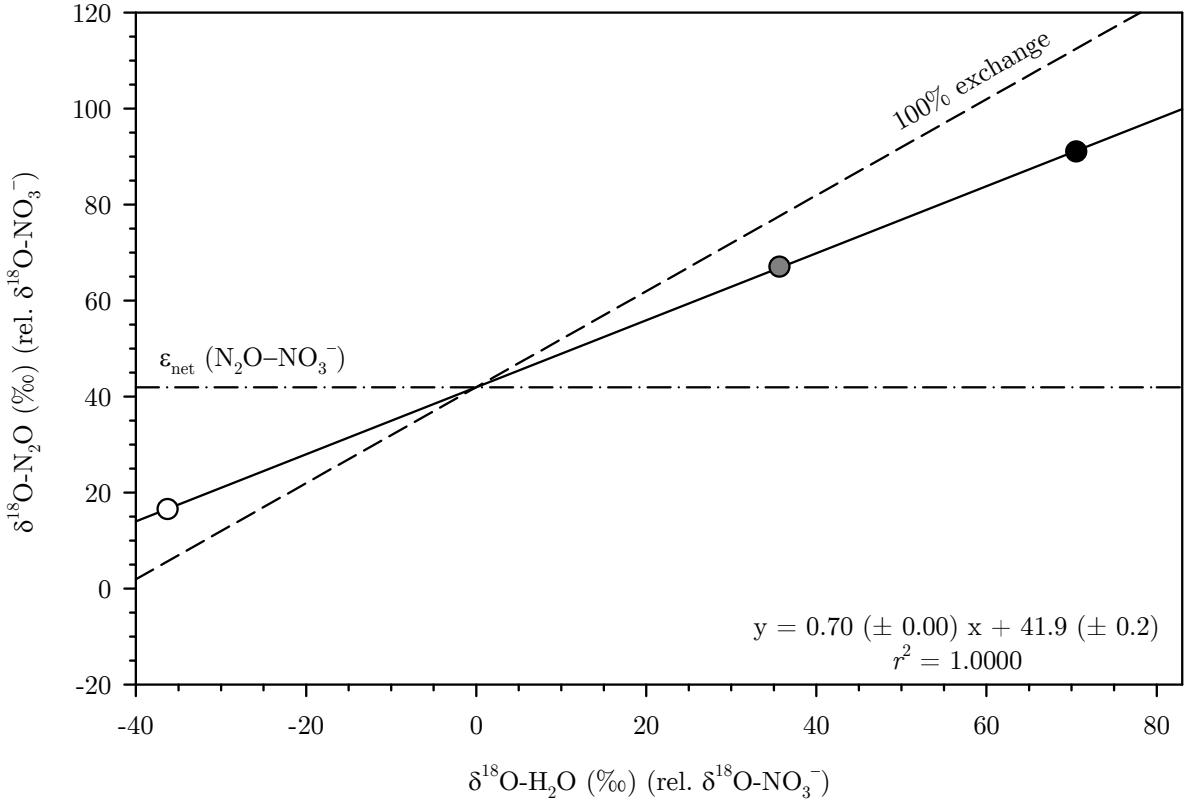


Figure 2.3e. Treatment E - upland soil, wet and warm

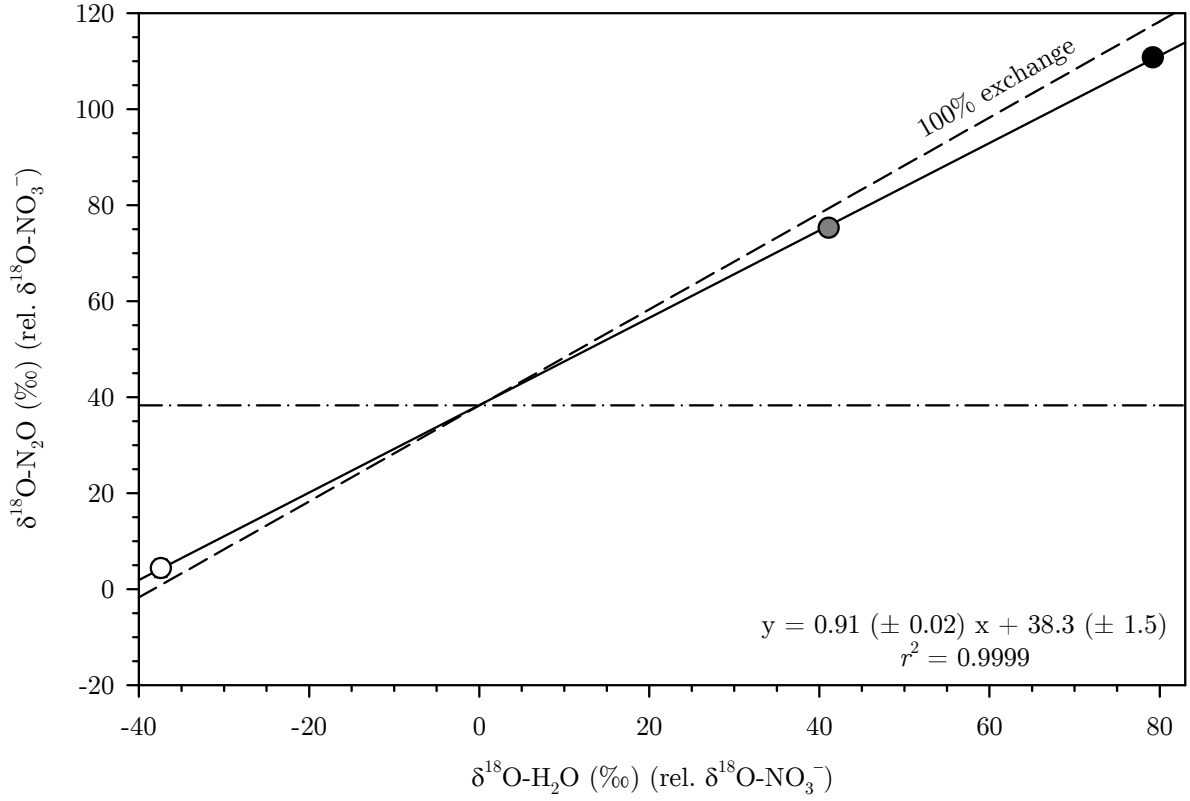


Figure 2.3a–e. The fraction of oxygen exchange between H_2O and N_2O precursors during dissimilatory reduction of NO_3^- to N_2O. The $\delta^{18}O\text{-}N_2O$ and $\delta^{18}O\text{-}H_2O$ have been normalized to the $\delta^{18}O\text{-}NO_3^-$ to facilitate comparison of different treatments. The slope of the line represents the fraction of H_2O-oxygen that was incorporated into the N_2O precursors ($\pm 1\sigma$). The y-intercept is the mean net oxygen isotope effect (ε_{net}) (N_2O–NO_3^-) ($\pm 1\sigma$). Each circle symbol represents a mean ($\pm 1\sigma$) of the $\delta^{18}O\text{-}N_2O$ measured from the fourth and fifth samplings ($n = 6$), and corresponds to incubation waters of bulk Nanopure DI (white), level 2 (grey) and level 1 (black). Many points do not have observable error bars because 1σ is less than the size of their symbol.

3 The $\delta^{15}N$ and $\delta^{18}O$ of nitrous oxide produced during denitrification in agricultural soils and stream sediment

Overview

Anaerobic incubations of agricultural soils and stream sediment were conducted with ^{18}O-labelled water to investigate the stable isotope ratios ($\delta^{15}N$ and $\delta^{18}O$) of nitrous oxide (N_2O) produced from denitrification. The rate of N_2O production and the $\delta^{15}N$ and $\delta^{18}O$ values of N_2O were measured. Oxygen exchange (O-exchange) and nitrogen and oxygen isotope effects (ε) were calculated. Soils were incubated under flooded and non-flooded conditions to assess the effects of soil moisture on the measured parameters.

The ^{15}N isotope effect for denitrification in this study varied from $-30‰$ to $-9‰$. The net ^{18}O isotope effect ranged between $+32‰$ and $+60‰$ and was negatively correlated to the total fraction of O-exchange, which varied between 0.40 and 0.94. The highest $\delta^{18}O$-N_2O values were measured in the flooded stream sediment, which had the largest net ^{18}O isotope effect and the least amount of O-exchange. The lowest $\delta^{18}O$-N_2O values were measured in a well-drained soil, which had the smallest net ^{18}O isotope effect and the greatest amount of O-exchange. The net ^{18}O isotope effect for denitrification was partially controlled by the fractions of O-exchange and N_2O reduction, which were likely influenced by the actively denitrifying microbial community and soil moisture.

Given the results of ^{15}N and ^{18}O isotopic discrimination and O-exchange determined in this study, the *in situ* $\delta^{15}N$-N_2O and $\delta^{18}O$-N_2O produced by denitrification in the agricultural soils would be isotopically different from N_2O formed in the temperate forest soils of Chapter 2 (given similar NO_3^- endmembers). This is because the ^{15}N isotope effects for denitrification in the agricultural soils were smaller than in the forested soils. Additionally, each of the agricultural soils incubated in this study would have a distinct *in situ* N_2O isotope composition. Differences in O-exchange and the net oxygen isotope effect would produce low $\delta^{18}O$-N_2O values in the well-drained (low OM) agricultural soil and higher values in the poorly-drained soil

and the stream sediment. The poorly-drained soil and the stream sediment could hypothetically be separated using $\delta^{15}N$-N_2O because the ^{15}N isotope effects in these soils differed significantly. Additionally, in most cases the isotopic composition of N_2O produced under flooded conditions would likely differ from N_2O produced in unsaturated soils or sediment.

3.1. *Introduction*

Globally, the agricultural sector has great potential to lower its climate change impact by reducing emissions of greenhouse gases (GHGs) like methane (CH_4) and nitrous oxide (N_2O). The agricultural sector contributes nearly one-third (32%) of all the anthropogenic GHG emissions worldwide (including carbon dioxide); with the energy sector (61%), and the industry and waste sectors (e.g., landfill and wastewater treatment) making up the remainder (3% each; US EPA 2006). Of these four sectors, agriculture is the leading contributor of CH_4 and N_2O, representing 52% and 84%, respectively, of the total emissions for these GHGs (yr. 2000). The vast majority of agricultural N_2O emissions originate from soil (85%), with manure management (8%) and other agriculturally-related sources (7%) accounting for the rest (US EPA 2006). Consequently, there is great interest in understanding the soil nitrogen (N) processes responsible for N_2O production so that effective policies and management practises can be implemented to successfully mitigate emissions.

N_2O is produced in soils through microbially-mediated redox reactions that occur in both impacted and pristine environments under a variety of geochemical settings. In oxygenated environments, when ammonium (NH_4^+) is oxidized to nitrate (NO_3^-) (nitrification), N_2O is an alternate end-product formed by the oxidation of hydroxylamine (NH_2OH), or by the reduction of nitrite (NO_2^-) (nitrifier-denitrification). In oxygen-depleted zones, N_2O is an obligatory intermediate compound of denitrification. There are many knowledge gaps that still need to be addressed if we are to successfully implement mitigation strategies. Our current inability to unequivocally separate nitrifier-produced N_2O from denitrifier-derived N_2O is

of paramount importance (Chen *et al.* 2008), because management strategies may affect each N_2O-producing process differently.

The stable isotope analysis of N and oxygen (O) ($\delta^{15}N$ and $\delta^{18}O$) in N_2O is a promising approach that may help constrain N_2O production pathways, because the magnitude of isotopic fractionation associated with each pathway differs. The ^{15}N isotope effect of denitrification ($\varepsilon_{\text{nitrous oxide}-\text{nitrate}} = -10‰$ to $-45‰$; Chapter 2, Table 2.1) is smaller than the ^{15}N isotope effect of nitrifier-denitrification. The latter has been measured using cultures of single organisms and estimates of $\varepsilon_{\text{nitrous oxide}-\text{ammonium}}$ range from $-47‰$ to $-55‰$ (Sutka *et al.* 2006; Mandernack *et al.* 2009). Perez *et al.* (2006) calculated much larger (negative) values of the ^{15}N isotope effect for nitrifier-denitrification in soils ($\varepsilon = -111 \pm 12‰$), however, such large ε values have not yet been corroborated by any other study. The ^{15}N ε for N_2O produced by NH_2OH oxidation is poorly constrained ($+8‰$ to $-32‰$, Sutka *et al.* 2003; 2004; 2006). These initial estimates would suggest that the $\delta^{15}N$-N_2O formed from NH_2OH oxidation may be indistinguishable from the $\delta^{15}N$-N_2O formed from denitrification if the endmembers have similar $\delta^{15}N$ values. Other parameters such as $\delta^{18}O$ values or isotopomeric nitrogen ratios ($\delta^{15}N^{\alpha}$ and $\delta^{15}N^{\beta}$) are tools that might prove useful in separating N_2O produced by these two pathways.

The use of $\delta^{18}O$-N_2O to partition N_2O sources is complicated by several O endmembers (NO_3^-, H_2O, and O_2), oxygen exchange (O-exchange) between H_2O and N_2O precursors [Chapter 2 (Snider *et al.* 2009); Chapter 4 (Snider *et al.* 2010); Chapter 5], and multiple isotope effects (ε); many of which are not measured or robustly defined. Despite this, it appears that $\delta^{18}O$ values of N_2O from NH_2OH oxidation and nitrifier-denitrification range between $+13‰$ and $+31‰$ regardless of variations in $\delta^{18}O$-H_2O, $\delta^{18}O$-O_2, isotope effects, or O-exchange.

Experiments with upland and wetland temperate forest soils (Snider *et al.* 2009) showed that $\delta^{18}O$ values of denitrifier-N_2O were largely controlled by the net ^{18}O isotope effect (^{18}O $\varepsilon_{\text{net}} = +37‰$ to $+43‰$, with the exception of one treatment ^{18}O $\varepsilon_{\text{net}} = +17‰$), and the %O-exchange with soil H_2O (upland soil, 86–94%; wetland soil, 64–70%). Given these find-

ings, the $\delta^{18}O$ value of denitrifier-derived N_2O could be as low as +30‰ (provided $\delta^{18}O$-H_2O = −10‰; $\delta^{18}O$-NO_3^- = −5‰; ^{18}O ε_{net} = +40‰). This lower boundary estimate for $\delta^{18}O$-N_2O from denitrification might decrease (even further into the range reported for nitrifier-derived N_2O) if $\delta^{18}O$-H_2O or $\delta^{18}O$-NO_3^- are more negative, or if the net ^{18}O isotope effect is smaller.

Despite this, almost all of the published $\delta^{18}O$-N_2O data reported to be produced by denitrification in soils is higher than +30‰ and ranges between approximately +35‰ and +45‰ (e.g., Toyoda *et al.* 2005, 2009; Opdyke *et al.* 2009; Ostrom *et al.* 2010). Denitrifier-produced N_2O in saturated environments (e.g., oceans, rivers, groundwaters) is even more enriched in ^{18}O with $\delta^{18}O$ values that typically range between +45‰ and +55‰ (e.g., Boontanon *et al.* 2000; Ostrom *et al.* 2000). Well *et al.* (2005) have even measured groundwater $\delta^{18}O$-N_2O with an astonishingly high value of +90‰. To date, there is no clear understanding why denitrifier-N_2O produced in these differing environments has distinct $\delta^{18}O$-values.

The results described in Chapter 2 (Snider *et al.* 2009) were quite striking because prior to that study reports of the ^{18}O ε for denitrification differed by ~48‰ (Chapter 1, Table 1.1) and O-exchange had never been demonstrated or quantified in soil. The objectives of this Chapter were to repeat the experiments of Chapter 2 with agricultural soils and quantify O-exchange and ^{18}O ε_{net} for denitrification in flooded soils and non-flooded soils at field capacity. The results of these experiments are compared and contrasted to those presented in Chapter 2, and robust estimates of O-exchange and ^{18}O ε_{net} in denitrifying soils are summarized. Additionally, a new (mathematical) approach to calculate these estimates is evaluated and compared to the methods developed in Chapter 2.

3.2. *Materials and Methods*

3.2.1. *Soil Collection*

Soils and stream sediment were collected in bulk from the Strawberry Creek Watershed, Maryhill, Ontario, Canada [Figure 3.1 (a–b)] on July 5, 2007. One mineral soil with low or-

ganic matter (OM) was collected from an upland site [Figure 3.1b, S2], and another mineral soil with high OM was collected from a wetter site [Figure 3.1b, R3]. At both sites, late vegetative stage corn was being grown at the time of collection. Crop residue and stones were removed from the surface and the soils were collected from the ground surface down to the top of a dense, till layer (~25 cm deep). There were no distinguishable soil-horizons present in this shallow zone of soil. This was probably a result of the historical cropping of these sites, which employed mechanical tillage practises.

In addition to the mineral soils, sediment was collected [Figure 3.1b, SS] from a reach of Strawberry Creek located near R3 and the meteorological tower. At the time of collection the creek was not flowing so the water table was below the surface of the sediment. Riparian vegetation (mostly grasses) and an upper layer of medium-textured sand (~15 cm) were removed, and the underlying sediment was collected in bulk. Both the sand and sediment layers were wet, but not saturated. The depth to the water table was not determined.

3.2.2. *Soil Processing, Geochemical Characterization and Incubation Protocols*

Detailed descriptions of the methods used to process and characterize the soils are described in Chapter 2. Any deviation from these methods or experimental protocols will be explicitly described here. Briefly, all soils were air-dried, homogenized, sieved to 2 mm, and stored in resealable freezer bags in darkness at room temperature. Total carbon (TC), total nitrogen (TN), δ^{13}C-TC, and δ^{15}N-TN were analyzed on an elemental analyzer (EA) coupled to an isotope ratio mass spectrometer (IRMS). Carbon:nitrogen ratios are reported on a molar basis for a non-acidified sample. Organic matter content (%) was quantified by loss on ignition (LOI). Soils were extracted with 2 M potassium chloride (KCl) and Nanopure deionized water (DI) (Barnstead International, Dubuque, IA) for analysis of extractable NH_4^+ and NO_3^- concentrations, respectively. Soil pH was determined in calcium chloride ($CaCl_2$) and water following ASTM methods (ASTM International 2007). A particle size analysis (% sand, % silt, % clay) was determined for each soil after oxidizing the organic matter with hydrogen peroxide (Laboratory Services, University of Guelph, Guelph, ON).

The incubation waters used in this study were prepared following methods outlined in Chapter 2. Any water remaining in the air-dried soils was extracted by azeotropic distillation, and the $\delta^{18}O$-H_2O was analyzed. The final $\delta^{18}O$ values of the soil water (after soils were moistened to their target moisture content) was calculated and the results are shown in Table 3.1.

Five separate anaerobic incubation experiments (treatments 1–5) were conducted in this study. In each treatment 22.5 grams of oven-dry soil [dry weight (dw.)] was wet up to either 100% water holding capacity (WHC) (i.e., field capacity) or flooded to 200% WHC. The flooded soils were not suspended in screening as described in Chapter 2. The well-drained, low OM soil (treatment 1) was only incubated at 100% WHC because this site does not experience flooding *in situ*. The gravimetric soil water content of each treatment was determined by drying soils overnight in an oven at 105°C. All soil waters prepared for this study were made anoxic (to minimize the introduction of O_2 into the incubations) by bubbling ultra-high purity (UHP) helium (He) through them for a short time to minimize evaporation losses. Soil water was used immediately or stored in Tedlar® gas bags for future use.

All treatments were conducted in the dark at laboratory temperature (20–22 °C). All treatments were fertilized with potassium nitrate (KNO_3) (1.47 mg N / g-soil$_{dw.}$, $\delta^{15}N = +13.8 \pm 0.3‰$ and $\delta^{18}O = +28.0 \pm 0.8‰$) after an anaerobic pre-incubation period (5 days). Anaerobiosis was maintained throughout the study by flushing incubation jars with He for 25 minutes at 600 mL/min. Flushing occurred after the onset of pre-incubation, throughout the pre-incubation period, after fertilization, and after each sampling event. The flooded soils (treatments 3 and 5) were slowly swirled on a reciprocal shaker throughout the pre-incubation and experimental periods to minimize diffusion effects and increase the rate of equilibration between the headspace and the flooded soil. To assess the amount of abiotic N_2O production, controls were performed with sterilized soils. Three replicate jars of each sterilized soil were fertilized, and the concentration of N_2O that accumulated over 5 days was monitored.

Incubations were sampled for N_2O concentration, $\delta^{15}N$-N_2O, and $\delta^{18}O$-N_2O five times (treatments 1, 2 and 4) or four times (treatments 3 and 5) over the ~8 hour experimental period. A detailed description of N_2O sample storage, and concentration and isotopic analysis is

provided in Chapter 2. Nitrogen and oxygen isotope ratios (R) of N_2O are expressed in delta (δ) notation ($R_{sample} \div R_{standard} - 1$) and reported in units of per mill (‰), where the international standards for N and O are atmospheric N_2 (AIR) and Vienna Standard Mean Ocean Water (VSMOW), respectively. Instantaneous nitrogen isotope effects (ε) are calculated as ($\alpha - 1$) and reported in ‰ units, where $\alpha = {}^{15}N/{}^{14}N$ product $\div$ ${}^{15}N/{}^{14}N$ substrate.

3.2.3. *Determination of Oxygen Isotope Exchange and Fractionation (Method I)*

Following the methods used in Chapter 2, ${}^{18}O/{}^{16}O$ ratios of N_2O and H_2O were normalized by expressing these values in delta (δ) notation relative to the ${}^{18}O/{}^{16}O$ ratio of the NO_3^- end-member (${}^{18}O/{}^{16}O$ of NO_3^- fertilizer = 0.0020613) (Equation 3.1a–b). As a result, the linear regression of $\delta^{18}O\text{-}N_2O$ $_{(rel.\ \delta^{18}O\text{-}NO_3^-)}$ vs. $\delta^{18}O\text{-}H_2O$ $_{(rel.\ \delta^{18}O\text{-}NO_3^-)}$ has a slope (m) that approximates the mean fraction of O-exchange that occurred between H_2O and N_2O precursors, and an intercept (b) that approximates the net ${}^{18}O$ isotope effect (${}^{18}O$ ε_{net}) for denitrification ($NO_3^- \rightarrow N_2$). The results of this regression analysis are shown in Table 3.1.

$$\delta^{18}O\text{-}N_2O\ (rel.\ \delta^{18}O\text{-}NO_3^-) = (R_{N_2O} \div R_{NO_3^-} - 1) \times 1000 \quad [3.1a]$$

$$\delta^{18}O\text{-}H_2O\ (rel.\ \delta^{18}O\text{-}NO_3^-) = (R_{H_2O} \div R_{NO_3^-} - 1) \times 1000 \quad [3.1b]$$

3.2.4. *Determination of Oxygen Isotope Exchange and Fractionation (Method II)*

In this study a new approach to calculate O-exchange and fractionation during denitrification is evaluated (Method II) and the results of this method are compared to those derived using Method I. Method II is similar to the approaches used in Chapter 4 and Chapter 5, and involves the step-wise reduction of NO_3^- to N_2 (Figure 3.2). This approach defines O-exchange and the net ${}^{18}O$ isotope effect as mathematical expressions (Equations 3.2–3.9).

$$\delta^{18}O\text{-}NO_2^- = \delta^{18}O\text{-}NO_3^- + \varepsilon_1 \quad [3.2]$$

$$\delta^{18}\text{O-NO} = (1 - f_{\text{exch.-}nir}) \times (\delta^{18}\text{O-NO}_2^- + \varepsilon_2) + f_{\text{exch.-}nir} \times (\delta^{18}\text{O-H}_2\text{O} + \varepsilon_5) \quad [3.3]$$

$$\delta^{18}\text{O-N}_2\text{O} = (1 - f_{\text{exch.-}nor}) \times (\delta^{18}\text{O-NO} + \varepsilon_3) + f_{\text{exch.-}nor} \times (\delta^{18}\text{O-H}_2\text{O} + \varepsilon_6) \quad [3.4]$$

where, isotope effects (ε) are defined as product−substrate, $\varepsilon = (\alpha - 1) \times 1000$, and $\alpha = {}^{18}\text{O}/{}^{16}\text{O}$ of $N_2O \div {}^{18}\text{O}/{}^{16}\text{O}$ of NO_3^-;

and, ε_1 is an O isotope effect of two processes:

(i) the inter-molecular ${}^{18}\text{O}/{}^{16}\text{O}$ fractionation associated with NO_3^- reduction to NO_2^- in the inner bacterial membrane (Granger *et al.* 2008), where the rate of $N^{16}O^{16}O^{16}O$ reduction occurs faster than the rate of $N^{16}O^{16}O^{18}O$ reduction (e.g., Böttcher *et al.* 1990, −8‰; Mengis *et al.* 1999, −18‰) [negative ε];
and,

(ii) the intra-molecular ${}^{18}\text{O}/{}^{16}\text{O}$ fractionation associated with NO_3^- reduction, where the rate of $\cdots N \cdots {}^{16}O$ bond breakage occurs faster than the rate of $\cdots N \cdots {}^{18}O$ bond breakage. This yields ^{18}O-depleted H_2O and ^{18}O-enriched NO_2^- [positive ε];

and, ε_2 is the intra-molecular O isotope effect associated with NO_2^- reduction (similar to that described above for NO_3^- reduction) [positive ε];

and, ε_3 is the inter-molecular O isotope effect resulting from the reduction of $2NO \rightarrow N_2O$, where the rate of $N \cdots {}^{16}O$ bond breakage occurs faster than the rate of $N \cdots {}^{18}O$ bond breakage. This yields ^{18}O-depleted H_2O and ^{18}O-enriched N_2O [positive ε];

and, $f_{\text{exch.-}nir}$ and $f_{\text{exch.-}nor}$ are the fractions (f) of O-exchange that occur at nitrite reductase (*nir*) and nitric oxide reductase (*nor*), respectively;

and, ε_5 and ε_6 are the O isotope effects associated with enzymatic O-exchange at *nir* and *nor*, respectively. This inter-molecular fractionation is hypothesized to occur similarly to the ${}^{18}\text{O}/{}^{16}\text{O}$ fractionation that occurs during the O_2 and H_2O uptake reac-

tions of nitrification [described by Casciotti *et al.* (2010) and Buchwald and Casciotti (2010)]. If the rate of $H_2\cdots{}^{16}O$ bond breakage occurs faster than the rate of $H_2\cdots{}^{18}O$ bond breakage, then ^{16}O is more readily incorporated into NO_2^- and NO during O-exchange [negative ε].

When there is no N_2O consumption the $\delta^{18}O\text{-}N_2O$ can be modelled by Equation 3.5, which is derived by substituting Equations 3.2–3.3 into Equation 3.4:

$$\delta^{18}O\text{-}N_2O = \left\langle f_{\text{exch.-}nir} + f_{\text{exch.-}nor} - (f_{\text{exch.-}nir} \times f_{\text{exch.-}nor}) \right\rangle \times \delta^{18}O\text{-}H_2O + \left\langle [\varepsilon_6 \times f_{\text{exch.-}nor}] + [1 - f_{\text{exch.-}nor}] \times [\varepsilon_3 + (\varepsilon_5 \times f_{\text{exch.-}nir}) + (1 - f_{\text{exch.-}nir}) \times (\varepsilon_1 + \varepsilon_2 + \delta^{18}O\text{-}NO_3^-)] \right\rangle \quad [3.5]$$

Note that Equation 3.5 is presented here in the linear form ($y = mx + b$), where $y = \delta^{18}O\text{-}N_2O$; $x = \delta^{18}O\text{-}H_2O$; and m and b are the slope and the intercept of the linear regression of $\delta^{18}O\text{-}N_2O$ versus $\delta^{18}O\text{-}H_2O$, respectively.

When N_2O reduction does occur, the $\delta^{18}O\text{-}N_2O$ after partial reduction to N_2 ($\delta^{18}O\text{-}N_2O_{\text{red.}}$) can be approximated by a Rayleigh distillation (Equation 3.6, Mariotti *et al.* 1981) shown here using delta and epsilon units rather than ratios and alphas.

$$\delta^{18}O\text{-}N_2O_{\text{red.}}/1000 + 1 = (\delta^{18}O\text{-}N_2O/1000 + 1) \times (1 - f_{\text{N2O red.}})^{(\varepsilon_4/1000)} \quad [3.6]$$

where, $\delta^{18}O\text{-}N_2O$ is the initial value prior to reduction (Equation 3.5), and $\delta^{18}O\text{-}N_2O_{\text{red.}}$ is the final value after some fraction of N_2O has been consumed ($f_{N_2O\ \text{red.}}$);

and, $(1 - f_{N_2O\ \text{red.}})$ is the fraction of N_2O that remains;

and, ε_4 is the inter-molecular O isotope effect associated with N_2O reduction, where the rate of $N\cdots{}^{16}O$ bond breakage occurs faster than the rate of $N\cdots{}^{18}O$ bond breakage. This yields ^{18}O-depleted H_2O and ^{18}O-enriched N_2O [positive ε].

The substitution of Equation 3.5 into Equation 3.6, and the re-arrangement into a linear form ($y = mx + b$, where $y = \delta^{18}\text{O-N}_2\text{O}_{\text{red.}}$; $x = \delta^{18}\text{O-H}_2\text{O}$; and m and b are the slope and the intercept of the linear regression of $\delta^{18}\text{O-N}_2\text{O}_{\text{red.}}$ versus $\delta^{18}\text{O-H}_2\text{O}$, respectively) yields Equations 3.7:

$$\begin{aligned}\delta^{18}\text{O-N}_2\text{O}_{\text{red.}} = {} & \left\langle [f_{\text{exch.-}nir} + f_{\text{exch.-}nor} - (f_{\text{exch.-}nir} \times f_{\text{exch.-}nor})] \times [1 - f_{\text{N2O red.}}]^{\varepsilon_4/1000} \right\rangle \times \delta^{18}\text{O-H}_2\text{O} \\ & + \left\langle \langle [\varepsilon_6 \times f_{\text{exch.-}nor}] + [1 - f_{\text{exch.-}nor}] \times [\varepsilon_3 + (\varepsilon_5 \times f_{\text{exch.-}nir}) + (1 - f_{\text{exch.-}nir}) \times \right. \\ & \left. (\varepsilon_1 + \varepsilon_2 + \delta^{18}\text{O-NO}_3^-)] + 1000 \rangle \times \langle 1 - f_{\text{N2O red.}} \rangle^{\varepsilon_4/1000} - 1000 \right\rangle \end{aligned} \quad [3.7]$$

When $f_{\text{exch.-}nir} = 0$ and $f_{\text{exch.-}nor} = 0$ (i.e., no O-exchange), then Equation 3.7 reduces to Equation 3.8:

$$\delta^{18}\text{O-N}_2\text{O}_{\text{red.}} = (\delta^{18}\text{O-NO}_3^- + \varepsilon_1 + \varepsilon_2 + \varepsilon_3 + 1000) \times (1 - f_{\text{N2O red.}})^{\varepsilon_4/1000} - 1000 \quad [3.8]$$

When $f_{\text{exch.-}nir} = 1$ and $f_{\text{exch.-}nor} = 1$ (i.e., complete O-exchange), then Equation 3.7 reduces to Equation 3.9:

$$\delta^{18}\text{O-N}_2\text{O}_{\text{red.}} = \left\langle (1 - f_{\text{N2O red.}})^{\varepsilon_4/1000} \right\rangle \times \delta^{18}\text{O-H}_2\text{O} + \left\langle (\varepsilon_6 + 1000) \times (1 - f_{\text{N2O red.}})^{\varepsilon_4/1000} - 1000 \right\rangle \quad [3.9]$$

Algebraic rearrangements of Equations 3.2–3.9 were completed with MuPAD® from the Symbolic Math Toolbox for MATLAB®. To interpret the data measured in this study and obtain estimates of O-exchange and the net ^{18}O isotope effect, the $\delta^{18}\text{O-N}_2\text{O}$ values are regressed against the $\delta^{18}\text{O-H}_2\text{O}$ values of the soil water. The linear regression results are shown in Table 3.1, and are discussed using Methods I and II in Sections 3.3.4–3.3.5 and 3.3.8–3.3.9, respectively.

3.3. *Results and Discussion*

3.3.1. *Soil Parameters*

The mineral soils incubated in this study were low in carbon (1.9–8.7%; Table 3.1) and nitrogen (0.2–0.6%; Table 3.1), which is typical of many agricultural soils in Southern Ontario. Soil collected from the upland site (treatment 1) contained a very low OM content (4.2%). The wetter soil (treatment 2–3) and the stream sediment (treatment 4–5) contained higher amounts of OM (14.9% and 7.1%, respectively; Table 3.1), however all three soils in this study contained relatively low OM contents compared to the organic soils described in Chapter 2 (upland, 36–46%; wetland, 79%). The total amount of inorganic N extracted from all soils was relatively low (2.4–17.4 μg N/g $soil_{dw.}$). The soil pH was typical (7.0–7.5) for soils of the region, which are heavily influenced by the carbonate-rich bedrock.

3.3.2. *Net N_2O Production Rates*

The levels of N_2O that accumulated in the control incubations were lower than the detection limit of the gas chromatograph (100 ppb N_2O) so abiotic N_2O production was a negligible source of N_2O in these soils. The rates of N_2O produced in all treatments varied from almost zero (treatment 3) to ~35 nmol N_2O/hr/g $soil_{dw.}$ (treatment 4) (Table 3.1; Figure 3.3). Given these N_2O production rates and an initial NO_3^- fertilization of 105 μmol/g $soil_{dw.}$, the denitrifying community was not N-limited. Simulating a worst-case-scenario, if 99% of the NO_3^- in treatment 4 was reduced to N_2 (i.e., a constant N_2O:N_2 ratio of 0.01), after 8 hours of incubation, only 20% of the supplied NO_3^- would be consumed (given a constant N_2O production rate ≈ 25 nmol N_2O/hr/g $soil_{dw.}$). Additionally, the $\delta^{15}N$ and $\delta^{18}O$ values of the N_2O in treatment 4 remained constant over the course of the incubations (Figure 3.3d), which would not be expected if the NO_3^- pool was limiting.

The range of N_2O production rates observed in this study (<1–35 nmol N_2O/hr/g $soil_{dw.}$) were very similar to the rates observed in the temperate forest soils (Chapter 2; 1–39 nmol N_2O/hr/g $soil_{dw.}$). In this study, however, divergent production rates among treatments were not attributable to variations in temperature because all incubations were conducted at

room temperature. Instead, variation in N_2O production rates measured in this study were based upon differences in soil type (and its geochemical properties such as organic carbon), H_2O saturation, and the fraction of N_2O reduction ($f_{N2O\ red.}$).

The mean rates of N_2O production in the terrestrial soils incubated at 100% WHC (9–10 nmol N_2O/hr/g $soil_{dw.}$; treatments 1–2) were not statistically different (2-tailed t-test, unequal variance, $p = 0.052$), suggesting that both soils have a similar potential to emit N_2O *in situ*. In contrast, the stream sediment had a much higher N_2O production rate (29 nmol N_2O/hr/g soildw.; treatment 4) at the same H_2O saturation (field capacity), and this was statistically different (2-tailed t-test, unequal variance, $p < 10^{-12}$) from the terrestrial soils. The stream sediment is an aquatic soil that is flooded for most of the year by nutrient-rich agricultural drainage waters. As such, the characteristics of the microbial community (such as species composition, density of denitrifiers, etc...) in this soil are likely very different than those of the terrestrial soils. The high rates of N_2O production in the stream sediment suggest that the overall potential denitrification rate in this sediment is comparatively high.

In general, the flooded incubations (treatments 3 and 5) had mean rates of net N_2O production that were lower than the rates observed in the same soils incubated at 100% WHC (Table 3.1). In this study net N_2O production is a net rate balanced by gross N_2O production and N_2O consumption. Lower net N_2O production in the flooded soils suggests that either: (i) the overall denitrification rate was lower in these soils; (ii) the N_2O:N_2 end-product ratio was different in these soils; or, (iii) the rate of extracellular N_2O uptake and subsequent consumption by N_2O-reducers was elevated in these treatments (Figure 3.2). Of the two soils that were flooded, the stream sediment exhibited the largest difference in mean net N_2O production rate (~⅓ the rate measured from soils incubated at 100% WHC). Although the mean N_2O production rates in the flooded and non-flooded high OM soils (treatments 2–3) were not statistically different at $\alpha = 0.01$ (2-tailed t-test, unequal variance, $p < 0.014$), N_2O production in the flooded soil declined over the course of the experiment and did not plateau (reach a quasi steady-state).

3.3.3. $\delta^{15}N$-N_2O and ^{15}N isotope effects (ε)

The mean $\delta^{15}N$-N_2O produced from all treatments ranged from $-16.1‰$ to $+4.5‰$ (treatments 4 and 3, respectively; Table 3.1, Figure 3.3). The $\delta^{15}N$-N_2O of the last three samplings in all treatments remained relatively constant (quasi steady-state). Instantaneous isotope effects ($^{15}N\ \varepsilon_{\text{nitrous oxide}-\text{nitrate}}$) calculated in this study (as defined in Chapter 2) varied between $-29.5‰$ and $-9.2‰$, which is similar to values described in the literature ($^{15}N\ \varepsilon = -45‰$ to $-10‰$; Chapter 1, Table 1.1). The ^{15}N isotope effects reported here for agricultural soils are slightly lower than those reported for temperate forest soils in Chapter 2 ($-35‰$ to $-19‰$).

There is a negative exponential relationship between the $\delta^{15}N$-N_2O (and $^{15}N\ \varepsilon$) and the rate of N_2O production (Figure 3.4) in this study that was not observed in the temperate forest soils (Chapter 2). This relationship is mainly driven by the data from treatments 3 and 4, and the standard deviations of the mean N_2O production rates are outside the 95% confidence intervals of the regression, which suggests the relationship is weak (Figure 3.4). Furthermore, a negative correlation is not intuitively logical. A positive relationship would be expected (if any); because as the rate of N_2O production increases the $^{15}N\ \varepsilon$ might decrease due to limited N supply.

It is important to remember that N_2O is an obligatory intermediate, and changes in net N_2O production may be due, in part, to differing rates of N_2O reduction. This N_2O-consuming process also affects the $\delta^{15}N$-N_2O by enriching the residual pool of N_2O in ^{15}N. Therefore, changing rates of N_2O reduction provide a partial explanation for the negative correlation shown in Figure 3.4. In fact, the datum with the highest $^{15}N\ \varepsilon$ value and the lowest N_2O production rate was measured in the flooded, high OM soil (treatment 3), which may have experienced significant N_2O reduction that changed with time. On the other hand, the flooded stream sediment (treatment 5) had one of the lowest values of $^{15}N\ \varepsilon$, and significant N_2O reduction did occur in this treatment (see Section 3.3.6). Therefore the observed relationship in Figure 3.4 may be fortuitous, and the high $^{15}N\ \varepsilon$ datum from treatment 3 and the low $^{15}N\ \varepsilon$ datum from treatment 4 may be caused by non-steady-state rates of N_2O production (Figure 3.3).

3.3.4. $\delta^{18}O$-N_2O and Oxygen Isotope Exchange (Method I)

Linear regression analysis of $\delta^{18}O$-N_2O versus $\delta^{18}O$-H_2O indicated that $\delta^{18}O$-N_2O values measured in this study were highly influenced by the $\delta^{18}O$ values of the soil water (r^2 = 0.97–1.00; Table 3.1). Determinations of O-exchange and ^{18}O ε_{net} were made using Method I following the procedures outlined in Section 2 (this study) and Chapter 2. The total fraction of O-exchange ($f_{exch.\text{-}nir}$ + $f_{exch.\text{-}nor}$) between H_2O and N_2O precursors varied widely across all treatments. Very high amounts of O-exchange occurred in the low OM soil (94%, treatment 1). Moderate amounts of O-exchange occurred in the high OM soil (64% and 65%, treatment 2 and 3, respectively), which was independent of the soil moisture content and N_2O production rate. Finally, lower amounts of O-exchange occurred in the non-flooded and flooded stream sediment (50% and 40%, treatments 4 and 5, respectively).

For the results of both this study and Chapter 2, there is a trend between the amount of O-exchange that occurred during denitrification and the soil's landscape position with respect to hydrology. Both the upland agricultural soil (treatment 1) and the upland forested soil (Chapter 2, treatments A, C, and E) exhibited high amounts of O-exchange (87–94%). Although these soils have very different histories and OM contents, neither of them experiences *in situ* saturated conditions for any considerable length of time. In contrast, the high OM agricultural soil (treatment 2–3) and the forested wetland (Chapter 2, treatments B and D) experience flooding during snowmelt and high precipitation events throughout the year. These soils exhibited lower amounts of O-exchange (64–70%). Finally, the agricultural stream sediment (treatment 4–5), which is flooded for most of the year (except during low flow, drought summer months) exhibited the lowest amounts of O-exchange (non-flooded, 50%; flooded, 40%).

This overall trend suggests that O-exchange during denitrification in soils is controlled by the composition of the microbial denitrifier community, which in turn, is controlled by the soil's landscape position and its antecedent hydrological conditions. Admittedly, this claim is speculative and only a hypothesis that remains to be tested with future research. However, the ranges of O-exchange calculated in this thesis are well-constrained for each soil type. Nei-

ther flooded nor non-flooded conditions, nor cold or warm temperatures, nor high or low net N_2O production rates affected this narrow range in O-exchange. This further suggests that the main controls on O-exchange lie within the composition of the microbial community.

3.3.5. *$\delta^{18}O$-N_2O and Oxygen Isotope Fractionation (Method I)*

The net $^{16}O/^{18}O$ fractionation that occurs from denitrification (^{18}O ε_{net}; Figure 3.2) is a cumulative isotope effect composed of: (i) ε_1, the negative isotope effect associated with active uptake of NO_3^- (−18‰ to −8‰, Mengis *et al.* 1999 and Böttcher *et al.* 1990, respectively) and the positive isotope effect associated with NO_3^- reduction; (ii) ε_2—ε_4, the positive isotope effects associated with NO_2^-, NO, and N_2O reduction; and, (iii) ε_5—ε_6, the (hypothesized) negative isotope effects associated with O-exchange. The cumulative value of the isotope effects of these processes (^{18}O ε_{net}) calculated using Method I varied from +32‰ to +60‰ (Table 3.1). In Chapter 2, the ^{18}O ε_{net} in the temperate forest soils was tightly constrained to +40 ± 3‰, with the exception of one treatment that had a lower ^{18}O ε_{net} equal to +17‰.

In all soils, the ^{18}O ε_{net} was not correlated to the N_2O production rate (Figure 3.4), but there was a negative correlation between ^{18}O ε_{net} and O-exchange (Figure 3.5). As it was explained in Chapter 2, when the fraction of O-exchange decreases, a larger proportion of the early isotope effects (e.g., $\varepsilon_1 + \varepsilon_2$, Figure 3.2) are expressed in the $\delta^{18}O$-N_2O (Equation 3.8). When the amount of O-exchange increases, a smaller portion of the early isotope effects are expressed in the $\delta^{18}O$-N_2O (Equation 3.9). Therefore, a correlation between ^{18}O ε_{net} and O-exchange is expected.

It is unknown if O-exchange is a fractionating process in soils and this cannot be independently determined with the data available in this study. O-exchange during denitrification occurs at the NO_2^- and NO reduction steps, which are reversible hydrolysis reactions (Kool *et al.* 2007). Presumably, as the rate of the backward reaction increases (e.g., Equation 3.10), so

$$NO_2^- + 2H^+ \rightleftharpoons NO + H_2O \qquad [3.10]$$

does the amount of O-exchange. The exact mechanism of O-exchange, however, is not well-defined. A better conceptual model of O-exchange is required; including a thermodynamic explanation that identifies the biogeochemical conditions that support significant rates of the backward reaction(s).

If O-exchange is a fractionating process, the isotope effect might be similar to the $^{18}O/^{16}O$ fractionations that occur during O_2 and H_2O uptake in nitrification, which have recently been determined in marine nitrifiers by Casciotti *et al.* (2010) and Buchwald and Casciotti (2010). As an example, the isotope effect for H_2O uptake during the final oxidation of NO_2^- to NO_3^- ranges from −25‰ to −9‰ (Buchwald and Casciotti 2010). If ε_5 and ε_6 were also large and negative values, then ^{18}O ε_{net} would decrease as O-exchange increased. This provides a further explaination for the negative correlation that was observed in this study between ^{18}O ε_{net} and O-exchange (Figure 3.5).

3.3.6. *Evidence of N_2O Reduction*

The consumption of N_2O to N_2 causes the remaining portion of the N_2O pool to become enriched in ^{18}O and ^{15}N. The ratio of the isotope effects for N_2O consumption (^{18}O ε_4:^{15}N ε) ranges between 2.3 and 3.0 (Chapter 1, Table 1.1) and N_2O isotope samples that have undergone consumption may plot along a trajectory with a slope close to 2.5 ($\delta^{18}O$-N_2O:$\delta^{15}N$-N_2O). Demonstrations of this distinctive relationship in soil-N_2O studies are provided by Jinuntuya-Nortman (2008) and Well and Flessa (2009b).

Most of the treatments in this study had $\delta^{15}N$-N_2O and $\delta^{18}O$-N_2O values that did not change appreciably with time (Figure 3.3). These incubations were designed to reach a quasi steady-state with continuous net N_2O production (i.e., open system). As such, cross-plots of $\delta^{18}O$-N_2O versus $\delta^{15}N$-N_2O for individual treatments cannot be used in this study to look for evidence of N_2O consumption. However, it is probable that N_2O reduction did occur in the flooded soils (treatments 3 and 5). Saturated environments present ideal conditions for N_2O reduction to N_2 because the rate of N_2O escape to the atmosphere is greatly reduced. If the values of ε_1–ε_3 and ε_5–ε_6 were the same in the non-flooded and flooded treatments of each soil,

then any differences in net isotope effects ought to be a result of differences in N_2O consumption (ε_4).

The $\delta^{18}O$-N_2O and $\delta^{15}N$-N_2O in the flooded stream sediment were higher than the values measured in the non-flooded sediment, and a line drawn through the ^{18}O ε:^{15}N ε ratios of treatments 4 and 5 had a slope of 3.2 (Figure 3.6). However, the variability of the ^{15}N ε estimates was large and the slope varied from 1.8 up to 15. Given the mean slope was close to 2.5, and the net rate of N_2O production in the flooded sediment was ~⅓ of the rate measured in the non-flooded sediment (Table 3.1), it is probable that N_2O reduction occurred to a greater extent in treatment 5 than in treatment 4.

This distinctive trajectory was not observed in the N_2O isotope ratios of treatments 2 and 3 (Figure 3.6). Although the ^{15}N ε of the flooded soil was 7.2‰ higher than the non-flooded soil, there was very little difference (~2‰) in ^{18}O ε_{net} between treatments 2 and 3. Additionally, the net rates of N_2O production in these incubations were not significantly different at $\alpha = 0.01$ (2-tailed t-test, unequal variance, $p < 0.014$). This suggests that regardless of the differences in WHC, both treatments experienced similar amounts of N_2O reduction.

3.3.7. *Predicting N_2O isotope ratios in Open and Closed Systems*

The net production of N_2O is the difference between gross production ($NO_3^- \rightarrow N_2O$) and gross consumption ($N_2O \rightarrow N_2$). When there is no N_2O reduction (i.e., the gross consumption rate = zero) the $\delta^{18}O$-N_2O can be modelled by Equation 3.5. When N_2O reduction does occur Equations 3.6–3.7 can be used to predict $\delta^{18}O$-N_2O values. These equations require knowledge of the fraction of N_2O reduced ($f_{N_2O\ red.}$). When a system is truly closed there is no N_2O production, and the $f_{N_2O\ red.}$ is entirely dependent upon the initial size of the N_2O pool and the rate of N_2O consumption. In this case, the classic Rayleigh distillation applies (Mariotti *et al.* 1981; Equation 3.6) and the $\delta^{18}O$-$N_2O_{red.}$ increases exponentially as the finite pool of N_2O diminishes (Figure 3.7a).

When a system is open, such as the soil incubation experiments of this study, N_2O is an intermediate compound that is continuously produced and consumed. In this case the f_{N_2O}

red. is dependent upon the relative rates of gross production and consumption. This can be expressed as the N_2O:N_2 ratio (Equation 3.11) or as the N_2O yield (%):

$$\begin{aligned} N_2O{:}N_2 \text{ ratio} &= \text{net } N_2O \text{ production} \div [\text{net } N_2O \text{ production} + N_2O \text{ consumption}] \\ \text{or,} \qquad &= N_2O \div [N_2O + N_2] \end{aligned} \qquad [3.11]$$

It is difficult to accurately measure the N_2O:N_2 ratio because the existing methods are fraught with errors (e.g., the acetylene block technique, Bollman and Conrad 1997a, 1997b; Wrage *et al.* 2004; Groffman *et al.* 2006) and the direct measurement of N_2 at low concentrations is prone to contamination by atmospheric air N_2 (~78% v/v).

A few studies have accurately quantified N_2O:N_2 ratios in soils using ^{13}N- or ^{15}N-labelling techniques, or by carefully measuring the N_2 production in soils incubated in artificial atmospheres (helium or argon, e.g., Scholefield *et al.* 1997; Delaune *et al.* 1998; Butterbach-Bahl *et al.* 2002; Bol *et al.* 2003; Meijide *et al.* 2010; Bergstermann *et al.* 2011). The N_2O:N_2 ratio in soils often increases following soil disturbance or N fertilization, and it can be highly variable over short time-scales (hours–days).

When the N_2O:N_2 ratio > 0 (i.e. net N_2O production $> N_2O$ consumption) the size of the N_2O pool will increase with time. The rate of increase of the N_2O pool is directly proportional to the N_2O:N_2 ratio (Figure 3.7b). This has important implications for the modelling of $\delta^{18}O\text{-}N_2O_{red.}$ because when the N_2O:N_2 ratio is high (~0.5 or greater), the fraction of N_2O remaining ($1 - f_{N_2O\ red.}$) quickly approaches 1. As a result, very little $^{18}O/^{16}O$ discrimination is observed because the isotopic 'signal' of N_2O consumption is quickly inundated by the newly produced N_2O. The fraction of N_2O remaining will also approach 1 when the N_2O:N_2 ratio is lower (0.01–0.1), albeit, it takes longer for the N_2O pool to build in size (Figure 3.7c).

None of the model simulations that are illustrated in Figure 3.7a–c accounts for any physical loss of N_2O. Diffusion is an important mechanism of N_2O loss in soils, and advection and gas exchange may be important in aqueous systems. The relative rate of N_2O loss out of the system will govern the upper size limit of the N_2O pool and may prevent the fraction of N_2O remaining from reaching 1. The imposition of physical N_2O losses will cause the slope of

the trajectories in Figures 3.7b–c to decrease. This is important because the magnitude of the observed isotopic separation increases as the fraction of N_2O remaining decreases (Figure 3.7a).

3.3.8. *Oxygen Isotope Exchange (Method II)*

The total O-exchange ($f_{\text{exch.-}nir} + f_{\text{exch.-}nor}$) is related to the slope of the linear regression of $\delta^{18}O\text{-}N_2O$ $_{\text{(rel. VSMOW)}}$ versus $\delta^{18}O\text{-}H_2O$ $_{\text{(rel. VSMOW)}}$ (Table 3.1) and is described in Equation 3.7. An expression of the slope term is given below in Equation 3.12.

$$\text{Slope (m)} = [f_{\text{exch.-}nir} + f_{\text{exch.-}nor} - (f_{\text{exch.-}nir} \times f_{\text{exch.-}nor})] \times [1 - f_{\text{N2O red.}}]^{\varepsilon_4/1000} \quad [3.12]$$

Equation 3.12 is non-determinate (there is no unique solution) and $f_{\text{exch.-}nir} + f_{\text{exch.-}nor}$ cannot be solved explicitly because there are too many unknown parameters. In an open system with a high N_2O:N_2 ratio (large fraction of N_2O remaining) the total O-exchange ($f_{\text{exch.-}nir} + f_{\text{exch.-}nor}$) is approximately equal to the slope (m) of the linear regression (Table 3.1) plus the product of the individual O-exchange terms ($f_{\text{exch.-}nir} \times f_{\text{exch.-}nor}$). Therefore, the slope (m) of the linear regression (as it is used in Method I) is a *minimum* estimate of O-exchange.

If the majority of the O-exchange occurs at only one enzyme, and $f_{\text{exch.-}nir} \gg f_{\text{exch.-}nor}$ (or vice-versa) then $f_{\text{exch.-}nir} \times f_{\text{exch.-}nor}$ becomes very small, and the slope (m) $\approx f_{\text{exch.-}nir} + f_{\text{exch.-}nor}$ (Table 3.2). However, if there is a large amount of O-exchange and it occurs at both enzymes ($f_{\text{exch.-}nir} \approx f_{\text{exch.-}nor}$), then $f_{\text{exch.-}nir} \times f_{\text{exch.-}nor}$ is a large and significant term. In this case the slope (m) $< f_{\text{exch.-}nir} + f_{\text{exch.-}nor}$ and it is a poor approximation of the true magnitude of O-exchange (Table 3.2).

When the remaining fraction of N_2O is small (such as in a closed system), the effect of N_2O reduction causes the slope (m) to increase slightly because consumption affects the $\delta^{18}O\text{-}N_2O$ (but not the $\delta^{18}O\text{-}H_2O$). As a result, as N_2O consumption increases, the difference between the slope (m) and the true O-exchange decreases (Table 3.2).

In many cases, estimates of O-exchange derived using Method I are a good approximation of the true O-exchange ($f_{\text{exch.-}nir} + f_{\text{exch.-}nor}$; derived using Method II). It is only when $f_{\text{exch.-}nir}$ and $f_{\text{exch.-}nor}$ are both large that Method I fails to accurately estimate the amount of O-exchange (with or without N_2O reduction).

3.3.9. *Oxygen Isotope Fractionation (Method II)*

The net ^{18}O isotope effect ($^{18}O\ \varepsilon_{net}$) is related to the intercept of the linear regression of $\delta^{18}O$-N_2O $_{\text{(rel. VSMOW)}}$ versus $\delta^{18}O$-H_2O $_{\text{(rel. VSMOW)}}$ (Table 3.1) and is described in Equation 3.7. An expression of the intercept term is given below in Equation 3.13.

$$\text{Intercept (b)} = \langle[\varepsilon_6 \times f_{\text{exch.-}nor}] + [1 - f_{\text{exch.-}nor}] \times [\varepsilon_3 + (\varepsilon_5 \times f_{\text{exch.-}nir}) + (1 - f_{\text{exch.-}nir}) \times (\varepsilon_1 + \varepsilon_2 + \delta^{18}\text{O-NO}_3^-)] + 1000\rangle \times \langle 1 - f_{\text{N2O red.}}\rangle^{\varepsilon_4/1000} - 1000 \quad [3.13]$$

The mathematical approach (Method II) used here to define the net ^{18}O isotope effect for denitrification demonstrates the complex nature of $^{18}O\ \varepsilon_{net}$, which depends on the $\delta^{18}O$-NO_3^- value, the individual isotope effects (ε_1–ε_6), and the fractions of O-exchange and N_2O reduction.

If the system is open and the N_2O:N_2 ratio is high (or there is a large fraction of N_2O remaining), then the isotope effect associated with N_2O consumption (ε_4) approaches zero. In this case, Equation 3.13 can be simplified to Equation 3.14:

$$\text{Intercept (b)} = [\varepsilon_6 \times f_{\text{exch.-}nor}] + [1 - f_{\text{exch.-}nor}] \times [\varepsilon_3 + (\varepsilon_5 \times f_{\text{exch.-}nir}) + (1 - f_{\text{exch.-}nir}) \times (\varepsilon_1 + \varepsilon_2 + \delta^{18}\text{O-NO}_3^-)] \quad [3.14]$$

It is not possible to isolate any further useful expressions of the ^{18}O isotope effects from Equations 3.13–3.14 because there are too many unmeasured or unknown parameters in this study. However, the mathematical approach of defining $^{18}O\ \varepsilon_{net}$ (and O-exchange) that is presented

here is useful for future studies that model the O isotope ratios of N_2O produced by denitrification.

3.4. *Conclusions*

The instantaneous ^{15}N isotope effect ($\varepsilon_{\text{nitrous oxide–nitrate}}$) for denitrification measured for three agricultural soils ranged from −30‰ to −9‰, which is consistent with reports described in the literature (Chapter 1, Table 1.1). The net ^{18}O isotope effect calculated for all treatments in this study varied from +32‰ to +60‰, and the approximate fraction of O-exchange ($f_{\text{exch.-}nir} + f_{\text{exch.-}nor}$) ranged from 0.40 in the flooded stream sediment to 0.94 in the non-flooded low OM soil. Moderate amounts of O-exchange occurred in the non-flooded and flooded high OM soil (0.64–0.65).

A new mathematical approach to calculate O-exchange revealed that the existing method (developed in Chapter 2) derives approximations of O-exchange that are minimum estimates. These approximations become less accurate as O-exchange increases and when significant proportions of the total O-exchange occur at both nitrite and nitric oxide reductase. This new mathematical approach also demonstrated the complex nature of the net ^{18}O isotope effect for denitrification which is dependent upon the $\delta^{18}O\text{-}NO_3^-$ value, multiple isotope effects, and the fractions of O-exchange and N_2O reduction.

The ^{18}O ε_{net} was negatively correlated to O-exchange, and the well-drained soil had the highest amount of O-exchange and the lowest apparent oxygen isotope enrichment. Correspondingly, the stream sediment had the lowest amounts of O-exchange and the highest apparent oxygen isotope enrichment calculated for the agricultural and forest soils studied in this thesis. This trend helps explain why the $\delta^{18}O\text{-}N_2O$ values measured in oceans, rivers and groundwaters tends to be higher than the $\delta^{18}O\text{-}N_2O$ values measured in soils. O-exchange is likely controlled by the microbial composition of the denitrifying community, which is influenced by the soil's landscape position and its associated hydrology (well-drained versus satu-

rated). The dominant denitrifying communities in well-drained soils may be very different than the communities found in saturated soils, groundwaters, surface waters, and oceans.

Based on the results of this study, the $\delta^{15}N$-N_2O and $\delta^{18}O$-N_2O that would be produced *in situ* by denitrification in the agricultural soils would be isotopically distinct from each other (given each soil had similar NO_3^- sources). The well-drained agricultural soil would yield lower $\delta^{18}O$-N_2O values than the poorly-drained soil and the stream sediment because the latter two soils exhibited less O-exchange and higher values of ^{18}O ε_{net}. Additionally, the poorly-drained soil and the stream sediment could be separated by their $\delta^{15}N$-N_2O values because the stream sediment had a larger ^{15}N isotope effect. The effects of flooding on the N_2O isotope ratios were less clear. In both cases the non-flooded soils had larger ^{15}N isotope effects than their flooded counterparts. The $\delta^{18}O$-N_2O values of the flooded sediment would be significantly higher than the non-flooded sediment; however, the $\delta^{18}O$-N_2O values in the poorly-drained soil would be similar regardless of flooded/non-flooded conditions. Finally, denitrifier-produced N_2O from the agricultural soils would be isotopically separable from the denitrifier-N_2O produced in the temperate forest soils (Chapter 2). This is largely because the ^{15}N isotope effects in the forested soils were larger than in the agricultural soils.

Table 3.1. The geochemical characteristics of the agricultural soils incubated in this study, the mean N_2O production rate, $\delta^{15}N\text{-}N_2O$, ^{15}N isotope effect, $\delta^{18}O\text{-}H_2O$, $\delta^{18}O\text{-}N_2O$, and the corresponding results of simple linear regression (Model I) of $\delta^{18}O\text{-}N_2O$ versus $\delta^{18}O\text{-}H_2O$ for treatments 1–5.

Treatment	**1**			**2**			**3**			**4**			**5**		
Soil	*low OM*			*high OM*			*high OM*			*stream sediment*			*stream sediment*		
texture (% sand, % silt, % clay)	silt loam (43, 41, 16)			loam (19, 64, 17)						fine sandy loam (55, 33, 12)					
water holding capacity (%)[a]	100			100			200			100			200		
gravimetric soil water content (g H_2O/g soil dw.)	0.52			0.79			1.58			0.69			1.38		
TC (%)	1.9			8.7			8.7			6.4			6.4		
$\delta^{13}C$-TC (‰ rel. to VPBD)	−21.8			−23.0			−23.0			−13.2			−13.2		
TN (%)	0.2			0.6			0.6			0.3			0.3		
$\delta^{15}N$-TN (‰ rel. to AIR)	6.7			6.1			6.1			6.7			6.7		
C:N ratio (mol:mol)	9.7			12.7			12.7			17.0			17.0		
LOI (%)	4.2			14.9			14.9			7.1			7.1		
extractable NH_4^+ (μg N/g soil dw.)	0.2			1.1			1.1			1.2			1.2		
extractable NO_3^- (μg N/g soil dw.)[b]	17.2			4.8			4.8			1.2			1.2		
soil pH (H_2O, 0.1 M $CaCl_2$)	7.3, 7.0			7.5, 7.2			7.5, 7.2			7.5, 7.3			7.5, 7.3		
mean[c] production rate (nmol N_2O/hr/g soil dw.) of last 3 samplings (± 1σ)	10.0 (1.8)			8.9 (2.5)			6.1 (5.0)			29.0 (7.7)			10.8 (8.1)		
mean[c] $\delta^{15}N\text{-}N_2O_{\text{ rel. AIR}}$ (‰) of last 3 samplings (± 1σ)	−6.9 (1.9)			−2.9 (1.1)			4.5 (2.7)			−16.1 (1.0)			−10.4 (3.5)		
mean[c] ^{15}N isotope effect (ε) (‰) of last 3 samplings (± 1σ)	−20.5 (1.9)			−16.4 (1.0)			−9.2 (2.7)			−29.5 (1.0)			−23.9 (3.4)		
$\delta^{18}O\text{-}H_2O_{\text{ rel. VSMOW}}$ (‰)[d]	–8.2	45.6	105.9	–9.5	45.6	106.5	–10.1	48.1	113.3	–9.5	47.6	111.5	–10.1	49.3	115.9
mean[e] $\delta^{18}O\text{-}N_2O_{\text{ rel. VSMOW}}$ (‰) of last 3 samplings (± 1σ)	25.5 (1.0)	80.7 (2.1)	133.5 (1.3)	53.4 (1.8)	87.5 (1.0)	128.0 (1.7)	54.2 (8.5)	93.5 (0.7)	134.5 (4.4)	52.6 (2.0)	80.2 (2.0)	113.5 (2.0)	73.7 (2.2)	99.2 (2.1)	124.2 (3.1)
linear regression analysis of $\delta^{18}O\text{-}N_2O$ (rel. VSMOW) versus $\delta^{18}O\text{-}H_2O$ (rel. VSMOW) of last 3 samplings															
slope (m) (± SE)	0.94 (0.01)			0.64 (0.01)			0.65 (0.02)			0.50 (0.01)			0.40 (0.01)		
intercept (b) (± SE)	32.8 (0.7)			59.0 (0.4)			61.3 (1.5)			57.0 (0.6)			78.3 (0.7)		
coefficient of determination (r^2)	0.9968			0.9973			0.9748			0.9938			0.9857		
linear regression analysis of $\delta^{18}O\text{-}N_2O$ (rel. $\delta^{18}O\text{-}NO_3^-$) versus $\delta^{18}O\text{-}H_2O$ (rel. $\delta^{18}O\text{-}NO_3^-$) of last 3 samplings															
slope (m) (± SE) [*total fraction of oxygen exchange*][f]	0.94 (0.01)			0.64 (0.01)			0.65 (0.02)			0.50 (0.01)			0.40 (0.01)		
intercept (b) (± SE) [*net ^{18}O isotope effect*][f]	32.4 (0.5)			47.7 (0.3)			50.1 (1.1)			41.9 (0.4)			59.9 (0.5)		
coefficient of determination (r^2)	0.9968			0.9973			0.9748			0.9938			0.9857		

[a] soil moisture at field capacity (100% WHC) or flooded (200% WHC).

[b] although antecedent NO_3^- was present in the field-collected soils, it was removed prior to fertilization (by soil denitrifiers during the pre-incubation period).

[c] $n = 27$ measurements.

[d] soils were incubated with 3 different waters: low, medium, and high $\delta^{18}O\text{-}H_2O$.

[e] $n = 9$ measurements.

[f] determined using Method I, which is described in Sections 3.2 and 3.3.

Table 3.2. The slope (m) of the linear regression of $\delta^{18}O\text{-}N_2O$ (rel. VSMOW) versus $\delta^{18}O\text{-}H_2O$ (rel. VSMOW) is a minimum estimate of O-exchange during denitrification. This table demonstrates the difference between the approximated O-exchange (Column A) and the true O-exchange (Column B) across the range of O-exchange measured in this study (0.40–0.94) when (i) $f_{\text{exch.-}nir} \approx f_{\text{exch.-}nor}$, (ii) $f_{\text{exch.-}nir} \neq f_{\text{exch.-}nor}$, (iii) $f_{\text{N2O red.}} = 0$, and (iv) $f_{\text{N2O red.}} > 0$.

slope (m) $= [f_{\text{exch.-}nir} + f_{\text{exch.-}nor} - (f_{\text{exch.-}nir} \times f_{\text{exch.-}nor})] \times [1 - f_{\text{N2O red.}}]^{\varepsilon_4/1000}$ .....Equation 3.12

A	B	C	D	E	F	G	H
approx. O-exchange (derived from slope of regression analysis)	true O-exchange ($f_{\text{exch.-}nir} + f_{\text{exch.-}nor}$, derived from Equations)	error |A – B|	Suitability of slope to predict O-exchange	$f_{\text{exch.-}nir}$	$f_{\text{exch.-}nor}$	$f_{\text{exch.-}nir} \times f_{\text{exch.-}nor}$	$f_{\text{N2O red.}}$
0.94	1.50	0.56	poor	0.75	0.75	0.56	0
0.94	0.98	0.04	good	0.94	0.04	0.04	0
0.97	1.50	0.53	poor	0.75	0.75	0.56	0.9
0.98	0.98	0.00	good	0.94	0.04	0.04	0.9
0.40	0.45	0.05	good	0.22	0.23	0.05	0
0.40	0.41	0.01	good	0.39	0.02	0.01	0
0.41	0.45	0.04	good	0.22	0.23	0.05	0.9
0.42	0.41	0.01	good	0.39	0.02	0.01	0.9

n.b. The value of ε_4 (within the range of literature estimates of ^{18}O $\varepsilon = -26‰$ to $-5‰$) has very little effect on the error (column C). As the strength of the isotope effect increases (ε_4 becomes more negative), the difference between the true and approximate O-exchange increases *slightly*. In these evaluations of Equation 3.12, ε_4 was held constant at $-15‰$.



Figure 3.1a. Approximate location of the Strawberry Creek Watershed in South-Central Ontario, Canada. The Grand River watershed boundary is shown by the black, solid line. This map was produced using information under License with the Grand River Conservation Authority, © Grand River Conservation Authority, 2011.



Figure 3.1b. The upper portion of the Strawberry Creek Watershed from the headwaters, which originate from the forested swamp north of Crowsfoot Road, to Maryhill Road ('Middle Road') in the bottom of the figure. The approximate positions of intensive study plots are shown, including the locations where soils were collected for this study [S2, treatment 1 (low OM soil); R3, treatment 2–3 (high OM soil); SS, treatment 4–5 (stream sediment)]. This map was produced using information under License with the Grand River Conservation Authority, ©Grand River Conservation Authority, 2011.

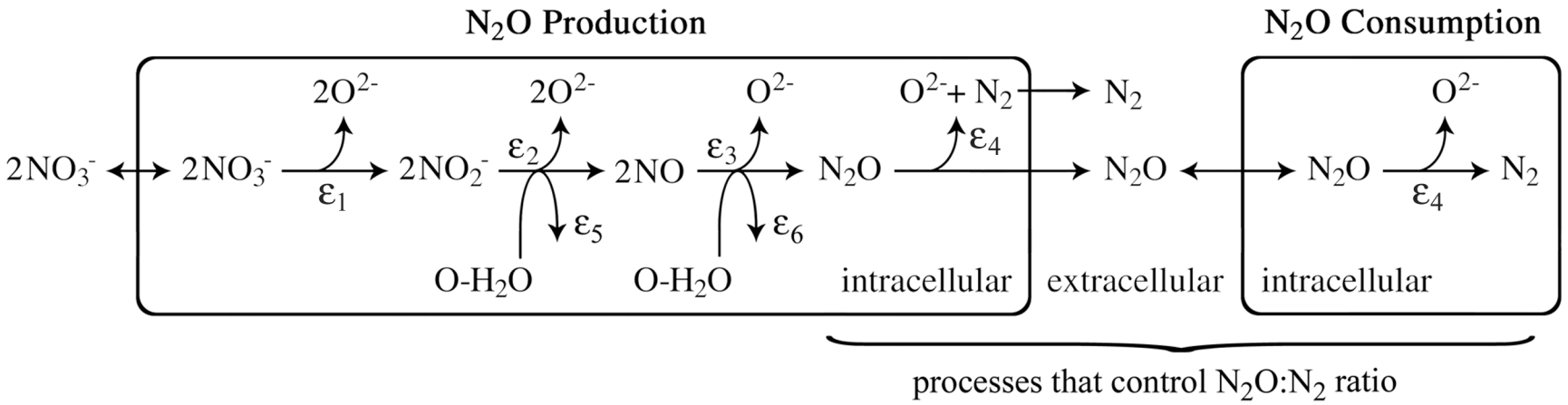


Figure 3.2. Proposed systematics of oxygen isotope enrichment and exchange during denitrification. The net O isotope effect measured between N_2O and NO_3^- ($^{18}O\varepsilon_{net}$) is a function of all the individual isotope effects (defined in Section 3.2.4), a variable fraction of O-exchange that occurs during NO_2^- and NO reduction, and the relative rates of N_2O production and N_2O consumption.

In this conceptual model of denitrification it is assumed that NO_3^- and N_2O are the only compounds that accumulate in the intra- or extracellular environments. If any other intermediate compounds accumulate and egress from the cell, then additional isotope effects could result if the steps are rate-limiting.

If 100% of the N_2O is reduced to N_2 (sequentially, within the same organism), then the observed $^{18}O/^{16}O$ discrimination is zero because no N_2O remains. If an organism is 'leaky' [as described in the 'hole-in-the-pipe' model by Firestone and Davidson (1989)], then a portion of the N_2O is reduced to N_2 (sequentially, within the same organism) and another portion is 'leaked' out of the cell. In this scenario $\varepsilon_4 >$ zero, and the accurate modelling of $^{18}O/^{16}O$ requires knowledge of the relative rates of N_2O production and N_2O consumption (the N_2O:N_2 ratio). Similarly, if extracellular N_2O is taken up by N_2O-consuming organisms, an intermolecular isotope effect occurs (ε_4) because the rate of $N_2{}^{16}O$ reduction to N_2 is faster than the reduction of $N_2{}^{18}O$ to N_2.

Figure 3.3a. Treatment 1 - low OM soil, 100% WHC

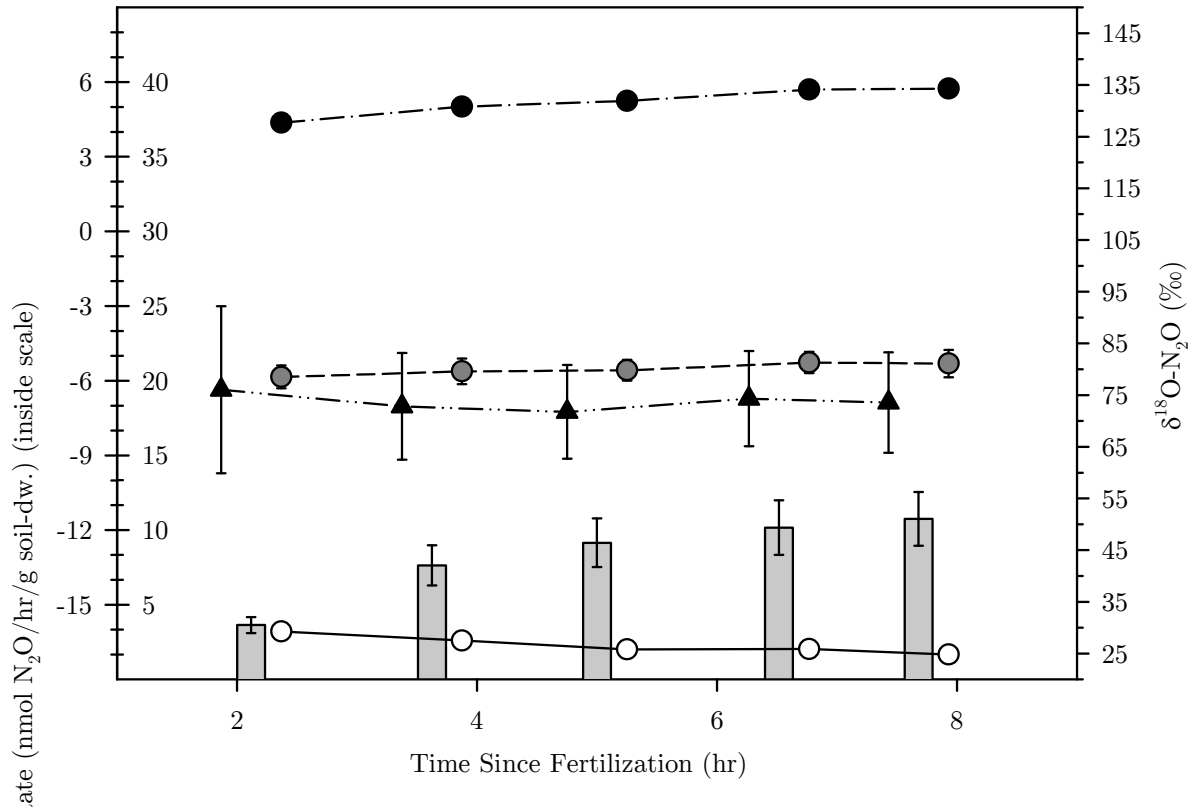


Figure 3.3b. Treatment 2 - high OM soil, 100% WHC

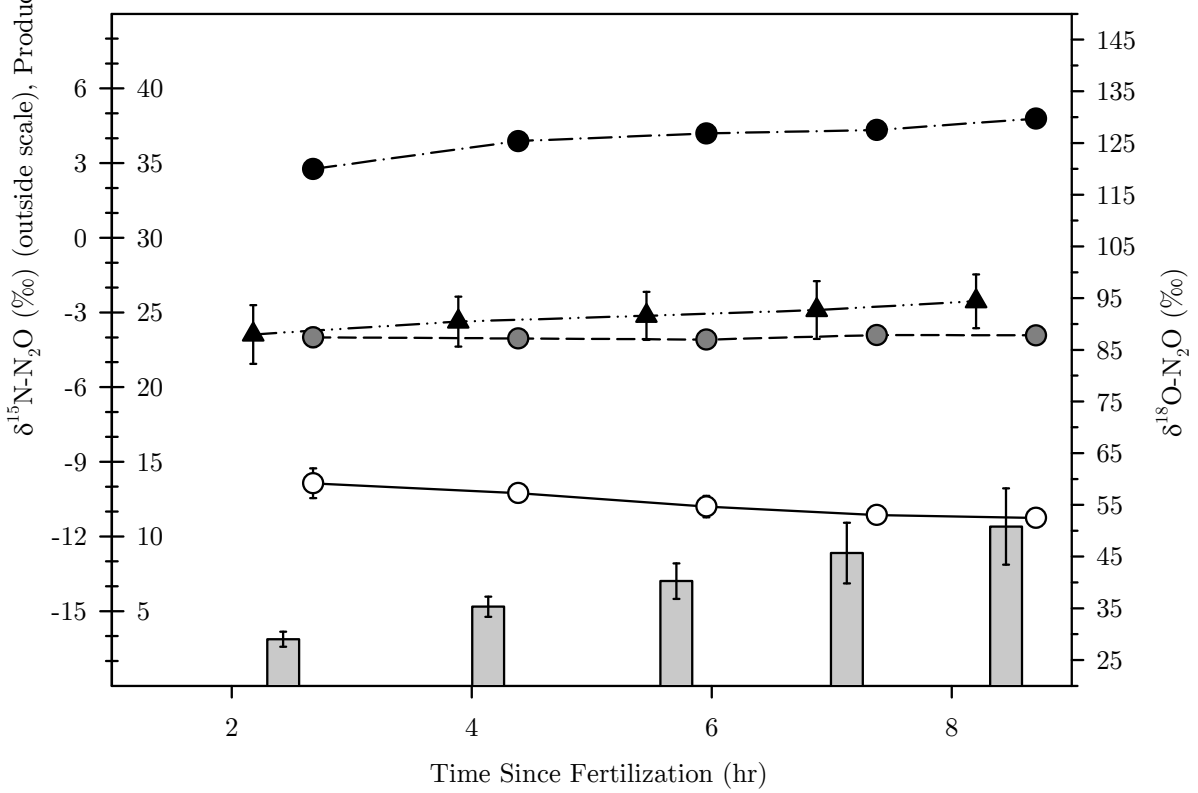


Figure 3.3c. Treatment 3 - high OM soil, 200% WHC (flooded)

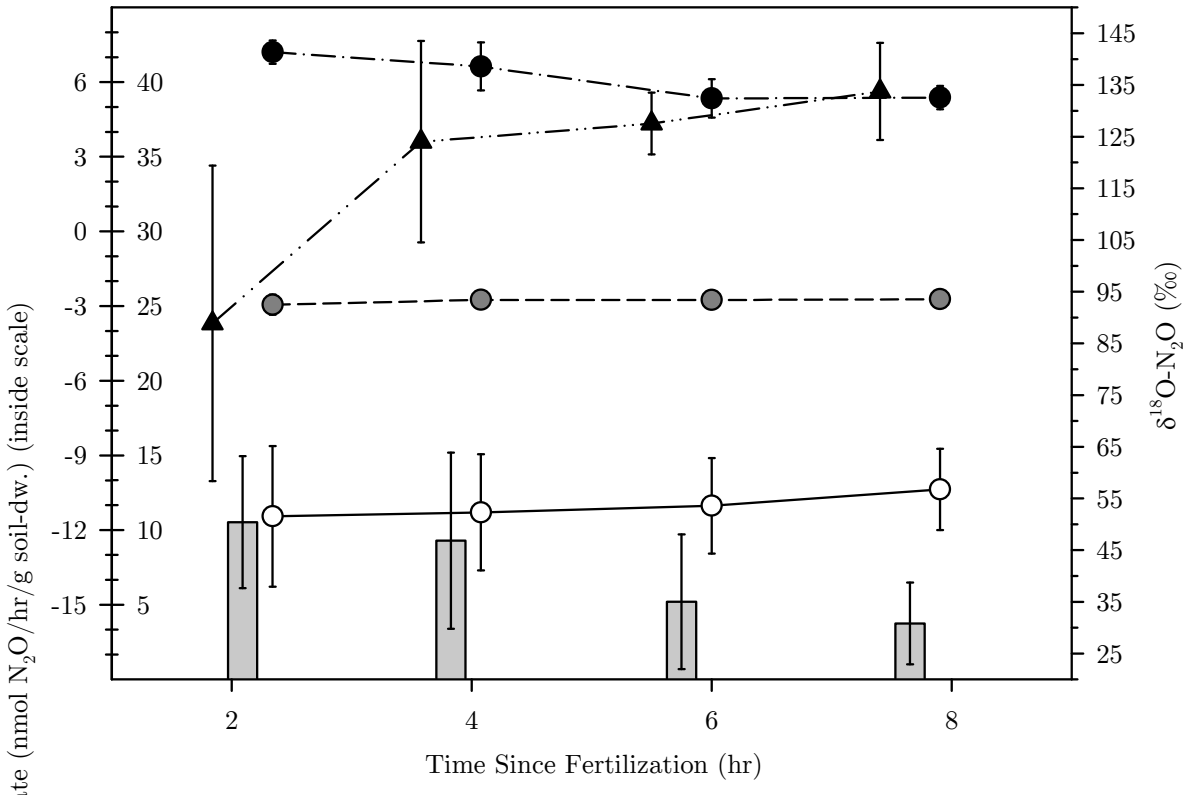


Figure 3.3d. Treatment 4 - stream sediment, 100% WHC

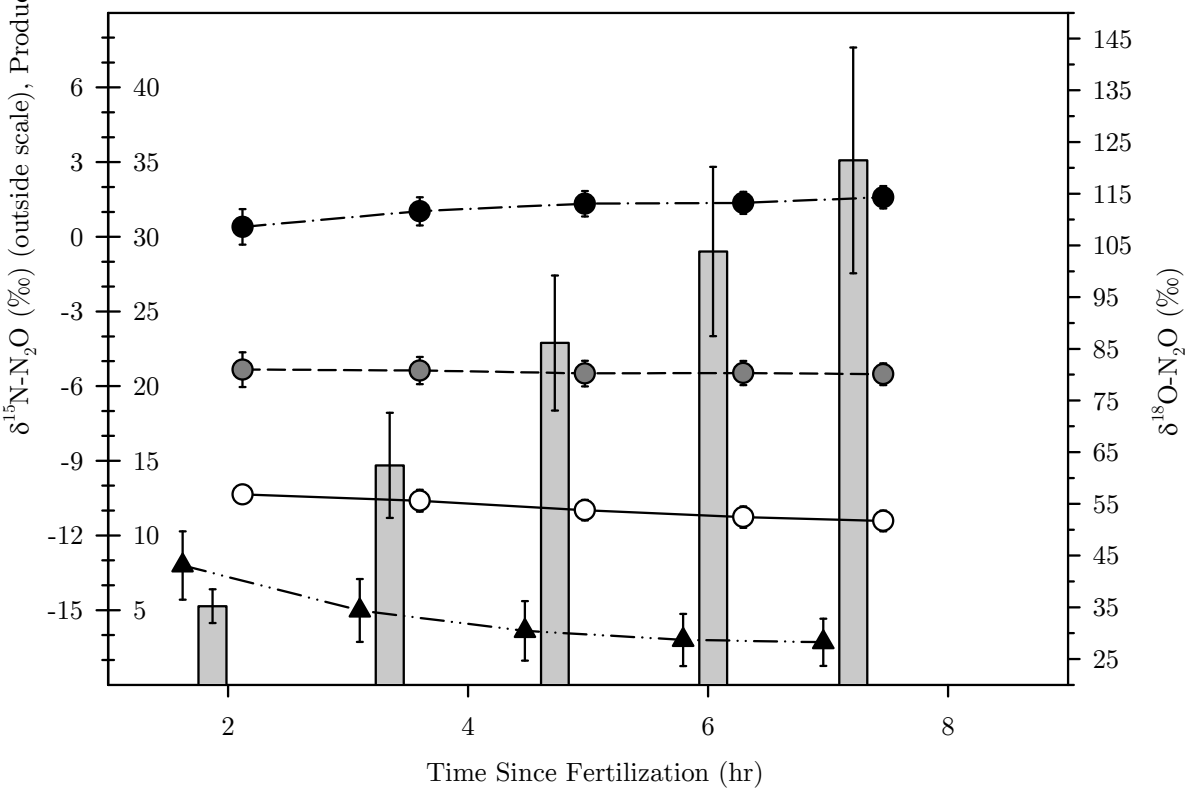


Figure 3.3e. Treatment 5 - stream sediment, 200% WHC (flooded)

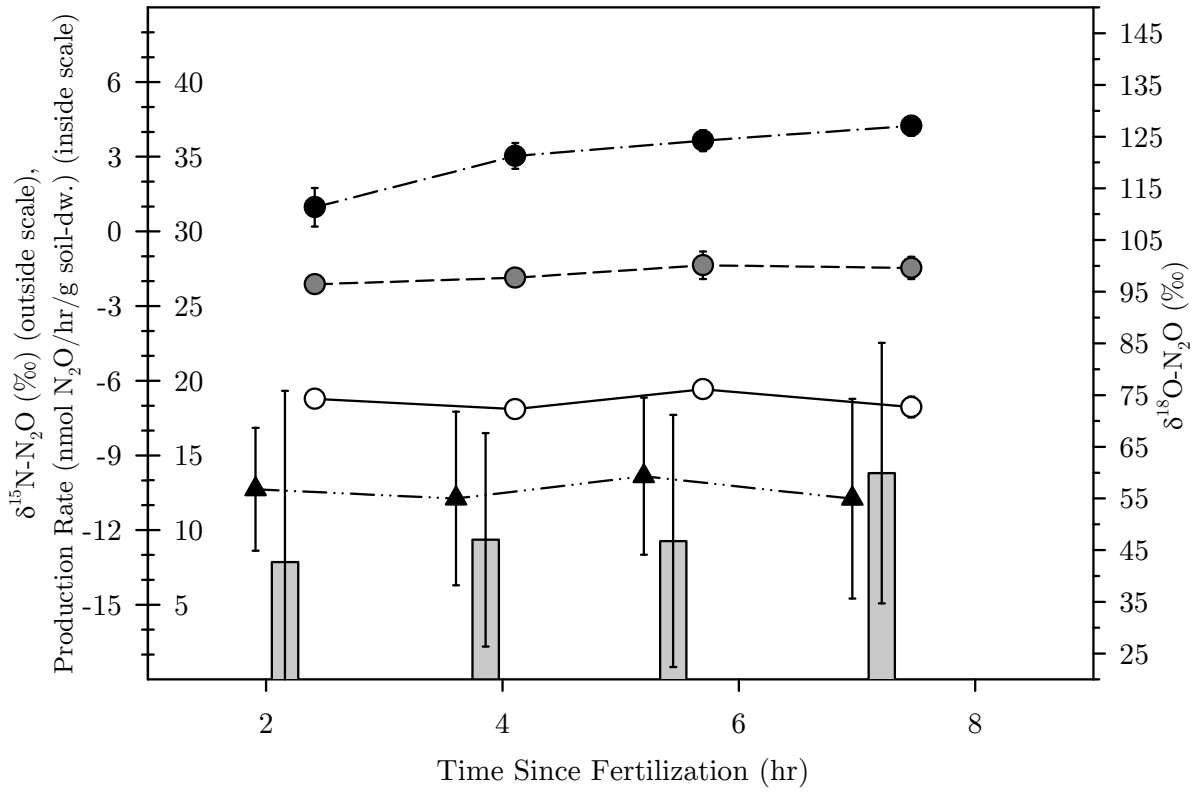


Figure 3.3a-e. N_2O production, δ^{15}N-N_2O (rel. AIR), and δ^{18}O-N_2O (rel. VSMOW) versus time for flooded and non-flooded anaerobic incubations of agricultural soil and stream sediment. Each N_2O production rate (bar plot) and δ^{15}N-N_2O symbol (triangle) represents a mean value with $n = 9$. Each δ^{18}O-N_2O symbol represents a mean value with $n = 3$, and corresponds to soils incubated with water at low (white circle), medium (grey circle), and high (black circle) ^{18}O-enrichment. Error bars represent 1σ from the mean, and, where they are absent, the error is smaller than the size of the symbol. All scales are identical on every plot.

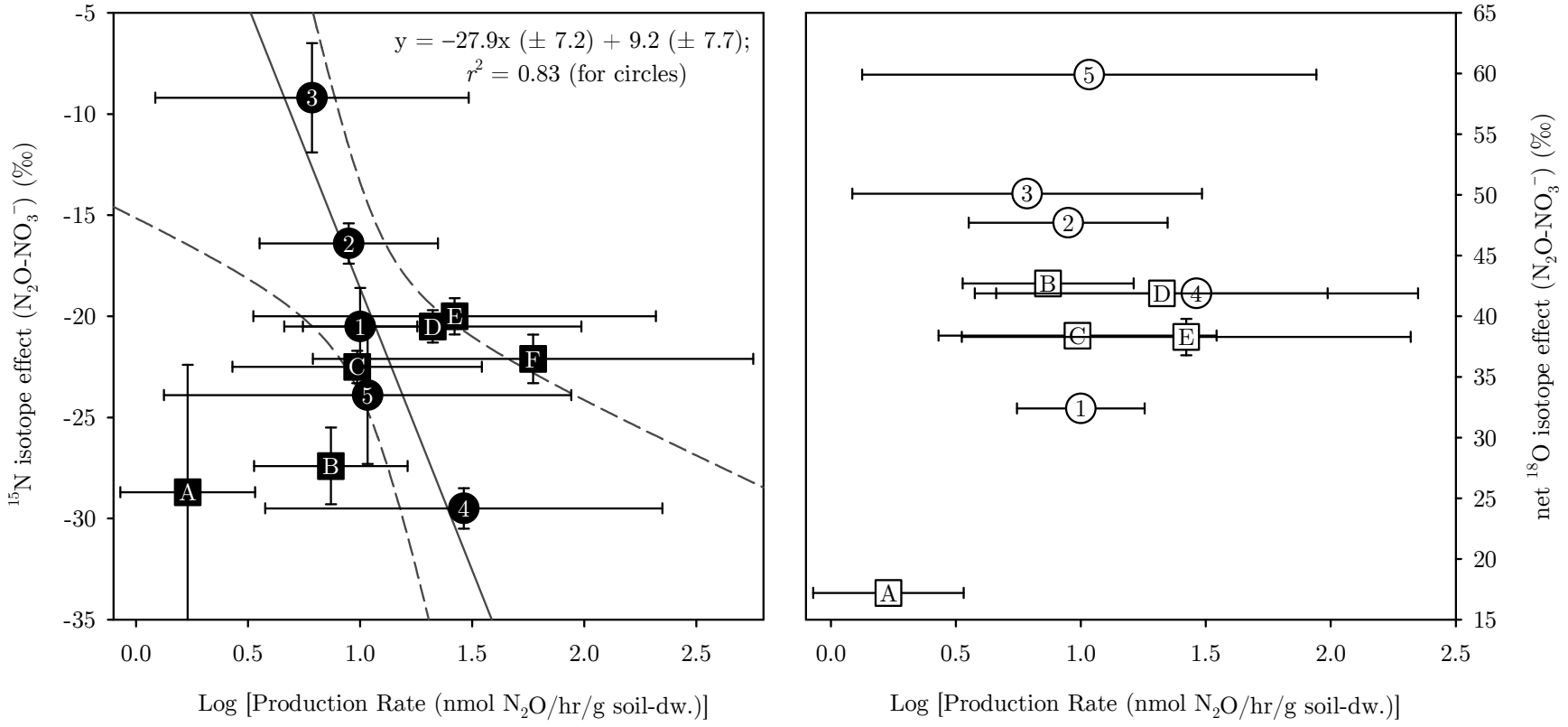


Figure 3.4. The relationship between the ^{15}N isotope effect (left side) and the ^{18}O isotope effect (right side) and the rate of net N_2O production by denitrification. Data collected in this study (circles) are labelled by treatment number, and data collected for Chapter 2 (squares) is labelled by treatment letter. There is a significant, negative exponential relationship (slope is not equal to zero) between the ^{15}N ε and the production rate in the agricultural soils (grey regression line, 95% confidence interval, and equation with standard error shown); yet the relation is weak and largely controlled by treatments 3 and 4. There are no other apparant relationships between the isotope effects and the N_2O production rate. The production rate data was $\log_{10}$ transformed to facilitate linear regression.

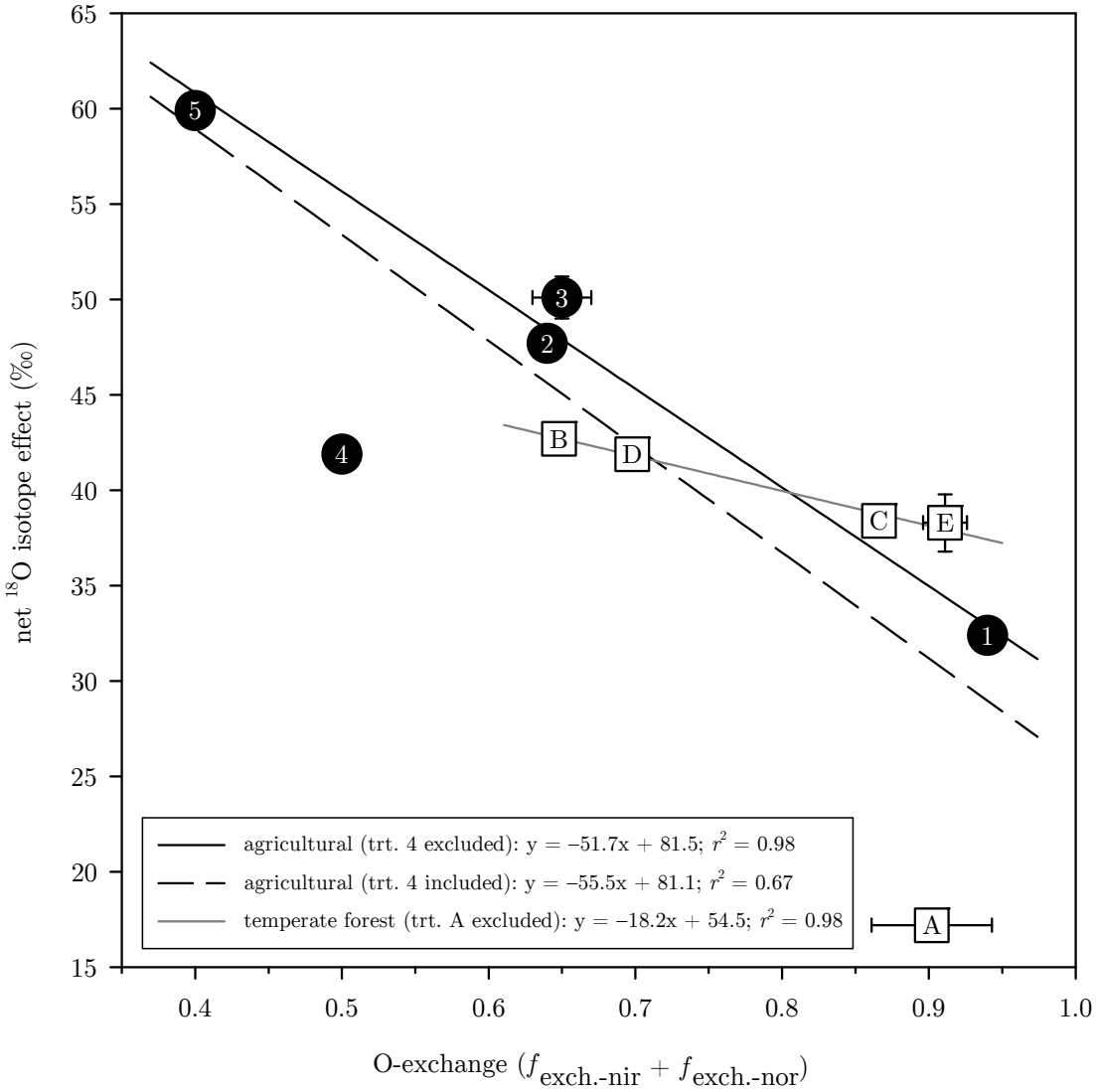


Figure 3.5. A regression of the net ^{18}O isotope effect versus O-exchange. Two lines are shown through the agricultural soils data (black circles with corresponding treatment numbers) representing regression with and without treatment 4 as an outlier. One regression line is shown through the forested soils data (white squares with corresponding treatment numbers) with treatment A excluded as an outlier. Model II linear regression (ranged major axis) is used because both ^{18}O ε_{net} and O-exchange are subject to natural variation.

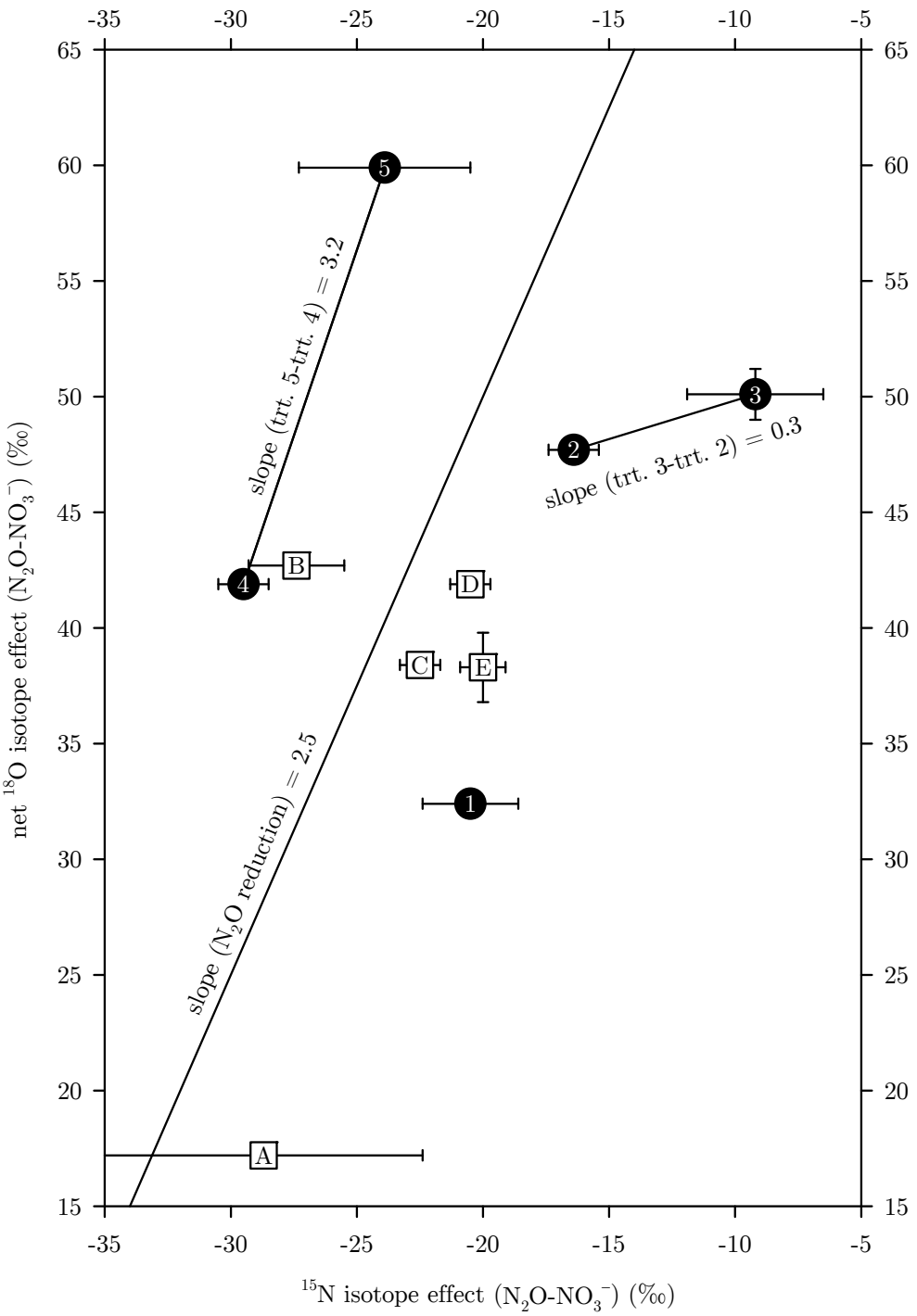


Figure 3.6. The oxygen and nitrogen isotope effects of the agricultural soils incubated in this study (black circles, labelled by treatment number) and the temperate forest soils of Chapter 2 (white squares, labelled by treatment letter). The ratio of the oxygen and nitrogen isotope effects for N_2O reduction is ~2.5:1 (Chapter 2, Table 2.1). This figure would suggest that in the stream sediment, more N_2O reduction occurred in treatment 5 (flooded) than in treatment 4 (non-flooded).

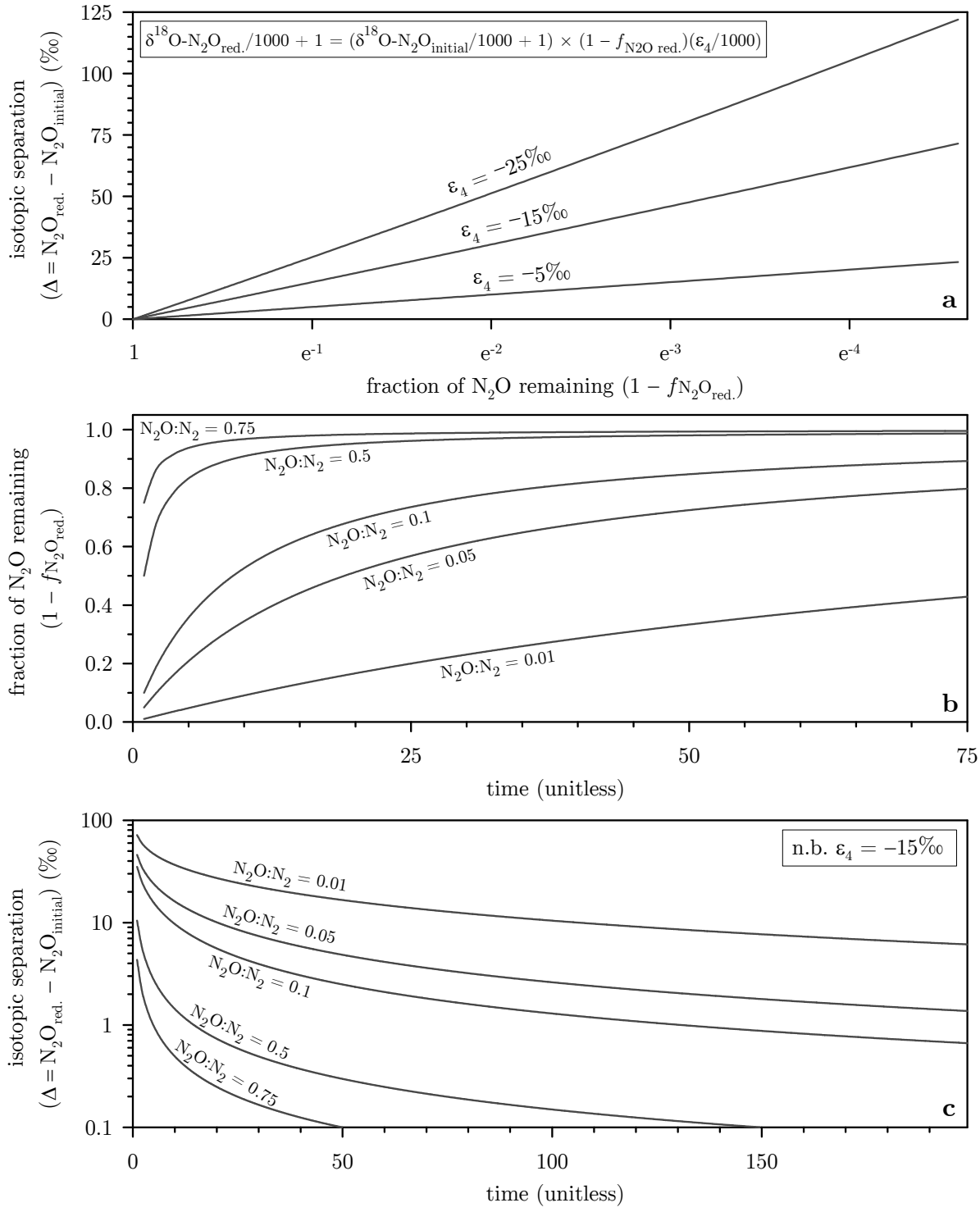


Figure 3.7. Predicting the δ^{18}O-$N_2O_{red.}$ value in open and closed systems. **a.** A closed system Rayleigh distillation of δ^{18}O-$N_2O_{red.}$ using different values of the isotope effect of N_2O consumption. **b.** In an open system with net N_2O production and N_2O consumption the fraction of N_2O remaining in the system increases with time and approaches 1. The rate of increase is governed by the N_2O:N_2 ratio. **c.** As the remaining fraction of N_2O approaches 1, the observed $^{18}O/^{16}O$ discrimination decreases, and the δ^{18}O-$N_2O_{red.}$ approaches the initial δ^{18}O value.

Reproduced with permission from:

Snider DM, Spoelstra J, Schiff SL, Venkiteswaran JJ (2010) Stable oxygen isotope ratios of nitrate produced from nitrification: ^{18}O-labeled water incubations of agricultural and temperate forest soils. *Environmental Science & Technology*, **44(14)**, 5358–5364. doi:10.1021/es1002567

© 2010 American Chemical Society

4 Stable oxygen isotope ratios of nitrate produced from nitrification: ^{18}O-labeled water incubations of agricultural and temperate forest soils

Overview

In many nitrate (NO_3^-) source partitioning studies, the $\delta^{18}O$ value for NO_3^- produced from nitrification is often assumed to reflect the isotopic compositions of environmental water (H_2O) and molecular oxygen (O_2) in a 2:1 ratio. Most studies that have measured or observed this microbial endmember have found that the $\delta^{18}O$-NO_3^- was more positive (up to +15‰ higher) than the assumed value. Current understanding of the mechanism(s) responsible for this discrepancy is limited.

Incubations of one temperate forest soil (organic) and two agricultural soils (mineral) were conducted with ^{18}O-labeled H_2O to apportion the sources of oxygen in NO_3^- generated from nitrification. The NO_3^- produced in all soils had $\delta^{18}O$ values that could not be explained by a simple endmember mixing ratio of 2:1. A more comprehensive model describing the formation of microbial NO_3^- was developed, which accounts for oxygen exchange between H_2O and NO_2^-, and includes terms for kinetic and equilibrium isotope effects. Oxygen isotope exchange (i.e., the fraction of NO_3^--oxygen that originates from the abiotic exchange of H_2O and NO_2^-) varied widely between the temperate forest soil (0.37) and the two agricultural soils (0.52 and 0.88). At present, the microbial endmember for nitrification cannot be successfully predicted.

4.1. *Introduction*

Stable isotope ratios of nitrogen ($^{15}N/^{14}N$) and oxygen ($^{18}O/^{16}O$) are often employed in studies investigating the sources of nitrate (NO_3^-) in the environment. Atmospherically-deposited NO_3^-, synthetic NO_3^- fertilizer, and NO_3^- generated from the nitrification of ammonium (NH_4^+) derived from: (i) soils; (ii) atmospheric deposition, and (iii) sewage and manure are isotopically unique (Xue *et al.* 2009). Dual NO_3^- isotope analysis ($\delta^{15}N$ and $\delta^{18}O$) has been successfully used to differentiate sources of NO_3^- in groundwaters (e.g., Aravena *et al.* 1993; Wassenaar 1995), surface waters (e.g., Mayer *et al.* 2002; Anisfeld *et al.* 2007; Lee *et al.* 2008), and catchment studies (e.g., Spoelstra *et al.* 2001; Burns and Kendall 2002; Pardo *et al.* 2004).

In most source apportionment studies, $\delta^{18}O$ values of microbially-derived NO_3^- are not measured. Instead, this endmember is estimated based upon knowledge of the fractional contributions and isotope ratios of water (H_2O) and molecular oxygen (O_2) during chemolithoautotrophic nitrification. The formation of hydroxylamine (NH_2OH) from NH_4^+ is catalyzed by ammonia monooxygenase and the oxygen atom incorporated during the reaction is derived from O_2 (Hollocher *et al.* 1981; Andersson and Hooper 1983). NH_2OH is then oxidized to NO_2^- by hydroxylamine oxidoreductase and H_2O is the source of the second oxygen atom (Andersson and Hooper 1983). The final oxidation step of nitrification is catalyzed by nitrite oxidoreductase and H_2O contributes the third oxygen atom to form NO_3^- (Aleem *et al.* 1965; Hollocher 1984; DiSpirito and Hooper 1986). Knowing this, the expected $\delta^{18}O$ value for microbial NO_3^- in units of per mill (‰) relative to (rel.) Vienna Standard Mean Ocean Water (VSMOW) is commonly given by Equation 4.1.

$$\delta^{18}O\text{-}NO_3^- \text{ (rel. VSMOW)} = [(\tfrac{1}{3}R_{O2} + \tfrac{2}{3}R_{H2O}) \div R_{VSMOW}] - 1 \qquad [4.1]$$

where, R is the $^{18}O/^{16}O$ ratio of O_2, H_2O or VSMOW.

A limited number of studies have actually measured $\delta^{18}O$ of microbial NO_3^- and the results vary between 0‰ and +16‰ (Figure 4.1). In most cases, these values are higher than

what would be predicted from Equation 1. Several reasons have been proposed to explain why $\delta^{18}O$ values of microbial NO_3^- may be higher than expected (Mayer *et al.* 2001; Spoelstra *et al.* 2007), and these primarily include mechanisms that cause the $\delta^{18}O$ values of O_2 and H_2O used by nitrifiers to deviate from commonly assumed values that are used in Equation 1. For example, the reservoir of O_2 used to oxidize NH_4^+ to NH_2OH may be different from atmospheric O_2 (+23.5‰; Kroopnick and Craig 1972) due to respiratory O_2 consumption. In addition, evaporation can cause an ^{18}O-enrichment of the soil water available to nitrifiers.

The first estimates of kinetic ^{18}O isotope fractionation during nitrification in cultures of marine bacteria were recently provided by Casciotti *et al.* (2010). The combined isotope effect (ε; where $\varepsilon = \alpha - 1$, and $\alpha = R_{product} \div R_{substrate}$) for O_2 and H_2O incorporation during the initial oxidations of NH_4^+ to NO_2^- ($\varepsilon_{k,O2} + \varepsilon_{k,H2O,1}$) ranged from −38‰ to −18‰. These findings are in accordance with what is commonly observed for O_2 uptake during respiration (e.g. bacterial respiration; ε = −29‰ to −8‰) (Lane and Dole 1956). Buchwald and Casciotti (2010) calculated the isotope effect for H_2O uptake during the final oxidation of NO_2^- to NO_3^- ($\varepsilon_{k,H2O,2}$ = −25‰ to −9‰). Prior to these studies, $^{18}O/^{16}O$ fractionation during uptake of O_2 and H_2O was not included in the simple 2:1 model that describes the formation of microbial NO_3^- (Equation 1).

Other researchers have suggested that, in addition to chemolithoautotrophic nitrification, other microbial processes may be involved in soils. Mayer *et al.* (2001) found that only one-third of the oxygen of microbial NO_3^- produced in raw humus was derived from water and suggested that heterotrophic nitrification was the predominant nitrifying process in their coniferous soil. Recent discoveries of high abundances of the Archaeal amoA gene in some soils questions whether or not ammonia-oxidizing Archaea may play a vital role in soil nitrification (e.g., Leininger *et al.* 2006; Jia and Conrad 2009).

It is also possible for $\delta^{18}O$ values of microbial NO_3^- to be lower than those calculated by Equation 1. Previous studies of *Nitrosomonas europaea* cultures observed an exchange of oxygen (O-exchange) between H_2O and NO_2^- that was concomitant with NH_4^+ oxidation (Andersson *et al.* 1982; Andersson and Hooper 1983). Casciotti *et al.* (2010) calculated that

1–25% of the oxygen atoms in NO_2^- had exchanged with H_2O during NH_4^+ oxidation in bacterial cultures of marine nitrifiers. The O-exchange observed in these studies is likely explained by the abiotic equilibration of H_2O and NO_2^- ($H_2{}^{18}O + N^{16}O_2 \rightleftharpoons N^{18}O_2 + H_2{}^{16}O$) (Casciotti *et al.* 2007). In contrast, Buchwald & Casciotti (2010) calculated very little O-exchange (0–3%) during NO_2^- oxidation to NO_3^- by *Nitrobacter* and *Nitrococcus spp.* Similar findings were reported in Hollocher (1984) and DiSpirito and Hooper (1986) although the latter observed active intermolecular O-exchange among NO_3^- molecules.

Oxygen exchange with H_2O during nitrification would reduce or eliminate the isotopic signal from the oxygen of O_2 incorporated during the initial NH_4^+ oxidation step, thereby producing soil NO_3^- with $\delta^{18}O$ values closer to those of the available H_2O. The occurrence of O-exchange during nitrification in natural soils has not yet been documented, nor has it been adequately explored. O-exchange with H_2O during denitrification in forest soils, however, is well-documented (Snider *et al.* 2009). If O-exchange during nitrification in soils does occur to an appreciable degree, researchers may unknowingly overestimate the contribution of microbial NO_3^- to a mixed-source pool. Consequently, estimates of N turnover and N sources may be miscalculated. The main objective of this study, therefore, is to quantify the fraction of NO_3^- oxygen atoms derived from H_2O and O_2 during nitrification in temperate forest and agricultural soils and develop a more comprehensive model of the formation of microbial NO_3^-.

4.2. *Materials and Methods*

4.2.1. *Soil Collection, Processing, and Characterization*

Soil was collected from a highly humified, organic-rich, Oh-horizon found in a mixed sugar maple-yellow birch upland temperate forest (Turkey Lakes Watershed, Sault Ste. Marie, Ontario, Canada; www.tlws.ca) described in (Jeffries *et al.* 1988). Bulk mineral soil was also collected (ground surface down to 25 cm) from two intensively tilled agricultural fields with distinct organic matter (OM) contents (Strawberry Creek Watershed, Maryhill, Ontario, Canada) described in (Petrone *et al.* 2006). Crop residue was removed before collection. All soils

were air-dried, homogenized, sieved to 2 mm, and stored for later use. Concentrations of total carbon (TC) and total nitrogen (TN) were determined by elemental analysis (EA). Organic matter (%) was quantified by loss on ignition (LOI). Soils were extracted with 2 M potassium chloride (KCl) and Nanopure deionized water (DI) (Barnstead International, Dubuque, IA) for determination of extractable NH_4^+ and NO_3^-, respectively. Soil pH was determined in H_2O and calcium chloride ($CaCl_2$) (ASTM International 2007). These methods are described in greater detail in Snider *et al.* (2009) and the results of these analyses are shown in Table 4.1.

4.2.2. *Incubations*

Soils were suspended within glass jars in rigid, porous sacs made from nylon screening to promote rapid and homogenous mixing of soil gases. A detailed description of the incubation chambers is provided by Snider *et al.* (2009). Agricultural soils were amended with reagent-grade NH_4Cl because pilot experiments with unfertilized soils revealed very slow N mineralization (results not shown). The ammonium salt was dissolved in deionized water (DI) and applied to the soils at the onset of incubation at an application rate of 0.15 mg N/g-soil (dry weight equivalent). NH_4^+ fertilization of the temperate forest soil was unnecessary because the rates of mineralization and nitrification in unamended soil were high enough to produce sufficient NO_3^- for isotopic analysis.

To assess the relative contributions of H_2O-oxygen and O_2-oxygen to NO_3^- during nitrification, each soil was amended with three waters that had distinct ^{18}O enrichments (Table 4.2). Each treatment was replicated three times, for a total of nine incubations per soil type. The soil waters were prepared by diluting 1.6 atom% $^{18}O\text{-}H_2O$ standard (Bio-Rad Laboratories, Hercules, CA) with Nanopure DI (Barnstead International, Dubuque, IA) ($\delta^{18}O = -10.8‰$). The air-dried soils contained small amounts of residual soil water that needed to be isotopically characterized. Azeotropic distillation with toluene (Revesz and Woods 1990) was used to extract water not bound within the particle matrices of the air-dried soils. The isolated water was subsequently analyzed for $\delta^{18}O\text{-}H_2O$ following methods outlined in Snider

et al (2009). The final $\delta^{18}O$-H_2O values of the soil water in the incubated soils were calculated (mixture of ^{18}O-labelled DI and residual endogenous soil water) (Table 4.2).

After the soils were moistened to 50% water holding capacity (WHC), incubation chambers were sealed and the headspace was flushed for 25 minutes at 600 mL/min with a commercial gas mixture (Praxair Canada, Inc.) containing 20.9% O_2 ($\delta^{18}O$-O_2 = +25.7‰ rel. VSMOW) balanced with ultra-high purity helium. $\delta^{18}O$-O_2 analysis was performed on a modified Micromass Isochrom IRMS and details of this method are described in Wassenaar and Koehler (1999). The incubation chamber headspace was flushed every 1–2 weeks throughout the experiment to maintain aerobic conditions (favouring nitrification with a constant $\delta^{18}O$-O_2 signature) and reduce the likelihood of denitrification. The masses of the incubation chambers were monitored throughout the experiment to assess the degree of evaporative H_2O loss that occurred during the short flushing events. In all replicates, the loss of H_2O was insufficient to cause measureable evaporative ^{18}O-enrichment of the soil waters (results not shown). Soils were incubated in the dark at room temperature (21–23 °C).

All replicates of temperate forest soil (n = 9) were incubated for 15 weeks (106 days), after which NH_4^+ and NO_3^- were extracted. Extractions of agricultural soils were conducted at different time intervals to investigate the temporal variation in the isotopic signature of NO_3^-. For both agricultural soils, one replicate of each treatment was extracted after 25, 37, and 52 days.

4.2.3. *Nitrate Isotope Analysis*

The $\delta^{18}O$ of NO_3^- was analyzed by methods adapted from Chang *et al.* (1999) and Silva *et al.* (2000) and are briefly described here. Samples were acidified to pH 5.0 with 10% HCl to remove carbonate species. Following acidification, sulphate and phosphate were removed from the extractants by precipitation with barium chloride and subsequent filtration through a 0.2 μm membrane filter. Excess barium was removed and NO_3^- was concentrated by passing samples through columns packed with BioRad AG 1-X8 (100–200 mesh, chloride form) anion exchange resin. NO_3^- was eluted from the columns with 3M HCl and the samples were neu-

tralized with Ag_2O. The AgCl precipitate was removed by filtration through a 0.2 μm membrane filter and the remaining solutions were freeze-dried. The solid $AgNO_3$ was stored in the dark in amber vials until analysis of stable isotopic ratios.

Dissolved organic matter (DOM) contains a large quantity of oxygen and this may interfere with the isotopic analysis of NO_3^- if the proportion of DOM relative to NO_3^- is high. In this study an additional DOM removal step was unnecessary because the anion exchange resin used had a high affinity for DOM, and even after the addition of 3M HCl, DOM was retained on the resin (Spoelstra *et al.* 2004, 2007). Additionally, the soil extractants contained very high concentrations of NO_3^- (80–90 mg N/L) and therefore the mass of NO_3^- was sufficient for isotopic measurement in small volumes of extractant (30 mL; i.e., high NO_3^-:DOM ratio). Samples were diluted to 300 mL with Nanopure DI before being passed through the anion exchange resin to facilitate sorption of DOM and quantitative retention of NO_3^-.

The $^{18}O/^{16}O$ ratio of NO_3^- was analyzed using a breakseal method described in Spoelstra *et al.* (2001) and analyzed on a VG PRISM mass spectrometer. Three standard reference materials for oxygen isotope analysis were converted to $AgNO_3$ and used to relate samples to VSMOW. These standards have $\delta^{18}O\text{-}NO_3^-$ values of −27.9‰ (USGS 34; Böhlke *et al.* 2003), +28.0‰ (commercial KNO_3 internal standard), and +57.5‰ (USGS 35; Böhlke *et al.* 2003) relative to VSMOW. The analytical precision for $\delta^{18}O$ was ± 0.8‰. All results are reported as delta (δ) values in units of per mill (‰), where $\delta = (R_{sample} \div R_{standard} - 1)$, and R is the isotopic ratio ($^{18}O/^{16}O$) of the sample or standard, respectively. All kinetic isotope effects ($^{18}\varepsilon_k$) are in ‰ units, where $\varepsilon = \alpha - 1$, and $\alpha = R_{product} \div R_{substrate}$.

4.3. *Results and Discussion*

4.3.1. *Nitrite Accumulation in High OM Agricultural Soil*

Large amounts of NO_2^- were detected in all replicates of the high OM agricultural soil extracted on day 25. The mass of NO_2^--N present in replicates a, d, and g was 68%, 65%, and 70% of the total pool of NO_3^- + NO_2^-, respectively. Incomplete nitrification of NH_4^+ to

NO_3^- is occasionally observed in cultivation, incubation, and field studies, and may be explained by slow growth rates of NO_2^- oxidizing bacteria. For example, bioreactor cultivations of nitrifiers revealed that *Nitrosomonas europaea* more readily recovered from starvation than did *Nitrobacter winogradskyi* (Tappe *et al.* 1999). Smith *et al.* (1997) observed NO_2^- accumulations in several streams of Northern Ireland that also contained free ammonia (NH_3). They explained that the presence of free NH_3 partially inhibits NO_2^- oxidation by *Nitrobacter spp.* but that it does not affect NH_4^+ oxidizers.

Regardless of the mechanism(s) responsible for NO_2^- accumulation in these replicates, there is obvious dissimilarity in the $\delta^{18}O$ values between the NO_3^- extracted from these soils at day 25 and the NO_3^- extracted at days 37 and 52 (Table 4.2). We conducted a separate test to examine the ability of the anion exchange resin to retain NO_2^- and found that in all cases, the masses of NO_2^--N in the high OM agricultural soils retained on the columns were incomplete and variable (rep. a–3%; rep. d–69%; rep. g–18%). Incomplete retention of NO_2^- could lead to isotopic fractionation because isotopically depleted NO_2^- may be preferentially bound to the resin (Silva *et al.* 2000). In addition, it is unknown if NO_2^- is chemically converted to NO_3^- or $AgNO_2$ in the later stages of the methods used here to prepare the samples for isotopic analysis. For these reasons, the $\delta^{18}O\text{-}NO_3^-$ values obtained from the extracts of high OM agricultural soils on day 25 (Table 4.2; italicized values) were excluded from any further data analysis and interpretation. We recommend that all isotopic studies of NO_3^- (regardless of the method used to analyze $^{18}O/^{16}O$) quantify NO_2^- and account for its presence to avoid complications in data interpretation (Casciotti *et al.* 2007). Current methods of NO_2^- removal using ascorbic acid (Granger *et al.* 2006) or sodium azide (McIlvin and Altabet 2005) have not been tested with the anion exchange method that was used in this study, and these methods may not be compatible with samples that contain high dissolved OM.

4.3.2. *Nitrogen Mineralization*

The NH_4Cl fertilizer was rapidly consumed in the agricultural soils. Mean ($\pm$ 1σ) accumulations of NO_3^- (and NO_2^-, where applicable) in all replicates of the low and high OM agricul-

tural soils were 114% (± 5%) and 118% (± 6%) of the applied NH_4^+, respectively. In most cases, replicates extracted at 37 and 52 days had the same amount of NO_3^- as replicates extracted at day 25, indicating that little to no NO_3^- was formed during the second half of the experiment and that the natural rate of ammonification in the agricultural soils is very low. $\delta^{18}O$ values of the NO_3^- extracted from these soils remained relatively unchanged with time (Table 4.2 - not including high OM soil replicates at day 25), indicating that once the NO_3^- was formed, there was little further processing of the newly formed NO_3^-. We are unable to calculate precise rates of mineralization and nitrification for the agricultural soils because all the added NH_4^+ was consumed by day 25. Estimates of net mineralization (net change in mass of NH_4^+-N plus NO_3^--N over the experimental period) range from 1.5 μg N/g soil dwt./day (high OM agricultural soil rep. g) to much lower values for most of the other replicates (~0.5 μg N/g soil dwt./day). Rates of net nitrification (net change in mass of NO_3^--N over the experimental period) in these soils were greater than 6 μg NO_3^--N/g soil dwt./day.

High concentrations of TN (1.2%) and TC (19.1%) in the temperate forest soil, with a corresponding C:N ratio of 18.4 (Table 4.1), presented favourable conditions for positive net mineralization of soil organic nitrogen (SON) (Jensen 1929). Extractions at the end of the experiment showed that large accumulations of inorganic N occurred in all replicates after 106 days of incubation, corresponding to net increases of NH_4^+ and NO_3^- of ~4100% and ~1400%, respectively. The mean rate of mineralization was 6.4 μg N/g soil dwt./day, and the mean rate of nitrification was 2.2 μg NO_3^--N/g soil dwt./day. These values are typical for soils collected from the TLW, which have an unusually high turnover of N and very large reserves of organic N (~750 kmol/ha) in the effective rooting zone (Foster *et al.* 1986, 1989). Our calculated nitrification rate is comparable to a mor soil (3.3 μg NO_3^--N/g soil dwt./day) and a raw humus soil (1.0 to 1.7 μg NO_3^--N/g soil dwt./day) reported in Mayer *et al.* (2001). The net accumulation of NO_3^--N measured in this study represents 36% of the total inorganic N (NO_3^- + NH_4^+) mineralized and is consistent with previous lab incubations of TLW soil (31.5%; Foster *et al.* 1986) and *in situ* buried bag incubations of forest floor (35%; Foster *et al.* 1989).

4.3.3. *Sources of ^{18}O in Microbial Nitrate*

The $\delta^{18}O\text{-}NO_3^-$ was strongly correlated to $\delta^{18}O\text{-}H_2O$ in all soils (r^2 range: 0.9974–0.9991; Figure 4.2), indicating that H_2O was a source of oxygen in the microbial NO_3^-. The slope of the linear regression of $\delta^{18}O\text{-}H_2O$ vs. $\delta^{18}O\text{-}NO_3^-$ is related to the fraction (f) of oxygen in the NO_3^- molecule derived from H_2O. For all soil types, this fraction (0.79–0.96) was much greater than the commonly invoked 0.67 (two-thirds).

Recent studies by Casciotti *et al.* (2010) and Buchwald and Casciotti (2010) with marine organisms have significantly improved our understanding of O-exchange and ^{18}O-fractionation during NO_2^- and NO_3^- generation. Here we show a similar, but further modified model of the formation of NO_3^- by bacterial nitrifiers (Figure 4.3). Large kinetic ^{18}O isotope effects ($^{18}\varepsilon$) are associated with the incorporation of O_2 ($^{18}\varepsilon_{k,O2}$) and H_2O ($^{18}\varepsilon_{k,H2O,1}$ and $^{18}\varepsilon_{k,H2O,2}$) (Casciotti *et al.* 2010; Buchwald and Casciotti 2010). Additionally, both intra- and extracellular abiotic O-exchange may occur between NO_2^- and H_2O (Casciotti *et al.* 2010). The equilibrium isotope effect ($^{18}\varepsilon_{eq}$) associated with this exchange is ~+14‰ at room temperature (Casciotti *et al.* 2007), so that at equilibrium, the $\delta^{18}O\text{-}NO_2^-$ value is ~14‰ higher than the $\delta^{18}O\text{-}H_2O$.

Equation 4.2 describes the formation of microbial NO_3^- based upon our improved understanding of the $\delta^{18}O$ systematics of bacterial nitrification.

$$\begin{aligned}\delta^{18}O\text{-}NO_3^- = \ & \tfrac{2}{3}\{[1 - f_{ABIOTIC}] \times [\tfrac{1}{2}(\delta^{18}O\text{-}O_2 + {}^{18}\varepsilon_{k,O2}) + \tfrac{1}{2}(\delta^{18}O\text{-}H_2O + {}^{18}\varepsilon_{k,H2O,1})] + \\ & [f_{ABIOTIC}] \times [\delta^{18}O\text{-}H_2O + {}^{18}\varepsilon_{eq}]\} + \tfrac{1}{3}[\delta^{18}O\text{-}H_2O + {}^{18}\varepsilon_{k,H2O,2}] \end{aligned} \quad [4.2]$$

The isotope effect for NO_2^- oxidation ($^{18}\varepsilon_{k,NO2\text{-}}$) does not appear in Equation 4.2 because it is not expressed in the $\delta^{18}O\text{-}NO_3^-$ when NO_2^- is fully consumed (Buchwald and Casciotti 2010). Additional O-exchange of H_2O with NO_2^- during oxidation to NO_3^- has not been observed to occur to any appreciable degree (Hollocher 1984; DiSpirito and Hooper 1986; Buchwald and Casciotti 2010), thus no enzyme-catalyzed O-exchange mechanism appears in our model. The inclusion of such a mechanism would add an additional O-exchange

term (e.g., f_{ENZYME}) to Equation 4.2, and would require a thorough understanding of if, how, and where ^{18}O-fractionation occurs during this additional O-exchange mechanism. Rearrangement of Equation 4.2 into a linear function produces Equation 4.3.

$$\delta^{18}\text{O-NO}_3^- = \tfrac{1}{3}(2 + f_{\mathrm{ABIOTIC}}) \times \delta^{18}\text{O-H}_2\text{O} + \tfrac{1}{3}[f_{\mathrm{ABIOTIC}}(2 \times {}^{18}\varepsilon_{\mathrm{eq}} - \delta^{18}\text{O-O}_2 - {}^{18}\varepsilon_{\mathrm{k,O2}} - {}^{18}\varepsilon_{\mathrm{k,H2O,1}}) + \delta^{18}\text{O-O}_2 + {}^{18}\varepsilon_{\mathrm{k,O2}} + {}^{18}\varepsilon_{\mathrm{k,H2O,1}} + {}^{18}\varepsilon_{\mathrm{k,H2O,2}}] \quad [4.3]$$

From the slopes of the linear regressions (Figure 4.2) and Equation 4.3, we can derive the fraction of abiotic O-exchange (f_{ABIOTIC}) that occurred during the incubation of our soils. The f_{ABIOTIC} for the temperate forest, low OM agricultural, and high OM agricultural soils were 0.37, 0.52, and 0.88, respectively. This shows that large fractions of NO_2^--oxygen exchanged with H_2O-oxygen in our soils, and that the $\delta^{18}\text{O-NO}_2^-$, which controls two-thirds of the $\delta^{18}\text{O-NO}_3^-$, is highly dependent upon f_{ABIOTIC}, $\delta^{18}\text{O-H}_2\text{O}$, and ${}^{18}\varepsilon_{\mathrm{eq}}$.

The rate of abiotic oxygen exchange ($H_2O \rightleftharpoons HNO_2$) is pH dependent (pKa = 3.25, Lide 2010) and at low pH rapid exchange may occur. Nitrification is an acid-generating process so at the intra- and pericellular level, pH may be much lower than the surroundings. At near-neutral pH (6 and 8) and +4 °C, Casciotti *et al.* (2007) measured 10–30% exchange within 3 weeks. They also showed that the rate of abiotic O-exchange increases with temperature.

In addition, the magnitude of f_{ABIOTIC} is a function of how much un-reacted NO_2^- is present at any given time, and how long it remains available to equilibrate with H_2O. Presumably, when the rate of nitrification has not reached a quasi steady-state ($NH_4^+ \rightarrow NO_2^- \rightarrow NO_3^-$), a build-up of NO_2^- occurs, and f_{ABIOTIC} increases. In this study, f_{ABIOTIC} was inversely related to the net nitrification rates, showing that at slower rates, there was more opportunity for H_2O–NO_2^- oxygen exchange. The high OM agricultural soil, in which a build-up of NO_2^- was observed at day 25, had the highest f_{ABIOTIC} (0.88). In contrast, the acidic temperate forest soil had the highest nitrification rate and the lowest f_{ABIOTIC} (0.37). This begs the question: does O-exchange occur appreciably in natural environments, or is it an ar-

tefact of lab-scale experiments and caused by disturbance effects? Generally, it is reported that NH_4^+ oxidation is the rate limiting step in nitrification (Schmidt *et al.* 2004), and reports of high NO_2^- concentrations in natural environments are rare. Further research is required to better understand O-exchange during nitrification, including field studies to confirm that it significantly affects $\delta^{18}O\text{-}NO_3^-$ *in situ*.

The intercept expression shown in Equation 4.3 is a function of several factors: $f_{ABIOTIC}$, $\delta^{18}O\text{-}O_2$, and four ^{18}O-isotope effects ($^{18}\varepsilon_{product-substrate}$). When the calculated values of $f_{ABIOTIC}$ and the measured value of $\delta^{18}O\text{-}O_2$ (+25.7‰) are substituted into this expression, a simplified expression is obtained that includes only terms for the ^{18}O-isotope effects. Unfortunately, there are too many unmeasured and unknown terms in our model to obtain useful estimates of the individual isotope effects or even a combined, net isotope effect. A proper estimation of the kinetic ^{18}O-isotope effects for nitrification requires an experimental approach with laboratory cultures where NH_4^+ oxidation is measured separately from NO_2^- oxidation. This cannot be done in samples containing a consortium of N cycling microorganisms such as in our soil incubation approach.

4.3.4. *Implications of O-exchange and ^{18}O Fractionation on Estimations of $\delta^{18}O\text{-}NO_3^-$*

The $\delta^{18}O\text{-}NO_3^-$ generated in the temperate forest and high OM agricultural soils were similar (fortuitously) with what would be predicted by Equation 4.1 (Figure 4.2 inset). In other words, the combined $f_{ABIOTIC}$ and ^{18}O isotope effects that occurred in these soils resulted in $\delta^{18}O\text{-}NO_3^-$ values that approximate a simple 2:1 endmember mixing model ($\delta^{18}O\text{-}H_2O$:$\delta^{18}O\text{-}O_2$). Conversely, the $\delta^{18}O\text{-}NO_3^-$ of the agricultural low OM soil was ~7‰ lower than what would be predicted by Equation 4.1.

Based on our current understanding of the ^{18}O systematics for nitrification (Equation 4.2), we cannot explain why previous measurements of $\delta^{18}O\text{-}NO_3^-$ (Figure 4.1 and references therein) are up to +15‰ higher than what would be predicted by Equation 4.1. No combination of $f_{ABIOTIC}$ (0.0–1.0) with the ^{18}O isotope effects provided by Casciotti *et al.* (2010) and Buchwald and Casciotti (2010) can produce these high $\delta^{18}O\text{-}NO_3^-$ values. This implies that

either ^{18}O enrichment mechanisms (such as respiration, evaporation, or denitrification) affected the $\delta^{18}O$ values of the O_2, H_2O, or NO_3^- in these studies (Figure 4.1), or the important kinetic ^{18}O isotope effects for O_2 and/or H_2O incorporation in soil microbial consortia differ from those measured in laboratory cultures studies.

Further experiments are required to determine the importance of O-exchange *in situ*. In the meantime, researchers using the dual NO_3^- isotope method should carefully consider the implications of a poorly defined microbial NO_3^- endmember when drawing conclusions in source partitioning studies. Common prediction approaches (e.g., Equation 4.1) that use a 2:1 endmember mixing model ($\delta^{18}O\text{-}H_2O$:$\delta^{18}O\text{-}O_2$), and neglect to account for isotope effects or O-exchange may result in inaccurate estimation of $\delta^{18}O\text{-}NO_3^-$ produced from nitrification. Scientists undertaking source-partitioning research may then make inaccurate estimations of the contribution of microbial NO_3^- to a mixed-source pool. Because the magnitude of O-exchange varies widely (this study; Casciotti *et al.* 2010), and appears to be rate related, it is unlikely that the microbial endmember for nitrification can be accurately predicted.

Table 4.1. Soil characteristics.

Soil	**temperate forest soil**	**agriculture (low OM)**	**agriculture (high OM)**
mass of soil incubated (g)[a]	26.4	60.0	60.0
water holding capacity (%)[b]	50	50	50
gravimetric soil moisture (g H_2O/g oven-dry soil)	1.13	0.26	0.39
pH (H_2O, 0.1 M $CaCl_2$)	5.1, 4.2	7.3, 7.0	7.5, 7.2
%C	19.1	1.9	8.7
%N	1.2	0.2	0.6
C:N (mol:mol)	18.4	9.7	12.7
Loss on ignition (%)	36.0	4.2	14.9
NH_4^+ (µg N / g-$soil_{dw.}$)[c]	10.4	0.2	1.1
NO_3^- (µg N / g-$soil_{dw.}$)[c]	17.3	17.2	4.8
$\delta^{18}O\text{-}NO_3^-$ (‰ $_{rel.\ VSMOW}$)[c]	5.0	15.8	8.5

[a] expressed as oven-dry weight equivalent.
[b] expressed as a percentage of gravimetric moisture content of soil at field capacity.
[c] initial N contents and $\delta^{18}O\text{-}NO_3^-$ prior to incubation or fertilization (if applicable).

Table 4.2. The net production of NO_3^- and NH_4^+, and the $\delta^{18}O$ values of soil H_2O and measured NO_3^-.

soil	replicate	incubation length (days)	ΔNO_3^- ($+ NO_2^-)_{final-initial}$ ($\mu g\ N/g\text{-}soil_{dw}$)	$\Delta NH_4^+{}_{final-initial}$ ($\mu g\ N/g\text{-}soil_{dw}$)	$\delta^{18}O\text{-}H_2O$ (‰ rel. VSMOW)[a]	Measured $\delta^{18}O\text{-}NO_3^-$ (‰ rel. VSMOW)[b]
temperate forest	a	106	239.7	420.2	−10.4	+0.9
	b	106	271.1	377.7		+3.5
	c	106	260.4	421.6		+2.5
	d	106	239.0	451.2	+68.0	+63.4
	e	106	233.4	405.0		+62.3
	f	106	231.2	465.1		+62.9
	g	106	234.4	472.0	+106.0	+93.7
	h	106	233.3	452.8		+95.3
	i	106	250.5	434.4		+95.6
agriculture (low OM)	a	25	172.6	−150.2	−6.3	−2.0
	b	37	163.3			−3.3
	c	52	179.1			−2.1
	d	25	174.6	−150.2	+41.4	+38.2
	e	37	169.6			+37.2
	f	52	172.3			+36.6
	g	25	157.9	−150.2	+94.8	+86.0
	h	37	180.4			+78.8
	i	52	175.1			+81.9
agriculture (high OM)	a	25	183.8	−151.1	−8.2	*+8.3* [c]
	b	37	171.5			+1.1
	c	52	190.4			+0.1
	d	25	171.6	−151.1	+39.4	*+22.6* [c]
	e	37	161.7			+44.6
	f	52	176.4			+43.8
	g	25	187.9	−151.1	+92.7	*+36.6* [c]
	h	37	173.5			+96.6
	i	52	187.2			+98.5

[a] ^{18}O of soil waters are calculated as: $^{18}O/^{16}O_{soil\ water} = {}^{18}O/^{16}O_{antecedent\ water} \times f_{antecedent\ water} + {}^{18}O/^{16}O_{deionized\ water} \times f_{deionized\ water}$; where, $f_{antecedent\ water} + f_{deionized\ water} = 1$.

[b] isotope ratios of NO_3^- are corrected for endogenous NO_3^- present in air-dry soils prior to incubation so that the data presented represents newly formed NO_3^-.

[c] NO_2^- accumulation in the high OM agricultural soil on day 25 affected the $\delta^{18}O$ values of the NO_3^- extracted from these soils. As a result, this data is excluded from further analysis and interpretation.

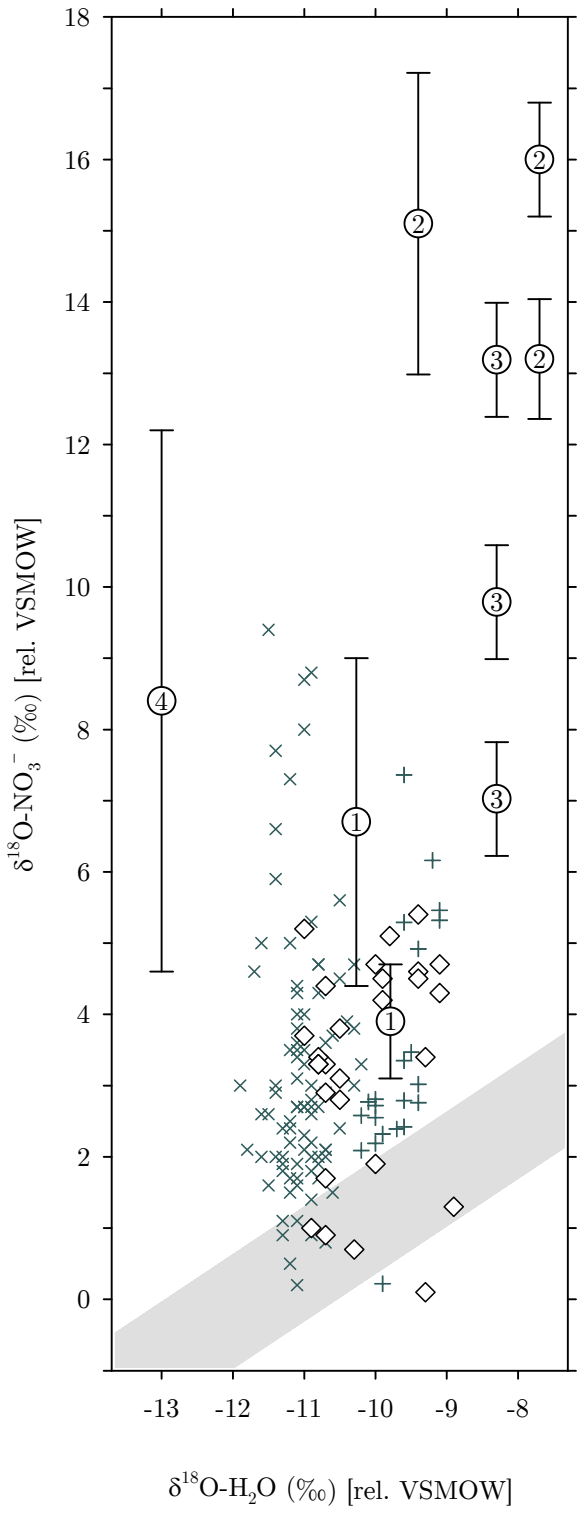


Figure 4.1. Field observations of δ^{18}O-NO_3^- produced from nitrification in groundwater [black diamond ($\diamond$) symbols (Aravena *et al.* 1993); grey thin 'ex' ($\times$) symbols (Wassenaar 1995)] and surface water [grey crosshair (+) symbols (Lee *et al.* 2008)]. Also shown are experimental measurements of microbial NO_3^- in a temperate hardwood forest [open circles #1 (Spoelstra *et al.* 2007)], and laboratory incubations of soil [open circles #2 (Burns and Kendall 2002); open circles #3 (Mayer *et al.* 2001); open circle #4 (Williard *et al.* 2001)]. Data was obtained from published tables or extracted from published figures using g3data software [http://frantz.fi/software/g3data.php (Bauer and Reynolds 2008)]. Error bars indicate 1 standard deviation from the mean value or analytical precision ($\pm$ 0.8‰) (whichever is greater). The solid grey area represents theoretical values of δ^{18}O-NO_3^- ($\pm$ 0.8‰) formed from nitrification with varying δ^{18}O-H_2O and constant δ^{18}O-O_2 (+23.5‰), and oxygen derived from H_2O and O_2 in a ratio of 2:1, respectively (Equation 5.1).

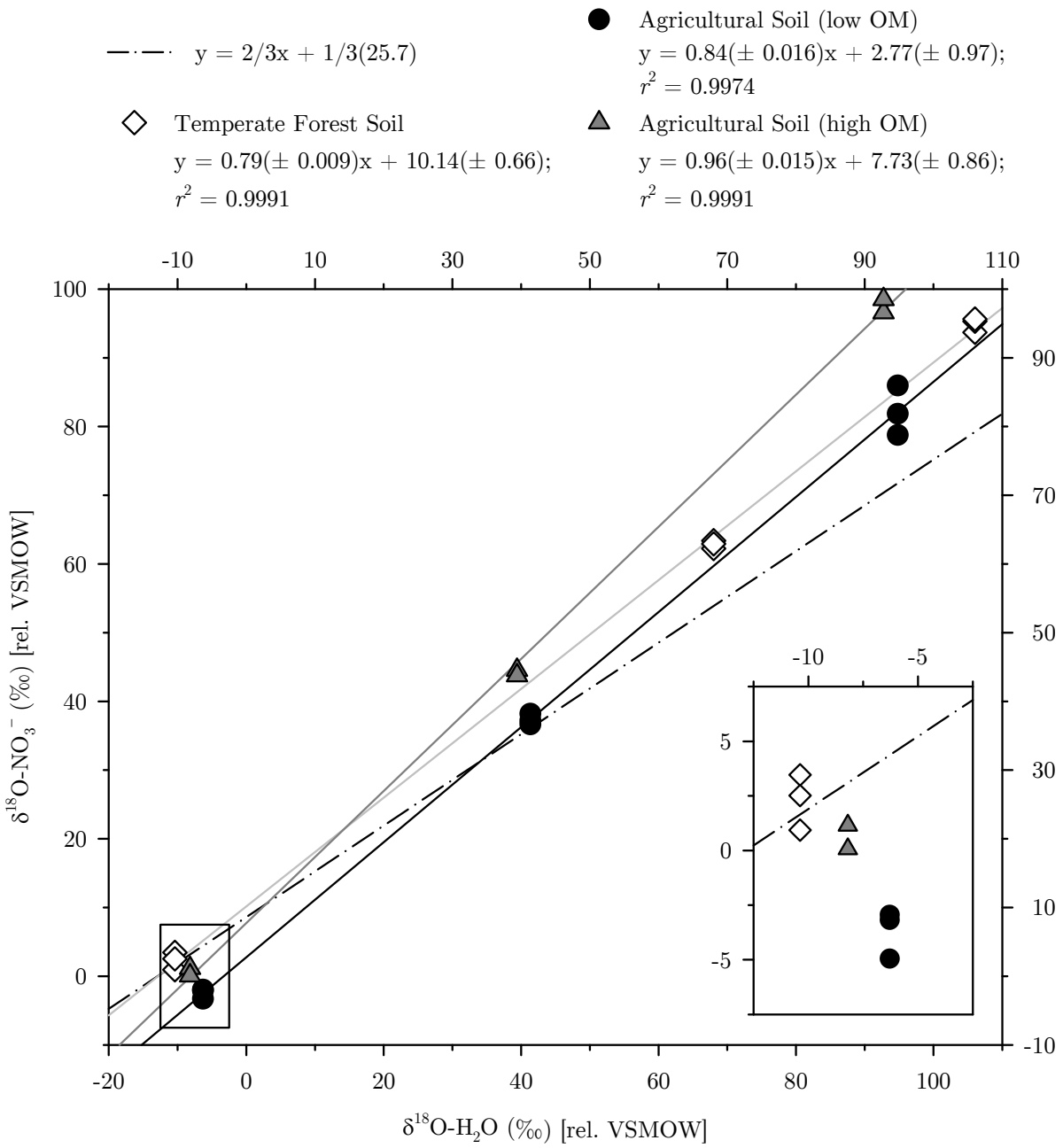


Figure 4.2. δ^{18}O-NO_3^- produced from nitrification of temperate forest and agricultural soils incubated with waters of varying δ^{18}O-H_2O. Linear regressions (± standard error) of the data and r^2 values are also shown. The dash-dot line represents δ^{18}O-NO_3^- with varying δ^{18}O-H_2O and constant δ^{18}O-O_2 (commercial gas mixture = +25.7‰), and oxygen sourced from H_2O and O_2 (in a ratio of 2:1). The inset shows an enlargement of the area of the main graph where δ^{18}O-NO_3^- is formed from soils incubated with waters at natural abundance for δ^{18}O.

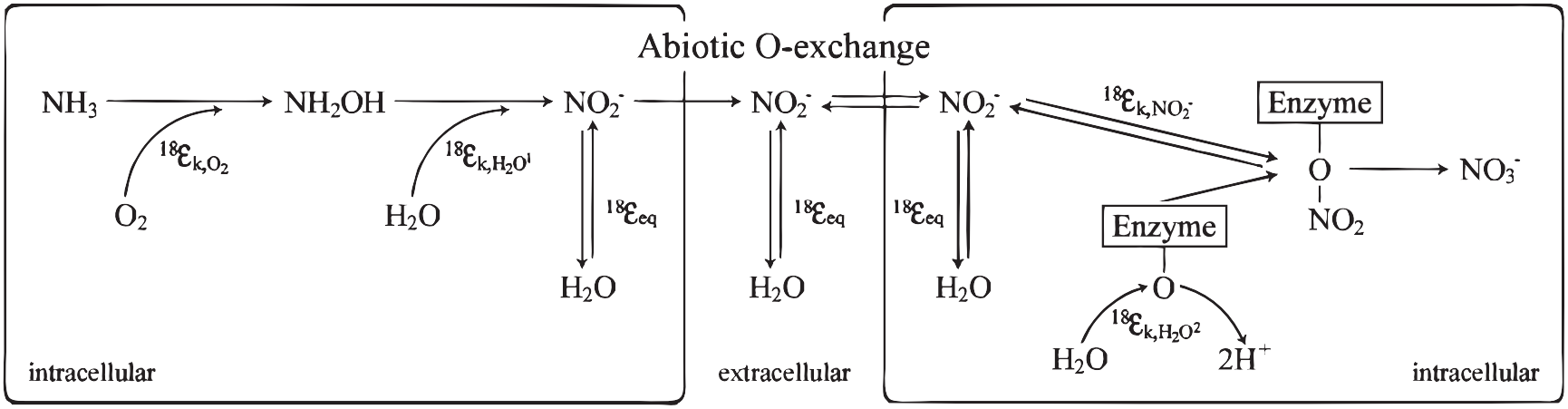


Figure 4.3. A schematic representation of bacterial nitrification modified from Casciotti *et al.* (2010) and Buchwald *et al.* (2010). The $\delta^{18}O$ of NO_3^- is largely controlled by: (i) the $\delta^{18}O$ values of O_2 and H_2O and the kinetic isotope effects ($^{18}\varepsilon_k$) that occur during their incorporation; and (ii) the fraction of intra- and extracellular abiotic oxygen exchange of H_2O and NO_2^- that occurs ($f_{ABIOTIC}$) and its associated equilibrium isotope effect ($^{18}\varepsilon_{eq}$).

5 Deciphering the oxygen isotope composition of nitrous oxide produced by nitrification

Overview

The ability to use $\delta^{18}O$ values of nitrous oxide (N_2O) to apportion environmental emissions is currently hindered by a poor understanding of the controls on $\delta^{18}O$-N_2O from nitrification (hydroxylamine oxidation to N_2O and nitrite reduction to N_2O). In this study fertilized agricultural soils and unfertilized temperate forest soils were aerobically incubated with different $^{18}O/^{16}O$ waters, and conceptual and mathematical models were developed to systematically explain the $\delta^{18}O$-N_2O formed by nitrification.

Modelling exercises used a set of defined input parameters to emulate the measured soil $\delta^{18}O$-N_2O data (Monte Carlo approach). The Monte Carlo simulations implied that abiotic oxygen (O) exchange between NO_2^- and H_2O is important in all soils, but that biological, enzyme-controlled O-exchange does not occur during the reduction of NO_2^- to N_2O (nitrifier-denitrification). Similarly, the model results indicated that N_2O consumption is not characteristic of aerobic N_2O formation.

The results of this study and a synthesis of the published literature data indicate that $\delta^{18}O$-N_2O formed in aerobic environments is well-constrained between +13‰ and +31‰ relative to VSMOW. N_2O formed via hydroxylamine oxidation and nitrifier-denitrification cannot be separated using $\delta^{18}O$ unless ^{18}O tracers are employed. The natural range of nitrifier $\delta^{18}O$-N_2O is discussed and explained in terms of our conceptual model, and the major and minor controls that define aerobically-produced $\delta^{18}O$-N_2O are identified. Despite the highly complex nature of $\delta^{18}O$-N_2O produced by nitrification this $\delta^{18}O$ range is narrow. As a result, in many situations $\delta^{18}O$ values may be used in conjunction with $\delta^{15}N$-N_2O data to apportion nitrifier- and denitrifier-derived N_2O. However, when biological O-exchange during denitrification is high and N_2O consumption is low, there may be too much overlap in $\delta^{18}O$ values to distinguish N_2O formed by these pathways.

5.1. *Introduction*

Over the last 150 years, humans have profoundly altered the global nitrogen (N) cycle by synthesizing large amounts of biologically reactive N (Galloway *et al.* 2008). A rising concentration of atmospheric nitrous oxide (N_2O) is one of the many negative consequences of increased N loads in the environment (Denman *et al.* 2007). N_2O is a potent, long-lived greenhouse gas that has a global warming potential 310 times greater than carbon dioxide over a 100-year timescale (Forster *et al.* 2007) and it continues to play an important role in the destruction of stratospheric ozone (Chipperfield 2009).

N_2O can be produced in a variety of biogeochemical settings by a number of different mechanisms. It is an obligate intermediate species of denitrification ($NO_3^- \rightarrow NO_2^- \rightarrow NO \rightarrow N_2O \rightarrow N_2$) and large N_2O emissions can occur when denitrification does not go to completion. N_2O is also a possible end-product of nitrification (ammonium oxidation). In aerobic environments N_2O can be formed by the oxidation of hydroxylamine (NH_2OH) or by the reduction of NO_2^- (nitrifier-denitrification) (Figure 5.1). Nitrifier-denitrification can be a significant source of N_2O in soils, including forest, grassland and arable soils (Kool *et al.* 2010, 2011). Much less is known about the environmental significance of the NH_2OH oxidation pathway.

Efforts to apportion different sources of N_2O emissions have included the analysis of stable isotopologue ($\delta^{15}N^{bulk}$ and $\delta^{18}O$) and isotopomeric ($\delta^{15}N^{\alpha}$ and $\delta^{15}N^{\beta}$) ratios at natural abundance, and they have yielded a better understanding of N_2O production and consumption processes (e.g., Ostrom *et al.* 2000, 2010; Perez *et al.* 2001, 2006; Bol *et al.* 2003; Well *et al.* 2005; Sutka *et al.* 2006; Toyoda *et al.* 2009; Maeda *et al.* 2010). Our current understanding of $\delta^{18}O$-N_2O produced in aerobic and sub-oxic environments is inadequate and this limits our ability to use $\delta^{18}O$ values to differentiate nitrifier-derived N_2O from N_2O formed by denitrification in anaerobic environments. A census of $\delta^{18}O$ values for N_2O reported to be formed by NH_2OH oxidation and nitrifier-denitrification yields surprisingly little data (Figure 5.2). Interestingly, all the available $\delta^{18}O$-N_2O data range between +13‰ and +29‰ (Figure 5.2a). A systematic explanation and interpretation of this narrow range in $\delta^{18}O$ values is currently unavailable, partly because all the controls on $\delta^{18}O$-N_2O are not known. There are two poten-

tial reaction pathways of N_2O formation (Figure 5.1) and a variable degree of abiotic O-exchange with H_2O and NO_2^- may occur (Casciotti *et al.* 2010; Snider *et al.* 2010). Further, there are numerous $^{18}O/^{16}O$ fractionating reaction steps and the enrichment factors may have large ranges or are currently unquantified.

One method used to investigate O isotope dynamics in the N cycle is soil incubation experiments using multiple treatments with different $\delta^{18}O$-H_2O tracers at or slightly above natural abundance (Mayer *et al.* 2001; Snider *et al.* 2009, 2010). Plots and linear regression analysis of $\delta^{18}O$-N_2O versus $\delta^{18}O$-H_2O provide constraints on the relative contributions of O endmembers (H_2O and O_2) and the fraction of O-exchange with H_2O. However, to properly interpret the slope and intercept of these plots, it is necessary to develop conceptual and mathematical models to elucidate the controlling processes involved. Such a tool does not currently exist for interpreting $\delta^{18}O$ values of N_2O generated by NH_2OH oxidation or nitrifier-denitrification.

The main purpose of this study was to gain a better understanding of the controls on $\delta^{18}O$ values of N_2O produced in aerobic settings and explain why the published global data ranges between +13‰ and +29‰ (objective 1). To achieve this, aerobic soil incubations were conducted to further characterize $\delta^{18}O$ values of N_2O produced by nitrification, including a series of incubations at multiple $\delta^{18}O$-H_2O values. To properly interpret our incubation results it was necessary to create a conceptual and mathematical model of O systematics during aerobic N_2O production and develop equations that described the slope and intercept of the linear regressions of $\delta^{18}O$-N_2O versus $\delta^{18}O$-H_2O (objective 2). Finally, using the soil incubation data and the equations derived from the mathematical model, a Monte Carlo modelling approach was employed to place constraints on the fractions of O-exchange and N_2O reduction that occurred in the soil incubations (objective 3).

5.2. *Materials and Methods*

5.2.1. *Experimental*

Mineral agricultural soils with varying organic matter (OM) contents (Table 5.1) were collected from two locations in the Strawberry Creek Watershed, located approximately 20 km northeast of Waterloo, ON, Canada (Petrone *et al.* 2006). These soils were under continuous cultivation and mechanically tilled so there were no distinct soil horizons present. In both locations bulk soil was collected from the surface down to a depth of 25 cm. In addition, organic-rich upland (Oh horizon) and wetland (peat) temperate forest soils were collected from the Turkey Lakes Watershed (TLW), located approximately 50 km north of Sault Ste. Marie, ON, Canada (www.tlws.ca; Jeffries *et al.* 1988). All soils were air-dried, sieved to 2 mm, and thoroughly homogenized prior to storage in air-tight, plastic freezer bags.

In order to characterize the $\delta^{18}O$ values of N_2O produced by nitrification, six separate experiments, differing in soil type, moisture and temperature, were conducted (Table 5.1). The experiments were not designed to directly compare different environmental effects; rather, our goal was to achieve a wide range in $\delta^{18}O$-N_2O across experiments so that the variability of the processes that control $\delta^{18}O$-N_2O (e.g., O-exchange) could be estimated. All incubations were conducted in the dark at ambient laboratory temperatures (~22 °C) except for Experiment 5, which was cooled to 9 °C in a dark refrigerated chamber.

Experiments 1–3 were incubated with $\delta^{18}O$-H_2O at natural abundance and at two higher ^{18}O-H_2O enrichments (treatments a–c, Table 5.1). The $\delta^{18}O$-H_2O was varied to quantify the amount of O-exchange during the formation of N_2O (this study) and nitrate (NO_3^-) by nitrification (Snider *et al.* 2010). The different $\delta^{18}O$-H_2O incubations were replicated 3 times, so that each of Experiments 1–3 had 9 replicate incubation jars. Experiments 4–6 were only incubated with $\delta^{18}O$-H_2O at natural abundance (Table 5.1). Analysis of $\delta^{18}O$-H_2O was done by CO_2 equilibration (Epstein and Mayeda 1953) on an isotope ratio mass spectrometer (IRMS) VG MM 903 (Environmental Isotope Laboratory, University of Waterloo, Waterloo, ON).

Incubations were conducted in 500 mL media jars (actual volume ≈ 590 mL) sealed with thick, halo-butyl rubber stoppers (43 mm, 2-leg lyophilization) that were washed in sodium hydroxide and baked prior to use. Additional silicon septa were placed on top of the stoppers and the jars were sealed with open-topped screw caps. Approximately 60 g of agricultural soil or 26 g of temperate forest soil (oven-dry equivalent) was placed inside the incubation chambers on top of rigid, porous sacs made from nylon screening. The soil/screening apparatus was suspended in the jars to increase the soil's surface area and promote homogenous mixing of gases. The total gas-filled volume of the incubation chamber was 92% (± 2%) of the total jar volume.

The gravimetric water content of each soil was determined by drying a known weight of air-dried soil in an oven at 105 °C until a constant weight was obtained. The water holding capacity (WHC) was determined by filling 100 cm^3 cylinders with a known weight of soil to a density that approximated the incubation conditions (soils were not packed). The bottoms of the cylinders were covered with coffee filters. The soils were placed inside a large desiccator and saturated (but not submerged) with deionized water (DI) overnight under a vacuum. After a 24-hour drainage period at ambient pressure the %WHC was determined gravimetrically. Three replications were conducted for each soil type, and the contribution of water held in the coffee filters after 24-hours was determined using empty cylinder blanks.

At the onset of incubation, air-dried soils were slowly moistened with DI to moisture contents corresponding to 50–75% WHC (Table 5.1). Experiments 1 and 2 were fertilized with reagent-grade ammonium chloride (NH_4Cl; 0.15 mg N/g-$soil_{dry\text{-}weight}$) because the mineralization rates in the unamended agricultural soils were very low (~0.5 μg N/g-$soil_{dry\text{-}weight}$/day; Snider *et al.* 2010), and consequently N_2O production rates were negligible in unfertilized aerobic incubations of the agricultural soils (results not shown). Fertilization of the temperate forest soils was unnecessary because N mineralization and N_2O production were sufficient to accumulate enough N_2O for isotopic analysis every 1–2 weeks.

Incubation jars were sealed and the headspace was purged at a rate of 500 mL/min. for 15 minutes with a commercial gas mixture containing 20.9% molecular oxygen (O_2) bal-

anced with ultra-high purity helium (He). The $\delta^{18}O$-O_2 of this gas mixture was +25.7‰ determined via a modified version of the Wassenaar and Koehler (1999) method as described by Venkiteswaran (2008). In this study, the natural air was replaced by an O_2/He atmosphere so that no exogenous N_2O was introduced into the incubations, which would have compelled additional data correction measures. Although the rate of N_2O diffusion in He is much greater than in air, Scholefield *et al.* (1997) found that neither the rate nor the amount of N_2O efflux from soil was affected by the use of a synthetic He atmosphere. Instead, it is the boundary layer between the water film and the atmosphere that controls the rate of gas diffusion.

Every 1–2 weeks the incubations were sampled for N_2O concentration, and if a sufficient amount was present, jars were sampled for $\delta^{18}O$-N_2O. Before gas samples were withdrawn from a jar, an equal volume of the commercial O_2/He mixture was injected into the jar, and the headspace was mixed thoroughly using a syringe. This prevented large pressure differentials between the laboratory atmosphere and the incubations, while at the same time ensuring a homogenous headspace prior to gas sampling. N_2O concentration was determined by gas chromatography on an electron capture detector (Varian Greenhouse Gas Analyzer), and the $\delta^{18}O$-N_2O was measured on a continuous flow-IRMS in-line with a TraceGas preconcentration system (GV instruments). Further methodological details of $\delta^{18}O$-N_2O analysis are found in Snider *et al.* (2009).

After sampling, the headspace was purged again with the commercial gas mixture to remove all the remaining N_2O prior to the onset of the next 1–2 week incubation period. The total length of incubation for the temperate forest soils ranged from 27 days (Experiment 6) to 106 days (Experiment 3). Agricultural soils were incubated for 52 days, with sacrificial samplings for NO_3^- extraction on days 25 and 37 [$\delta^{18}O$-NO_3^- results in Snider *et al.* (2010)].

Oxygen isotope ratios of N_2O were expressed in delta (δ) notation, (calculated as $R_{sample} \div R_{standard} - 1$) and reported in units of per mill (‰), where R_{sample} and $R_{standard}$ are the $^{18}O/^{16}O$ of the sample and Vienna Standard Mean Ocean Water (VSMOW), respectively. Data were corrected for isotopologues that contribute to mass 46, followed by daily linearity and drift corrections. The analytical precision (1σ) for $\delta^{18}O$-N_2O was 0.4‰.

In this study, $^{15}N/^{14}N$ isotope ratios of N_2O ($\delta^{15}N_{bulk}$ at natural abundance) were concurrently analyzed. This data is ancillary to the main objectives of this study (to gain a better understanding of $\delta^{18}O$-N_2O), and for the sake of brevity these results are not published here but are the focus of another manuscript (Chapter 6). With the exception of Experiment 6 (wetland forest soil) the $\delta^{15}N$-N_2O data produced in the aerobic incubations of this study were 20–25‰ lower (more ^{15}N-depleted) than the $\delta^{15}N$-N_2O data produced in anaerobic incubations of the same soils (Snider *et al.* 2009; Chapter 3). This evidence provides further confirmation that nitrification was the dominant N_2O-forming pathway in this study (Perez *et al.* 2001, 2006).

5.2.2. *Model Development*

To interpret $\delta^{18}O$-N_2O values a conceptual model was developed that describes N_2O produced by NH_2OH oxidation and nitrifier-denitrification (Figure 5.1). This is accompanied by several mathematical expressions (Equations 5.1–5.11) that describe N_2O formation. Many of the parameters that control $\delta^{18}O$-N_2O are unknown in this study. As such, a series of Monte Carlo simulations were employed to see if some of the unknown parameters could be constrained. This necessitated many different assumptions about the pathway of N_2O formation and the magnitudes of the individual isotope effects (ε_1–ε_{10}). In the following model description, oxygen isotope effects (ε) are defined as ($\alpha - 1$) and reported in ‰ (10^3) units, where $\alpha = R_{product}/R_{substrate}$. There is a broad range of uncertainty in the ε values so that most (or all) of the literature reports are taken into account. The overall importance of specific parameters to the final $\delta^{18}O$-N_2O value is discussed in Section 5.4.3 and the accompanying Table 5.3.

The $\delta^{18}O$ value of N_2O formed by NH_2OH oxidation is represented by Equation 5.1, and the isotope effects (ε_1 and ε_{10}) are approximated from others' findings. The O isotope effect for O_2 consumption (ε_1; Figure 5.1) by bacterial respirers ranges from -29‰ to -8‰ (Lane and Dole, 1956). Recently, Mandernack *et al.* (2009) investigated N_2O formation by methanotrophs and calculated ε_1 to be -17.5 ± 5.4‰. Casciotti *et al.* (2010) measured the

net O isotope effect for NO_2^- formation ($\varepsilon_1 + \varepsilon_2$) with marine bacteria, and this ranged from $-38‰$ to $-18‰$. For the purpose of setting the initial parameters for the modelling component, the range of ε_1 is defined from the findings of Mandernack *et al.* (2009).

$$\delta^{18}O\text{-}N_2O_{\text{ (via NH2OH oxid.)}} = \delta^{18}O\text{-}O_2 + \varepsilon_1 + \varepsilon_{10} \quad [5.1]$$

N_2O formation by NH_2OH oxidation is a poorly-understood process. For example, the number of reaction steps and whether or not they are enzyme-catalyzed is not clearly identified (Stein and Yung 2003). Very little is known about the magnitude of ε_{10}. Sutka *et al.* (2003, 2006) measured $\delta^{18}O$ values of N_2O produced by cell cultures fertilized with NH_2OH; however, the $\delta^{18}O$ value of the NH_2OH was unknown and the relative proportion of N_2O formed by NH_2OH oxidation versus nitrifier-denitrification was not explicitly determined.

Sutka *et al.* (2006) conducted a separate experiment with *N. europaea* cultures that were fertilized with NH_4^+. The N_2O site-preference (SP: $\delta^{15}N^{\alpha}$ - $\delta^{15}N^{\beta}$) in this experiment was $+31.4 \pm 4.2‰$, which was similar to the NH_2OH oxidizers (SP $\approx +32‰$ to $+35‰$), yet it was different from the SP of the N_2O produced by the NO_2^- reducers ($\approx 0‰$). This suggests that the N_2O formed in that experiment was generated via NH_2OH oxidation. Furthermore, the NH_4^+-fertilized incubations of *N. europaea* were enclosed with an atmospheric air headspace, where the $\delta^{18}O\text{-}O_2$ can be estimated from the $\delta^{18}O\text{-}O_2$ of tropospheric air ($+23.5‰$; Kroopnick and Craig 1972). Because the $\delta^{18}O\text{-}N_2O$ formed from this experiment was $+23.5 \pm 1.3‰$ (Sutka *et al.* 2006), it is plausible that the net O isotope effect ($\varepsilon_1 + \varepsilon_{10}$) was close to $0‰$ (Equation 5.1). Frame and Casciotti (2010) recently confirmed this by measuring the net O isotope effect of $NH_4^+ \rightarrow NH_2OH \rightarrow N_2O$ in the marine bacterium *Nitrosomonas marina* C-113a ($\varepsilon_1 + \varepsilon_{10} = -2.9 \pm 0.8‰$).

Substituting the estimates of $\varepsilon_1 + \varepsilon_{10}$ (Frame and Casciotti 2010) and ε_1 ($-17.5 \pm 5.4‰$, Mandernack *et al.* 2009) into Equation 5.1, a value for ε_{10} ($+14.6 \pm 5.5‰$) can be defined for use in this study (Table 5.2). This estimate is similar to other positive O isotope effects (e.g., ε_5 or ε_7) that result from O-loss reactions. If it is assumed that the rate of

$\cdots N \cdots {}^{16}O$ bond breakage occurs faster than the rate of $\cdots N \cdots {}^{18}O$ bond breakage, then when two NH_2OH molecules combine to form $N_2O + H_2O + 4H^+$, the N_2O is ^{18}O-enriched and the H_2O is ^{18}O-depleted.

Equations 5.2 and 5.3 describe the formation of $\delta^{18}O\text{-}NO_2^-$ from NH_4^+ by chemolitho-autotrophic nitrifiers, where O_2 and H_2O each contribute one O atom (Hollocher *et al.* 1981; Andersson and Hooper 1983). For modelling purposes, we need to approximate ε_2. Although ε_2 is not known, the O isotope effect of H_2O incorporation during $NO_2^- \rightarrow NO_3^-$ was determined by Buchwald and Casciotti (2010) ($\varepsilon_4 = -22.5‰$ to $-9.3‰$; means of all experiments $\pm$ 1σ). It is likely that the values of ε_2 and ε_4 are similar because in both cases the O atom is derived from H_2O. As such, ε_2 is defined here as $-16 \pm 7‰$ (Table 5.2).

$$\delta^{18}O\text{-}NH_2OH = \delta^{18}O\text{-}O_2 + \varepsilon_1 \qquad [5.2]$$

$$\delta^{18}O\text{-}NO_2^- = ½(\delta^{18}O\text{-}NH_2OH) + ½(\delta^{18}O\text{-}H_2O + \varepsilon_2) \qquad [5.3]$$

A recent study of marine nitrifiers showed that NO_2^--oxygen can exchange with H_2O-oxygen (Casciotti *et al.* 2010), however, the exact mechanism (biotic or abiotic) was not identified. Here and in Snider *et al.* (2010), it is assumed that this exchange is abiotic because Casciotti *et al.* (2007) demonstrated that NO_2^- and H_2O rapidly exchange O atoms in the absence of bacteria. The equilibrium isotope effect (ε_3) associated with this process is $+14‰$ at room temperature (Casciotti *et al.* 2007). Equation 5.4 describes the $\delta^{18}O\text{-}NO_2^-$ after abiotic equilibrium with H_2O.

$$\delta^{18}O\text{-}NO_2^-{}_{\text{(exchange-abiotic)}} = (1 - f_{\text{exchange-abiotic}}) \times \delta^{18}O\text{-}NO_2^- + f_{\text{exchange-abiotic}} \times (\delta^{18}O\text{-}H_2O + \varepsilon_3) \qquad [5.4]$$

The fractions (f) of abiotic O-exchange ($f_{\text{exchange-abiotic}}$; Figure 5.1) in Experiments 1–3 were previously estimated from $\delta^{18}O\text{-}NO_3^-$ measurements (0.37–0.88, Snider *et al.* 2010). Although these results are from the same soil incubation experiments as this study, $f_{\text{exchange-abiotic}}$

is treated here as an unknown parameter in the Monte Carlo simulations (Table 5.2). Early model runs that used values of $f_{\text{exchange-abiotic}}$ from Snider *et al.* (2010) ($\pm$ 1σ) produced results that had a greater error than later model runs that used $f_{\text{exchange-abiotic}}$ values that ranged in a random-normal fashion between 0 and 1. By treating $f_{\text{exchange-abiotic}}$ as an unknown parameter in this study, the modelled results can be directly compared to the measured results reported in Snider *et al.* (2010), and the likelihood that the simulation results represent real (or plausible) combinations can be assessed.

Further biological O-exchange (enzyme-controlled) by nitrifiers has not been documented during NO_2^- reduction to N_2O. During denitrification large amounts of O-exchange can occur (Ye *et al.* 1991; Kool *et al.* 2007; Snider *et al.* 2009; Snider *et al.* unpublished results Chapter 3), but the mechanisms responsible for this O-exchange are not well-defined. Kool *et al.* (2007) noted that this process is a reversible hydrolysis (e.g., $NO_2^- + 2H^+ \rightleftharpoons NO + H_2O$). Presumably, as the backward reaction rate increases relative to the forward reaction rate, the amount of H_2O-O incorporation increases. The genes that encode for NO_2^- and NO reductase enzymes in denitrifiers are very similar to those found in nitrifiers (Casciotti and Ward 2001; Cantera and Stein 2007; Garbeva *et al.* 2007). Therefore, the occurrence of enzyme-catalyzed O-exchange during NO_2^- and NO reduction by nitrifiers ($f_{\text{exchange-}nir}$ and $f_{\text{exchange-}nor}$; Figure 5.1) must be included in our conceptual model (Equations 5.5–5.6).

$$\delta^{18}\text{O-NO} = (1 - f_{\text{exchange-}nir}) \times (\delta^{18}\text{O-NO}_2^{-}{}_{\text{(exchange-abiotic)}} + \varepsilon_5) + f_{\text{exchange-}nir} \times (\delta^{18}\text{O-H}_2\text{O} + \varepsilon_6) \qquad [5.5]$$

$$\delta^{18}\text{O-N}_2\text{O}_{\text{(via nit.-denit.)}} = (1 - f_{\text{exchange-}nor}) \times (\delta^{18}\text{O-NO} + \varepsilon_7) + f_{\text{exchange-}nor} \times (\delta^{18}\text{O-H}_2\text{O} + \varepsilon_8) \qquad [5.6]$$

Fractionation during biological O-exchange (ε_6 and ε_8) has not been adequately studied. If the process is a reversible hydrolysis, then there may be an associated isotope effect that is similar to the $^{18}O/^{16}O$ fractionation that occurs during the H_2O uptake reactions of NH_2OH oxidation (Equation 5.3) and NO_2^- oxidation to NO_3^- (Buchwald and Casciotti 2010). Consequently, in this rudimentary model of nitrifier-derived $\delta^{18}O$-N_2O we define ε_6 =

$-16 \pm 7‰$ and $\varepsilon_8 = -16 \pm 7‰$ (Table 5.2). The importance of these parameters to the final δ^{18}O-N_2O value is directly proportional to the amounts of biologically-catalyzed O-exchange that occur (Equations 5.5–5.6). That is, if biological O-exchange is low then the importance in the uncertainty of ε_6 and ε_8 is also low (and vice-versa).

When a reaction step is rate-limiting, and the substrate is abundant, inter-molecular isotope effects can occur. This is often observed in NO_3^- as it is consumed during denitrification. The reduction of NO_3^- causes the δ^{18}O-NO_3^- to increase as the remaining fraction of NO_3^- decreases (Böttcher *et al.* 1990, $\varepsilon = -8‰$; Mengis *et al.* 1999, $\varepsilon = -18‰$). In nitrifier-denitrification, it is unknown if NO_2^- accumulates in the intra- or extra-cellular environment to levels that allow $NO_2^- \rightarrow NO$ to be rate-limiting. The majority of the NO_2^- produced by ammonia-oxidizing bacteria is 'normally' excreted and taken up by nitrite-oxidizing bacteria. However, when nitrifier-denitrification occurs, it is not known if an accumulated pool of NO_2^- is consumed, or if $NH_2OH \rightarrow NO_2^- \rightarrow NO$ occurs sequentially within the same organism with no build up of NO_2^-. If the reduction of NO_2^- to NO by nitrifier-denitrifiers is rate-limiting, then an additional negative inter-molecular isotope effect associated with NO_2^- uptake is likely (similar to the $^{18}O/^{16}O$ fractionation associated with NO_3^- uptake). In this case, the extracellular δ^{18}O-NO_2^- pool would be dependent on the relative yields of N_2O and NO_3^- (the assumed end-products of NO_2^- consumption) and the isotope effect associated with NO_3^- consumption (ε_4) must be considered.

In this conceptual model of nitrifier-denitrification we assume that NO_2^- reduction is not rate-limiting. Instead, it is assumed that ε_5 reflects the positive intra-molecular isotope effect associated with the reductive loss of NO_2^--O to form H_2O (Figure 5.1). Theoretically, this process should have a positive isotope effect (ε_5) because the rate of $\cdots N \cdots {}^{16}O$ bond breakage occurs faster than the rate of $\cdots N \cdots {}^{18}O$ bond breakage. This would yield ^{18}O-depleted H_2O and ^{18}O-enriched NO.

Similarly, it is assumed that the subsequent reduction of $2NO + 2H^+ \rightarrow N_2O + H_2O$ has a positive isotope effect (ε_7) because the rate of $\cdots N \cdots {}^{16}O$ bond breakage occurs faster than the rate of $\cdots N \cdots {}^{18}O$ bond breakage (yielding ^{18}O-depleted H_2O and ^{18}O-enriched N_2O). Addi-

tionally, this model assumes that NO does not accumulate and egress to/from the organism. If this did occur, there would be an inter-molecular $^{18}O/^{16}O$ fractionation that would cause the emitted NO to be ^{18}O-enriched relative to the substrate NO. While there are studies that have measured large environmental NO emissions (e.g., Davidson 1992, 1993; Perez *et al.* 2006), the isotope effects associated with this process are unknown. Future modelling attempts may incorporate this information once it becomes available.

There is one report of the net isotope effect ($\varepsilon_5 + \varepsilon_7$) for NO_2^- reduction by a marine nitrifier ($+8.4 \pm 1.4$‰; Frame and Casciotti 2010). This estimate probably includes both an inter-molecular and intra-molecular isotope effect because the marine nitrifiers were fertilized with NO_2^-. If the inter-molecular isotope effect for NO_2^- uptake was similar to the estimates reported by Böttcher *et al.* (1990) and Mengis *et al.* (1999) for NO_3^- uptake, then the net isotope effect associated with O-loss during NO_2^- and NO reduction could conceivably be several per mill higher (10–20‰). Therefore, it is reasonable to expect that $\varepsilon_5 + \varepsilon_7$ could be larger than the values reported by Frame and Casciotti (2010). For modelling purposes, we set $\varepsilon_5 = 10 \pm 6$‰ and $\varepsilon_7 = 10 \pm 6$‰ (Table 5.2) so that the combined isotope effect ($\varepsilon_5 + \varepsilon_7$) ranged between +8‰ to +32‰.

Equation 5.7 illustrates a simplified mixing expression for the $\delta^{18}O$ of N_2O formed by NH_2OH oxidation and nitrifier-denitrification [$\delta^{18}O\text{-}N_2O_{\text{ (total)}}$]. The substitution of Equations 5.1–5.6 into Equation 5.7 yields the long-form of this expression (Equation 5.8), which is shown to demonstrate the complexity of all the currently known controls of N_2O formation.

$$\delta^{18}O\text{-}N_2O_{\text{ (total)}} = (1 - f_{\text{N2O via nit.-denit.}}) \times \delta^{18}O\text{-}N_2O_{\text{ (via NH2OH oxid.)}} + f_{\text{N2O via nit.-denit.}} \times \delta^{18}O\text{-}N_2O_{\text{ (via nit.-denit.)}} \quad [5.7]$$

where, $f_{\text{N2O via NH2OH oxid.}} = 1 - f_{\text{N2O via nit.-denit}}$

$$\begin{aligned}\delta^{18}O\text{-}N_2O_{\text{ (total)}} = {} & f_{\text{N2O via nit.-denit.}} \times \langle f_{\text{exchange-}nor} \times (\delta^{18}O\text{-}H_2O + \varepsilon_8) - (f_{\text{exchange-}nor} - 1) \times \langle \varepsilon_7 + \\ & f_{\text{exchange-}nir} \times (\delta^{18}O\text{-}H_2O + \varepsilon_6) - (f_{\text{exchange-}nir} - 1) \times \langle \varepsilon_5 + f_{\text{exchange-abiotic}} \times \\ & (\delta^{18}O\text{-}H_2O + \varepsilon_3) - (f_{\text{exchange-abiotic}} - 1) \times \langle \tfrac{1}{2}(\delta^{18}O\text{-}O_2 + \varepsilon_1 + \\ & \delta^{18}O\text{-}H_2O + \varepsilon_2)\rangle\rangle\rangle - (f_{\text{N2O via nit.-denit.}} - 1) \times (\delta^{18}O\text{-}O_2 + \varepsilon_1 + \varepsilon_{10}) \end{aligned} \quad [5.8]$$

Although it is largely accepted that most nitrifier-denitrifiers are incapable of N_2O reduction (Arp and Stein 2003), Poth (1986) and Shrestha *et al.* (2002) have provided experimental evidence that N_2 can be produced by *Nitrosomonas* isolates. In contrast, N_2O consumption by denitrifiers (under anoxia) is well-documented. Therefore, to make our model complete, Equations 5.9a–b describe the reduction of N_2O following a typical Rayleigh distillation (Mariotti *et al.* 1981), where Equation 5.9a is the commonly recognized form and Equation 5.9b is an equivalent form derived using delta and epsilon units.

$$^{18}O/^{16}O\text{-}N_2O_{\text{ (final)}} = {}^{18}O/^{16}O\text{-}N_2O_{\text{ (initial)}} \times (1 - f_{\text{N2O red.}})^{(\alpha\,-\,1)} \qquad [5.9a]$$

$$\delta^{18}O\text{-}N_2O_{\text{ (N2O red.)}} = \langle(\delta^{18}O\text{-}N_2O_{\text{ (total)}} \div 1000 + 1) \times (1 - f_{\text{N2O red.}})^{(\varepsilon 9\,\div\,1000)} - 1\rangle \times 1000 \qquad [5.9b]$$

where, $\delta^{18}O\text{-}N_2O_{\text{ (N2O red.)}}$ and $\delta^{18}O\text{-}N_2O_{\text{ (total)}}$ are the final and initial $\delta^{18}O$ values, respectively, after some fraction of N_2O reduction ($f_{\text{N2O red.}}$) has occurred,

and, $(1 - f_{\text{N2O red.}})$ is the fraction of un-reacted N_2O that remains,

and, $\varepsilon = 10^3(\alpha - 1)$ (Mariotti *et al.* 1981).

Reports of the O isotope effect associated for N_2O reduction in soils (ε_9; Figure 5.1) vary between $-26‰$ and $-5‰$ (Schmidt and Voerkelius 1989; Mandernack *et al.* 2000; Menyailo and Hungate 2006; Ostrom *et al.* 2007; Vieten *et al.* 2007; Jinuntuya-Nortman *et al.* 2008; Well and Flessa 2009). For modelling purposes, ε_9 was assigned a value of $-15.5 \pm 10.5‰$ (Table 5.2).

The substitution of Equation 5.8 into Equation 5.9b and the subsequent rearrangement of this expression into a linear form ($y = mx + b$), where $y = \delta^{18}O\text{-}N_2O_{\text{ (N2O red.)}}$ and $x = \delta^{18}O\text{-}H_2O$, yields an expression for the slope (m; Equation 5.10) and an expression for

the intercept (b; Equation 5.11). The linearization of $\delta^{18}O\text{-}N_2O_{\ (N2O\ red.)}$ facilitates the interpretation of our measured data ($\delta^{18}O\text{-}N_2O$, $\delta^{18}O\text{-}H_2O$, and $\delta^{18}O\text{-}O_2$).

$$\text{slope } (m) = f_{\text{N2O via nit.-denit.}} \times \langle (1 - f_{\text{N2O red.}})^{(\varepsilon 9 \div 1000)} \rangle \times \langle f_{\text{exchange-}nor} - \langle \langle f_{\text{exchange-}nir} - (½ \times f_{\text{exchange-abiotic}} + ½) \times (f_{\text{exchange-}nir} - 1) \rangle \times (f_{\text{exchange-}nor} - 1) \rangle \rangle \quad [5.10]$$

$$\begin{aligned}\text{intercept } (b) = {} & (1 - f_{\text{N2O red.}})^{(\varepsilon 9 \div 1000)} \times \langle -f_{\text{N2O via nit.-denit.}} \times \langle (f_{\text{exchange-}nor} - 1) \times \\ & \langle \varepsilon_7 + \varepsilon_6 \times f_{\text{exchange-}nir} - (f_{\text{exchange-}nir} - 1) \times \langle \varepsilon_5 + \varepsilon_3 \times f_{\text{exchange-abiotic}} - \\ & (f_{\text{exchange-abiotic}} - 1) \times \langle ½ \times (\delta^{18}O\text{-}O_2 + \varepsilon_1 + \varepsilon_2) \rangle \rangle \rangle - \varepsilon_8 \times f_{\text{exchange-}nor} \rangle - \\ & (f_{\text{N2O via nit.-denit.}} - 1) \times (\delta^{18}O\text{-}O_2 + \varepsilon_1 + \varepsilon_{10}) + 1000 \rangle - 1000 \end{aligned} \quad [5.11]$$

Algebraic rearrangements of Equations 5.1–5.11 were completed with MuPAD® from the Symbolic Math Toolbox for MATLAB®. In order to place constraints on the fractions of O-exchange and N_2O reduction that occurred in the soil incubation experiments with multiple $\delta^{18}O\text{-}H_2O$ values, $\delta^{18}O\text{-}N_2O_{\ (N2O\ red.)}$ (i.e., Equations 5.10–5.11) was modelled in MATLAB® using a Monte Carlo approach. Values for $f_{\text{exchange-abiotic}}$, $f_{\text{exchange-nir}}$, $f_{\text{exchange-nor}}$, ε_1–ε_3 and ε_5–ε_{10} were randomly generated (with a non-normal distribution) using the ranges summarized in Table 5.2 and defined previously in this section. N_2O reduction was modelled under four different scenarios: $f_{\text{N2O red.}} = 0$ (*scenario a*); $f_{\text{N2O red.}} = 0$–0.25 (*scenario b*); $f_{\text{N2O red.}} = 0.25$–$0.5$ (*scenario c*); and $f_{\text{N2O red.}} = 0.5$–$0.75$ (*scenario d*). For each scenario of Experiments 1–3, 100,000 model runs were performed and $\delta^{18}O\text{-}N_2O$ values were calculated using Equations 5.10–5.11 and the three different $\delta^{18}O\text{-}H_2O$ values. To determine the goodness-of-fit, the modelled $\delta^{18}O\text{-}N_2O$ values were compared to the measured values of $\delta^{18}O\text{-}N_2O$ from the soil incubation experiments. All modelled $\delta^{18}O\text{-}N_2O$ values that were within the 95% confidence bands of the linear regression of the measured $\delta^{18}O\text{-}N_2O$ versus $\delta^{18}O\text{-}H_2O$ were deemed acceptable solutions.

Initial model calculations allowed $f_{\text{N2O via NH2OH oxid.}}$ and $f_{\text{N2O via nit.-denit.}}$ to vary randomly between 0–1, provided that the total $f_{\text{N2O}} = 1$ (i.e., no other sources of N_2O other than NH_2OH oxidation and nitrifier-denitrification). Under these conditions the simulation results

were poorly constrained and the values of $f_{\text{exchange-abiotic}}$, $f_{\text{exchange-nir}}$, and $f_{\text{exchange-nor}}$ did not converge to unique ranges at all levels of error (i.e., large scatter). Even when small amounts of $f_{\text{N2O via NH2OH oxid.}}$ were invoked (0–0.25; Supplementary Figure 5.1) the model fits were noticeably poorer than when $f_{\text{N2O via nit.-denit.}} = 1$ (Supplementary Figures 5.2–5.4). Therefore, in order to proceed further with the Monte Carlo modelling and constrain some of the unknown values in Equation 5.10–5.11, it was necessary to assume that nitrifier-denitrification was the sole N_2O generating process (i.e., $f_{\text{N2O via nit.-denit.}} = 1$ and $f_{\text{N2O via NH2OH oxid.}} = 0$). The validity of this assumption is discussed in Section 5.4.1.

5.3. *Results*

5.3.1. *Experimental*

The NH_4^+-fertilizer was rapidly consumed in Experiments 1 and 2, and by day 25 there was no measureable NH_4^+ in the agricultural soil extracts. In the first phase of Experiment 1 there was a temporary accumulation of NO_2^- (9.0 ± 0.7 μmol/g-soil$_{\text{dw.}}$) that comprised about two-thirds of the total [NO_2^- + NO_3^- pool] (13.3 ± 0.7 μmol/g-soil$_{\text{dw.}}$). By day 37, however, no NO_2^- remained and much more NO_3^- was present (12.4 ± 0.5 μmol/g-soil$_{\text{dw.}}$). At the end of Experiment 1 the mean (± 1σ) soil NO_3^- concentration was 13.5 ± 0.5 μmol/g-soil$_{\text{dw.}}$, which represented 125% ± 5 of the initial NH_4^+ applied. The amount of 'excess' NO_3^- was likely produced after the soils were moistened and the easily digestible portion of the organic N pool was mineralized. Most of the N_2O formed in Experiment 1 occurred within the first 25 days of incubation (day 0–25 cumulative amount = 0.52 ± 0.04 μmol/g-soil$_{\text{dw.}}$). The N_2O yield over the whole incubation was 3.8–4.4% of the total oxidized N pool (NO_3^- + NO_2^- + N_2O). The N_2O production rates in Experiment 1 ranged between 4–1600 pmol N_2O/hr/g-soil$_{\text{dw.}}$ and high rates were sustained for the first 37 days of incubation (Figure 5.3a).

No NO_2^- was detected in any extracts of Experiment 2. All the NH_4^+ was nitrified in the first 25 days and 13.3 ± 0.7 μmol of NO_3^-/g-soil$_{\text{dw.}}$ was produced. This represented 124% ± 7 of the initial NH_4^+ application. Soils extracted on day 52 did not contain significantly

more NO_3^- (13.8 ± 0.2 μmol/g-soil$_{dw.}$). The vast majority of the N_2O formed in Experiment 2 occurred within the first 2 weeks (Figure 5.3b), and the cumulative amount produced over the entire incubation (0.02 ± 0.00 μmol/g-soil$_{dw.}$) represented an N_2O yield of ~0.1% of the total oxidized N pool. The rates of N_2O production in Experiment 2 were low (0.5–50 pmol N_2O/hr/g-soil$_{dw.}$), and N_2O production declined exponentially with time. After the second sampling event, N_2O production dropped below 10 pmol N_2O/hr/g-soil$_{dw.}$ and did not recover.

In Experiment 3 (unfertilized, upland forested soil) large amounts of NH_4^+ and NO_3^- accumulated after 106 days of incubation (30.9 and 17.4 μmol/g-soil$_{dw.}$, respectively). The mean rates of net ammonification (Organic N → NH_4^+) and net nitrification (NH_4^+ → NO_3^-) were 4.2 and 2.2 μg N/g-soil$_{dw.}$/day, respectively, which are typical rates of soil N turnover in upland soils of the Turkey Lakes Watershed (Foster *et al.* 1986, 1989). The mean cumulative amount of N_2O produced in Experiment 3 was 0.13 ± 0.08 μmol/g-soil$_{dw.}$, which represented an N_2O yield of ~0.7% of the total oxidized N pool. The N_2O production rates were variable among replicates incubations ranging from 3 to 220 pmol N_2O/hr/g-soil$_{dw.}$ (Figure 5.3c).

The rates of N_2O production in the other upland soil incubations (Experiments 4 and 5) ranged between 5–167 pmol N_2O/hr/g-soil$_{dw.}$. In the forested wetland soil (Experiment 6) the N_2O production rate increased from 19 pmol N_2O/hr/g-soil$_{dw.}$ near the beginning of the incubation to a maximum of 4350 pmol N_2O/hr/g-soil$_{dw.}$ near the end of the experiment. The soils in Experiments 4–6 were not extracted for chemical analyses at the end of their incubations.

Despite large differences in N_2O production rates among experiments, the production-weighted $\delta^{18}O$-N_2O values for all experimental treatments with $\delta^{18}O$-H_2O at natural abundance was small (range of mean values ± 1σ = +17‰ to +31‰; Table 5.1; Figure 5.2b). Incubations with multiple $\delta^{18}O$-H_2O values (Experiments 1–3) yielded N_2O that fell into three distinct $\delta^{18}O$ ranges (Figure 5.3). The results of the linear regressions of $\delta^{18}O$-N_2O and $\delta^{18}O$-H_2O are shown in Table 5.1.

5.3.2. *Monte Carlo Simulations*

Model fits of Experiments 1–3 that satisfied Equations 5.10–5.11 are shown in the Supplementary Figures 5.2–5.4, respectively. These data are summarized and shown as histograms in Figure 5.4. Tests for normality (Anderson-Darling and Shapiro-Wilk) showed that none of the results were normally distributed ($\alpha = 0.05$). Consequently, the output parameters are discussed in approximate terms and their values will be described as ranges. The results of the simulated isotope effects (ε_1–ε_{10}) are not shown. These values were operationally defined, and for each model run a discrete ε value was chosen in a random non-normal fashion based upon the input ranges summarized in Table 5.2. As such, scatter plots of their results at high and low error covered the entire defined range of ε.

5.4. *Discussion*

5.4.1. *Soil Incubation Experiments*

Net nitrification in the agricultural soils was rapid in the early phase of incubation (greater than 6 μg NO_3^--N/g $soil_{dw.}$/day; Snider *et al.* 2010). The vast majority of the NO_3^-, NO_2^- (Experiment 1 only), and N_2O were generated in the first 25 days. The temporary accumulation of NO_2^- in Experiment 1 was gone by the 37th day. This coincided with a decline in the N_2O production rate in this experiment and suggests that nitrifier-denitrification was a dominant N_2O-forming process in this soil.

The N_2O yields of Experiments 1–3 ranged from 0.1%–4.4%. The N_2O yields of *Nitrosomonas* and *Nitroso* bacteria were reviewed by Colliver and Stephenson (2000) and they reported N_2O yields (relative to the total NO_2^- produced) of fully-aerated cultures that ranged from 0.05% to 3.3%. The yields of oxygen-limited cultures ranged from 0.8% to 11%. Well *et al.* (2008) reported the N_2O yields from nitrification in three arable soils incubated with a range of fertilization and moisture treatments. In their experiments the N_2O yields (expressed as a % of the NH_4^+ lost) ranged from 0.07% ± 0.02 to 0.45% ± 0.10. In comparison, the N_2O yields from Experiments 1 and 2 of this study were 5.2% ± 0.2 and 0.2% ± 0.0 of the NH_4^+

lost, respectively. Based on this evidence the N_2O yields of Experiments 2 and 3 were similar to previous estimates. The N_2O yields of Experiment 1 were higher than what has been measured from well-aerated cultures and soil microcosms.

It is not clear why Experiment 1 had higher rates of N_2O production. It may simply be because NO_2^-, which is the substrate for the reductive portion of nitrifier-denitrification, accumulated to high levels and the microbial community was not NO_2^- limited. However, oxygen-limitation cannot be discounted in this experiment because the high organic matter soils of Experiment 1 can retain a lot of water, and at 50% WHC the gravimetric soil moisture was almost 40% (Table 5.1). Therefore, oxygen-limitation may have stimulated higher rates of nitrifier-denitrification.

If the microbial community in Experiment 1 was oxygen-limited, then denitrification must also be considered as a route of N_2O production. In this study the incubation headspace was flushed with 20.9% O_2 after each sampling. Periodic checks of the headspace did not reveal any noticeable O_2 declines in Experiments 1–5. In the temperate forest wetland soil (Experiment 6) the headspace O_2 decreased to a minimum concentration of $\approx$ 17% and the rate of N_2O production was high. Although the experimental design favoured nitrification, it is possible that anoxic microsites or 'hotspots' capable of supporting denitrification were localized on or between SOM particles (Parkin 1987). This is an inherent limitation of soil incubation studies that examine nitrification with whole microbial communities in their natural media. If some of the N_2O in Experiment 1 was NO_3^--derived then the N_2O yield from NH_4^+ would be closer to the value measured from Experiments 2 and reported in Well *et al.* (2008).

The $\delta^{18}O$-N_2O values of Experiments 1–3 were highly correlated to $\delta^{18}O$-H_2O (r^2 = 0.97–1.00; Table 5.1). This implies that NH_2OH oxidation, which uses O_2 as the sole oxygen source (Equation 5.1), was not a significant N_2O-forming mechanism. If NH_2OH oxidation was an important N_2O formation pathway in Experiments 1–3, the variability of the $\delta^{18}O$-N_2O data would not be so well-explained by the different $\delta^{18}O$-H_2O treatments. For the Monte Carlo simulations, this evidence supports the assumption that all the N_2O was formed by nitrifier-denitrification.

5.4.2. *Monte Carlo Simulations*

The development of this model and its systematic account of the controls of δ^{18}O-N_2O generated by nitrification is a valuable scientific contribution. No clear, holistic explanation of δ^{18}O-N_2O production in aerobic environments has been provided prior to this study. The Monte Carlo modelling approach employed here provides a means to constrain some of the unknown parameters that control δ^{18}O-N_2O formed in aerobic environments. The accuracy of the results of each modelled parameter (i.e., their likeness to the true values) cannot be independently confirmed. In this study, the only measured parameters are δ^{18}O-N_2O, δ^{18}O-H_2O, and δ^{18}O-O_2 (and $f_{\text{exchange-abiotic}}$, Snider *et al.* 2010). This model provides a foundation for future modelling attempts that have greater certainty in the input parameters. Given the rudimentary nature of these Monte Carlo simulations, the following results are interpreted cautiously.

The model output values of $f_{\text{exchange-abiotic}}$ were inversely proportional to the $f_{\text{N2O red.}}$ values (Experiments 1–3, *scenarios a–d*) (Figure 5.4). This relationship is an artefact of the model and is a function of how the two parameters are associated in the model equations. In most cases, if the $f_{\text{N2O red.}}$ value was high, then the $f_{\text{exchange-abiotic}}$ value had to be low (and vice versa) if the solution was to be a good fit and closely approximate the measured δ^{18}O-N_2O value. The isotope effect for N_2O reduction (ε_9) is normal and the $\delta^{18}O$ value of the residual N_2O rises as $f_{\text{N2O red.}}$ increases. Also, the δ^{18}O-NO_2^- pool rises as the degree of $NO_2^- \rightleftharpoons H_2O$ O-exchange increases because the equilibrium isotope effect is positive ($\varepsilon_3 = +14‰$). The latter point may not be intuitive because O-exchange often results in a product with a $\delta^{18}O$ value that is lower than its substrate (e.g., denitrification). However, prior to abiotic O-exchange, the $\delta^{18}O$ of the newly formed NO_2^- (Equation 5.3) is very similar to the $\delta^{18}O$ value of H_2O. Using representative values of: δ^{18}O-$H_2O = -5‰$; δ^{18}O-$O_2 = +23.5‰$; $\varepsilon_1 = -17.5‰$; and $\varepsilon_2 = -16‰$, an example of the δ^{18}O-NO_2^- prior to abiotic O-exchange is shown below (Equation 5.12). After abiotic O-exchange occurs, the fraction of NO_2^- that equilibrates with H_2O is 14‰ higher.

$$\begin{aligned}\delta^{18}\text{O-NO}_2^- &= ½ \times (\delta^{18}\text{O-H}_2\text{O} + \delta^{18}\text{O-O}_2 + \varepsilon_1 + \varepsilon_2) \\ &= ½ \times \langle(-5) + (+23.5) + (-17.5) + (-16)\rangle \\ &= -7.5‰ \end{aligned} \quad [5.12]$$

Comparing the known values of $f_{\text{exchange-abiotic}}$ derived from $\delta^{18}\text{O-NO}_3^-$ measurements (Snider *et al.* 2010) to the modelled values of $f_{\text{exchange-abiotic}}$, inferences can be made about the amount of N_2O reduction that occurred in the soil incubation experiments. In Experiment 1 the measured $f_{\text{exchange-abiotic}}$ value (0.88 ± 0.05, Snider *et al.* 2010) is best described by *scenarios a* and *b* (Figure 5.4). In *scenario a* 82% of the modelled $f_{\text{exchange-abiotic}}$ values were between 0.75–0.90. In *scenario b* 90% of the modelled $f_{\text{exchange-abiotic}}$ values were between 0.70–0.90. *Scenario c* also approximates the known range of $f_{\text{exchange-abiotic}}$, but all the simulated parameters had a much wider distribution under this scenario. Therefore, the $f_{\text{N2O red.}}$ in the high OM agricultural soil was probably greater than or equal to zero, but did not exceed 25%.

The Monte Carlo simulations of Experiment 1 suggested that additional O-exchange occurred during NO_2^- and NO reduction (Figure 5.4). In *scenario a* 71% of the modelled $f_{\text{exchange-nir}}$ values were between 0–0.25, and in *scenario b* 84% of the values were between 0–0.35. Similarly, in *scenario a* 84% of the modelled $f_{\text{exchange-nor}}$ values were between 0–0.20, and in *scenario b* 85% of the values were between 0–0.25. The correlation between $f_{\text{exchange-nir}}$ and $f_{\text{exchange-nor}}$ was poor under both scenarios (r^2 = 0.07–0.12).

Oxygen-exchange during NO_2^- and NO reduction by nitrifier-denitrifiers has not been documented in any research study to date. Additionally, there is insufficient empirical evidence to suggest that nitrifiers readily consume N_2O. Given the uncertain nature of the simulated estimates of $f_{\text{N2O red.}}$, $f_{\text{exchange-nir}}$, and $f_{\text{exchange-nor}}$ in Experiment 1, and the lack of evidence supporting O-exchange and N_2O reduction by nitrifier-denitrifiers, it is conceivable that a portion of the N_2O produced in this experiment was produced by denitrification. In contrast to nitrifying organisms, denitrifiers do catalyze O-exchange and N_2O reduction to N_2. Given this, a small amount of denitrification can explain the higher N_2O yields that were measured in this high OM agricultural soil. However, the rate of net N_2O production by denitrification

would have been small compared to the N_2O production rate by nitrification. Anoxic incubation experiments (helium atmosphere) examining denitrification in this soil revealed average net N_2O production rates that were one to two orders of magnitude higher (Chapter 3, unpublished results not shown).

In Experiment 2 *scenario a* provided the best fit of the measured $f_{\text{exchange-abiotic}}$ value (0.52 ± 0.05, Snider *et al.* 2010), however all four scenarios significantly underestimated the known value (Figure 5.4). For example, 96% of the modelled $f_{\text{exchange-abiotic}}$ values in *scenario a* were between 0–0.40. The remaining scenarios provided lower values of $f_{\text{exchange-abiotic}}$. This suggests that one or more of the defined parameters (Table 5.2) did not adequately represent the true value or range of ε_1–ε_{10}. When a small amount of the N_2O in Experiment 2 was formed by NH_2OH oxidation (Supplementary Figure 5.1) the simulated range of $f_{\text{exchange-abiotic}}$ was much larger, and 82% of the values were between 0.15–0.80. Therefore, it may be that some of the N_2O formed in this low OM agricultural soil was generated by NH_2OH oxidation. The Monte Carlo simulations of Experiments 2 suggested that biologically catalyzed O-exchange during NO_2^- and NO reduction was absent. For all levels of N_2O consumption (*scenarios a–d*) the modelled values of $f_{\text{exchange-nir}}$ and $f_{\text{exchange-nor}}$ trended towards zero.

In Experiment 3 the known $f_{\text{exchange-abiotic}}$ value (0.37 ± 0.03, Snider *et al.* 2010) was most similar to *scenarios a* and *b* (Figure 5.4). In *scenario a* 83% of the modelled $f_{\text{exchange-abiotic}}$ values were between 0.30–0.65. In *scenario b* 80% of the modelled $f_{\text{exchange-abiotic}}$ values were between 0.25–0.65. Accordingly, the $f_{\text{N2O red.}}$ in upland temperate forest soils of Experiment 3 was likely greater than or equal to zero, but not more than 25%. If the $f_{\text{N2O red.}}$ was greater than zero in this experiment then a portion of the total N_2O pool may have been produced by denitrification. This organic forest soil was 36% organic matter (by weight), and at 50% WHC the soils contained ~two times their oven-dry weight in water (Table 1). Consequently, it is plausible that anoxic microsites were present these incubations. However, if denitrification did produce some of the N_2O in Experiment 3 then the relative portion was small. Anaerobic incubations of the upland temperate forest soil exhibited average net N_2O production rates that were two to three orders of magnitude higher (9,000–26,000 pmol N_2O/hr/g-

$soil_{dw.}$, Snider *et al.* 2009). Additionally, very high amounts of denitrifier-catalyzed O-exchange occurred in this soil (87–91%). In this study there was no evidence of biologically catalyzed O-exchange. The modelled values of $f_{\text{exchange-nir}}$ and $f_{\text{exchange-nor}}$ trended towards zero for all levels of N_2O consumption except for *scenario d*.

5.4.3. *The modelled range of $\delta^{18}O$-N_2O formed by nitrification in soils*

The mean ($\pm$ 1σ) production-weighted $\delta^{18}O$-N_2O measured in this study from incubations with $\delta^{18}O$-H_2O at natural abundance ranged from +17‰ to +31‰ (Table 5.1). In the published literature the reported $\delta^{18}O$ values of nitrifier-derived N_2O ranges from +13‰ to +29‰ (Figure 5.2a). Combining these results gives an overall range of +13‰ to +31‰ that is surprisingly narrow given the complexity and number of parameters that control the isotopic composition of N_2O formed by nitrification.

The substitution of the mean, minimum, and maximum values of input parameters (Table 5.2) into Equations 5.10 and 5.11 yields interesting findings that are summarized in Table 5.3. The widest possible range in $\delta^{18}O$-N_2O generated by NH_2OH oxidation ranges from +9.7‰ to +31.5‰. Consequently, most of the natural abundance $\delta^{18}O$-N_2O data measured in this study and provided in the literature (Figure 5.2) could hypothetically be formed by NH_2OH oxidation. Using the mean values of ε_1 and ε_{10} (Mandernack *et al.* 2009; Frame and Casciotti 2010), a more moderate estimate of $\delta^{18}O$-N_2O is derived (+20.6‰).

The $\delta^{18}O$-O_2 in the troposphere is +23.5‰ (Kroopnick and Craig 1972) and slightly higher in solution (+24.2‰; air-equilibrium value). This value may increase if high metabolic respiration rates persist and localized ^{18}O-enrichment of O_2 occurs. The $\delta^{18}O$-O_2 may also be several per mill lower in highly productive, nutrient-rich rivers impacted by pollution (e.g., Wassenar *et al.* 2010). As shown in Equation 5.1, the $\delta^{18}O$-N_2O formed by NH_2OH oxidation is directly proportional to the $\delta^{18}O$-O_2 endmember and it will increase or decrease in a 1:1 fashion as $\delta^{18}O$-O_2 changes.

The Monte Carlo simulations presented here suggest that biological O-exchange does not occur in nitrifier-denitrification ($f_{\text{exchange-}nir} + f_{\text{exchange-}nor} = 0$). Similarly, there is little

empirical evidence to indicate that nitrifier-denitrifiers consume N_2O. If $f_{\text{exchange-}nir}$, $f_{\text{exchange-}nor}$, and $f_{\text{N2O red.}}$ were significant in any of the soils studied here (e.g., Experiment 1), then a fraction of that N_2O was probably denitrifier-derived. As such, a simplified expression for the $\delta^{18}O$-N_2O formed by nitrifier-denitrification is provided in Equation 5.13.

$$\begin{aligned}\delta^{18}\text{O-N}_2\text{O}_{\text{ (via nit.-denit.)}} = \; & [1 - f_{\text{exchange-abiotic}}] \times [½(\delta^{18}\text{O-O}_2 + \varepsilon_1) + ½(\delta^{18}\text{O-H}_2\text{O} + \varepsilon_2)] + \\ & [f_{\text{exchange-abiotic}} \times (\delta^{18}\text{O-H}_2\text{O} + \varepsilon_3)] + \varepsilon_5 + \varepsilon_7 \end{aligned} \quad [5.13]$$

The widest range of $\delta^{18}O$-N_2O produced by nitrifier-denitrification is between −5.4‰ and +46.6‰, however moderate values of the input parameters produce $\delta^{18}O$-N_2O equal to +22.4‰ (Table 5.3, columns d–f). This broad spectrum of $\delta^{18}O$ values is highly dependent upon the $\delta^{18}O$-H_2O and variations in $f_{\text{exchange-abiotic}}$ (Equation 5.13). Most of the significant N_2O-producing regions in the World have environmental $\delta^{18}O$-H_2O (at natural abundance) that ranges from −15‰ to +2‰ (Gat 1996). Rounded estimates of $f_{\text{exchange-abiotic}}$ reported in Snider *et al.* (2010) ranged between 0.3–0.9. Using a single representative value for $\delta^{18}O$-H_2O (−5‰), the maximum variation in $f_{\text{exchange-abiotic}}$ imparts a ~10‰ shift in $\delta^{18}O$-N_2O (Table 5.3, columns g–h). Nitrifier-denitrifier produced $\delta^{18}O$-N_2O is also heavily influenced by ε_5 and ε_7, and for every per mill change in $\varepsilon_5 + \varepsilon_7$, the $\delta^{18}O$-N_2O changes by a per mill unit. Consequently, a greater certainty in the magnitude of these isotope effects could significantly improve future modelling scenarios.

The remaining input variables impart less control on the $\delta^{18}O$-N_2O produced by nitrifier-denitrification. When abiotic O-exchange is high, large variations in $\delta^{18}O$-O_2, ε_1, and ε_2 impart <1‰ change in $\delta^{18}O$-N_2O. These parameters become more important as O-exchange decreases (Equation 5.13). Finally, the equilibrium isotope effect associated with $f_{\text{exchange-abiotic}}$ ($\varepsilon_3 \approx +14$‰ at 21 °C) does not deviate appreciably with pH or salinity (Casciotti *et al.* 2007); however ε_3 is inversely proportional to temperature. McIlvin and Casciotti (2006) showed that ε_3 decreased by ~1‰ for every ~7 °C increase in temperature between 4–37 °C.

To summarize, despite the complexity of $\delta^{18}O$-N_2O formation in aerobic environments, the $\delta^{18}O$ values of N_2O produced by nitrification are constrained between +13‰ and +31‰. N_2O produced by NH_2OH oxidation closely resembles its $^{18}O/^{16}O$ endmember (O_2), whereas N_2O produced by nitrifier-denitrification varies more in $\delta^{18}O$ because values are highly dependent upon $\delta^{18}O$-H_2O, abiotic O-exchange, and the kinetic fractionations associated with NO_2^- reduction to N_2O. Although $\delta^{18}O$ values cannot be used to distinguish between the two nitrifier N_2O-forming pathways, they may be used (in conjunction with $\delta^{15}N$ values) in some applications to differentiate between NH_4^+-derived and NO_3^--derived N_2O. The latter often has higher $\delta^{18}O$-N_2O values because N_2O reduction, which is exclusive to denitrifiers, can increase the $\delta^{18}O$-N_2O much higher than the upper $\delta^{18}O$ limit of aerobically-produced N_2O. However, in some instances large amounts of biological O-exchange with H_2O, which is a process that appears to be unique to denitrifiers, can lead to overlapping $\delta^{18}O$ source signatures.

Table 5.1. The experimental conditions and the mean rates of N_2O produced by nitrification in this study, and the linear regression analyses of mean production-weighted $\delta^{18}O$-N_2O versus $\delta^{18}O$-H_2O.

field site	**agricultural**						**temperate forest**					
experiment	**1**			**2**			**3**			**4**	**5**	**6**
identifier (Canadian soil classification)	high OM (Melanic Brunisol)			low OM (Gray-Brown Luvisol)			upland 2005 (Oh horizon of Ferro-Humic Podzol)			upland 2006 (*idem*)	wetland (Mesisol)	
texture (% sand, % silt, % clay)	loam (19, 64, 17)			silt loam (43, 41, 16)			clay-loam (20, 46, 34)			n.d.	silty-clay (17, 43, 40)	
water holding capacity (%)	50			50			50			75	68	59
gravimetric soil moisture (g H_2O/g soil dw.)[a]	0.39			0.26			1.03			1.59	1.59	2.70
temperature (°C)	22			22			22			22	9	22
incubation length (days)	25, 37, 52[b]			25, 37, 52[b]			106			93	42	27
replicate incubations (n)	9, 6, 3			9, 6, 3			9			5	3	3
NH_4^+ fertilized?	yes			yes			no			no	no	no
organic matter (%)[c]	15			4			36			36	46	79
total C:total N (mol:mol)	12.7			9.7			18.4			18.4	17.7	20.3
soil pH (H_2O, 0.1 M $CaCl_2$)	7.5, 7.2			7.3, 7.0			5.1, 4.2			5.1, 4.2	5.2, 4.5	5.4, 5.1
mean N_2O production rate (pmol N_2O/hr/g-soil$_{dw.}$) ± 1σ (n)	590 ± 573 (45)			16 ± 20 (45)			53 ± 47 (81)			42 ± 34 (55)	21 ± 6 (9)	1254 ± 1600 (24)
treatment[d]	**a**	**b**	**c**	**a**	**b**	**c**	**a**	**b**	**c**	**a**	**a**	**a**
linear regression analysis ($y = mx + b$)												
mean production-weighted $\delta^{18}O$-N_2O [y] (‰) ± 1σ (n)[e]	17.7 ± 1.1 (13)	61.0 ± 1.1 (13)	111.6 ± 0.8 (13)	24.3 ± 6.6 (6)	51.6 ± 2.4 (7)	85.3 ± 6.7 (7)	25.3 ± 3.1 (27)	84.5 ± 4.7 (27)	103.9 ± 10.1 (27)	25.3 ± 0.5 (55)	29.3 ± 0.1 (9)	26.6 ± 1.5 (24)
$\delta^{18}O$-H_2O [x] (‰)	−8.2	39.4	92.7	−6.3	41.4	94.8	−10.4	68.0	106.0	−10.4	−6.4	−9.3
slope [m] ± standard error	0.931 ± 0.009			0.604 ± 0.042			0.687 ± 0.048			n/a	n/a	n/a
intercept [b] ± standard error	25.0 ± 0.5			27.6 ± 2.5			33.8 ± 3.5			n/a	n/a	n/a
r^2 (coefficient of determination)	1.00			0.97			0.97			n/a	n/a	n/a
95% confidence band[f]	± 1.33			± 6.47			± 9.22			n/a	n/a	n/a

[a] The gravimetric soil water content under experimental conditions.

[b] Three replicates (one from each ^{18}O enrichment) were extracted for $\delta^{18}O$-NO_3^- on days 25, 37 and at the end of the incubation.

[c] Determined by loss on ignition (LOI) at 550 °C for 4 hours.

[d] Treatments a, b, and c refer to the $^{18}O/^{16}O$ ranges of the soil waters (a = natural abundance, b = medium enrichment, c =high enrichment)

[d] The production-weighted $\delta^{18}O$-N_2O value of each replicate incubation was calculated as:

$$\sum_{t=0}^{final} (\delta^{18}O\text{-}N_2O \times \text{fraction of total } N_2O \text{ produced})_t$$, where t = sampling event.

The mean production-weighted $\delta^{18}O$-N_2O value [± 1σ or analytical uncertainty of $\delta^{18}O$-N_2O (0.4‰), whichever is greater] was calculated for each experiment or treatment and is listed in this table with the size of the sample mean (n).

[e] Linear regression confidence bands were calculated using the least squares method.

n/a – not applicable because experiments were not done with multiple $\delta^{18}O$-H_2O treatments.

n.d. – not determined.

Table 5.2. Input parameters used in the Monte Carlo simulations of Equations 5.10–5.11.

parameter	**input value or range**
δ^{18}O-H_2O[a]	*measured*
δ^{18}O-O_2	$+25.7‰$
$f_{\text{exchange-abiotic}}$	$0 \leq f \leq 1$
$f_{\text{exchange-}nir}$	$0 \leq f \leq 1$
$f_{\text{exchange-}nor}$	$0 \leq f \leq 1$
$f_{\text{N2O red}}$[b]	$0 \leq f \leq 0.75$
$f_{\text{N2O via NH2OH oxid.}}$	0
$f_{\text{N2O via nit.-denit.}}$	1
ε_1	$-17.5 \pm 5.4‰$
ε_2	$-16 \pm 7‰$
ε_3	$+14‰$
ε_5	$+10 \pm 6‰$
ε_6	$-16 \pm 7‰$
ε_7	$+10 \pm 6‰$
ε_8	$-16 \pm 7‰$
ε_9	$-15.5 \pm 10.5‰$
ε_{10}	$+14.6 \pm 5.5‰$

[a] Refer to Table 5.1 for δ^{18}O-H_2O values of each experiment's treatments.

[b] δ^{18}O-N_2O was simulated under four different scenarios with varying N_2O reduction (*scenario a*, $f = 0$; *scenario b*, $0 \leq f \leq 0.25$; *scenario c*, $0.25 \leq f \leq 0.5$; and *scenario d*, $0.5 \leq f \leq 0.75$).

Table 5.3. The range of $\delta^{18}O\text{-}N_2O$ produced by nitrification when the $\delta^{18}O$ values of O_2 and H_2O are not artificially ^{18}O-enriched. The column labels (letters) are referenced in the text. The bolded table cells show those values that differ from the 'moderate scenarios' shown in columns b and e.

$y = mx + b$; $\delta^{18}O\text{-}N_2O$ = Equation 5.10 × $\delta^{18}O\text{-}H_2O$ + Equation 5.11											
		N_2O (via NH2OH oxid.)			N_2O (via nit.-denit.)						
		a	b	c	d	e	f	g	h	i	j
parameter	input range	minimum value	moderate value	maximum value	minimum value	moderate value	maximum value	varying $f_{\text{exchange-abiotic}}$		invoking $f_{\text{exchange-nir}}$ and $f_{\text{exchange-nor}}$	invoking N_2O consumption
$\delta^{18}O\text{-}H_2O$ (‰)	−15 to +2	n/a	n/a	n/a	**−15**	−5	**+2**	−5	-5	−5	−5
$\delta^{18}O\text{-}O_2$ (‰)	+23.5	+23.5	+23.5	+23.5	23.5	+23.5	+23.5	+23.5	+23.5	+23.5	+23.5
$f_{\text{N2O via nit.-denit.}}$	0 or 1	0	0	0	1	1	1	1	1	1	1
$f_{\text{exchange-abiotic}}$	0.3–0.9	n/a	n/a	n/a	**0.3**	0.6	**0.9**	**0.3**	**0.9**	0.6	0.6
$f_{\text{exchange-}nir}$	0 (0.3)	n/a	n/a	n/a	n/a	n/a	n/a	n/a	n/a	**0.3**	n/a
$f_{\text{exchange-}nor}$	0 (0.2)	n/a	n/a	n/a	n/a	n/a	n/a	n/a	n/a	**0.2**	n/a
$f_{\text{N2O red.}}$	0 (0.25)	n/a	n/a	n/a	n/a	n/a	n/a	n/a	n/a	n/a	**0.25**
ε_1 (‰)	−17.5 ± 5.4	**−22.9**	−17.5	**−12.1**	**−22.9**	−17.5	**−12.1**	−17.5	−17.5	−17.5	−17.5
ε_2 (‰)	−16 ± 7	n/a	n/a	n/a	**−23**	−16	**−9**	−16	−16	−16	−16
ε_3 (‰)	+14	n/a	n/a	n/a	+14	+14	+14	+14	+14	+14	+14
ε_5 (‰)	+10 ± 6	n/a	n/a	n/a	**+4**	+10	**+16**	+10	+10	+10	+10
ε_6 (‰)	−16 ± 7	n/a	n/a	n/a	n/a	n/a	n/a	n/a	n/a	**−16**	n/a
ε_7 (‰)	+10 ± 6	n/a	n/a	n/a	**+4**	+10	**+16**	+10	+10	+10	+10
ε_8 (‰)	−16 ± 7	n/a	n/a	n/a	n/a	n/a	n/a	n/a	n/a	**−16**	n/a
ε_9 (‰)	−15.5 ± 10.5	n/a	n/a	n/a	n/a	n/a	n/a	n/a	n/a	n/a	**−15.5**
ε_{10} (‰)	+14.6 ± 5.5	**+9.1**	+14.6	**+20.1**	n/a	n/a	n/a	n/a	n/a	n/a	n/a
$\delta^{18}O\text{-}N_2O$ (‰)		**+9.7**	**+20.6**	**+31.5**	**−5.4**	**+22.4**	**+46.6**	**+17.5**	**+27.4**	**+5.7**	**+27.0**

n/a – not applicable.

n.b. $f_{\text{N2O via NH2OH oxid.}} = 1 - f_{\text{N2O via nit.-denit.}}$

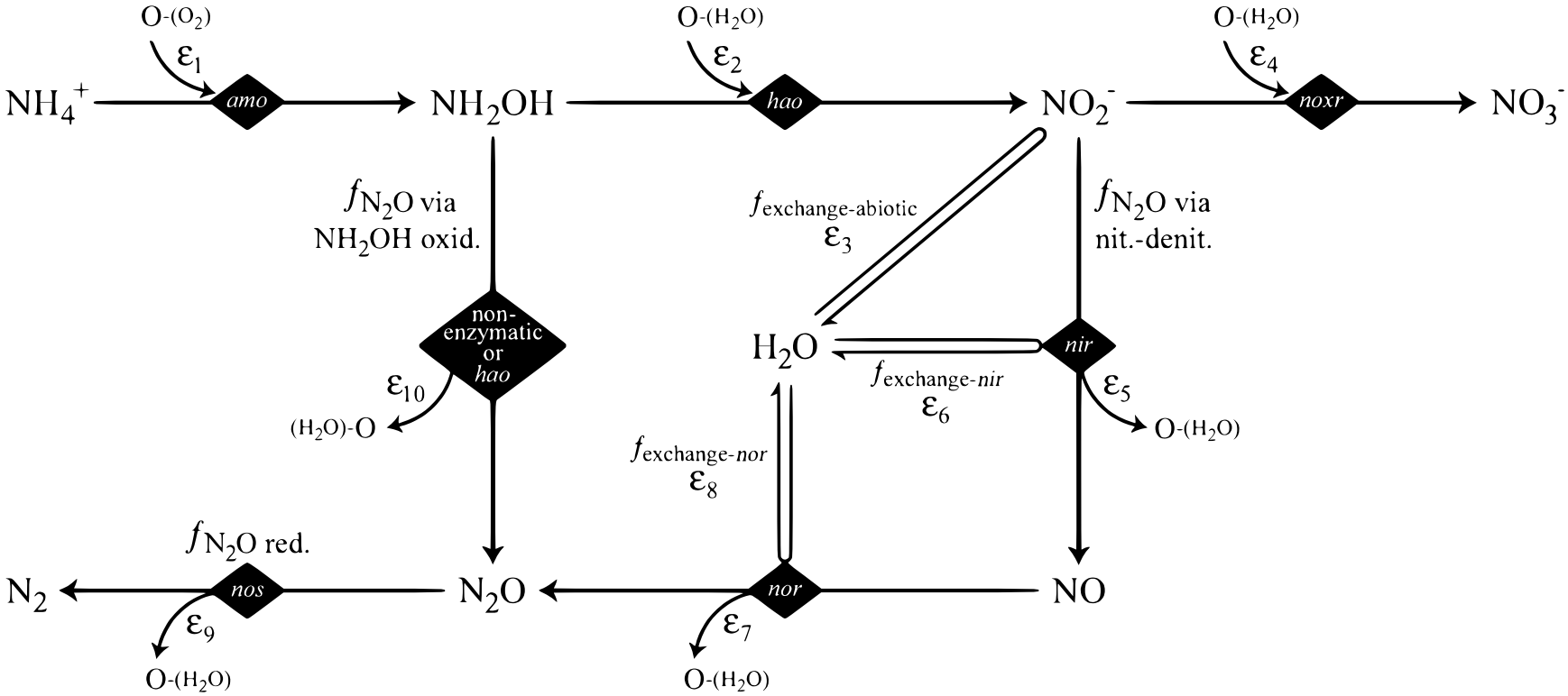


Figure 5.1. A schematic representation of the biogeochemical processes that form N_2O in aerobic environments. The total pool of nitrifier-N_2O is comprised of fractions (f) formed by: (i) the direct oxidation of NH_2OH to N_2O ($f_{\text{N2O via NH2OH oxid.}}$), and (ii) the reduction of NO_2^- to N_2O ($f_{\text{N2O via nit.-denit.}}$). N_2O may be consumed ($f_{\text{N2O red.}}$) within anoxic microsites of an otherwise aerobic environment. Oxygen atoms of NO_2^- can abiotically exchange with H_2O ($f_{\text{exchange-abiotic}}$); and further, enzyme-catalyzed O-exchange may occur between H_2O and NO_2^- and/or NO ($f_{\text{exchange-nir}}$, $f_{\text{exchange-nor}}$). This diagram accounts for O isotope effects (ε) at each oxidation, reduction and O-exchange step, regardless if they have been previously measured or not. Black diamond symbols represent enzymes, whose names are abbreviated to *amo* (ammonia monooxygenase), *hao* (hydroxylamine oxidoreductase), *noxr* (nitrite oxidoreductase), *nir* (nitrite reductase), *nor* (nitric oxide reductase), and *nos* (nitrous oxide reductase). In anoxic microsites the full denitrification pathway may occur starting with NO_3^- reduction to NO_2^-, which is catalyzed by nitrate reductase (*nar*, not shown).

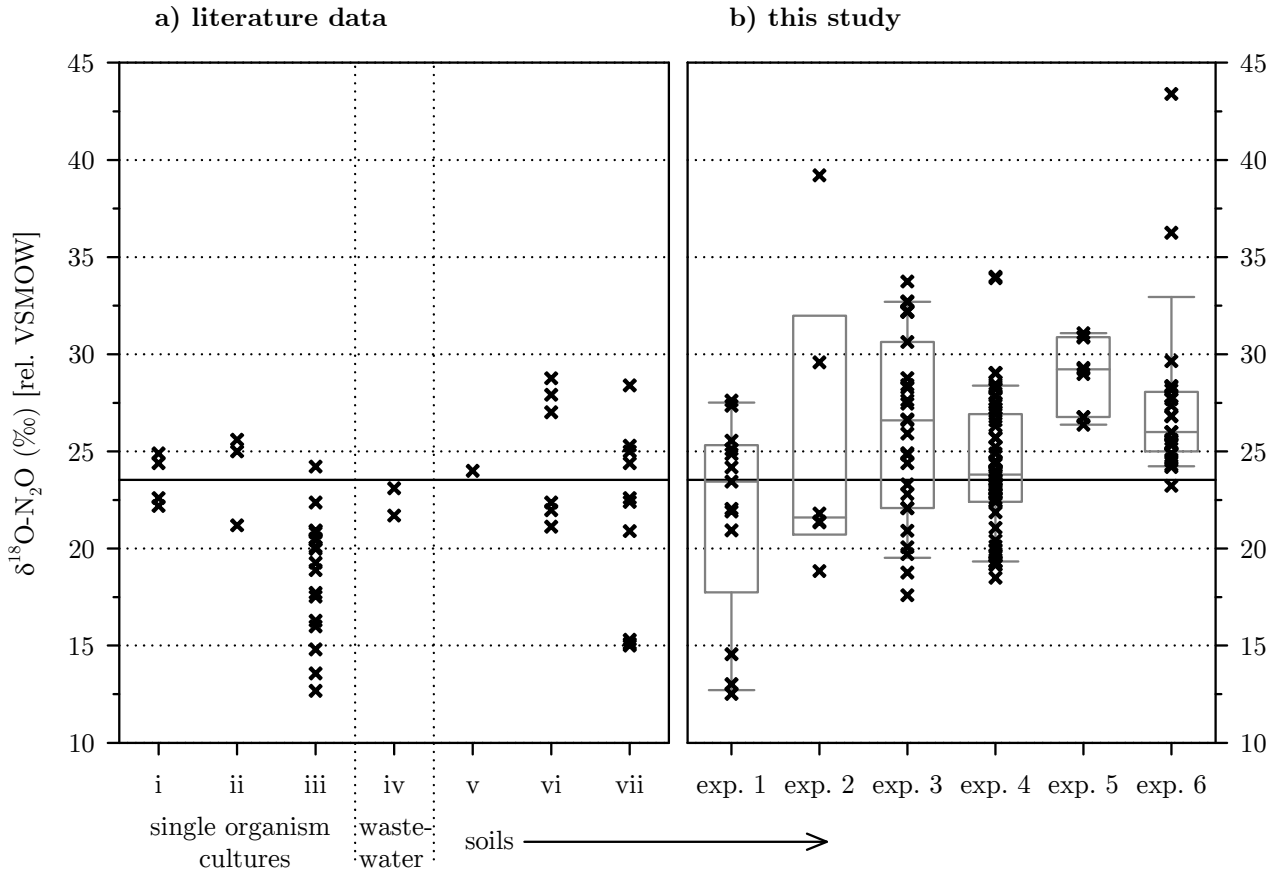


Figure 5.2a. Literature reports of $\delta^{18}O$ values of N_2O produced during ammonium (NH_4^+) oxidation by single organism cultures [*Nitrosomonas europaea*, Sutka *et al.* 2006 (i); *Methylosinus trichosporium* OB3b, Mandernack *et al.* 2009 (ii); *N. marina* C-113a, Frame & Casciotti 2010 (iii)] or the microbial consortia found in wastewater [Yoshinari & Wahlen 1985 (iv)] and soils [Wahlen & Yoshinari 1985 (v); Perez *et al.* 2001 (vi); Well *et al.* 2008 (vii)]. Data was obtained from published tables or extracted from published figures using g3data software (http://frantz.fi/software/g3data.php, Bauer & Reynolds 2008). **Figure 5.2b.** $\delta^{18}O$ values of N_2O collected from this study (with $\delta^{18}O$-H_2O at natural abundance) is plotted for comparison with literature data ($n = 134$). The dark grey vertical box plots show the median, 25th and 75th percentiles of experiments (exp.) 1-6, and the whiskers (where present) represent the 10^{th} and 90^{th} percentiles. The solid black horizontal line shows the $\delta^{18}O$ value of atmospheric O_2 (+23.5‰; Kroopnick & Craig 1972).

Figure 5.3a. Experiment 1

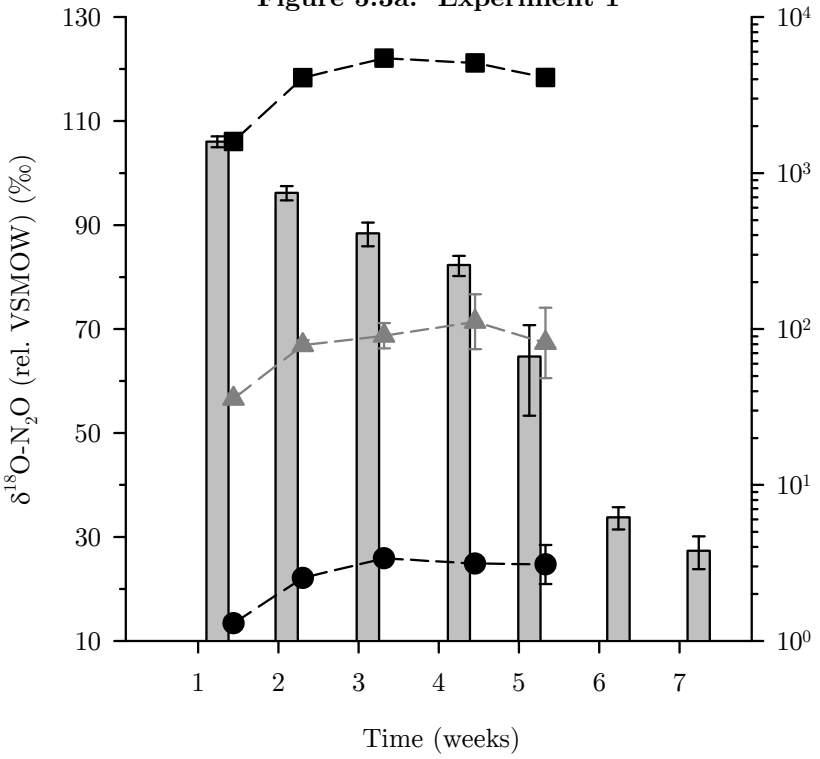


Figure 5.3b. Experiment 2

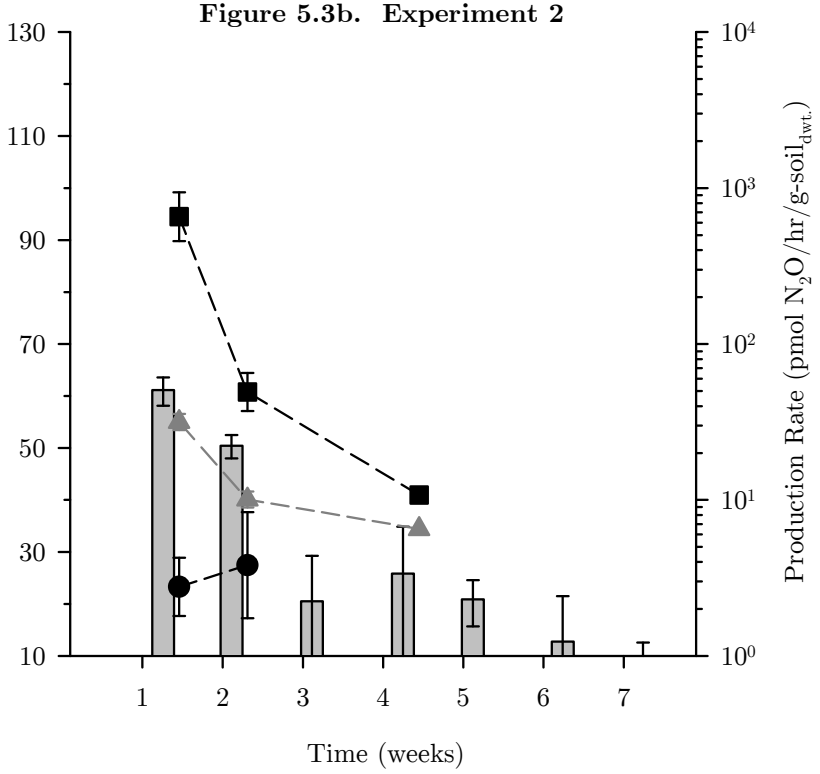


Figure 5.3c. Experiment 3

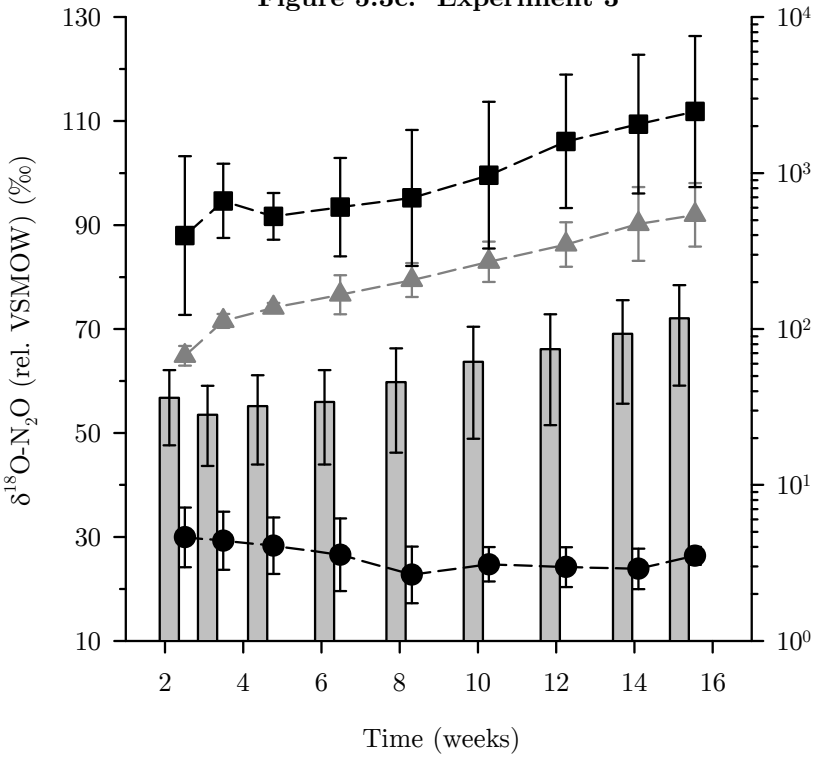
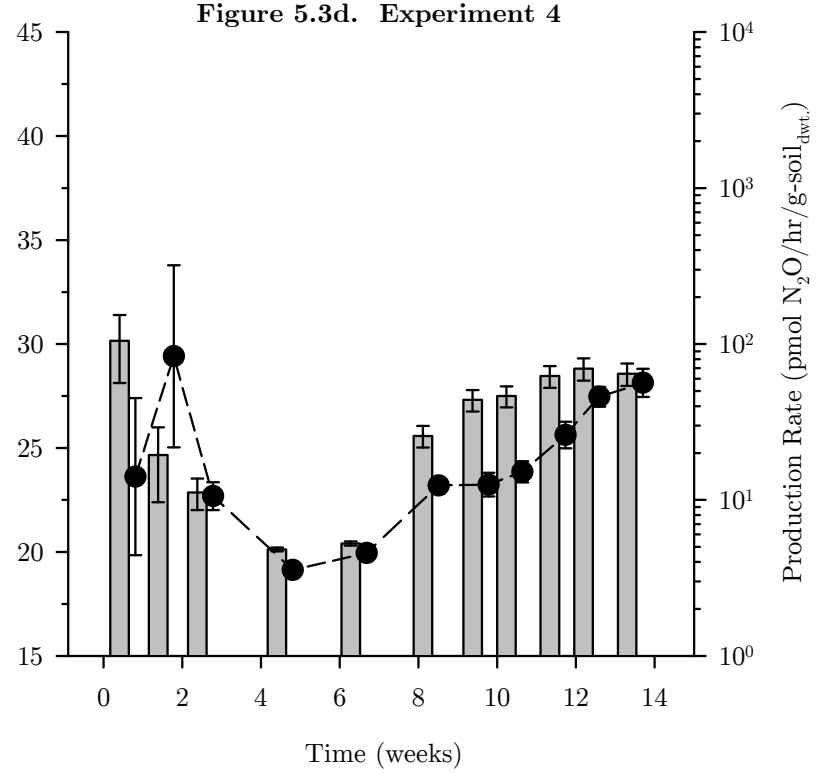
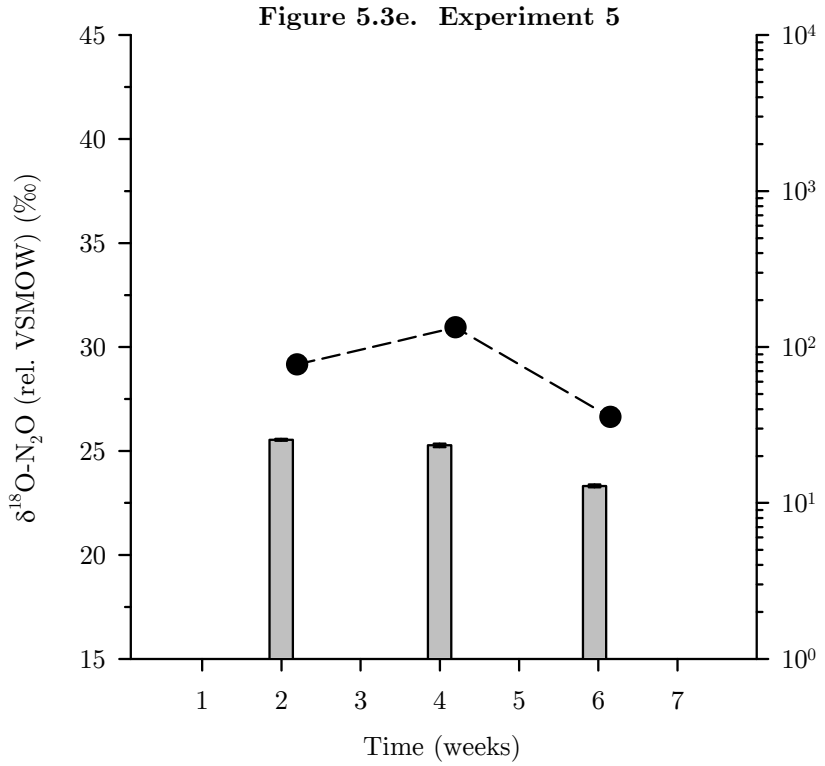


Figure 5.3d. Experiment 4





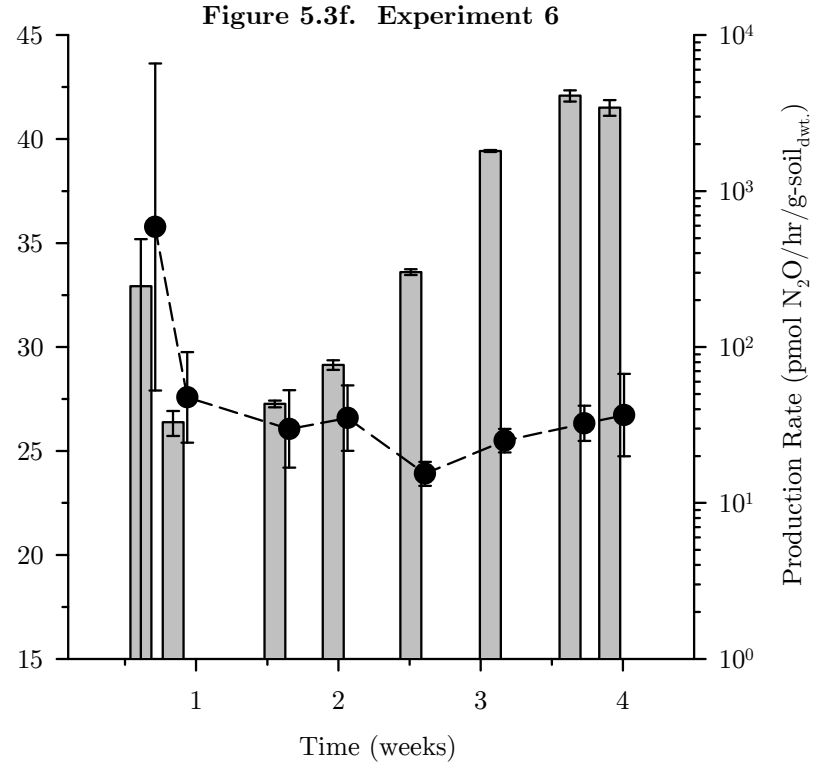


Figure 5.3a–f. The $\delta^{18}O\text{-}N_2O$ (scatter plots, left vertical axis) and rates of N_2O production (bar plots, right vertical axis) measured with time (horizontal axis) for experiments 1–6. The $\delta^{18}O\text{-}N_2O$ of experiments 1–3 spanned across distinct ranges that corresponded to $\delta^{18}O\text{-}H_2O$ at natural abundance (black circles), medium ^{18}O enrichment (grey triangles), and high ^{18}O enrichment (black squares). In a few cases, incubations were not sampled for $\delta^{18}O\text{-}N_2O$ because there was insufficient N_2O production for isotopic analysis. Error bars represent 1σ from the mean and, where they are absent, the error is smaller than the size of the symbol.

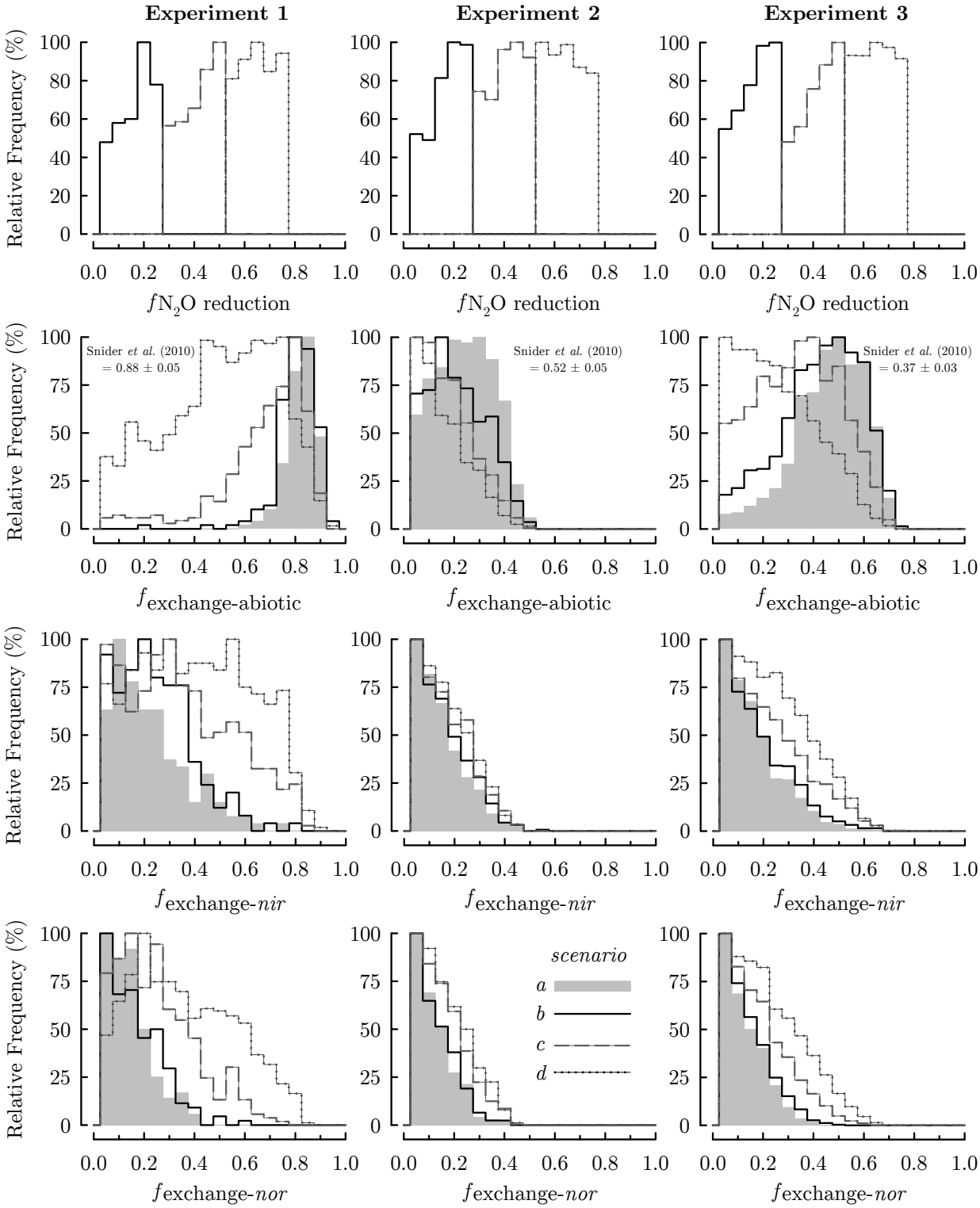
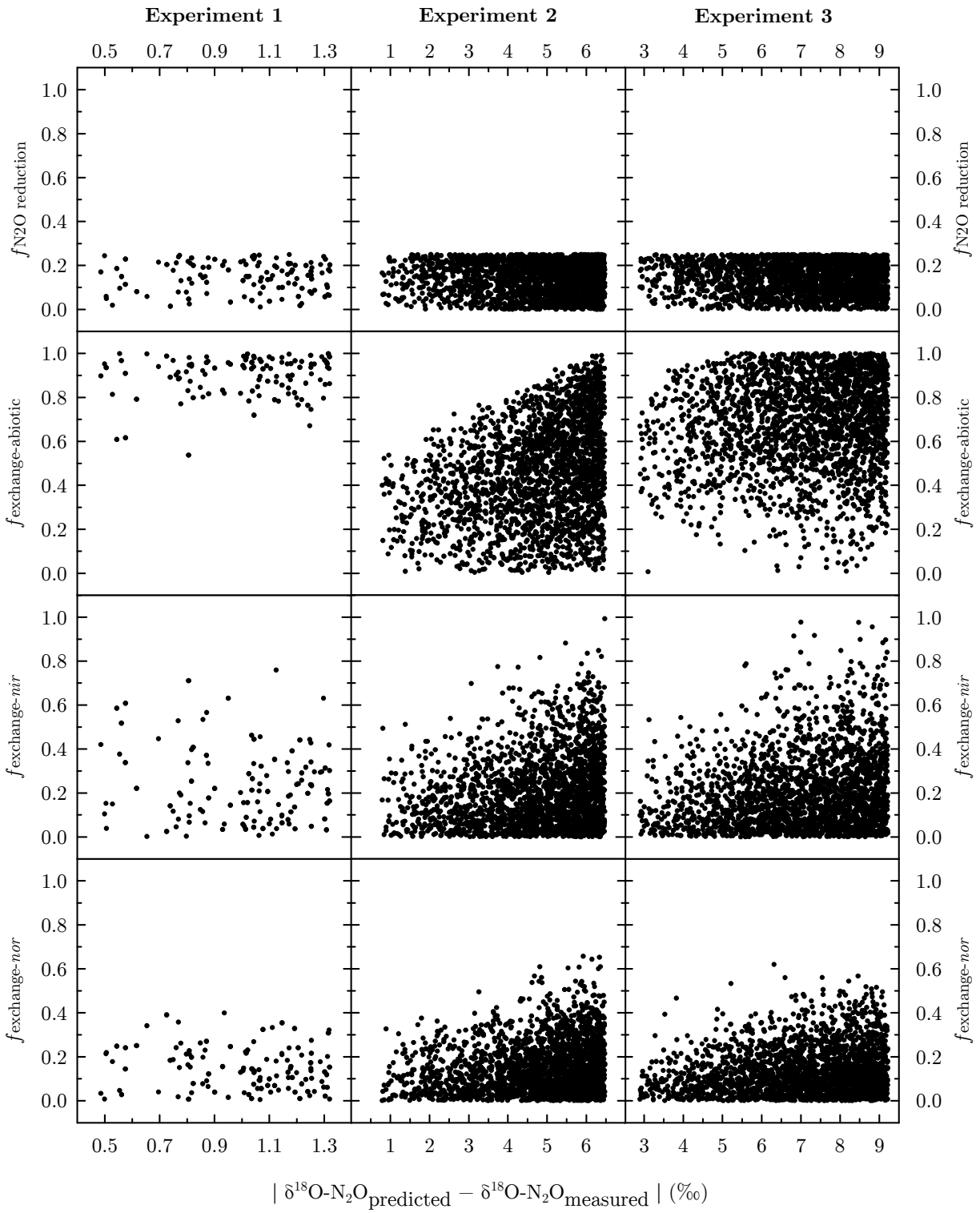
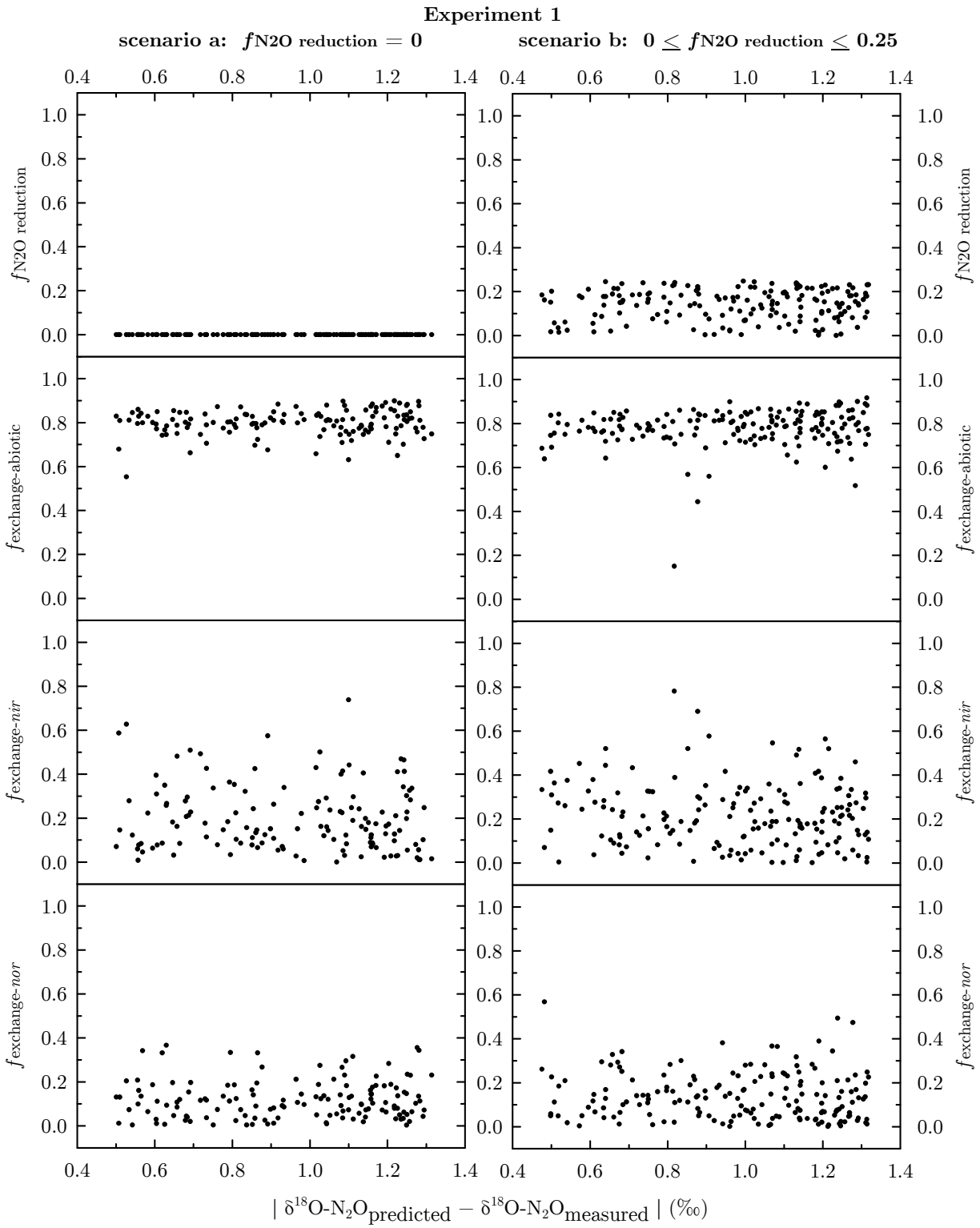


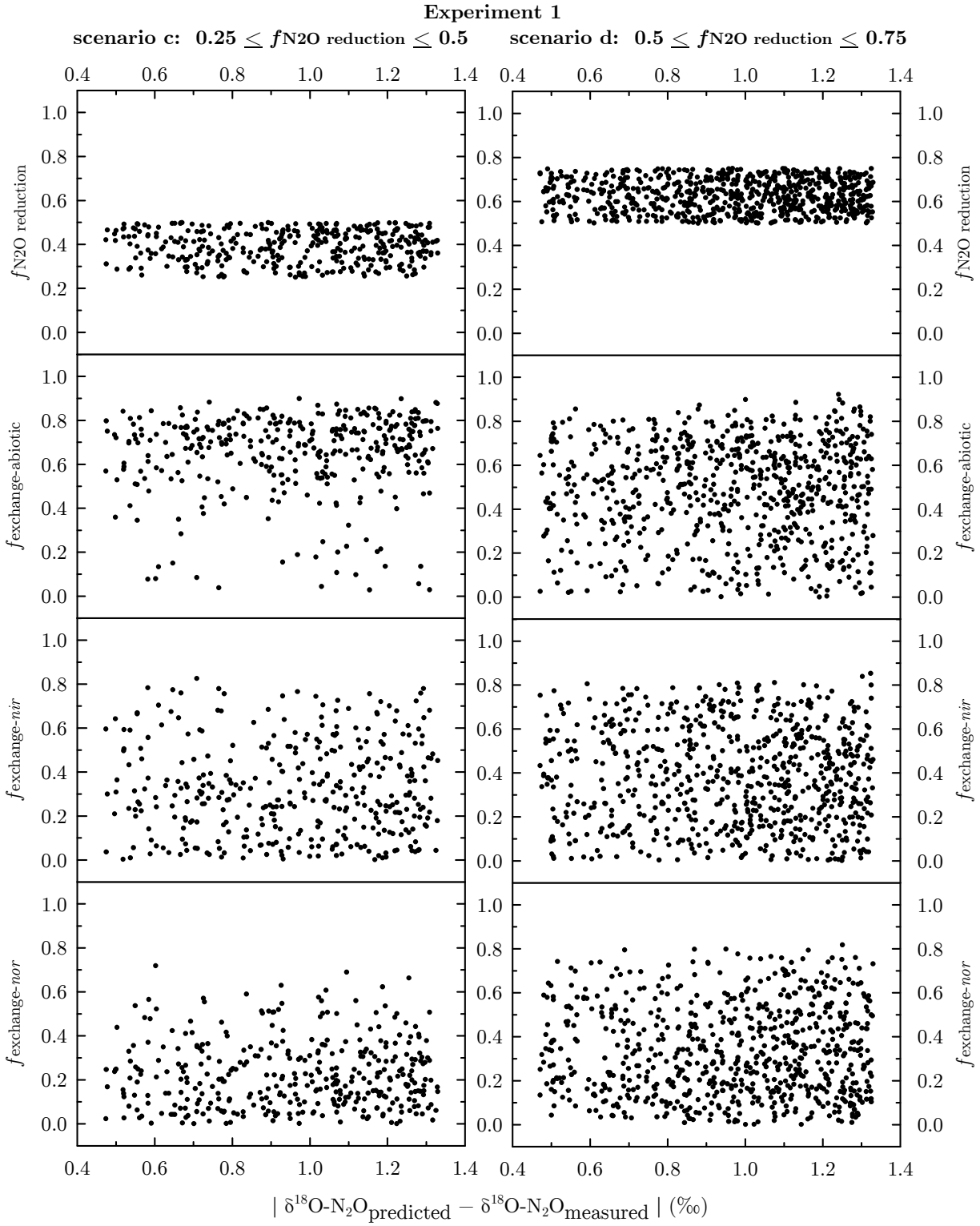
Figure 5.4. Histograms of model parameters predicted using Monte Carlo simulations. Solutions are within the 95% C.I. of the linear regressions of the measured δ^{18}O-N$_2$O versus δ^{18}O-H$_2$O. The solid grey step-plots depict the results of *scenario a* (fN2O red. = 0); the black solid line step-plots represent *scenario b* ($0 \leq f$N2O red. ≤ 0.25); the grey dashed line step-plots represent *scenario c* ($0.25 \leq f$N2O red. ≤ 0.5); and the grey dotted line step-plots represent *scenario d* ($0.5 \leq f$N2O red. ≤ 0.75). The frequency [count (n)] in each bin is expressed relative to the maximum count observed across all bins (bin size = 0.05).



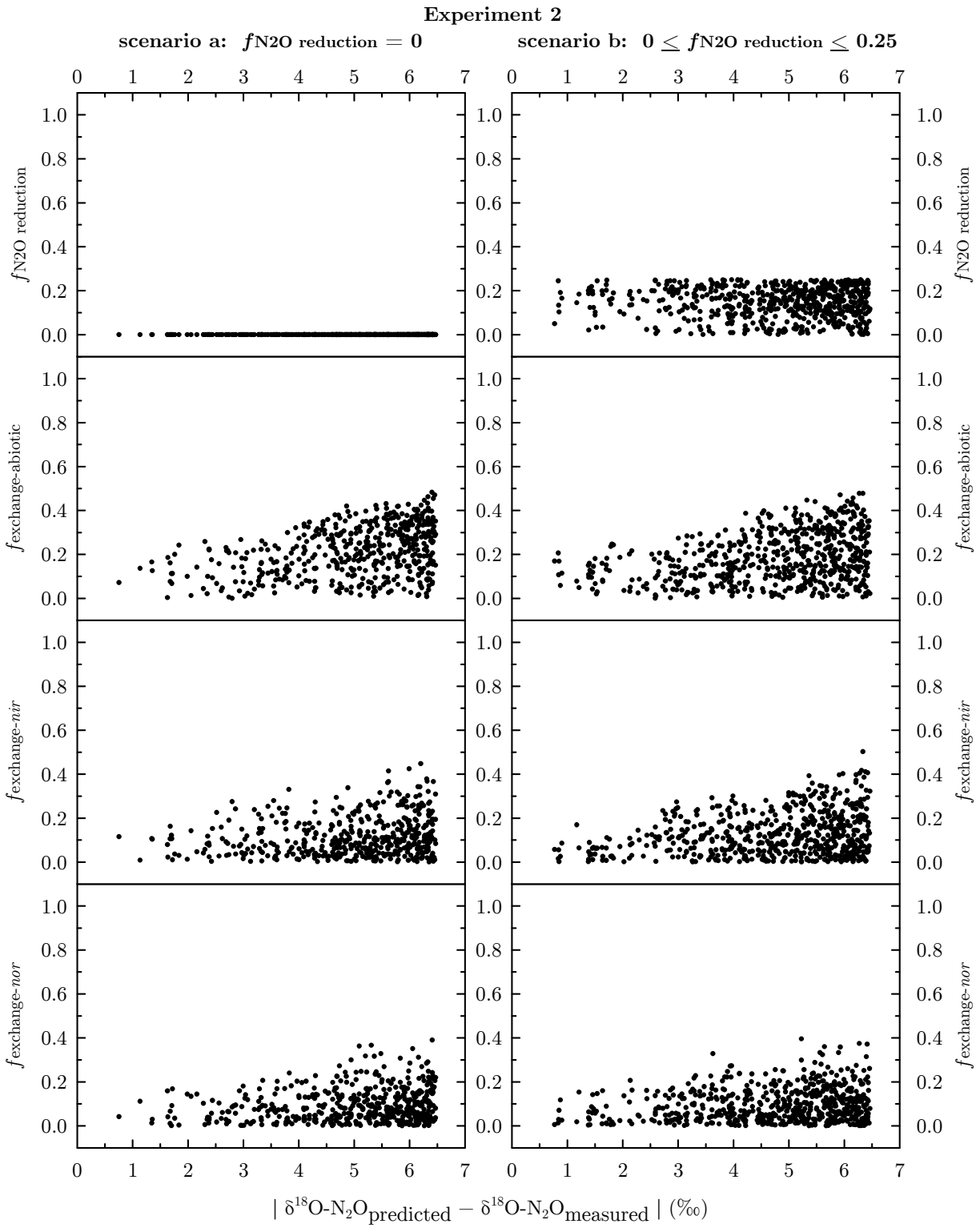
Supplementary Figure 5.1. The Monte Carlo simulation results for Experiments 1-3 (*scenario b*) with variable fractions of N_2O produced via nitrifier-denitrification (0.75-1) and via NH_2OH oxidation (0-0.25) [where the total N_2O from both pathways = 1]. Only those results that yielded $\delta^{18}O\text{-}N_2O$ within the 95% confidence bands of the measured $\delta^{18}O\text{-}N_2O$ are shown (n = 165 for Expt. 1; n = 2276 for Expt. 2; n = 2296 for Exp. 3). 300,000 and 100,000 model runs were performed for Expt. 1 and Expts. 2-3, respectively.



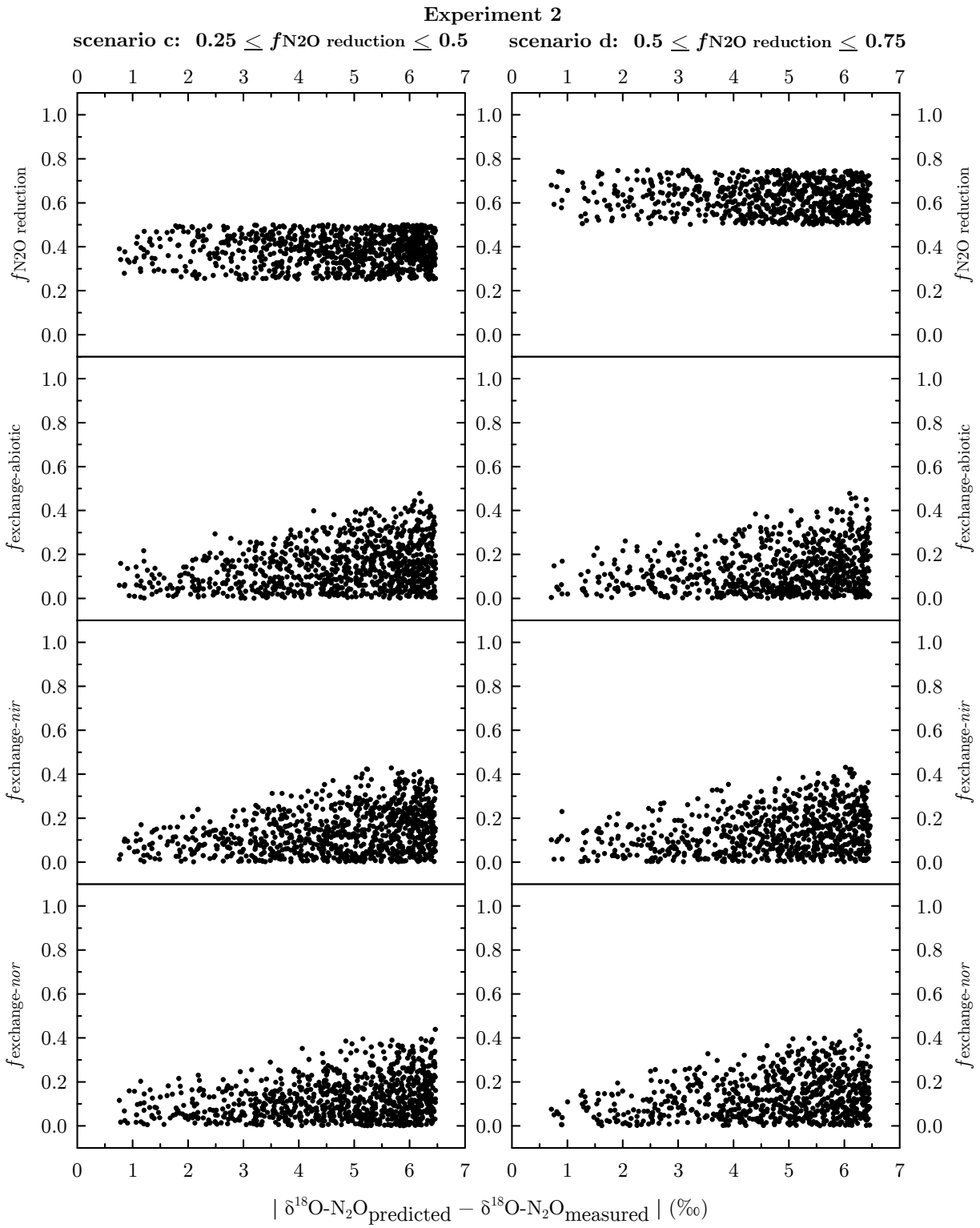
Supplementary Figure 5.2a. The Monte Carlo simulation results for Experiment 1 when the fraction of N_2O reduction is zero (*scenario a*) or varies between zero and 0.25 (*scenario b*). Of the total 100,000 model runs conducted for each scenario, only those results that yielded $\delta^{18}O\text{-}N_2O$ predictions that were within the 95% confidence bands (± 1.33‰) of the measured $\delta^{18}O\text{-}N_2O$ are shown here ($n = 140$ for *scenario a*; $n = 172$ for *scenario b*).



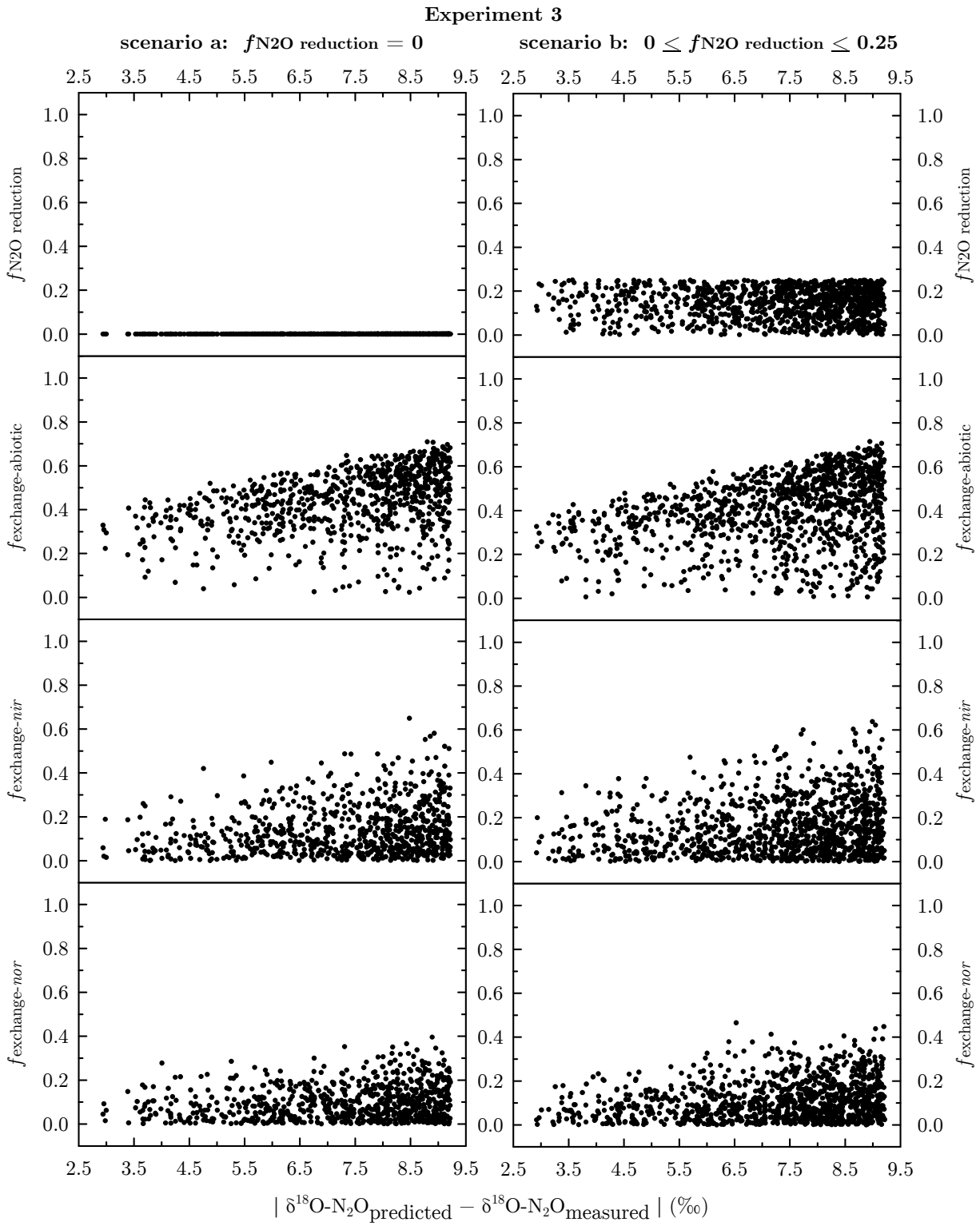
Supplementary Figure 5.2b. The Monte Carlo simulation results for Experiment 1 when the fraction of N_2O reduction varies between 0.25-0.5 (*scenario c*) or between 0.5-0.75 (*scenario d*). Of the total 100,000 model runs conducted for each scenario, only those results that yielded $\delta^{18}O$-N_2O predictions that were within the 95% confidence bands (± 1.33‰) of the measured $\delta^{18}O$-N_2O are shown here (n = 363 for *scenario c*; n = 713 for *scenario d*).



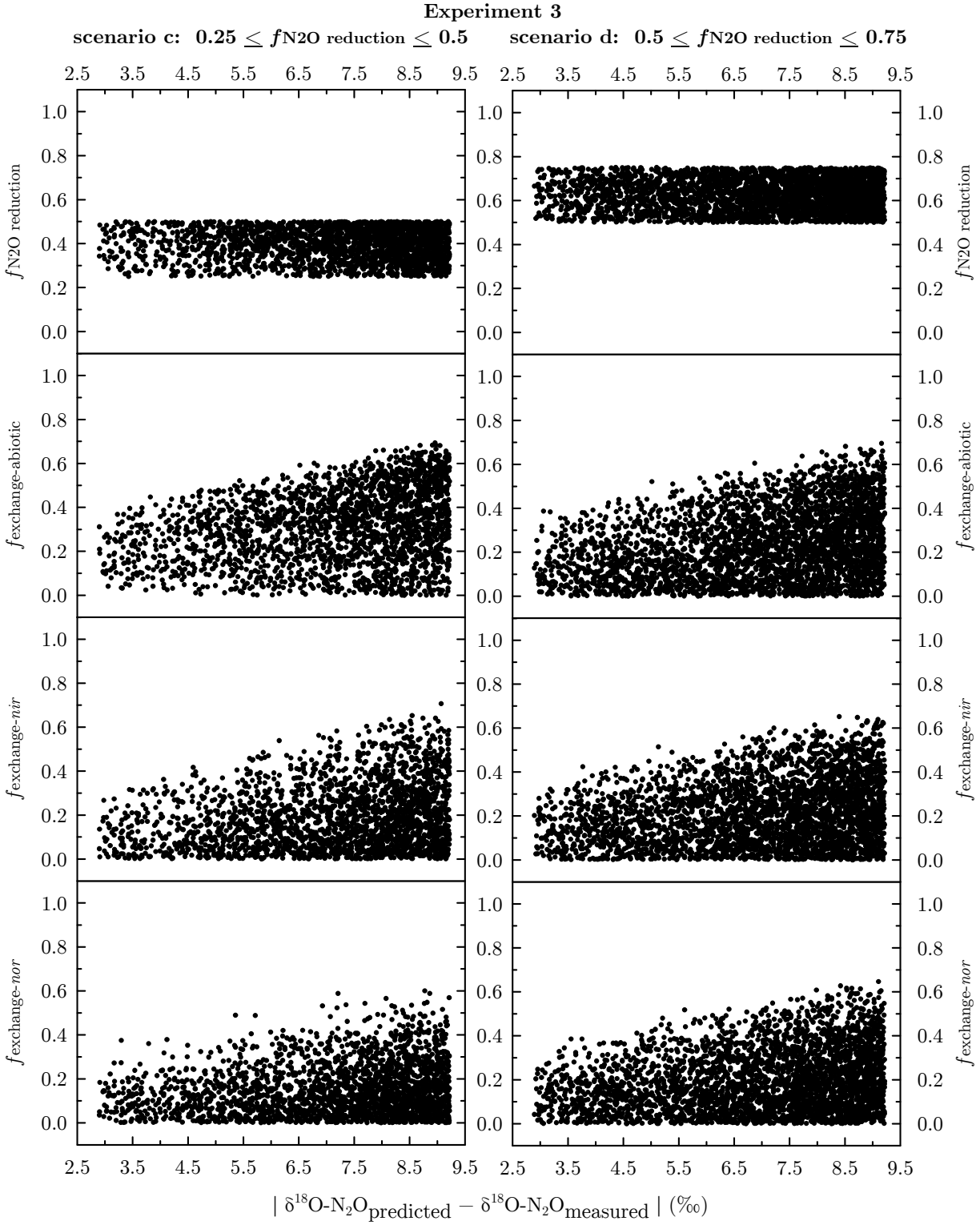
Supplementary Figure 5.3a. The Monte Carlo simulation results for Experiment 2 when the fraction of N_2O reduction is zero (*scenario a*) or varies between zero and 0.25 (*scenario b*). Of the total 100,000 model runs conducted for each scenario, only those results that yielded $\delta^{18}O\text{-}N_2O$ predictions that were within the 95% confidence bands (± 6.47‰) of the measured $\delta^{18}O\text{-}N_2O$ are shown here ($n = 484$ for *scenario a*; $n = 614$ for *scenario b*).



Supplementary Figure 5.3b. The Monte Carlo simulation results for Experiment 2 when the fraction of N_2O reduction varies between 0.25-0.5 (*scenario c*) or between 0.5-0.75 (*scenario d*). Of the total 100,000 model runs conducted for each scenario, only those results that yielded $\delta^{18}O$-N_2O predictions that were within the 95% confidence bands (± 6.47‰) of the measured $\delta^{18}O$-N_2O are shown here (n = 931 for *scenario c*; n = 783 for *scenario d*).



Supplementary Figure 5.4a. The Monte Carlo simulation results for Experiment 3 when the fraction of N_2O reduction is zero (*scenario a*) or varies between zero and 0.25 (*scenario b*). Of the total 100,000 model runs conducted for each scenario, only those results that yielded $\delta^{18}O$-N_2O predictions that were within the 95% confidence bands (± 9.22‰) of the measured $\delta^{18}O$-N_2O are shown here (n = 797 for *scenario a*; n = 1139 for *scenario b*).



Supplementary Figure 5.4b. The Monte Carlo simulation results for Experiment 3 when the fraction of N_2O reduction varies between 0.25-0.5 (*scenario c*) or between 0.5-0.75 (*scenario d*). Of the total 100,000 model runs conducted for each scenario, only those results that yielded $\delta^{18}O$-N_2O predictions that were within the 95% confidence bands (± 9.22‰) of the measured $\delta^{18}O$-N_2O are shown here (n = 2380 for *scenario c*; n = 3528 for *scenario d*).

6 The $\delta^{15}N$ of nitrous oxide and nitrate produced by nitrification in agricultural and temperate forest soils

Overview

Fertilized and unfertilized incubations of agricultural and temperate forest soils were conducted to examine the $\delta^{15}N$ values of nitrous oxide (N_2O) and nitrate (NO_3^-) generated by nitrification. The rate of N_2O production spanned five orders of magnitude with minimum rates of <1 picomol N_2O/hr/g-soil$_{dw.}$ measured in a well-drained agricultural soil and maximum rates >4000 picomol N_2O/hr/g-soil$_{dw.}$ measured in a forested peat.

An unfertilized upland forest soil generated $\delta^{15}N$-NO_3^- that was 11.5‰ lower than the $\delta^{15}N$ of the organic nitrogen pool, which is a characteristic ^{15}N-depletion for NO_3^- produced by microbial nitrification. Ammonium (NH_4^+) fertilizer applied to the agricultural soils was rapidly consumed by nitrification. As a result, the $\delta^{15}N$-NO_3^- in these soils was equal to, or higher, than the $\delta^{15}N$ of the NH_4^+ fertilizer.

The mean production-weighted $\delta^{15}N$-N_2O in all treatments varied from −48‰ to −13‰, and the $\delta^{15}N$-N_2O was well-correlated with the N_2O production rate in many of the soils. The isotopic separation (Δ) between N_2O and NH_4^+ in the agricultural soils and the forested peat ranged from −35‰ to −16‰. These Δ separations were less negative than the expected ^{15}N-depletion for nitrification because the supply of substrate was limited in these treatments. The ^{15}N isotope effect ($\varepsilon_{\text{nitrous oxide−total nitrogen}}$) in the upland forested soils varied from −55‰ to −37‰. The greatest ^{15}N-depletions in the forest soils were measured towards the end of the incubations when N_2O production rates were highest and the substrate pool was large.

With the exception of the temperate forest peat, all soils incubated in this study produced nitrifier-N_2O with $\delta^{15}N$ values lower than the denitrifier-derived N_2O produced by the same soils in Chapters 2 and 3. This shows that $\delta^{15}N$-N_2O can be used to separate different N_2O sources, provided that the $\delta^{15}N$ values of the endmembers are well-characterized.

6.1. *Introduction*

The soil nitrogen (N) cycle is a complicated and fascinating network of redox reactions that are catalyzed by many different microorganisms for metabolism or N nutrition. Several different species of inorganic N exist in oxidation states that range from −3 to +5 (Figure 6.1). Stable N isotope ratio ($^{15}N/^{14}N$) measurements are a useful addition to a geochemist's toolbox because they often allow the identification of unique N sources. For example, the $\delta^{15}N$ of fertilizer NO_3^- is distinct from the $\delta^{15}N$ of sewage and manure NO_3^- (Xue *et al.* 2009). Oftentimes, $\delta^{15}N$ measurements are useful in apportionment studies because the isotopic fractionation associated with a particular reaction pathway imparts a unique isotopic fingerprint on the measured compound. The latter approach is used in this study to examine $\delta^{15}N$ values of N_2O and NO_3^-.

The $\delta^{15}N$ values of N_2O produced from nitrifier-denitrification are thought to be much lower than the $\delta^{15}N$-N_2O produced from denitrification (e.g., Yoshida 1988; Webster and Hopkins 1996; Perez *et al.* 2006, 2001). The results of these studies suggest that nitrifier-derived $\delta^{15}N$-N_2O is 50–75‰ lower than the $\delta^{15}N$ value of its substrate. Many of the early (and recent) works demonstrated this with pure cultures of nitrifying organisms and very little research has been done in soils or other natural media to confirm our expectations. However, to properly demonstrate the utility of $\delta^{15}N$ to separate nitrifier-derived N_2O from denitrifier-derived N_2O, research using soils (which contain a consortium of N-cycling organisms) must be done.

Well *et al.* (2008) conducted microcosm studies of fertilized arable soils to determine the isotopic composition of N_2O produced by nitrification. They concluded that $\delta^{15}N$ measurements are a poor indicator of nitrifier-produced N_2O because they often change significantly over short periods of time. They observed an increase in the $\delta^{15}N$-N_2O produced in their experiments because the nitrifiers' voracious appetite for fertilizer resulted in a ^{15}N enrichment of the substrate and product pools.

Only one published study has defined the $\delta^{15}N$ values of nitrifier and denitrifier-N_2O in the same soils. Perez *et al.* (2006) incubated Amazonian rain forest soils and they calculated

^{15}N isotope effects ($\varepsilon_{\text{nitrous oxide}-\text{ammonium}}$) for nitrification of $-112‰$ to $-102‰$ [where $\varepsilon = (\alpha - 1) \times 1000$, and $\alpha = {}^{15}N/{}^{14}N$–product $\div$ $^{15}N/^{14}N$–substrate]. These results were puzzling because the values were so different than any of the previously reported estimates. A careful examination of their methodological approaches revealed that their $\delta^{15}N\text{-}N_2O$ values from nitrification were not measured. Instead, the data was modelled using a combination of acetylated and non-acetylated soil incubations to apportion the fractions of N_2O from nitrification and denitrification. The nitrification-N_2O endmember was derived using a 'Keeling Plot' approach. Additionally, the $\delta^{15}N\text{-}NH_4^+$ endmember used to calculate ε in their study was up to $22‰$ higher than the $\delta^{15}N$-TN suggesting other important factors were not accounted for (e.g., volatilization).

At steady-state, the rate-limiting step for nitrification is expected to be the slow oxidation of NH_4^+ to NO_2^- (Kendall 1998). Experiments with different chemolithoautotrophic ammonia-oxidizing bacteria (AOB) have shown that NH_4^+ must accumulate to intracellular concentrations of ~1 M before the first NO_2^- molecules are produced (Schmidt *et al.* 2004). Under these conditions, maximum ^{15}N fractionation between NH_4^+ and NO_2^- can occur, which varies between $-37‰$ and $-25‰$ in *N. europaea* (Mariotti *et al.* 1982; Yoshida 1988).

Upon oxidation of NH_4^+ by AOB, the NO_2^- product is further oxidized to NO_3^- by a separate group of organisms termed nitrite-oxidizing bacteria (NOB) (Figure 6.1). Casciotti *et al.* (2009) recently discovered that NO_2^- oxidation in *Nitrococcus mobilis* (a marine NOB) imparts an *inverse* isotope effect of $+13‰$. Given the estimates of ε for $NH_4^+ \rightarrow NO_2^-$ ($-37‰$ to $-25‰$, Mariotti *et al.* 1982; Yoshida 1988) and the ε for $NO_2^- \rightarrow NO_3^-$ ($+13‰$, Casciotti *et al.* 2009), the combined ε for $NH_4^+ \rightarrow NO_3^-$ is $-24‰$ to $-12‰$. This overall isotope effect for nitrification is amazingly similar to the observed ^{15}N isotope effect in soils ($-29‰$ to $-12‰$; Kendall 1998).

This may be fortuitous, however, because NO_2^- rarely accumulates in the environment and this must happen if the inverse isotope effect for NO_2^- oxidation is to be expressed in the $\delta^{15}N\text{-}NO_3^-$. Instead, the lower estimates of $\varepsilon_{\text{nitrate}-\text{ammonium}}$ that are often observed in soils are likely due to non-steady-state reaction rates (k) of N assimilation, mineralization, and nitrifi-

cation (NO_3^- and N_2O production). In fact, in many soil systems, the observed $\Delta_{\text{nitrate–ammonium}}$ is often ~0‰ and very little net fractionation occurs.

Yoshida (1988) and Sutka *et al.* (2003, 2004, 2006) have measured the ^{15}N ε for NO_2^- reduction to N_2O (−38‰ to −24‰) by supplying *Nitrosomonas* bacteria with exogenous NO_2^- and measuring the $\delta^{15}N$-N_2O. These studies have led to the belief that the overall $\delta^{15}N$ isotope effect for N_2O produced by nitrifier-denitrification ($NH_4^+ \rightarrow NO_2^- \rightarrow N_2O$) is large and negative (−75‰ to −50‰) because it is assumed that $\varepsilon_{\text{nitrite–ammonium}}$ and $\varepsilon_{\text{nitrous oxide–nitrite}}$ can be summed to yield $\varepsilon_{\text{nitrous oxide–ammonium}}$. However, these independently measured estimates can only be added together to derive an overall N isotope effect ($NH_4^+ \rightarrow N_2O$) when NO_2^- (or another intermediate compound) accumulates and a second rate-limiting step occurs.

Admittedly, this is a major point of contention that needs further study and clarification in the literature. There is currently nothing to indicate that NH_4^+ oxidation and NO_2^- reduction are two separate, uncoupled reaction mechanisms in nitrifier-denitrifiers. Instead, it is probable that NH_4^+ oxidation is coupled to NO_2^- reduction and the whole reaction mechanism is intracellular and sequential (Figure 6.1) because AOB are capable of metabolizing the entire sequence of oxidations and reductions.

The potential for $\delta^{15}N$ to separate N_2O produced by denitrification and nitrifier-denitrification remains uncertain. Although many studies using bacterial cultures suggest that there is clear ^{15}N separation between denitrification and nitrifier-denitrification, Well *et al.* (2008) suggests that there is too much overlap to successfully apportion N_2O sources in soils. Therefore, the main objective of this chapter is to characterize the $\delta^{15}N$-N_2O produced from soil incubations under different nitrifying conditions, and to calculate the associated ^{15}N enrichment factors (ε). A secondary objective of this chapter is to report the $\delta^{15}N$ values of NO_3^- generated by soil nitrification.

6.2. *Materials and Methods*

Almost all of the methodologies used to generate the data presented in this chapter have been described elsewhere in this thesis, particularly in Chapters 4–5. The following information only briefly describes the experimental protocols used in this Chapter. Particular attention is given to those methods that are not described elsewhere in this thesis.

6.2.1. *Soil Collection, Processing, and Geochemical Characterization*

Two agricultural soils were collected in bulk from the Strawberry Creek Watershed, Maryhill, Ontario, Canada (Chapter 3, Figure 3.1a–b). Both were nutrient-poor, mineral soils that were planted with late vegetative-stage corn at the time of collection. One silt-loam soil was collected from a well-drained site low in organic matter (OM) (treatment 1). The other agricultural soil (loam) was collected from a wetter site with a higher amount of OM (treatment 2).

Temperate forest soils were collected from the Turkey Lakes Watershed (TLW), near Sault Ste. Marie, Ontario, Canada (www.tlws.ca). Two batches of an organic-rich, Oh-horizon clay-loam soil (Agriculture and Agri-Food Canada, The Canadian System of Soil Classification, 3rd ed., 1998) were collected from the same plot within an upland site in 2005 (treatments 3–5) and 2006 (treatment 6). Additionally, a peat (silty-clay soil) was collected from a forested swamp in 2006 (treatment 7).

All soils were air-dried, homogenized, sieved to 2 mm, and stored in resealable freezer bags at room temperature in a dark cabinet for future incubation use. The % total carbon (TC), δ^{13}C-TC, % total nitrogen (TN), and δ^{15}N-TN were analyzed on an elemental analyzer (EA) coupled to an isotope ratio mass spectrometer (IRMS). Carbon:nitrogen ratios were calculated and reported on a molar basis for an non-acidified sample (Table 6.1). The % OM was determined by loss on ignition (LOI), and a particle size analysis of the soils was conducted. The concentrations of extractable NH_4^+ and NO_3^- were quantified by extracting soils with 2 M potassium chloride (KCl) and Nanopure deionized water (DI) (Barnstead International, Dubuque, IA), respectively. Soil pH was determined in calcium chloride ($CaCl_2$) and

water following ASTM methods (ASTM International 2007). The results of these analyses are shown in Table 6.1.

Detailed descriptions of the methods used to analyze N_2O concentration and $\delta^{15}N\text{-}N_2O$ are provided in Chapter 2. NO_3^- isotopes were determined using ion exchange methods developed by Chang *et al.* 1999 and Silva *et al.* 2000 and are described in greater detail in Chapter 4. The values of $\delta^{15}N\text{-}NO_3^-$ were determined by EA-IRMS by combining 1 mg of silver nitrate ($AgNO_3$) and 2 mg of sucrose into tin capsules. All samples were analyzed alongside internal $\delta^{15}N\text{-}NO_3^-$ standards that had been previously calibrated against international reference materials. The analytical precision (1σ) for $\delta^{15}N\text{-}NO_3^-$ was $\pm$ 0.3‰.

Nitrogen isotope ratios of N_2O and NO_3^- are expressed in delta (δ) notation, calculated as ($^{15}N/^{14}N$ sample $\div$ $^{15}N/^{14}N$ standard $-$ 1) and reported in units of per mill (‰), where the $^{15}N/^{14}N$ of the standard reference material (atmospheric N_2 – AIR) is 0.003663 (Coplen *et al.* 2002). Instantaneous nitrogen isotope effects (ε) are calculated as ($\alpha - 1$) and reported in ‰ units, where α = $^{15}N/^{14}N$ product $\div$ $^{15}N/^{14}N$ substrate. Further definition of the instantaneous ε and justification for its usage in this study is given in Section 6.3.5.

6.2.2. *Soil Incubation Protocol*

In order to characterize the $\delta^{15}N\text{-}N_2O$ and $\delta^{15}N\text{-}NO_3^-$ produced by nitrification, seven separate incubations were conducted that differed in soil type, moisture and temperature. The ultimate goal of the different experimental conditions was to generate a wide range of nitrification rates (N_2O and NO_3^- production rates) and characterize the $\delta^{15}N\text{-}N_2O$ and $\delta^{15}N\text{-}NO_3^-$. All incubations were conducted in the dark at ambient laboratory temperatures (~22 °C) except for treatments 5–6, which were cooled to 9 °C in a dark, refrigerated chamber. Incubations of treatment 5 began at room temperature and were cooled for the final quarter of the experiment to see how abrupt changes in temperature affected the rate of N_2O production and the $\delta^{15}N\text{-}N_2O$ values.

The agricultural soils were fertilized with reagent-grade ammonium chloride (NH_4Cl; 0.15 mg N/g-$soil_{dw.}$; $\delta^{15}N\text{-}NH_4^+ = -0.84 \pm 0.1$‰) because the rates of N_2O production in

unamended soils were negligible (results not shown). The temperate forest soils did not require NH_4^+ fertilization because production rates were high enough to produce sufficient N_2O for isotopic analysis every 1–2 weeks.

After the incubation jars were sealed, the headspace was purged with a commercial gas mixture containing 20.9% molecular oxygen (O_2) balanced with ultra-high purity helium. Incubations were sampled for N_2O concentration every 1–2 weeks, and if sufficient N_2O existed, jars were sampled for $\delta^{15}N\text{-}N_2O$. After sampling, the headspace was purged again to remove all the N_2O prior to the onset of the next 1–2 week incubation period. Agricultural soils (treatments 1–2) were incubated for 52 days, with sacrificial samplings for $\delta^{15}N\text{-}NO_3^-$ that occurred on days 25 and 37. The length of the temperate forest soil incubations ranged from 27 days (treatment 7) to 199 days (treatment 5). At the end of treatment 3, soils were extracted for $\delta^{15}N\text{-}NO_3^-$ analysis. NO_3^- extractions were not performed in any of the remaining temperate forest soils (treatments 4–7).

6.3. *Results and Discussion*

6.3.1. *Ammonification, Nitrification and N_2O Production (Treatments 1–2)*

The rates of ammonification (organic N $\rightarrow$ NH_4^+) in unfertilized agricultural soil incubations were very slow (results not shown), and consequently, their natural rates of nitrification ($NH_4^+ \rightarrow NO_3^-$) and N_2O production were also slow. Once fertilized, treatments 1 and 2 rapidly consumed all the NH_4^+, and by day 25 there was no measureable NH_4^+ in the soil extracts (Table 6.2).

The vast majority of the NO_3^- in treatment 1 was produced following fertilization in the first 25 days. Soils extracted on day 37 and at the end of the experiment (day 52) did not contain more NO_3^- (Table 6.2). The overall rates of N_2O production in treatment 1 were low (0.5–50.1 pmol N_2O/hr/g-$soil_{dw.}$). N_2O production declined exponentially with time, and after the second sampling event, N_2O production dropped below 10 pmol N_2O/hr/g-$soil_{dw.}$ and did

not recover (Figure 6.2a). It is clear that nitrification in the low OM agricultural soil was limited by the available supply of NH_4^+.

In the initial phase of treatment 2 (day 25) there was a temporary accumulation of nitrite (NO_2^-) (9.0 μmol/g-soil$_{dw.}$) that comprised ~two-thirds of the total NO_2^- + NO_3^- pool (13.3 μmol/g-soil$_{dw.}$; Table 6.2). By day 37, however, no NO_2^- remained and much more NO_3^- was present in this soil (12.4 μmol/g-soil$_{dw.}$).

The rates of N_2O production in treatment 2 (4–1600 pmol N_2O/hr/g-soil$_{dw.}$) were much higher than in treatment 1. N_2O production also declined exponentially in this soil; however, greater rates were sustained for the first 37 days of incubation (Figure 6.2b) despite the fact that the NH_4^+-fertilizer was exhausted by the 25th day. The elevated rates of N_2O production in this treatment likely resulted from the NO_2^- accumulation because NO_2^- is an intermediate compound of nitrifier-denitrification (Figure 6.1). By day 37, the rates of N_2O production began declining, and the NO_2^- was no longer present in the soil extractions. As discussed in Chapter 5 (Experiment 1), it is possible that a small amount of denitrification occurred in this incubation and this resulted in the higher rates of N_2O production.

6.3.2. *Ammonification, Nitrification and N_2O Production (Treatments 3–6)*

After 106 days of incubation, large amounts of NH_4^+ and NO_3^- (30.9 and 17.4 μmol/g-soil$_{dw.}$, respectively) had accumulated in the upland forested soil (Table 6.2; treatment 3). The mean rates of net ammonification (Organic N → NH_4^+) and net nitrification (NH_4^+ → NO_3^-) were 4.2 and 2.2 μg N/g-soil$_{dw.}$/day, respectively (Chapter 4, Section 4.3.2). These unusually high rates of soil N turnover have been measured in other upland soils collected from the TLW (Foster *et al.* 1986, 1989).

The rate of N_2O production measured in treatment 3 was highly variable among replicates incubations (Figure 6.2c). Soils are inherently variable entities and although they were well-mixed after collection, sieved, air-dried, and then well-mixed again, the treatment replicates showed a heterogeneous response to the incubation conditions. Higher intra-treatment

variability also occurred among replicates of the other upland forest soil incubations (treatments 4–5).

The rates of N_2O production in the forested soils did not reach a *quasi* steady-state by the end of most experiments (Figure 6.2c–e and Figure 6.2g). In contrast to the agricultural soils, N_2O production in these soils generally increased with time. Also, the duration of upland forested soil experiments was much longer so the microbial communities likely evolved differently. In the upland forested soils incubated at room temperature (treatments 3–5) the rates of N_2O production increased substantially after ~8 weeks. In the forested wetland (treatment 7), this period was shorter (~2 weeks). An increase of N_2O with time was also observed in the denitrification incubations of Chapters 2–3, which were much shorter (~8 hours) but subject to a period of pre-incubation to establish the soil denitrifier community. There was no pre-incubation period in this nitrification study, so the initial low rates of N_2O production were likely a result of the 'lag-time' required for the microbial communities of organic-N mineralizers and AOB to develop and establish the N supplies required for N_2O production.

At the onset of incubation, a short 'burst' of N_2O was measured in treatments 4 and 7. This is likely attributable to the respiration of easily available soil organic matter (SOM). Rapid surges of nitrification following soil disturbance is a well-documented artefact that is often observed in soil nutrient cycling studies (e.g., Hales and Ross 2008). Interestingly, although treatments 4 and 5 were essentially replicate treatments (until treatment 5 was cooled), the first sampling of treatment 5 was not anomalously high. In fact, considering the incubations of treatments 4 and 5 were the same soil (upland forest, collected in 2005) and they were initially subjected to the same conditions (Table 6.1), it is surprising that the maximum rate of N_2O production in treatment 4 (weeks 11–13, Figure 6.2d) was approximately half the maximum rate of N_2O production measured in treatment 5 (weeks 11–21, Figure 6.2e). The only other conceivable difference between the two treatments was the length of time the soils were stored (dried, in air-tight, Ziploc® freezer bags). However, even this cannot explain the observed differences, because the soils used in treatment 5 were stored 5

months longer than the soils used in treatment 4. Perhaps if treatment 4 was not terminated at day 93, and allowed to nitrify longer, the rates of N_2O production would have increased.

Soil moisture (within the tested range of WHC) did not have any clear control on the rates of N_2O production measured in treatments 3–5 because adjustments from 50% WHC to 75% WHC did not yield markedly different N_2O production (Figure 6.2c–e). The effect of temperature, however, was readily apparent in treatments 5–6. N_2O production in treatment 5 decreased significantly once it was cooled to 9 °C and did not recover by the end of the experiment. Treatment 6 was cooled from the onset of the experiment until it ended 7 weeks later when the air-conditioned incubation chamber malfunctioned, prompting the termination of treatments 5–6. Only 3 measurements were made in treatment 6 and the rates of N_2O production did not exceed ~25 picomol N_2O/hr/g-soil$_{dw.}$, which was very close to the rates observed in Treatment 5 when it was cooled. Depending on the values chosen to estimate the temperature coefficient (Q_{10}) [a unitless factor by which a biological rate (R) increases as the temperature (T) increases by 10 °C (Equation 6.1)], the Q_{10} for aerobic N_2O production in the upland forested soils varied from ~2–3, which is typical for most biological systems.

$$Q_{10} = \left(\frac{R_2}{R_1}\right)^{\left(\frac{10}{T_2\text{-}T_1}\right)} \qquad [6.1]$$

6.3.3. *N_2O Production (Treatment 7)*

Much more N_2O was formed in the temperate forest wetland than in any of the other treatments. During the third week of treatment 7 the rate of N_2O production ranged between 1800–4400 pmol N_2O/hr/g-soil$_{dw.}$ Such high rates of N_2O production are not commonly associated with nitrifier-generated N_2O but are usually attributed to denitrification. During the experiment, it was suspected that treatment 7 became sub-oxic as a result of high O_2 consumption by aerobic respirers and that much of the measured N_2O was actually produced by denitrifiers. Periodic checks of the % O_2 in the incubation chamber's headspace revealed minor declines in O_2 concentration (largest decline ≈ 4%; data not shown). This does not com-

pletely rule out the possibility of denitrification, however, because it is possible that anoxic microsites ('hotspots') were localized on or between SOM particles (Parkin 1987).

Anaerobic incubations of this wetland soil (helium headpace, same moisture and temperature) yielded denitrifier-N_2O at rates equal to 21,100 ± 4600 pmol N_2O/hr/g-soil$_{dw.}$ (Chapter 2, treatment D). These rates were at least 5 times greater than the rates measured in this study. Finally, the mean production-weighted $\delta^{18}O$ value of the N_2O produced in this wetland soil would suggest that it was produced by nitrification ($\delta^{18}O$-N_2O = +27‰; Chapter 5, treatment 6). In comparison, the $\delta^{18}O$ values of denitrifier-derived N_2O in this wetland would range between +37‰ and +41‰ (provided: $\delta^{18}O$-NO_3^- = 0–9‰; $\delta^{18}O$-H_2O = -8‰; O-exchange = 67%; ^{18}O isotope effect = +42‰; Chapter 2).

6.3.4. *The End-Product Ratios (NO_3^-:N_2O) of Nitrification*

The main end-product of nitrification in treatments 1–3 was NO_3^-. A budget of the N masses in treatments 1 and 2 showed that ~25% more NO_3^- was produced than what would be expected if the only available substrate was the NH_4^+ fertilizer (Table 6.2). Furthermore, most of this 'excess' NO_3^- was generated during the first 25 days of incubation. Therefore, it was likely produced from NH_4^+ made available from the mineralization of the easily digestible (labile) portion of the organic N pool after treatments 1 and 2 were moistened.

The ratio of the nitrification end-products (NO_3^-:N_2O) provides a means to compare a soil's potential to generate N_2O by nitrification (Table 6.2). The NO_3^-:N_2O ratios of treatment 1 (~700–1300) were the highest of all the soils because very little N_2O was produced in this treatment. The NO_3^-:N_2O ratios in treatment 2 (~20–30) and treatment 3 (~50–220) were lower because the rates of N_2O production in these soils were higher. These values correspond to N_2O yields of 0.07–0.15% (treatment 1), 3.8–4.4% (treatment 2), and 0.7% (treatment 3) of the total oxidized N pool (NO_3^- + NO_2^- + N_2O). In comparison, Colliver and Stephenson (2000) have reviewed and summarized the N_2O yields from fully aerated and oxygen limited cultures of autotrophic nitrifiers (*Nitrosomonas* spp. and other *Nitroso* bacteria). The N_2O yields (relative to the total NO_2^- produced) in aerated cultures ranged from 0.05%

to 3.3%, and from 0.8 to 11% under oxygen limitation. Therefore, the N_2O yields of treatments 1 and 3 were typical of fully aerated cultures of nitrifiers, and the N_2O yield of treatment 2 suggests the incubations were oxygen limited.

6.3.5. *The $\delta^{15}N$-NO_3^- Values of Treatments 1–3*

The $\delta^{15}N$ values of the soil NO_3^- in treatments 1 and 2 were high (Table 6.2). In treatment 1, the mean $\delta^{15}N$-NO_3^- of seven of the replicates was $+0.1 \pm 0.3$‰, which corresponds to a mean ^{15}N isotopic separation (Δ) between NH_4^+ and NO_3^- of +0.9‰ (Table 6.3). This provides further evidence that the NH_4^+ substrate was completely consumed because the $\delta^{15}N$ difference between the fertilizer ($\delta^{15}N$-$NH_4^+ = -0.8$‰) and the NO_3^- is almost zero. In an open system where nitrifiers are not limited by the supply of NH_4^+, the $\delta^{15}N$ of microbial NO_3^- is expected to be 12–29‰ lower than the $\delta^{15}N$-NH_4^+ (Kendall 1998). However, in a closed system, when 100% of the substrate is consumed to form one product, the isotopic composition of the cumulative product is equal to the initial isotopic composition of the substrate (Kendall 1998).

The $\delta^{15}N$-NO_3^- of the remaining two replicates in treatment 1 had a higher mean $\delta^{15}N$-NO_3^- equal to $+11.3 \pm 1.2$‰ ($^{15}N\ \Delta = +12.1$‰). These anomalous values cannot be clearly explained given the data measured in this study (Table 6.2). Somehow ^{15}N-depleted N was removed from the NH_4^+ pool, but it was not oxidized to NO_3^-. Obviously the $\delta^{15}N$-N_2O is a ^{15}N-depleted end-product, but the net N_2O accumulation and $\delta^{15}N$-N_2O values in these two replicates were not different from the other treatment replicates. Additionally, the NO_3^- accumulation in these two replicates was not significantly less than the other treatment replicates (Table 6.2). Perhaps the 'missing' ^{15}N-depleted N was assimilated by microorganisms? It is doubtful that this small amount of N could be isotopically detected as a decrease in the $\delta^{15}N$-TN pool because the total inorganic N species in treatment 1 only comprised ~9% (by mass) of the TN pool. Alternatively, perhaps a fraction of the NH_4^+ was volatilized in these replicates and ^{15}N-depleted NH_3 was lost from the system? Volatilization is known to increase the residual pool of NH_4^+ by several per mill (Fogel and Cifuentes 1993), and the initial pH of

these soils was 7.0–7.3 (Table 6.1). However, even this is not a satisfactory explanation because a) the total accumulation of NO_3^- in these high δ^{15}N-NO_3^- replicates was similar to the other replicates, and b) nitrification is an acid-generating process, and rapid rates of nitrification in these soils would lower the potential for volatilization.

The NO_3^- extracted on day 25 from treatment 2 had a very high mean δ^{15}N value of $+39.5 \pm 3.0$‰ (Table 6.2). A large proportion (65–70%) of the oxidized N in these replicates was NO_2^-. Tests of the anion exchange column eluent revealed that a variable amount of the NO_2^- loaded onto the columns was retained by the resin (3–69%). However, all the NO_3^- loaded onto the resin was retained even when NO_2^- was present. Incomplete retention of an anion on an exchange resin can cause isotopic fractionation (Silva *et al.* 2000). Additionally, the effect(s) of the hydrochloric acid (HCl) and silver oxide (AgO) additions on NO_2^- are untested and its fate is largely unknown for this method. For example, it is unknown if NO_2^- is chemically oxidized to NO_3^- at low pH. Therefore, the δ^{15}N-NO_3^- data collected from the first extraction of these soils is not reliable because a large portion of the δ^{15}N sample may have been subject to isotopic fractionation and other methodological artefacts.

The remaining six replicates of treatment 2 (days 37 and 52) did not contain any NO_2^- and had a narrowly confined mean δ^{15}N-NO_3^- value of 9.3 ± 0.3‰ (Table 6.2). This corresponds to a mean ^{15}N isotopic separation (Δ) of $+10.1$‰ (Table 6.3). This is ~9‰ greater than the majority of the treatment 1 replicates, and similar to the two anomalous treatment 1 replicates ($\Delta = +12.1$‰).

Finally, the mean δ^{15}N-NO_3^- value of treatment 3 was -6.1 ± 1.8‰ ($n = 9$). This treatment was not fertilized, nor was the rate of nitrification limited by the supply of NH_4^+ because the substrate pool increased ~44 times its initial size over the 106 day incubation (positive net ammonification; Table 6.2). The instantaneous isotope effect [or enrichment factor (ε)] is a valid estimate of kinetic isotope fractionation when the substrate reservoir is infinitely large, and only a small proportion ($<$ ~5%) of the substrate pool is consumed (Mariotti *et al.* 1981). Enrichment factors ($\varepsilon_{\text{nitrate–ammonium}}$) can be calculated for this treatment because the net rate of NH_4^+ removal (nitrification – 2.2 μg N/g-soil$_{\text{dw.}}$/day) was smaller than the net

rate of NH_4^+ production (ammonification – 4.2 μg N/g-soil$_{dw.}$/day). As such, after a short period of incubation time, the size of the NH_4^+ pool would have been much larger than the instantaneous product (NO_3^-).

The $\varepsilon_{\text{nitrate–total nitrogen}}$ for treatment 3 was -11.5 ± 1.8‰ (Table 6.3), which is within the range of reported ^{15}N fractionation for nitrification of NH_4^+ to NO_3^- in soils (-29‰ to -12‰; Kendall 1998). The δ^{15}N-TN (+5.6‰; Table 6.1, treatment 3) is a good proxy for δ^{15}N-NH_4^+ in the TLW soils because >99.99% of the TN is organic, and little to no isotopic discrimination occurs from organic N mineralization (± 1‰; Kendall 1998). This has been independently confirmed in soils of various sub-catchments at the TLW by Dr. J. Spoelstra (*unpublished results*). The estimate of $\varepsilon_{\text{nitrate–total nitrogen}}$ reported here for treatment 3 is very similar to the isotopic separation ($\Delta = -9.3 \pm 1.6$‰) measured between the δ^{15}N-NO_3^- (-8.6 ± 1.2‰) and the δ^{15}N-TN ($+0.7 \pm 1.0$‰) during an *in situ* study of microbial NO_3^- production (Spoelstra *et al.* 2007), which examined the NO_3^- produced in the litter (Ol) and fibric (Of) layers of upland, organic soil at the TLW [the soil horizons directly above the humic soil (Oh) incubated in this study]. The results of treatment 3 are also very similar to the isotopic separation measured between the TN and NO_3^- produced by nitrification in forest floor percolates of a deciduous forest (mor: -11.1 ± 2.9‰) and a coniferous forest (raw humus: -9.8 ± 0.7‰) (Mayer *et al.* 2001). Therefore, the δ^{15}N-NO_3^- values (and enrichment factors) measured here are in accordance with other studies that examined microbial nitrate production.

6.3.6. *The $\delta^{15}N$-N_2O of the Agricultural Soils and the Isotopic Separation (Δ: N_2O–NH_4^+)*

The most ^{15}N-depleted N_2O was measured from the agricultural soils at the first sampling (day 9) when the fertilizer pool was large and its δ^{15}N-NH_4^+ value was most similar to its initial δ^{15}N value. As time progressed, δ^{15}N-N_2O values in the agricultural soils increased and the production rates decreased (Figure 6.3). Higher rates of N_2O production were sustained in treatment 2 until week 5, when production decreased and δ^{15}N-N_2O increased sharply (Figure 6.2b). At some point between the 2nd and 5th sampling the soil NO_2^- was completely con-

sumed because none of it remained in the extractions that were conducted on day 37 (Table 6.2).

In most of the treatments of this study, steady-state rates of N_2O production and $\delta^{15}N$-N_2O values were not observed (Figure 6.2). Additionally, in all but treatment 7, the lowest $\delta^{15}N$-N_2O values were coupled with the highest N_2O production rates (Figure 6.3). Therefore, production-weighted $\delta^{15}N$-N_2O values were calculated for all replicates of each treatment in this study (Table 6.2).

Upon comparing the N_2O yield of treatment 1 with the N_2O yield of treatment 2, there is a direct relationship with the mean production-weighted $\delta^{15}N$-N_2O values. As the N_2O yield changed from ~0.1% (treatment 1) to ~4% (treatment 2), the $\delta^{15}N$-N_2O values also changed from −36‰ (treatment 1) to −30‰ (treatment 2). In a closed system with two end-products (NO_3^- and N_2O), in order for mass to be conserved, N_2O can only be highly ^{15}N-depleted (with respect to the NH_4^+) when the vast majority of the NH_4^+ is oxidized to NO_3^-. The opposite is also true, and as the rate of $NO_2^- \rightarrow N_2O$ increases relative to the rate of $NO_2^- \rightarrow NO_3^-$, (i.e., treatment 1 vs. treatment 2), then the $\delta^{15}N$ value of the produced N_2O must also increase.

The mean ($\pm$ 1σ) production-weighted $\delta^{15}N$-N_2O values of treatments 1 and 2 were -35.7 ± 3.4‰ and -29.9 ± 1.0‰, respectively. These values are 35‰ and 29‰ lower than the $\delta^{15}N$ of the NH_4^+-fertilizer (Δ). Ideally, the isotope effects in these treatments would be best approximated by a Rayleigh distillation, which requires knowledge of the fraction of substrate that remains. Although replicate incubations of treatments 1–2 were sacrificed in order to determine time course values of $[NH_4^+]$ and $\delta^{15}N$-NH_4^+, all the NH_4^+ fertilizer in the agricultural soils was consumed before the first extraction occurred (day 25). As a result, it was not possible to determine the $\varepsilon_{\text{nitrous oxide}-\text{ammonium}}$ for these treatments.

Despite this, the production-weighted ^{15}N Δ of nitrifier-derived N_2O in these soils (Table 6.3) was isotopically distinct and lower than the ^{15}N $\varepsilon_{\text{nitrous oxide}-\text{nitrate}}$ of denitrifier-derived N_2O in these soils (Chapter 3, treatment 1 = -20.5 ± 1.9‰; treatment 2 = -16.4 ± 1.0‰). This is an important finding because the NO_3^- and NH_4^+ endmembers in these soils have

similar $\delta^{15}N$ values and therefore, the N_2O generated by denitrification and nitrification ought to be isotopically separable.

6.3.7. *The $\delta^{15}N$-N_2O Values and N Isotope Effects of the Upland Forested Soils*

Positive net ammonification was measured in treatment 3, and it is inferred that similar NH_4^+ accumulations occurred in the remaining upland forest soils (treatments 4–6). As time progressed and the size of the NH_4^+ pool increased, the rates of N_2O production increased and the $\delta^{15}N$-N_2O values declined (Figure 6.2c–f). As in the case of the agricultural soils, the $\delta^{15}N$-N_2O of the upland forest soils was inversely proportional to the rates of N_2O production (Figure 6.3). However, compared to the agricultural soils, the data from the upland soils progressed in an opposite direction with time because the forest soil system was open (with respect to the NH_4^+ substrate). Therefore, as time progressed and the NH_4^+ pool was replenished, the nitrifiers were not limited by supply requirements, and the isotopic composition of the NH_4^+ likely remained constant.

The abrupt cooling of treatment 5 had a clear effect on the $\delta^{15}N$-N_2O (and the N_2O production rate) as data from the final four samplings of this treatment ceased to decline and remained constant near $-40‰$. By the 145^{th} day, when these soils were cooled, the NH_4^+ pool was likely large, and the sudden decrease in N_2O production rate spurred a maximal isotope effect. Similarly, the $\delta^{15}N$-N_2O values measured in treatment 6 were the lowest of any of the treatments in this study (Figure 6.2f). A maximal isotope effect was observed in the first two samplings when the NH_4^+ pool was likely large and non-limiting. However, by the sixth week the N_2O production rates decreased and the $\delta^{15}N$-N_2O increased. This suggests that changes in the nitrification or ammonification rates were occurring, or the nitrification end-product ratio was changing.

The mean production-weighted $\delta^{15}N$-N_2O values of the upland forest soils (including $\pm$ 1σ) ranged between $-29‰$ and $-48‰$, (Table 6.2). The calculated mean ^{15}N isotope effects ($\varepsilon_{\text{nitrous oxide}-\text{total nitrogen}}$) for treatments 3–6 were $-36.8‰$, $-40.2‰$, $-39.1‰$, and $-55.1‰$, respectively (Table 6.3). These estimates encompass the ^{15}N $\varepsilon_{\text{nitrous oxide}-\text{ammonium}}$ calculated for

nitrifier-denitrification by Sutka *et al.* (2006) (−47‰) who supplied pure cultures of *Nitrosomonas europaea* with NH_4^+ and measured the resulting $\delta^{15}N\text{-}N_2O$. On the other hand, Perez *et al.* (2006) reported much larger (modelled) estimates of ^{15}N fractionation (−112‰ to −102‰) from tropical forest soils that have not been measured or modelled by any other study to date.

Importantly, the ^{15}N isotope effects calculated here for nitrifier-produced N_2O in upland temperate forest soils are isotopically distinct and lower than the ^{15}N isotope effects calculated for denitrification using the same soils ($\varepsilon_{\text{nitrous oxide−nitrate}} = -29‰$ to $-20‰$; Chapter 2). As such, $\delta^{15}N$ is a useful parameter for separating N_2O produced by multiple pathways in these soils.

6.3.8. *The $\delta^{15}N\text{-}N_2O$ of the Forested Wetland and the Isotopic Separation (Δ: $N_2O-NH_4^+$)*

The forested wetland (treatment 7) generated the most N_2O of all the soils incubated in this study and production rates increased dramatically with time (Figure 6.2g). Additionally, the production rates were positively correlated with $\delta^{15}N\text{-}N_2O$ (Figure 6.3), which was the highest $\delta^{15}N\text{-}N_2O$ measured in this study (mean production-weighted $\delta^{15}N\text{-}N_2O = -13.5 \pm 0.5‰$). The mean ^{15}N $\Delta_{\text{nitrous oxide−total nitrogen}}$ of the forested wetland was −16.4‰.

There are two possible explanations for the unique data of treatment 7. First, a coupling of nitrification with denitrification would yield an overall increased production rate and $\delta^{15}N\text{-}N_2O$. However, as explained in Section 6.3.3, the O_2 concentrations within the soil headspace did not decline severely; the rates observed in this study were less than one-fifth the rates observed in fully anoxic incubations; and the $\delta^{18}O$ values of this N_2O would indicate it was nitrifier-derived. Therefore, there is no clear line of evidence that implicates denitrification as a dominant N_2O-producing pathway in this treatment.

There is an alternative explanation for the ^{15}N-enriched N_2O generated in this treatment. It is possible that the N_2O was totally nitrifier-derived, but the system was not truly open and N_2O production was limited by the rate of ammonification. If the rate of nitrification (substrate removal) increased proportionally with the ammonification rate (substrate re-

generation), and the rates were approximately equal, then the NH_4^+ pool may have become ^{15}N-enriched as it grew with time. This scenario can account for both high N_2O production rates and $\delta^{15}N$-N_2O values.

Importantly, if the N_2O generated from the forested wetland is a representative nitrification endmember, $\delta^{15}N$ values cannot be reliably used to apportion different N_2O sources in this soil. Anaerobic incubations at 59% WHC and 22 °C generated denitrifier-derived N_2O with a mean ^{15}N $\varepsilon_{\text{nitrous oxide–nitrate}}$ of -20.5 ± 0.8‰. This is likely too close to the isotopic composition of nitrifier-derived N_2O in this soil because the mean ^{15}N $\Delta_{\text{nitrous oxide–total nitrogen}}$ in this study was -16.4‰.

6.4. *Conclusions*

The rates of N_2O production in this study were highly variable across all treatments spanning 5 orders of magnitude (from <1 to >4000 picomol N_2O/hr/g-$soil_{dw.}$). In contrast to the short denitrification experiment of Chapters 2–3 (~8 hours), which yield much more N_2O (up to ~60,000 picomol N_2O/hr/g-$soil_{dw.}$; Chapter 2), the aerobic nitrification incubations conducted in this study lasted 4–28 weeks. These are some of the longest incubations ever conducted in a soil N_2O study.

The mean production-weighted $\delta^{15}N$-N_2O produced by nitrification in the agricultural and temperate forest soils ranged from -48‰ to -13‰. In the agricultural soils and the forested peat these values were higher than expected; likely because of limitations in the substrate supply.

The ^{15}N isotope effect ($\varepsilon_{\text{nitrous oxide–total nitrogen}}$) in the upland forested soils (-55‰ to -37‰) was greatest near the end of the experiments when the rates of N_2O production were high and there was ample substrate for nitrification. Although these estimates were not as strong as the literature reports suggest, they were more ^{15}N-depleted than the $\varepsilon_{\text{nitrous oxide–nitrate}}$ for denitrification in the same soils (Chapter 2). The most ^{15}N-depleted N_2O was measured in the upland soil that was cooled to 9 °C.

The isotopic separation (Δ) between N_2O and the nitrification endmember in the agricultural soils ranged from $-35‰$ to $-16‰$. Despite restrictions in substrate supply, the calculated $\Delta_{\text{nitrous oxide}-\text{ammonium}}$ in the agricultural soils was still greater than the $\varepsilon_{\text{nitrous oxide}-\text{nitrate}}$ for denitrification in these same soils (Chapter 3). The results of this study show that different soils exhibit different isotope effects (ε) and isotopic separations (Δ), and the forested and agricultural soils produce isotopically distinct N_2O.

The $\delta^{15}N$ values of N_2O can be used to isotopically separate denitrification and nitrification sources, provided that the $\delta^{15}N$ of NO_3^- and NH_4^+ endmembers are measured. In most environments, the $\delta^{15}N$ values of these endmembers are not widely different. Most NO_3^- derived from the nitrification of SOM ranges in $\delta^{15}N$ from $0‰$ to $+8‰$. The $\delta^{15}N$ of synthetic NH_4^+ fertilizers fall between $-4‰$ and $+4‰$, and NO_3^- fertilizers vary from $-6‰$ and $+7‰$ (Hübner 1986; Wassennar 1995; Xue *et al.* 2009). Manure and sewage $\delta^{15}N\text{-}NO_3^-$ sources range between $+4‰$ and $+25‰$, and fresh NH_4^+ from these sources often falls between $+2‰$ and $+10‰$ (Hübner 1986; Fogel and Cifuentes 1993; Wassennar 1995; Kendall 1998). However, manure and sewage N is commonly ^{15}N-enriched (up to $+30‰$ or more) as a result of denitrification or volatilization. This is most commonly observed from land applications of sewage/manure, or from lagoon or manure storage facilities. Therefore, in certain rare situations where the $\delta^{15}N\text{-}NH_4^+ > \delta^{15}N\text{-}NO_3^-$, the $\delta^{15}N\text{-}N_2O$ from mixed sources/pathways may be isotopically inseparable.

Table 6.1. The experimental conditions and geochemical parameters measured in this study.

	agricultural						**temperate forest**				
treatment	**1**			**2**			**3**	**4**	**5**	**6**	**7**
soil	low OM			high OM			upland 2005	upland 2005	upland 2005	upland 2006	wetland
texture (% sand, % silt, % clay)	silt loam (43, 41, 16)			loam (19, 64, 17)			clay-loam (20, 46, 34)			n.d.	silty-clay (17, 43, 40)
water holding capacity (%)	50			50			50	75	75	68	59
gravimetric soil water content (g H_2O/g soil dw.)	0.26			0.39			1.06	1.59	1.59	1.59	2.70
temperature (°C)	22			22			22	22	22/9[a]	9	22
NH_4^+ fertilized?	yes			yes			no	no	no	no	no
TC (%)	1.9			8.7			19.1	19.1	19.1	25.4	45.2
δ^{13}C-TC (‰ rel. to VPBD)	−21.8			−23.0			−25.8	−25.8	−25.8	−25.3	−26.9
TN (%)	0.2			0.6			1.2	1.2	1.2	1.7	2.6
δ^{15}N-TN (‰ rel. to AIR)	+6.7			+6.1			+5.6	+5.6	+5.6	+7.3	+2.9
C:N ratio (mol:mol)	9.7			12.7			18.4	18.4	18.4	17.7	20.3
LOI (%)	4.2			14.9			36.0	36.0	36.0	46.4	79.3
initial extractable NH_4^+ (µg N/g soil dw.)	0.2			1.1			10.4	10.4	10.4	16.8	21.8
initial extractable NO_3^- (µg N/g soil dw.)	17.2			4.8			17.3	17.3	17.3	19.1	39.6
soil pH (H_2O, 0.1 M $CaCl_2$)	7.3, 7.0			7.5, 7.2			5.1, 4.2	5.1, 4.2	5.1, 4.2	5.2, 4.5	5.4, 5.1
incubation length (days)[b]	25	37	52	25	37	52	106	93	199	42	27
replicate incubations (n)[b]	3	3	3	3	3	3	9	5	6	3	3

[a] Treatment 5 was cooled to 9 °C in an air-conditioned incubation chamber on the 145th day.

[b] There were nine replicate incubations in each of treatments 1 and 2. Three replicates were sacrificially extracted for δ^{18}O-NO_3^- on days 25, 37 and 52 (Chapter 4).

n.d. – not determined.

Table 6.2. An account of select N species after 25 days and 37 days of incubation (agricultural soils) and at the end of the experiments (all soils). Note: treatments 4–7 were not extracted for NH_4^+, NO_2^-, and NO_3^- at the experiment's termination.

treatment	replicate(s)	duration (days)	initial NH_4^+ (μmol/g soil dw.)[a]	total accumulation (μmol N/g soil dw.) (final−initial)				$[NO_3^-+NO_2^-]$ ÷ N_2O ratio	δ^{15}N-NO_3^- (‰)[b]	δ^{15}N-N_2O (production-weighted) (‰) [sample size (n)][c]
				NH_4^+	NO_2^-	NO_3^-	N_2O			
1	a	25	10.7	0	0	13.6	0.02		+0.5	−32.2 [2]
	d					13.7	0.02		+12.1	−39.0 [2]
	g					12.5	0.01		−0.5	−37.5 [2]
mean ± 1σ						**13.3 ± 0.7**	**0.02 ± 0.00**	**665 ± 35**		
relative change (% initial NH_4^+)[d]						**+124% ± 7**	**+0.2% ± 0.0**			
1	b	37	10.7	0	0	12.9	0.01		+0.1	−31.1 [2]
	e					13.3	0.01		+0.5	−40.6 [2]
	h					14.1	0.02		+0.3	−32.1 [3]
mean ± 1σ						**13.4 ± 0.6**	**0.01 ± 0.00**	**1340 ± 60**		
relative change (% initial NH_4^+)[d]						**+125% ± 6**	**+0.1% ± 0.0**			
1	c	52	10.7	0	0	14.0	0.01		+10.4	−36.7 [2]
	f					13.5	0.02		+0.1	−34.6 [3]
	i					13.7	0.01		+0.0	−37.9 [2]
mean ± 1σ						**13.8 ± 0.2**	**0.02 ± 0.00**	**690 ± 10**		
relative change (% initial NH_4^+)[d]						**+129% ± 2**	**+0.2% ± 0.0**			
TREATMENT 1 mean ± 1σ						**13.5 ± 1**	**0.01 ± 0.005**		**+3.0 ± 5.1**	**−35.7 ± 3.4 [20]**
2	a	25	10.8	0	9.2	4.3	0.55		+38.5	−28.4 [3]
	d				8.2	4.4	0.48		+37.2	−30.9 [3]
	g				9.6	4.1	0.52		+42.9	−31.7 [3]
mean ± 1σ					**9.0 ± 0.7**	**4.3 ± 0.1**	**0.52 ± 0.04**	**26 ± 2**	**+39.5 ± 3.0**	
relative change (% initial NH_4^+)[d]					**+83% ± 6**	**+40% ± 1**	**+4.8% ± 0.4**			
2	b	37	10.8	0	0	12.6	0.65		+9.2	−29.3 [5]
	e					11.9	0.50		+9.3	−30.0 [5]
	h					12.7	0.56		+9.5	−29.6 [5]
mean ± 1σ						**12.4 ± 0.5**	**0.57 ± 0.08**	**22 ± 3**	**+9.3 ± 0.2**	
relative change (% initial NH_4^+)[d]						**+115% ± 5**	**+5.3% ± 0.2**			

Table 6.2 continued.

treat-ment	repli-cate(s)	duration (days)	initial NH_4^+ (μmol/g soil dw.)[a]	total accumulation (μmol N/g soil dw.) (final−initial)				$[NO_3^-+NO_2^-]$ ÷ N_2O ratio	δ^{15}N-NO_3^- (‰)[b]	δ^{15}N-N_2O (production-weighted) (‰) [sample size (n)][c]
				NH_4^+	NO_2^-	NO_3^-	N_2O			
2	c	52	10.8	0	0	13.9	0.55		+9.0	−29.2 [5]
	f					12.9	0.55		+9.5	−29.7 [5]
	i					13.7	0.59		+9.3	−30.1 [5]
mean ± 1σ						**13.5 ± 0.5**	**0.56 ± 0.02**	**24 ± 1**	**+9.3 ± 0.3**	
relative change (% initial NH_4^+)[d]						**+125% ± 5**	**+5.2% ± 0.2**			
TREATMENT 2 mean ± 1σ							**0.55 ± 0.050**			**−29.9 ± 1.0 [39]**
3	a	106	0.7	30.0	0	17.1	0.16		−5.6	−34.8 [9]
	b			27.0		19.4	0.01		−6.9	−29.1 [9]
	c			30.1		18.6	0.26		−2.5	−29.9 [9]
	d			32.2		17.1	0.16		−5.9	−29.9 [9]
	e			28.9		16.7	0.20		−4.4	−28.0 [9]
	f			33.2		16.5	0.07		−8.5	−34.2 [9]
	g			33.7		16.7	0.14		−6.6	−35.5 [9]
	h			32.3		16.7	0.15		−6.8	−30.7 [9]
	i			31.0		17.9	0.02		−7.7	−30.9 [9]
TREATMENT 3 mean ± 1σ				**30.9 ± 2.2**		**17.4 ± 1.0**	**0.13 ± 0.082**	**134 ± 83**	**−6.1 ± 1.8**	**−31.4 ± 2.7 [81]**
4	a–e	93	0.7	nd.			**0.07 ± 0.006**		nd.	**−34.8 ± 2.2 [55][e]**
5	a–f	199	0.7	nd.			**0.36 ± 0.067**		nd.	**−33.7 ± 1.3 [114][e,f]**
6	a–c	42	1.2	nd.			**0.02 ± 0.000**		nd.	**−48.2 ± 0.2 [9][e]**
7	a–c	27	1.6	nd.			**0.78 ± 0.071**		nd.	**−13.5 ± 0.5 [24][e]**

[a] For treatments 1–2, the inital NH_4^+ values include the endogenous-NH_4^+ (Table 6.1) and the fertilizer-NH_4^+, which was applied at a rate of 0.15 mg NH_4^+-N/g $soil_{dw.}$ (δ^{15}N-NH_4^+ = −0.8 ± 0.1‰).

[b] Isotope ratios of NO_3^- are corrected for endogenous NO_3^- present in air-dry soils prior to incubation so that the data presented represents newly formed NO_3^-.

[c] The production-weighted δ^{15}N-N_2O value of each replicate incubation is calculated as:

$$\sum_{t=0}^{final} (\delta^{15}\text{N-}N_2O \times \text{fraction of total } N_2O \text{ produced})_t$$ [± 1σ or analytical uncertainty of δ^{15}N-N_2O (0.2‰), whichever is greater], where t = sampling event.

[d] The relative N changes listed here are slightly different than the values reported in Chapter 4, Section 4.3.2. In Chapter 4, units are expressed in μg N/g-$soil_{dw.}$

[e] The production-weighted δ^{15}N-N_2O of treatments 4–7 are mean values ± 1σ [n].

[f] This production-weighted δ^{15}N-N_2O value includes the data collected while soils were cooled.

nd. – not determined.

Table 6.3. The isotope effects (ε) or isotopic separations (Δ) measured in this study for the nitrification of NH_4^+ to NO_3^- (treatments 1–3) and NH_4^+ to N_2O (treatments 1–7).

	agricultural				**temperate forest**			
soil	**low OM**		**high OM**		**upland 2005**	**upland 2005**	**upland 2005**	**upland 2006**	**wetland**
treatment	**1**		**2**		**3**	**4**	**5**	**6**	**7**
soil δ^{15}N-TN (‰)	+6.7		+6.1		+5.6	+5.6	+5.6	+7.3	+2.9
fertilizer δ^{15}N-NH_4^+ (‰)	−0.8		−0.8		not applicable	not applicable			
	reps. a–b,e–i	reps. c–d	day 0–25	day 0–52	day 0–106	not determined			
mean δ^{15}N-NO_3^- (‰)	+0.1 ± 0.3	+11.3 ± 1.2	+39.5 ± 3.0[a]	+9.3 ± 0.3	−6.1 ± 1.8				
^{15}N ε or Δ (NO_3^-−substrate) (‰)	+0.9 (Δ)[b]	+12.1 (Δ)[b]	+40.3 (Δ)[a,b]	+10.1 (Δ)[b]	−11.5 (ε)[c]				
mean production-weighted δ^{15}N-N_2O (‰)	−35.7 ± 3.4		−29.9 ± 1.0		−31.4 ± 2.7	−34.8 ± 2.2	−33.7 ± 1.3	−48.2 ± 0.2	−13.5 ± 0.5
^{15}N ε or Δ (N_2O−substrate) (‰)[c,d]	−34.9 (Δ)[d]		−29.1 (Δ)[d]		−36.8 (ε)[e]	−40.2 (ε)[e]	−39.1 (ε)[e]	−55.1 (ε)[e]	−16.4 (Δ)[f]

[a] The soil solution extracted from treatment 2 on day 25 was composed of NO_2^- (~two-thirds) and NO_3^- (~one-third). As discussed in Chapter 4, Section 5.3.1, the fate of NO_2^- throughout the resin method for analysis of δ^{15}N-NO_3^- is largely unknown.

[b] Agricultural soils: $\Delta = \delta^{15}$N-nitrate − δ^{15}N-fertilizer.

[c] Upland forest soil: $\varepsilon = (\alpha - 1) \times 1000$, where $\alpha = {}^{15}N/{}^{14}N$-nitrate ÷ $^{15}N/^{14}N$-soil TN.

[d] Agricultural soils: $\Delta = \delta^{15}$N-nitrous oxide − δ^{15}N-fertilizer.

[e] Upland forest soils: $\varepsilon = (\alpha - 1) \times 1000$, where $\alpha = {}^{15}N/{}^{14}N$-nitrous oxide ÷ $^{15}N/^{14}N$-soil TN.

[f] Wetland forest soil: $\Delta = \delta^{15}$N-nitrous oxide − δ^{15}N-soil TN.

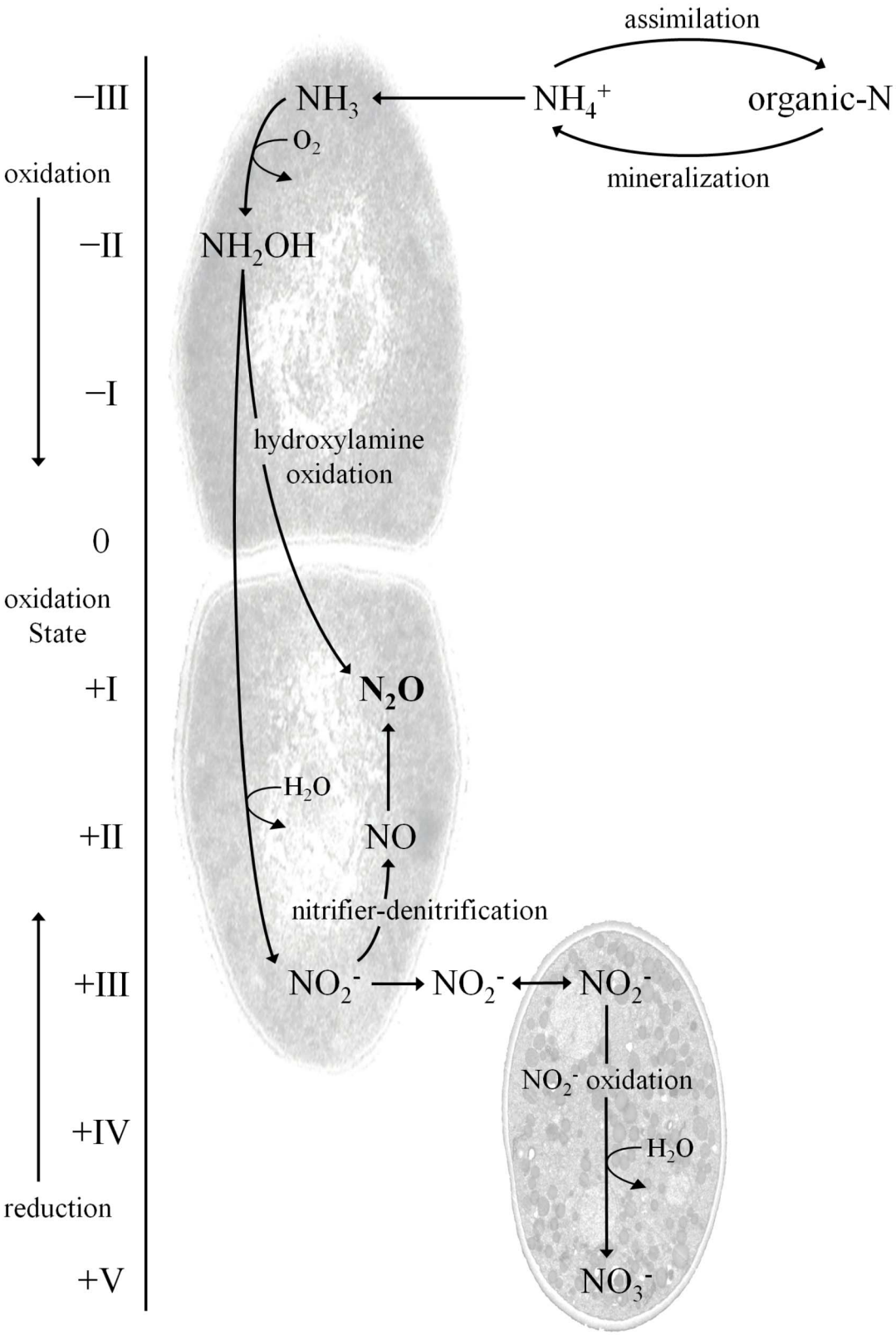


Figure 6.1. The nitrification of NH_4^+ can yeild NO_3^- and N_2O end-products. In aerobic environments N_2O is produced by hydroxylamine (NH_2OH) oxidation or by nitrifier-denitrification (NO_2^- reduction).

Figure 6.2a. Treatment 1 - low OM agricultural soil, 50% WHC

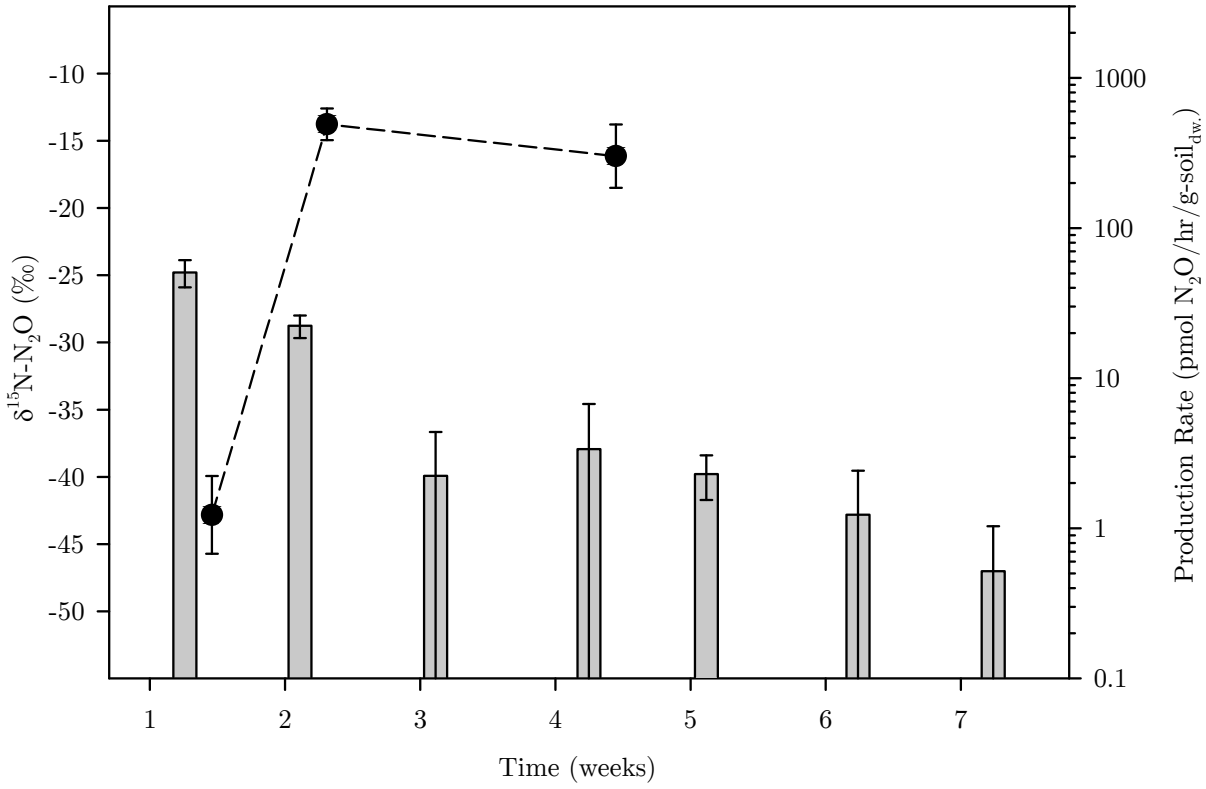


Figure 6.2b. Treatment 2 - high OM agricultural soil, 50% WHC

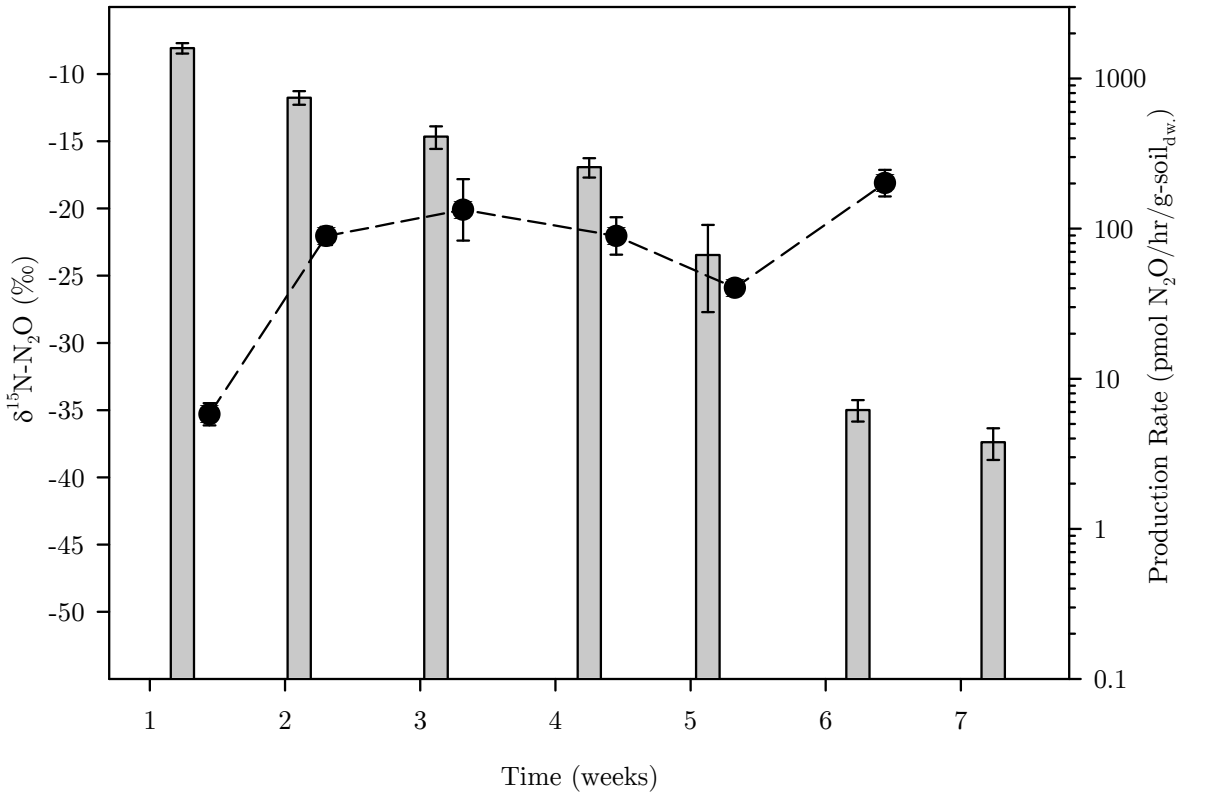


Figure 6.2c. Treatment 3 - upland forested soil, 50% WHC

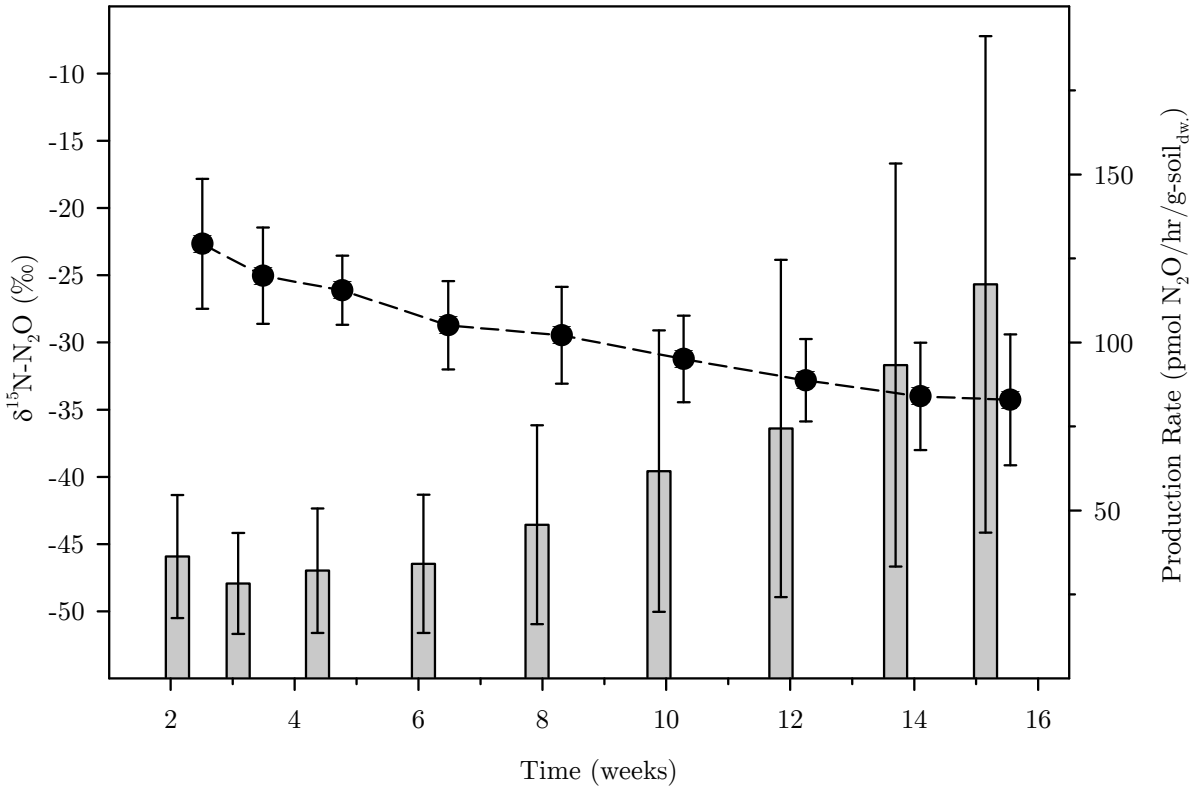


Figure 6.2d. Treatment 4 - upland forested soil, 75% WHC

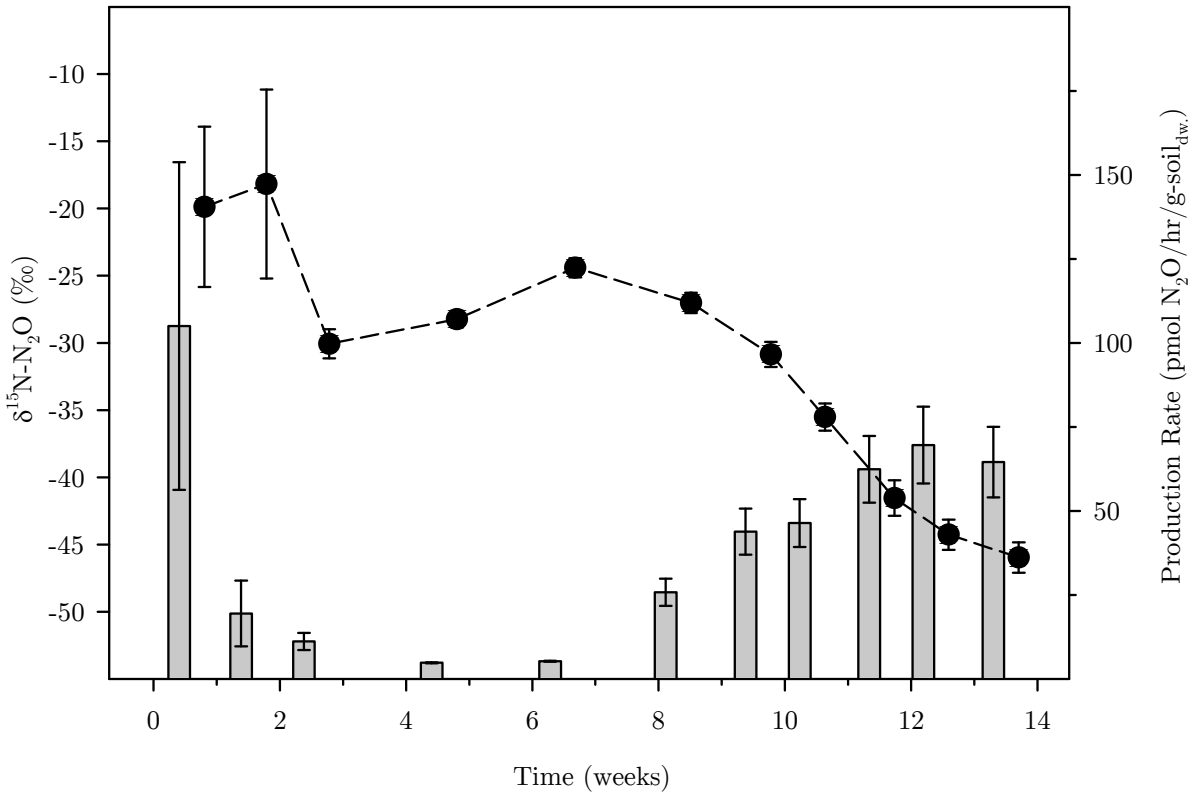


Figure 6.2e. Treatment 5 - upland forested soil, 75% WHC, 22 °C/9 °C

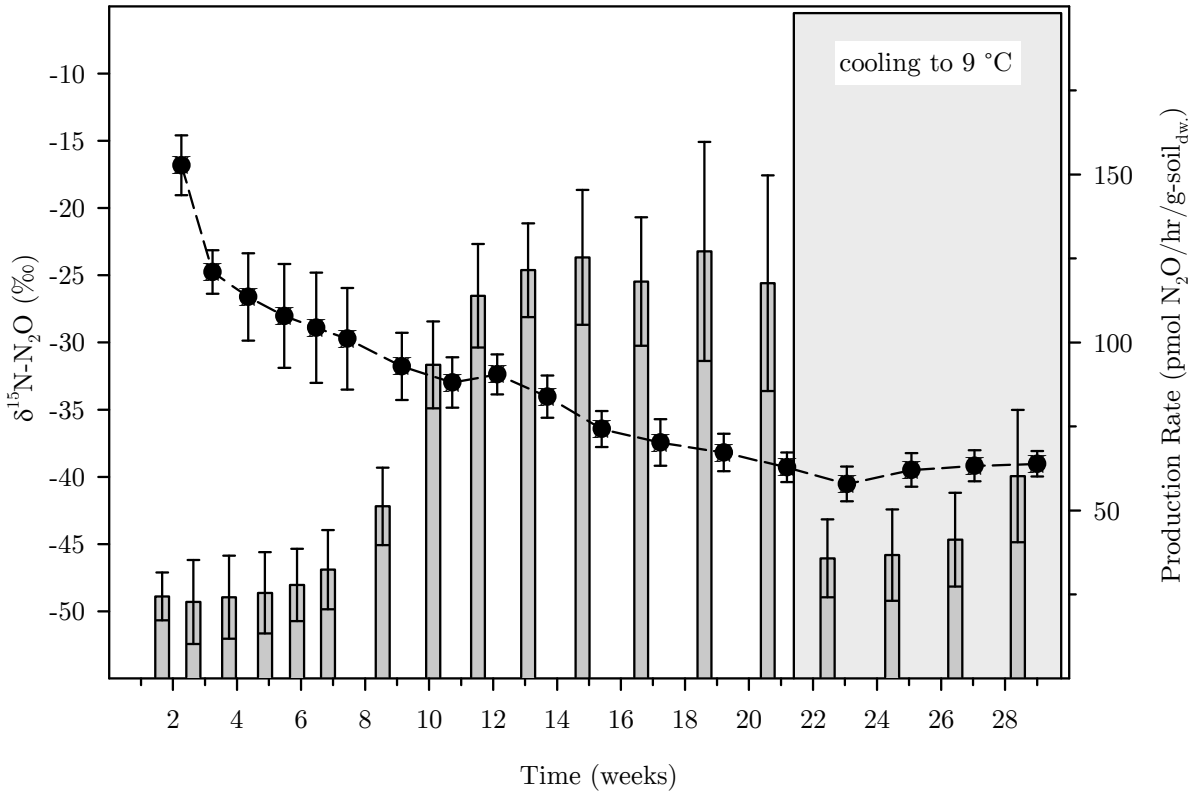


Figure 6.2f. Treatment 6 - upland forested soil, 70% WHC, 9 °C

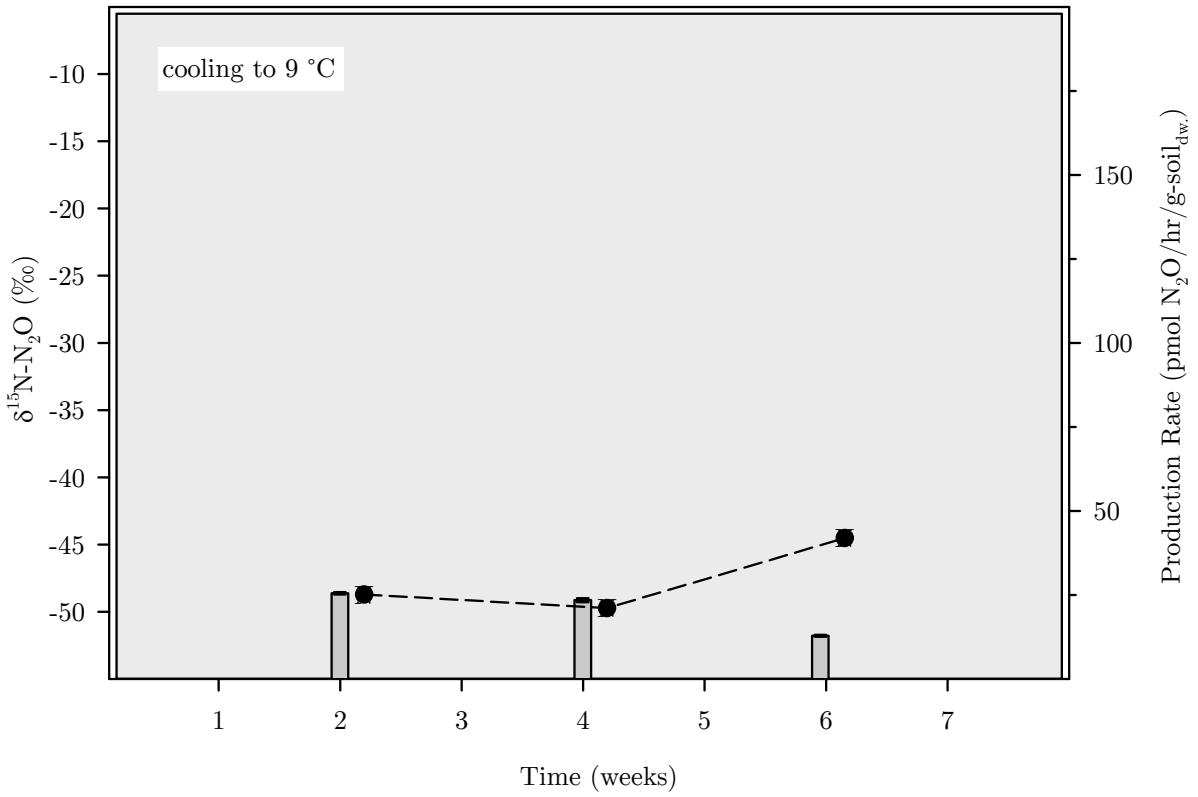


Figure 6.2g. Treatment 7 - wetland forested soil, 60% WHC

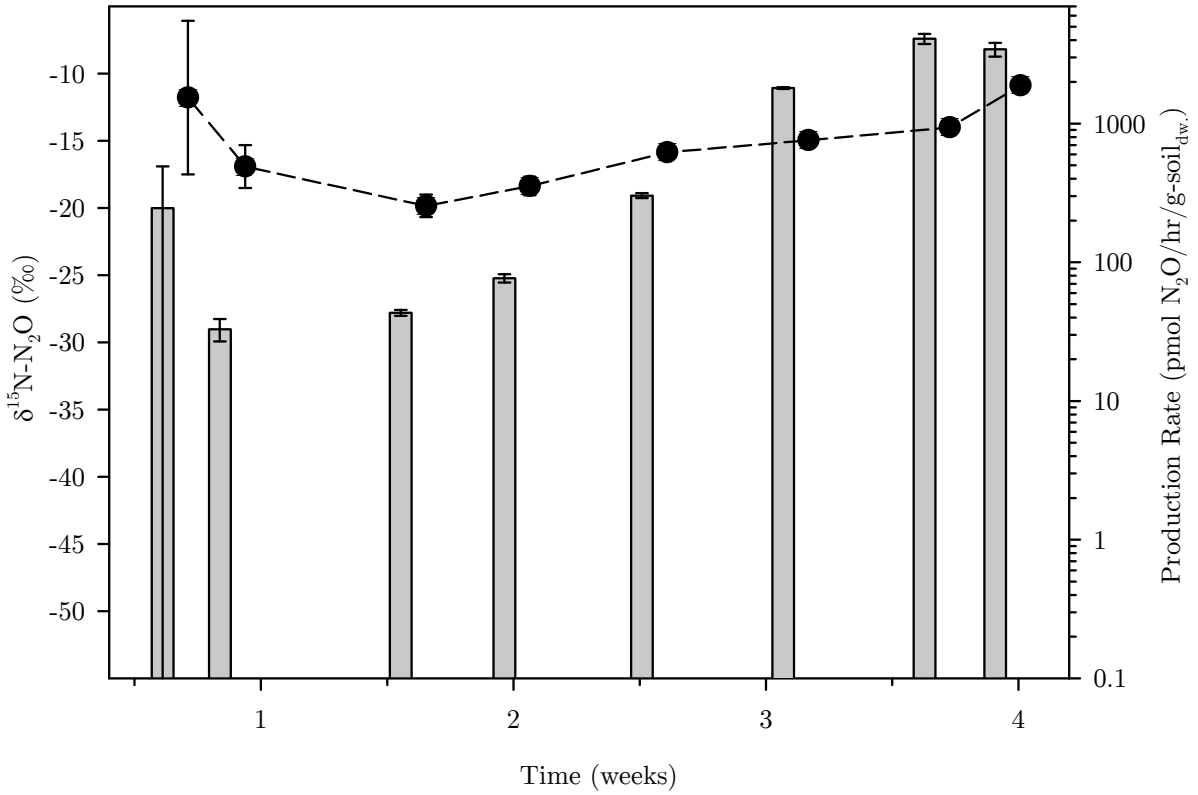


Figure 6.2a-g. δ^{15}N-N_2O (rel. AIR) and the rate of N_2O production versus time for treatments 1-7 of this study. Each N_2O production rate (bar plot) and δ^{15}N-N_2O symbol represents a mean value, and the number of replicate incubations (n) for each treatment can be found in Table 6.1. The error bars represent 1σ from the mean, and, where they are absent, the error is smaller than the size of the symbol. The δ^{15}N-N_2O is scaled identically on each plot. The N_2O production rate is not scaled the same on each plot. To improve visibility, δ^{15}N-N_2O symbols are displayed to the right of the bar plots.

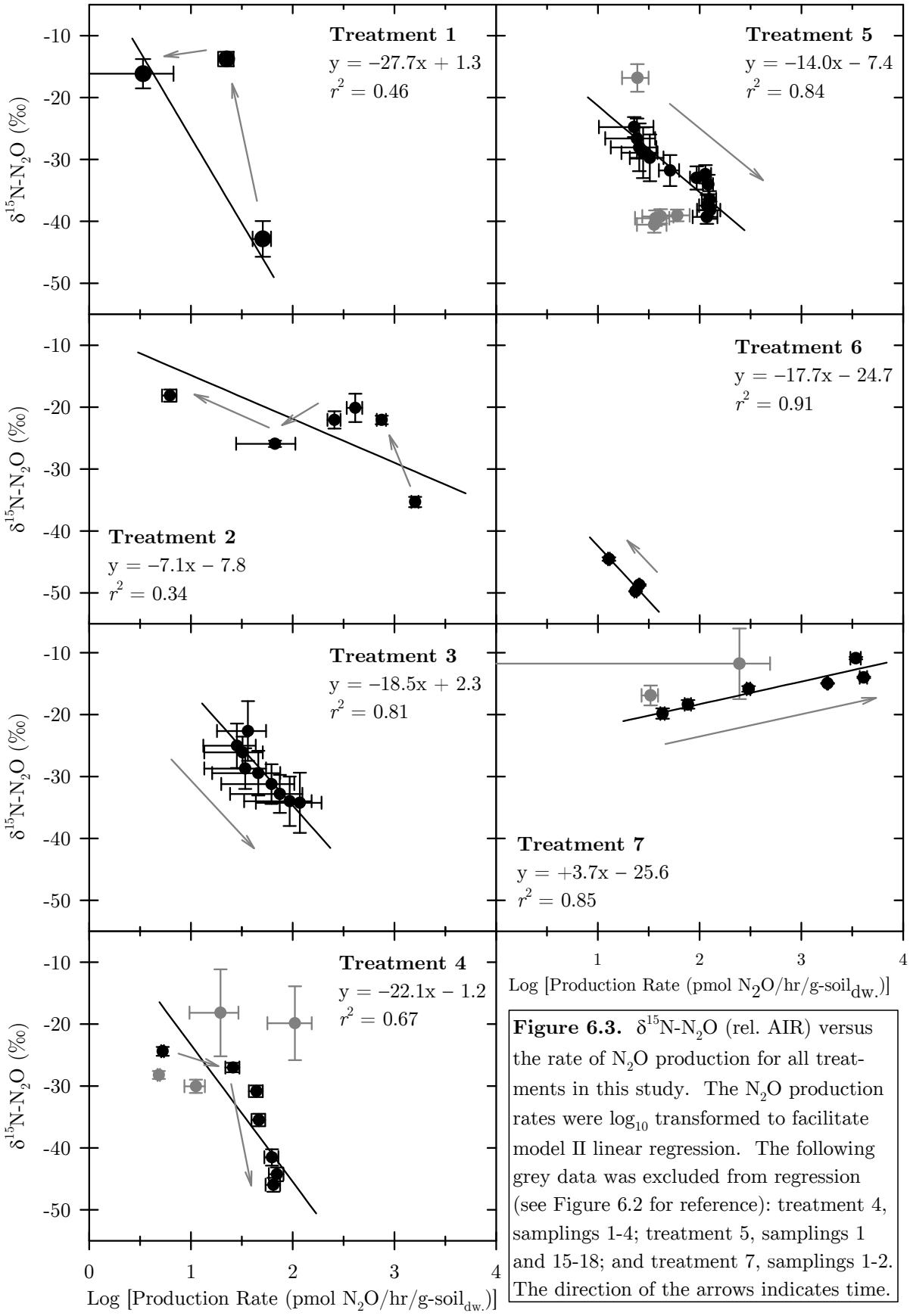


Figure 6.3. δ^{15}N-N_2O (rel. AIR) versus the rate of N_2O production for all treatments in this study. The N_2O production rates were $\log_{10}$ transformed to facilitate model II linear regression. The following grey data was excluded from regression (see Figure 6.2 for reference): treatment 4, samplings 1-4; treatment 5, samplings 1 and 15-18; and treatment 7, samplings 1-2. The direction of the arrows indicates time.

7 Conclusions and implications of this research, relevance to *in situ* nitrous oxide data, and recommendations for future studies

7.1. *Conclusions and Implications of this Research*

The overall objective of this thesis research is to characterize the nitrogen (N) and oxygen (O) isotope ratios of nitrous oxide ($\delta^{15}N$ and $\delta^{18}O$-N_2O) produced by denitrification and nitrification in temperate forest and agricultural soils. Soils contain a consortium of N-metabolizing microorganisms and this thesis builds upon earlier work examining the controls of N_2O isotope ratios. Incubation experiments with five different soils produced N_2O at rates that varied six orders of magnitude (from <1 picomol N_2O/hr/g-soil$_{dw.}$ to >60 nmol N_2O/hr/g-soil$_{dw.}$). Temperature and soil moisture were manipulated, and redox conditions were either completely aerobic or fully anoxic. Under these varying experimental conditions, the isotope effects of N_2O produced by denitrification and nitrification were well-characterized. Most experiments were replicated many times to ensure that robust datasets were generated. In total, 791 unique samples were collected and manually analyzed for $\delta^{15}N$ and $\delta^{18}O$-N_2O.

Tracer experiments using ^{18}O-labelled water (H_2O) targeted our poor comprehension of the controls on $\delta^{18}O$-N_2O. Tremendous amounts of information were gained from these experiments, including the first estimates of oxygen exchange (O-exchange) between H_2O and N_2O-precursors in soils and estimates of the ^{18}O isotope effect for denitrification not obscured by O-exchange (Chapters 2–3). The research presented in Chapter 4 developed a more comprehensive model to describe NO_3^- formation in soil by nitrification. Finally, the ^{18}O-H_2O tracer strategies employed in this research yielded the first holistic interpretation of $\delta^{18}O$-N_2O values generated by nitrification (Chapter 5). The experimental data and models (conceptual and mathematical) presented in Chapter 5 provided the first complete explanation of why nitrifier-N_2O has $\delta^{18}O$ values that range between +13‰ and +31‰. The outcomes of this research are far-reaching, and they will make large, positive impacts on scientific communities with interests in global climate change and N biogeochemistry.

Prior to this dissertation, several studies had investigated the $\delta^{15}N$-N_2O produced with laboratory-cultured organisms and there were a few reports of $\delta^{15}N$-N_2O from natural environments. If $\delta^{18}O$-N_2O values were reported, only a limited interpretation of the data was provided. These early works put forth the concept that stable isotope measurements could be the keystone that would allow researchers to conclusively identify N_2O production pathways in the environment. This hope remains today; yet the task of conclusively differentiating nitrifier-N_2O from denitrifier-N_2O appears significantly more complicated.

7.1.1. *The Use of $\delta^{15}N$ Measurements to Separate Nitrifier and Denitrifier-Produced N_2O*

Combining the results of this thesis (Figure 7.1a-b) with over two decades of research documenting $\delta^{15}N$-N_2O values measured from lab studies and field environments (Chapter 1, Table 1.1), it can be concluded that nitrifier-produced N_2O is more ^{15}N-depleted than denitrifier-produced N_2O *in most cases*. We cannot, however, rely on $\delta^{15}N$-N_2O alone to unequivocally separate production pathways. Many lab studies have shown that there are large ^{15}N fractionations associated with some segments of the nitrification pathway, yet experiments with soils (*this thesis*, Well *et al.* 2008) and *Nitrosomonas europaea* (Sutka *et al.* 2006) supplied with ammonium (NH_4^+) have shown that ^{15}N separation between nitrifier and denitrifier-N_2O is not as large as previously hoped (Chapter 1, Section 1.5.2).

In many cases, N_2O in oxic environments will contain a mixture of denitrifier-N_2O and nitrifier-N_2O. As such, in order to use $\delta^{15}N$-N_2O to propose a dominant production mechanism, a suitable degree of ^{15}N separation between pathways is required. Experiments conducted in this thesis have shown that, on a case-by-case basis, there may be sufficient and insufficient ^{15}N separation between N_2O sources to isotopically distinguish production pathways. When systems were closed, without continuous input of substrate, nitrifier-produced $\delta^{15}N$-N_2O became too high to be differentiated from denitrifier-N_2O (Figure 7.1a – forested wetland; well-drained and poorly-drained agricultural soils). However, when systems were open (at *quasi* steady-state) excellent ^{15}N separation between the pathways was observed (e.g., in a forested upland soil).

7.1.2. *The Use of $\delta^{18}O$ Measurements to Separate Nitrifier- and Denitrifier-Produced N_2O*

The experiments conducted in this thesis have made significant strides toward achieving a comprehensive understanding of the controls on $\delta^{18}O$-N_2O. This research has contributed important findings about O-exchange and ^{18}O-isotope effects in soils that have never been quantified before. The discovery that H_2O-O can exchange with N_2O precursors complicates the use of $\delta^{18}O$-N_2O to distinguish between production pathways. The results obtained from incubations of well-drained soils in this thesis have shown that it is possible to have overlapping nitrifier and denitrifier $\delta^{18}O$-N_2O signatures (Figure 7.2 – forested upland soil; well-drained agricultural soil). As such, before field data are interpreted, pilot experiments with soils should be conducted to determine the $\delta^{18}O$-N_2O denitrification endmember. This can be done either with or without ^{18}O-labelled water, depending on whether an estimate of O-exchange is desired.

The results of Chapter 5 buoyed optimism about the usefulness of $\delta^{18}O$-N_2O to apportion N_2O sources because it was revealed that nitrification-produced $\delta^{18}O$-N_2O values are narrowly confined between +13‰ and +31‰. Despite the remarkably complicated controls of nitrifier-produced N_2O (Chapter 5), this narrow range of $\delta^{18}O$ values may be the key distinguishing feature that is required in many environments to distinguish nitrifier- from denitrifier-produced N_2O. In this thesis, the denitrifier-derived $\delta^{18}O$-N_2O was higher than +33‰ in all the poorly drained soils (Figure 7.2). Furthermore, the reduction of N_2O to N_2, which is unique to denitrifiers, further increases $\delta^{18}O$-N_2O and helps segregate denitrifier-N_2O from nitrifier-N_2O. In the well-drained soils of this thesis the $\delta^{18}O$ separation of nitrifier- and denitrifier-N_2O is predicted to be poor. The high amounts of O-exchange (>90%) in these soils and the low ^{18}O-fractionation ($\varepsilon < +40$‰) generated modelled $\delta^{18}O$-N_2O results from +8‰ to +34‰ (Figure 7.2).

7.1.3. *Defining the Range of Soil-Derived $\delta^{15}N$-N_2O and $\delta^{18}O$-N_2O in this Thesis*

Summarizing the results of ^{15}N and ^{18}O isotope fractionation and O-exchange measured in this thesis (Chapters 2–3 and 5–6), the expected range of $\delta^{15}N$-N_2O and $\delta^{18}O$-N_2O values that

would be produced by denitrification and nitrification in the temperate forest and agricultural soils can be derived (Table 7.1–7.2; Figures 7.3–7.4). Normalization of the data (based on $\delta^{15}N$ and $\delta^{18}O$ of endmembers) is required to properly compare the denitrifier-produced N_2O (Chapter 2–3), nitrifier-produced N_2O (Chapter 5–6), and *in situ* data (Figure 7.5, Turkey Lakes Watershed; Figure 7.6, Strawberry Creek Watershed). In the future, these modelled ranges can be constrained further if more information is known (e.g., seasonal variations in endmembers such as $\delta^{18}O$-H_2O).

7.2. *General Observations of $\delta^{15}N$-N_2O and $\delta^{18}O$-N_2O Field Measurements*

The data illustrated in the figures of this chapter are compilations of $\delta^{15}N$-N_2O and $\delta^{18}O$-N_2O sampled from pristine and N-impacted environments. Many of the results were collected in Canada (mainly Southern Ontario) by several dedicated researchers affiliated with the Environmental Geochemistry Laboratory, University of Waterloo (Figure 7.8a). To date, none of these data are published in peer-reviewed publications, but several datasets have been documented in graduate and undergraduate theses (Vandenhoff 2007; Rempel 2008; Thuss 2008; Flood 2010; Li 2010; Rossi 2010; Hollingham 2011; Rosamond *unpublished results*; Senger *unpublished results*), or elsewhere (Schiff, Spoelstra, and Robertson *unpublished data*). An immense amount of time, effort and money is invested in this work and the author is tremendously grateful to those individuals who have shared their work in this thesis.

Almost all of the global *in situ* N_2O isotope results that have been published in peer-reviewed journals (up to February 2011) are shown in Figure 7.9a–b. If any references are missing then they were unintentionally omitted (the author is unaware of their existence), or they were deliberately omitted for a specific reason (e.g., the $\delta^{18}O$-N_2O data are not scaled relative to international reference materials; Yamulki *et al.* 2000). None of the published data shown here were generated from lab/field incubations, or determined using labelled ^{15}N or ^{18}O material. Some of the results were obtained from agricultural soils treated with fertilizers.

In total, (exactly) 1700 unique *in situ* $\delta^{15}N$-N_2O/$\delta^{18}O$-N_2O pairs are shown throughout this chapter. To the best of the author's knowledge, this is the most comprehensive summary of field-collected $\delta^{15}N$ and $\delta^{18}O$-N_2O ever collected, and it provides the foundation for powerful analyses and interpretations in this thesis and in future work.

The compiled data is shown here in order to place the results of this thesis into context, and in most circumstances *little to no interpretation of individual datasets is provided.* Each case study (published and unpublished) is a story on its own; a field site with a unique range of N_2O endmembers and environmental conditions (geochemical, climatological, and otherwise). With the exception of the *in situ* data collected from the Turkey Lakes and Strawberry Creek Watersheds, only broad generalizations about the data will be provided.

7.2.1. *N_2O from the Turkey Lakes Watershed*

Of the total *in situ* N_2O samples collected to date from the Turkey Lakes Watershed, only eleven have contained enough N_2O to be analyzed for isotopes (Figure 7.5). Of these, six samples were soil gas (flux chambers) collected from Catchment 38 (a peat wetland), which is the same location where peat was collected for this thesis. These samples were collected over a few hours during an intense fall storm after a long period of drought. Large amounts of NO_3^- had accumulated in the peat over the summer, and the N_2O fluxes were extremely high. These antecedent conditions, combined with a high rainfall event, provided ideal conditions for denitrification to occur. Interestingly, the $\delta^{15}N$ and $\delta^{18}O$ values of this episodic N_2O flux are closer to the range observed from the nitrification incubations of this peat soil. Therefore, either (i) the range of denitrifier-N_2O defined from the peat incubations in this thesis is not a good representation of the high flux event produced by denitrification in Catchment 38; or (ii) nitrification was the significant process responsible for the episodic N_2O flux measured in Catchment 38; or (iii) the N_2O was produced by denitrification in the upland soils directly above Catchment 38, then subsequently translocated via the shallow groundwater to the wetland below where it was discharged. The second possibility is the least likely explanation be-

cause the traditional geochemical evidence (wetland primed with NO_3^-, intense hydrological event) would strongly point to N_2O production by denitrification.

The remaining data collected from the Turkey Lakes Watershed are dissolved N_2O samples. One is a groundwater sample (5,600% N_2O saturation) collected from Catchment 50 (wetland) that is ^{15}N-depleted (−35‰) and within the $\delta^{18}O$ range of nitrifier-N_2O (+19‰). The other four samples were collected from streams at weirs. One drains Catchment 35 (upland; 7,000% N_2O saturation; $\delta^{15}N\text{-}N_2O = -22‰$; $\delta^{18}O\text{-}N_2O = +25‰$). The other three samples drain wetlands and the N_2O concentrations were high (Catchment 38 = 66,000% sat.; Catchment 60 = 31,000% sat.; Catchment 50 = 24,000% sat.). The $\delta^{15}N\text{-}N_2O$ of these three stream samples ranged between −5‰ and −16‰ and the $\delta^{18}O$ values were between +20‰ and +26‰, which is similar to the soil flux measurements from Catchment 38 and the forested wetland nitrification incubations conducted in this thesis.

7.2.2. *N_2O from the Strawberry Creek Watershed*

A large number of *in situ* N_2O isotope samples have been collected from the Strawberry Creek Watershed (Figure 7.6; Rempel 2008, Spoelstra and Schiff *unpublished*). Soil N_2O was collected at 10–50 cm depths during February–June 2007 and February–May 2008 (n = 181). The isotopic evidence suggests that the soil N_2O was produced by nitrification and denitrification. The cluster of data with $\delta^{18}O\text{-}N_2O$ above +30‰ is denitrifier-derived (n = 29). The highly ^{15}N-depleted values (down to −47‰) must be nitrifier-derived. The remaining data with $\delta^{18}O\text{-}N_2O < +30‰$ is nitrifier- and denitrifier-derived N_2O. O-exchange during denitrification in the well-drained Strawberry Creek soil incubations was very high (94% ± 1; Table 7.1). Most of the *in situ* soil N_2O samples < +30‰ were collected during snowmelt in February and March when the $\delta^{18}O$ of environmental H_2O is low. Although snowpack $\delta^{18}O\text{-}H_2O$ data from the Strawberry Creek site are unavailable, historical values collected from Simcoe, ON (~80 km south of Strawberry Creek) and Egbert, ON (~91 km northeast of Strawberry Creek) have declined to < −20‰ (Birks *et al.* 2003). Therefore, high amounts of O-exchange with very low $\delta^{18}O\text{-}H_2O$ during the winter and spring can explain these low $\delta^{18}O\text{-}N_2O$ values.

In this case, the range of denitrification $\delta^{18}O$-N_2O defined for this soil (24‰ ± 2; Table 7.1) may need to be adjusted using lower $\delta^{18}O$-H_2O values.

Most of the *in situ* stream samples (n = 42) collected at the outlet of Strawberry Creek are within the $\delta^{18}O$-N_2O range of the denitrifier-N_2O stream sediment incubations, yet more ^{15}N-enriched than the modelled range would predict. A significant amount of the N_2O in the creek's headwaters is lost to the atmosphere before the creek reaches the outlet (Rempel 2008). This not only lowers the dissolved concentration of N_2O in the stream, but influences its isotopic signature towards the mean tropospheric N_2O value ($\delta^{15}N$ = 6.7‰, $\delta^{18}O$ = 44.6‰; Kaiser *et al.* 2003). Gas exchange can explain the higher $\delta^{15}N$-N_2O values of the stream samples. It is also possible that the ^{15}N isotope effect measured in the stream sediment incubations was larger than what occurs in the field.

Groundwater N_2O at Strawberry Creek (n = 32) was widely distributed in $\delta^{15}N$-N_2O (from −33‰ to +5‰) and $\delta^{18}O$-N_2O (+30‰ to +62‰). A few samples had highly enriched in $\delta^{15}N$ and $\delta^{18}O$ values characteristic of N_2O consumption (Figure 7.7). The lowest $\delta^{18}O$-N_2O value was +30‰, which would suggest that all the groundwater N_2O was generated by denitrification.

Finally, the N_2O collected from the drainage tiles (n = 126) had an even wider distribution in $\delta^{15}N$ (from −43‰ to +14‰) and a similar distribution in $\delta^{18}O$ (from +25‰ to +53‰). This wide range in isotope values would suggest that both nitrification and denitrification were responsible for producing the dissolved N_2O in the tiles. Depending on the hydrological conditions, N_2O in the tile waters could be produced in the unsaturated soil (vadose zone) or the groundwater (saturated soil). A large number of the tile samples resemble the denitrification ^{18}O-endmembers of the stream sediment and the poorly drained soil (low O-exchange, large O isotope effect) (Figure 7.6). In contrast to the *in situ* stream samples, N_2O in the tiles is not affected by gas exchange with the troposphere, so the majority of these samples are more ^{15}N-depeleted than in the stream. Finally, consumption of N_2O entrained in the soil may be another important determinant of the $\delta^{15}N$ and $\delta^{18}O$ values of N_2O dissolved in tile waters.

7.2.3. *Soil-Derived N_2O*

Figure 7.8b (EGL data) and Figure 7.9b (published data) show all the available $\delta^{15}N$ and $\delta^{18}O$ values of soil-derived N_2O ($n = 445$). The vast majority of these *in situ* soil samples fall within the ranges defined in this thesis. Although only five soils (from two field sites) were incubated in this thesis, and soils were sieved, dried, stored for long periods of time, rewetted, and in some cases fertilized, the N_2O generated in these experiments spanned almost the entire range of $\delta^{15}N$-N_2O and $\delta^{18}O$-N_2O that is observed naturally in soils.

A high density of the published data lie close to the value of tropospheric N_2O ($\delta^{15}N = +6.7‰$, $\delta^{18}O = +44.6‰$; Kaiser *et al.* 2003). This suggests that a high proportion of the soil measurements in the literature may be low flux or low concentration samples that are more reflective of tropospheric N_2O than biologically-produced N_2O. Additionally, some of the data have $\delta^{15}N$ and $\delta^{18}O$-N_2O values higher than the tropospheric signal, which is symptomatic of N_2O reduction (Figure 7.7).

7.2.4. *Aquatic N_2O from Oceans, Rivers, and Streams*

A summary of dissolved $\delta^{15}N$-N_2O and $\delta^{18}O$-N_2O values from freshwater streams and rivers is shown in Figure 7.8c ($n = 590$; EGL data). Of the published data, there is a relatively small amount of stream and river N_2O isotope data ($n = 34$) and a larger collection of oceanic N_2O isotope results ($n = 197$) (Figures 7.9a–b). Most of the marine N_2O is centred near tropospheric N_2O; however some highly ^{15}N- and ^{18}O-enriched samples were collected from the Arabian Sea and Eastern Tropical North Pacific Ocean by Yoshinari *et al.* (1997) and Yamagishi *et al.* (2007). The lowest marine N_2O isotope values are reported by Westley *et al.* (2006) where minimum $\delta^{15}N$ and $\delta^{18}O$-N_2O values in the Black Sea reached $-11‰$ and $+40‰$, respectively.

Only three studies have reported $\delta^{15}N$ and $\delta^{18}O$ of freshwater N_2O. These samples were obtained from the Tama River, Tokyo, Japan (Toyoda *et al.* 2009), the Bang Nara River, Thailand (Boontanon *et al.* 2000), and an agricultural drainage ditch in Germany (Well *et al.* 2005). Similar to marine N_2O, these samples are close to tropospheric N_2O, which, de-

pending on sample flux/concentration, may indicate that gas exchange is a significant determinant of the $\delta^{15}N$ and $\delta^{18}O$-N_2O of these rivers and streams. The lowest published freshwater results originate from the Tama River, which is impacted by sewage treatment effluent, and these data are closer to the ranges of N_2O formation by nitrification and denitrification reported in this thesis (Figure 7.9b).

An extensive collection of N_2O isotope ratios from the Grand River Watershed is reported in Thuss (2008) ($n = 404$). A large proportion of the low concentration samples have $\delta^{15}N$ and $\delta^{18}O$-N_2O values that lie near tropospheric N_2O (Figures 7.8b and 7.12a). Some of these data are ^{15}N- and ^{18}O-enriched, indicating that these samples were altered by N_2O consumption.

The remainder of the Grand River dataset is widespread, and much of it falls within the ranges for nitrifier- and denitrifier-N_2O reported in this thesis. Of the 54 Grand River samples with $\delta^{18}O$-N_2O values $< +28‰$, 47 were collected from inside wastewater treatment plants in Guelph, Kitchener, and Waterloo, ON, or in the river downstream of their effluent discharge pipes. The highest concentration samples were collected from the Kitchener wastewater treatment plant in June 2007 (9,000-14,000% above atmospheric saturation). Interestingly, these samples have low $\delta^{18}O$ values but are ^{15}N-enriched (bottom-right corner of Figure 7.8c). The remaining EGL freshwater N_2O was collected from the Strawberry Creek, Turkey Lakes Watershed streams, Thames River, Innisfil Creek, and Black Brook Watershed stream ($n = 60$), and most of the data fall within the range of denitrifier-N_2O reported in this thesis (Figure 7.8c).

7.2.5. *Groundwater N_2O*

The groundwater $\delta^{15}N$ and $\delta^{18}O$-N_2O are shown in Figures 7.8c and 7.9a–b. There are 395 samples collected by EGL affiliates from ten different field sites across Canada (mainly Southern Ontario) and the results cover the entire combined range of $\delta^{15}N$ and $\delta^{18}O$-N_2O observed from soils, oceans, rivers, and streams. The Long Point groundwater N_2O results are especially striking because the $\delta^{15}N$-N_2O ranges from $-46‰$ to $+31‰$, and the $\delta^{18}O$-N_2O ranges

from +20‰ to +96‰ (Figure 7.11b). Groundwater N_2O isotope results from the Putnam site are also distributed widely (Figure 7.8d).

Groundwater systems are geochemically diverse environments and redox conditions can vary widely from site to site. As such, if the appropriate substrates exist, aerobic groundwaters can sustain nitrification and produce ^{15}N- and ^{18}O-depleted N_2O, and anoxic groundwaters can support denitrification and produce ^{15}N- and ^{18}O-enriched N_2O (that may be subsequently consumed and further enriched). Additionally, there are few groundwater N_2O isotope values that lie close to the isotopic signature of tropospheric N_2O. As explained in Section 7.3.5 (below), groundwaters are not in direct contact with the atmosphere and are not subject to the effects of gas exchange with tropospheric N_2O. However, in soil and aquatic environments, gas exchange can mask fractionating processes.

7.2.6. *A Statistical Description of the In Situ Data*

The vast assemblage of $\delta^{15}N$ and $\delta^{18}O$-N_2O data collected by EGL researchers ($n = 1180$) and others ($n = 520$) is shown in Figure 7.10a. This compilation of data reveals staggering variability in both $\delta^{15}N$ and $\delta^{18}O$. A descriptive statistical analysis of the data's distribution is shown in Figure 7.10b, where the median, $25^{th}/75^{th}$, $10^{th}/90^{th}$ and $5^{th}/95^{th}$ percentiles are identified. The median values of $\delta^{15}N$-N_2O and $\delta^{18}O$-N_2O are −8‰ and +41‰, respectively. Nine-tenths of all the $\delta^{15}N$-N_2O values are between −33‰ and +9‰ (a 42‰ range), and nine-tenths of all the $\delta^{18}O$-N_2O values lie between +19‰ and +64‰ (a 45‰ range).

Very few values lie within the upper left-hand and lower right-hand corners of Figures 7.10a–b. These areas, which are relatively devoid of data, have been affectionately termed the 'forbidden zones' by EGL researchers. Instead, there is a strong, positive correlation between $\delta^{15}N$ and $\delta^{18}O$, and a significant proportion of the data falls near the isotopic value of tropospheric N_2O (Figure 7.10 a–b). Of the few data points that do fall in the 'forbidden zone', most originate from two different field sites (a soil and a lake) in Antarctica that have truly unique conditions. In addition to very low $\delta^{18}O$-H_2O values, one study recorded abiotically-produced N_2O in soil that was formed by the reduction of NO_3^-/NO_2^- coupled to the oxida-

tion of ferrous iron minerals (Samarkin *et al.* 2010). The other study described biologically-produced N_2O that was formed >10,000 years ago. This dissolved N_2O was (and still is) trapped in a permanently ice-covered saline lake, and concentrations exceeded 700,000% atmospheric saturation (Priscu *et al.* 2008).

A descriptive statistical analysis of the soil data is shown in Figure 7.10c. The median soil δ^{15}N-N_2O and δ^{18}O-N_2O values are −15‰ and +30‰, respectively. Nine-tenths of all the δ^{15}N-N_2O values are between −34‰ and +6‰ (a 40‰ range), and nine-tenths of all the δ^{18}O-N_2O values lie between +17‰ and +50‰ (a 33‰ range). The ranges of nitrifier- and denitrifier-derived N_2O defined in this thesis (Figure 7.10c, grey polygon) span > 90% of this *in situ* soil data.

Finally, the flux-weighted average isotopic composition of soil-emitted N_2O measured in several different studies is shown in Figure 7.10d. These values are compared to modelled estimates of the average terrestrial N_2O source. These modelled estimates, presented in papers that discuss the global N_2O isotope budget (Rahn and Wahlen 2000; Kaiser 2002; Stein and Yung 2003), are derived from box-models that balance the masses and isotopic compositions of N_2O in the oceans, troposphere and stratosphere. The terrestrial N_2O source (mainly soil) is a residual, back-calculated term with high degree of uncertainty. Additionally, a concentration-weighted value of the shallow soil gas sampled from Strawberry Creek is also shown for comparison (Figure 7.10d). A detailed discussion of this data and the global isotopic N_2O budget is beyond the scope of this chapter. These flux-weighted estimates are shown here to place the results of this thesis into context (the nitrifier- and denitrifier-derived isotopic N_2O ranges).

7.3. *Key Controls of the Isotopic Range of In Situ N_2O*

7.3.1. *The Isotopic Variation of N_2O Substrates*

Molecular oxygen (O_2) and H_2O are two ^{18}O endmembers that need to be considered when interpreting the O isotopic variability of N_2O. The $\delta^{18}O$ value of atmospheric O_2 is +23.5‰

(Kroopnick and Craig 1972), and slightly higher in solution ($\delta^{18}O\text{-}O_2$ = +24.2‰; air-equilibrium value). The $\delta^{18}O\text{-}O_2$ may be greater in certain settings if high metabolic rates persist and localized ^{18}O-enrichment of O_2 occurs. The $\delta^{18}O\text{-}O_2$ may also be lower in highly productive, nutrient-rich rivers impacted by sewage treatment inputs (Wassenar *et al.* 2010). In the South Saskatchewan River, for example, high rates of daytime photosynthesis forced the $\delta^{18}O$-dissolved oxygen down to +8‰ at a site downstream of the Saskatoon sewage treatment plant.

The $\delta^{18}O\text{-}H_2O$ of environmental water is variable and dependent on many factors including: season, latitude, altitude, evaporative enrichment, proximity to glacial melt-waters, and inland distance from marine sources. In most areas where N_2O emissions are globally significant (moderate-heavy N loading), $\delta^{18}O\text{-}H_2O$ ranges from −15‰ to +2‰ (Gat 1996), however, there are many areas with lower $\delta^{18}O\text{-}H_2O$ that may prove to be important N_2O producing regions.

The NH_4^+ endmember for nitrification can vary in $\delta^{15}N$ by > 40‰. Atmospheric $\delta^{15}N\text{-}NH_4^+$ sources may be as low as −10‰ or as high as +4‰ (Hübner 1986; Kendall 1998). In many regions of the world the rate of NH_4^+ deposition is low relative to the loading of other N sources. Therefore, deposition is usually only a significant source of N in pristine environments downwind of agriculture. Synthetic NH_4^+ and urea fertilizers have $\delta^{15}N$ values near 0 ± 4‰ (Hübner 1986; Wassennar 1995) and this source can dominate in fertilized soils or surface waters and groundwaters that receive drainage from agriculture. Similarly, manure and sewage inputs from agriculture or wastewater treatment can be significant NH_4^+ sources in soils, surface waters and groundwaters. Fresh manure and sewage has $\delta^{15}N\text{-}NH_4^+$ values that range between +2‰ and ~+10‰, but can become much higher (>+30‰) when volatilization of NH_4^+ to NH_3 occurs (Hübner 1986; Fogel and Cifuentes 1993; Wassennar 1995; Kendall 1998).

The NO_3^- endmember for denitrification is highly variable in $\delta^{15}N$ (−6‰ to ~40‰) and $\delta^{18}O$ (>80‰), and these ranges have recently been reviewed by Xue *et al.* (2009). More commonly the isotopic range of both $\delta^{15}N$ and $\delta^{18}O$ is ~30‰. Atmospherically deposited

NO_3^- and NO_3^- derived from nitrification of atmospheric NH_4^+ ranges in $\delta^{15}N$ from −12‰ to +6‰. The $\delta^{18}O$ of NO_3^- in precipitation is very high and typically ranges from +45‰ to >+90‰. These depositional sources are most significant in pristine environments and are often masked by other NO_3^- sources that contribute a greater N load on the landscape.

Most NO_3^- derived from the nitrification of soil organic nitrogen ranges in $\delta^{15}N$ from 0‰ to +8‰ and $\delta^{18}O$ from 0‰ to +16‰, although lower $\delta^{15}N$ and $\delta^{18}O$ values have been recorded (e.g., Mitchell 2006; Rempel 2008; *this thesis*, Chapters 4 and 6). Heavily N impacted sites can receive NO_3^- from synthetic fertilizers and/or manure and sewage NO_3^-. Fertilizer NO_3^- (e.g., ammonium nitrate) $\delta^{15}N$ values range between −2‰ and +3‰, and $\delta^{18}O$ values range between +18‰ and +25‰. Manure and sewage NO_3^- sources are higher in $\delta^{15}N$ (+4‰ to +25‰), but their $\delta^{18}O$ values are reflective of microbial nitrification processes (0‰ to +16‰; Xue *et al.* 2009).

The denitrification of a NO_3^- reservoir that is closed (no input of substrate) causes the $\delta^{18}O$ and $\delta^{15}N$ values of the remaining NO_3^- to increase in a characteristic ~0.5:1 ratio (e.g., Böttcher *et al.* 1990; Mengis *et al.* 1999). At least ~5% of the total pool must be consumed before there is any observable shift in the NO_3^- isotopes, but as NO_3^- reduction progresses $\delta^{15}N$ and $\delta^{18}O$ values increase exponentially (Mariotti *et al.* 1981; Kendall 1998). N_2O produced from this changing NO_3^- pool may also become ^{18}O and ^{15}N-enriched in a ~0.5:1 ratio as time progresses illustrated by the NO_3^- consumption trajectories shown in Figure 7.7.

7.3.2. *Variable Fractionation and Oxygen Exchange*

Literature estimates of ^{15}N and ^{18}O fractionation for N_2O production are summarized in Chapter 1 (Table 1.1). In most cases, the $\delta^{15}N$-N_2O produced by denitrification ($\varepsilon_{\text{nitrous oxide–nitrate}}$: −40‰ to −10‰) is higher than the $\delta^{15}N$-N_2O produced from nitrification. Studies using cultured nitrifying organisms would suggest the ^{15}N $\varepsilon_{\text{nitrous oxide–ammonium}}$ is large and negative (−75‰ to −50‰). This has not been confirmed *in situ*, and the range of ^{15}N $\varepsilon_{\text{nitrous oxide–ammonium}}$ values observed in this thesis were lower (−55‰ to −30‰; excluding results obtained in forested wetland).

The $\delta^{18}O$ values of nitrifier-N_2O range between +13‰ and +31‰ (Chapter 5). The $\delta^{18}O$ values of denitrifier-N_2O are dependent upon a variable ^{18}O isotope effect (+17‰ to +60‰; Chapters 2-3) and a variable amount of O-exchange (40% to 95%; Chapters 2-3). The amount of O-exchange measured for individual denitrifier strains varies from almost zero to 100% (Chapter 1, Table 1.2), so the minimum amount of O-exchange in nature is probably lower than what was determined in this thesis (40%).

Given the large ranges of the $\delta^{15}N$ and $\delta^{18}O$ endmembers for nitrification and denitrification, the large ranges of N and O isotope effects, and the varying amounts of O-exchange that can occur, it is surprising that nine-tenths of both the $\delta^{15}N$-N_2O and $\delta^{18}O$-N_2O values produced in natural environments are confined to a 42–45‰ range and not more variable than it appears to be (Figure 7.10c).

7.3.3. *The Effect of N_2O Consumption on the Isotope Ratios of N_2O*

The N and O isotope effects associated with the reduction of N_2O to dinitrogen (N_2) are summarized in Chapter 1, Table 1.1. The consumption of a closed N_2O pool is modelled in Figure 7.7 using the minimum and maximum estimates of O and N isotope effects reported in the literature. The ^{15}N $\varepsilon_{\text{dinitrogen-nitrous oxide}}$ ranges from −9‰ to −2‰ and the ^{18}O $\varepsilon_{\text{dinitrogen-nitrous oxide}}$ ranges from −26‰ to −5‰ (Mandernack *et al.* 2000; Ostrom *et al.* 2007; Vieten *et al.* 2007; Well and Flessa 2009b). As N_2O is consumed, the N and O isotope values of the residual pool increase along a trajectory with a characteristic slope that varies between 2.3 and 3.0 ($\delta^{18}O$:$\delta^{15}N$, Figure 7.7; Menyailo and Hungate 2006; Vieten *et al.* 2007). Demonstrations of this distinctive relationship in soils are shown in Jinuntuya-Nortman (2008) and Well and Flessa (2009b).

N_2O consumption can explain much of the ^{18}O-enriched data of Figure 7.10c. In fact, most of the unpublished EGL $\delta^{18}O$-N_2O values within the upper 10th percentile ($\delta^{18}O$-N_2O > +56‰) are likely from N_2O sources that were subject to consumption. These surface and groundwater data were collected in Southern Ontario from the Lower Grand River, Putnam and Long Point. Maximum summer $\delta^{18}O$ values of NO_3^- and H_2O in this reach of the Grand

River are up to +7‰ and −8‰, respectively (Jamieson 2010; Schiff, Venkiteswaran, and Chen *unpublished data*). Assuming that the O-exchange is low (40%) and the O isotope effect is high (+60‰), the highest summertime δ^{18}O-N_2O that *could* be produced by denitrification in the river is +61‰. This is a maximum theoretical value because the actual O-exchange and O isotope effect are unknown. Therefore, in all likelihood an additional mechanism (such as N_2O consumption) is needed to explain the Grand River δ^{18}O-N_2O values that are higher than tropospheric N_2O (Figure 7.8c).

Similarly, the maximum δ^{18}O-NO_3^- values in the groundwaters of Putnam and Long Point do not exceed +13‰ and +17‰, respectively (Robertson and Schiff 2008; Aravena and Robertson 1998). The expected maximum δ^{18}O-H_2O values at these sites are close to −8‰ (e.g., Aravena *et al.* 1993). Therefore the maximum theoretical δ^{18}O-N_2O values produced by denitrification in the groundwaters at Putnam and Long Point are +65‰ and +67‰, respectively. Since there are several δ^{18}O-N_2O values higher than this theoretical production maximum (up to +99‰; Figure 7.8d), N_2O consumption must be invoked in order to explain this ^{18}O-enriched data.

7.3.4. *The Effect of Diffusion on δ^{15}N-N_2O and δ^{18}O-N_2O*

The isotopic fractionation from diffusion is greatest in a vacuum where molecular collisions are minimal. In natural media (air, soils/sediment, and water) the molecular collision frequency increases and the magnitude of isotopic fractionation decreases. The diffusional isotope effects of δ^{15}N-N_2O and δ^{18}O-N_2O are relatively unstudied, and its importance in soils is not clear. It is a significant consideration in studies of soil-respired carbon dioxide (e.g., Nadelhoffer and Fry 1988; Cerling *et al.* 1991) so it must be taken into account in soil N_2O studies, however, the role of external factors such as soil moisture or the physical length of the diffusion barrier (e.g., soil column) are unknown.

N_2O diffusion in soils was first discussed by Perez *et al.* (2000) who measured N_2O in profiles of tropical forest soils. At depths of 3 m and 5 m, the δ^{15}N and δ^{18}O values were 4.6‰ and 7.7‰ (respectively) lower than the N_2O in the production zone (0.75 m). This iso-

topic shift was remarkably similar to the theoretical isotope effect (4.4‰ and 8.7‰, respectively) that is expected for the diffusion of $\delta^{15}N$-N_2O and $\delta^{18}O$-N_2O in air (Perez *et al.* 2000). The authors concluded that the shallower N_2O had diffused down into the deep layers.

Another study conducted by Rock *et al.* (2007) described a conceptual model (netNpc) that explains the isotopic variability of N_2O in an agricultural soil influenced by the simultaneous effects of production, consumption, dissolution and diffusion. In this study, diffusion was not a dominant process controlling the isotopic signature of N_2O. Instead, a concentration gradient (with higher values at depth) was observed along a 90 cm profile and there was a concomitant increase in $\delta^{15}N$ and $\delta^{18}O$-N_2O values. N_2O production and consumption were the significant processes controlling the isotopes and concentrations in this soil (Rock *et al.* 2007).

One other study by Well and Flessa (2008) investigated the effects of diffusion on $\delta^{15}N$-N_2O and $\delta^{18}O$-N_2O by conducting lab simulations that measured the time-course residual N_2O contained in gas-filled reservoirs (Exetainers®). As the reservoir gas diffused through different sized needles, the concentration declined, and the diffusive isotope effects of $^{15}N^{14}N^{16}O/^{14}N^{14}N^{16}O$ and $^{14}N^{14}N^{18}O/^{14}N^{14}N^{16}O$ were determined (+5.2‰ and +7.8‰, respectively). These results agreed with the theoretical isotope effects for N_2O diffusion in air (calculation is found in Well and Flessa 2008), and were similar to the observations of Perez *et al.* (2000). These diffusive isotope effects are shown in Figure 7.7, where the diffusion trajectories have a slope of 1.5 ($\delta^{18}O$:$\delta^{15}N$).

Well and Flessa (2008) coupled these simulations with a model describing the diffusive isotope effects of N_2O emitted from soils. The isotopic separations between the (i) source-zone N_2O, (ii) pore-space N_2O, (iii) and emitted N_2O during steady-state and non-steady-state conditions are shown. Unfortunately, it is difficult to reconcile statements made in the text of this paper with the illustrated model results. For example, Figures 4–5 (Well and Flessa 2008) are incorrectly labelled (Reinhard Well, February 28, 2011, *personal communication*) and the magnitude and direction of the isotopic changes are hard to determine. What is known is that at steady-state, the soil flux to the atmosphere is isotopically identical to the

N_2O in the source-zone. When the system is not at steady-state the N_2O flux is not identical to the source-zone N_2O. When the rate of N_2O production declines or stops, the heavy isotopologues diffuse out of the soil, and the δ^{15}N-N_2O and δ^{18}O-N_2O values emitted from the soil surface increase.

7.3.5. *N_2O Gas Exchange with the Troposphere*

Gas exchange with tropospheric N_2O is an important isotope-altering process in low concentration environments that can effectively mask the isotopic evidence of biological N_2O formation and consumption. Groundwater N_2O is not affected by gas exchange with the troposphere because there is no direct atmospheric contact. In contrast, soil and aquatic environments are open to the atmosphere. This effect is readily apparent in the *in situ* N_2O data because there is a noticeable absence of groundwater δ^{15}N and δ^{18}O-N_2O that lie close to tropospheric N_2O (Figures 7.8–7.9).

A powerful illustration of the gas exchange effect is shown in the Grand River (Figure 7.11a). Most of the samples below ~400% saturation have a δ^{18}O-N_2O close to the δ^{18}O value of tropospheric N_2O ($\pm$ 10‰). On the other hand, the high concentration samples from sites impacted by wastewater treatment effluent in the Grand River have δ^{18}O-N_2O values that range between +10‰ and +35‰ (approximately), which is characteristic of nitrifier-produced N_2O.

Groundwater data from the Long Point site provide an equally powerful demonstration of the isotopic variability that can occur at one location when gas exchange is absent (Figure 7.11b). The results of this thesis provide a useful foundation for interpreting groundwater N_2O isotope case-studies (such as the Long Point data), because the diagnostic isotope effects of nitrification and denitrification are not masked by gas exchange with the troposphere.

The strong effect of gas exchange puts the usefulness of much of the low concentration soil and aquatic N_2O data into question. If a large fraction of the low concentration samples collected from near-surface soils and marine/freshwater environments contain tropospheric N_2O, can the formation process(es) be delineated if the data is so biased by tropospheric gas

exchange? To address this concern, models such as SIDNO (Thuss 2008) that account for gas exchange with tropospheric N_2O in low concentration aquatic environments must be used to interpret data. A model to 'correct' low concentration soil N_2O data for gas exchange effects does not currently exist. In any case, as the sample concentration approaches the tropospheric mixing ratio, the uncertainty of the 'corrected' result increases substantially.

7.4. *Recommendations for Future Studies*

At its most fundamental level, this thesis questioned whether or not $\delta^{15}N$ and $\delta^{18}O$ values can be used to apportion different N_2O sources. The answer to this question is a qualified "yes". The controls on $\delta^{15}N$-N_2O and $\delta^{18}O$-N_2O are far too complicated to infer the dominant N_2O production process based on isotopic measurements of N_2O alone. Instead, $\delta^{15}N$-N_2O and $\delta^{18}O$-N_2O must be measured in conjunction with other isotopic endmembers and traditional geochemical parameters. Provided that researchers take into account all the key pieces of information outlined in this chapter, and isotopically characterize all N_2O endmembers on a site-by-site basis, $\delta^{15}N$ and $\delta^{18}O$ values of N_2O can distinguish between denitrifier and nitrifier-derived N_2O. O-exchange need not be quantified in all cases. Alternatively, it is suggested that anaerobic incubations be conducted (with $\delta^{18}O$-H_2O at natural abundance) to characterize the denitrification N_2O endmember for each site.

The work presented in this thesis has made several important research contributions. Many questions were successfully addressed, and many more questions were conceived that remain unanswered. The following recommendations for future work represent the important research questions that are most relevant to this thesis.

7.4 i What controls O-exchange during soil denitrification? Is it a species-specific attribute that changes with shifts in the dominant denitrifying community? Is the dominant denitrifying community controlled by soil type and antecedent hydrological conditions? *(Chapters 2–3)*

Incredibly, O-exchange was not affected by changes in soil temperature and moisture, nor was O-exchange correlated to the rate of N_2O production. Very high O-exchange was observed in incubations of both the upland forested soil (87–91%) and the well-drained agricultural soil (94%). Although these soils have very different histories, soil texture and nutrient contents (organic-rich versus mineral), both soils are well-drained. Additionally, these soils exhibited some of the smallest ^{18}O isotope effects for denitrification measured in this thesis. Moderate amounts of O-exchange were observed in the forested wetland (65–70%) and the wetland agricultural soil (64%–65%). The smallest amount of O-exchange observed in this thesis occurred in the stream sediment, which is normally flooded throughout most of the year.

When we examine $\delta^{18}O\text{-}N_2O$ collected from various natural environments, much of the data from soil gases ranges between +35‰ and +45‰. The $\delta^{18}O\text{-}N_2O$ samples collected from streams, rivers and oceans generally ranges between +45‰ to +55‰. Is this segregation of $\delta^{18}O\text{-}N_2O$ based solely on different amounts of O-exchange unique to each environment?

7.4 ii Does O-exchange in denitrification occur appreciably during nitrite (NO_2^-) reduction *and* nitric oxide (NO) reduction? Or does the bulk of the O-exchange occur at only one step? *(Chapter 3)*

The mathematical derivations of O-exchange presented in Chapter 3 (Method II) reveal that the slope of the linear regression of $\delta^{18}O\text{-}N_2O$ versus $\delta^{18}O\text{-}H_2O$ is a good approximation of O-exchange when it occurs at one enzymatic site. If the fraction of O-exchange occurs equally at nitrite reductase and nitric oxide reductase, then the slope is a poor approximation of the total O-exchange. In this case, the slope underestimates the true O-exchange.

7.4 iii Does the abiotic equilibrium O-exchange between NO_2^- and H_2O occur appreciably in natural environments, or is it an artefact of lab-scale experiments and caused by disturbance effects? *(Chapter 4–5)*

The amount of abiotic O-exchange ($NO_2^- \leftrightarrow H_2O$) that occurs during nitrification is a function of how much unreacted NO_2^- is present at any given time, and how long it remains available to equilibrate with H_2O. There are very few reports of high environmental NO_2^- concentrations in the literature. Furthermore, NH_4^+ oxidation is thought to be the rate-limiting step of microbial NO_3^- production (Schmidt *et al.* 2004). In this thesis, the highest amount of O-exchange was recorded in a soil that experienced a temporary accumulation of NO_2^-, and the lowest amount of O-exchange was recorded in the soil with the highest rate of nitrification. Was this O-exchange induced by the soil incubation methodology (soil collection, sieving, drying, storage, and re-wetting)?

7.4 iv Can experiments with nitrifying bacteria confirm or deny the existence of biological O-exchange during nitrifier-denitrification? *(Chapter 5)*

Biologically catalyzed O-exchange is well documented during denitrification. The Monte Carlo simulations of N_2O production during nitrification suggested that biologically catalyzed O-exchange was absent. A more rigorous approach using cultures of nitrifying bacteria (following the methods of Ye *et al.* 1991) would conclusively identify if biologically-catalyzed O-exchange occurs during nitrifier-denitrification

7.4 v What proportion of nitrifier-derived N_2O is produced by hydroxylamine (NH_2OH) oxidation relative to nitrifier-denitrification? *(Chapters 5–6)*

Initial estimates of the ^{15}N isotope effect (N_2O—NH_2OH) would suggest that $\delta^{15}N$-N_2O produced by NH_2OH oxidation is indistinguishable from denitrifier-derived $\delta^{15}N$-N_2O (Sutka *et al.* 2003, 2004, 2006). Additionally, the ^{18}O-isotope effect for NH_2OH oxidation is unknown. How many reaction steps are involved in this reaction? Is NO a reaction intermediate? Is it an enzyme-catalyzed oxidation, or is it redox coupled (with Fe^{2+}, for example)?

7.4 vi Is the ^{15}N isotope effect (N_2O—NH_4^+) for N_2O produced by nitrification really as large (^{15}N-depleted) as single organism incubation experiments would suggest (^{15}N ε = −75‰ to −50‰; Yoshida 1988; Sutka *et al.* 2003, 2004, 2006)? *(Chapter 6)*

Lab culture experiments with chemolithoautotrophic nitrifiers have shown large ^{15}N-depletions for NH_4^+ oxidation to NO_2^-, and for NO_2^- reduction to N_2O. In the literature, these independently measured isotope effects are often summed to infer the total isotope effect for N_2O produced from NH_4^+. In nature, this is only valid if NO_2^- accumulates and the pool of NO_2^- is significantly large. Otherwise, if there is no accumulation of NO_2^- (and $NH_4^+ \rightarrow NO_2^- \rightarrow N_2O$ occurs within a single organism) the ^{15}N isotope effect (N_2O—NH_4^+) for N_2O produced by nitrification is likely smaller and controlled by NH_4^+ oxidation (the rate-limiting step).

Table 7.1. A summary of selected results from the denitrification experiments conducted in Chapters 2–3.

		soil **chapter # [treatment(s)]**	**^{15}N isotope effect (ε) measured in this thesis**	**representative δ^{15}N-NO_3^- endmember (*in situ*)[a]**	**δ^{15}N-N_2O (modelled)**	**oxygen exchange**	**net ^{18}O isotope effect (ε)**	**representative δ^{18}O-NO_3^- endmember (*in situ*)[a]**	**δ^{18}O-N_2O (modelled)[b]**
DENITRIFICATION	forested	*upland* 2 [A]	−29 ± 6‰	−8 ± 2‰	−37 ± 6‰	90 ± 4%	+17 ± 0‰	+3 ± 2‰	+10 ± 2‰
		upland 2 [C, E]	−21 ± 1‰		−29 ± 2‰	89 ± 3%	+38 ± 2‰	+3 ± 2‰	+31 ± 3‰
		wetland 2 [B, D, F]	−24 ± 5‰		−32 ± 5‰	67 ± 3%	+42 ± 0‰	+7 ±2 ‰	+39 ± 2‰
	agricultural	*well-drained* 3 [1]	−21 ± 2‰	+8 ± 6‰	−13 ± 6‰	94 ± 1%	+32 ± 0‰	−3 ± 3‰	+24 ± 2‰
		poorly-drained 3 [2–3]	−12 ± 5‰		−4 ± 8‰	65 ± 2%	+49 ± 2‰	0 ± 3‰	+44 ± 3‰
		stream sediment 3 [4–5]	−26 ± 5‰		−18 ± 8‰	45 ± 6%	+51 ± 9‰	−2 ± 5‰	+46 ± 10‰

[a] Representative δ^{15}N and δ^{18}O-NO_3^- ranges for each soil were chosen from data published in Chapter 4, Table 4.2; Spoelstra *et al.* 2007; Rempel 2008.

[b] Denitrification experiments were fertilized with KNO_3 with a $\delta^{18}O = +28‰$, which is not a representative $^{18}O/^{16}O$ endmember for these soils. As such, a range of possible δ^{18}O-N_2O values is shown for each soil that is calculated using the estimates of O-exchange and net ^{18}O isotope effect determined in this thesis. A δ^{18}O-H_2O range (−8 ± 2‰) was chosen from the values shown in Chapter 5, Table 5.1 (where δ^{18}O-H_2O is at natural abundance for $^{18}O/^{16}O$). This range can be expanded/condensed in the future if more information is known. For example, during snowmelt at Strawberry Creek the δ^{18}O-H_2O may be as low as −20‰ rel. VSMOW. Consequently, N_2O produced in the well-drained agricultural soil could be as low as ~12‰.

Mean δ^{18}O-N_2O values were calculated as:

δ^{18}O-N_2O = δ^{18}O-NO_3^- (1 − fraction of O-exchange) + δ^{18}O-H_2O(fraction of O-exchange) + net ^{18}O isotope effect

N.B. Uncertainty estimates are 1σ from the mean value, and the modelled results include a propagated uncertainty estimate. The following equation was used to propagate error:
when $d = a + b + c$,
where $d = \delta^{18}\text{O-N}_2\text{O}; a = \left(1 - f_{\text{oxygen exchange}}\right) \times \delta^{18}\text{O-NO}_3^-; b = f_{\text{oxygen exchange}} \times \delta^{18}\text{O-H}_2\text{O}; c =$ net ^{18}O isotope effect
then $\sigma_d = \sqrt{(\sigma_a)^2 + (\sigma_b)^2 + (\sigma_c)^2}$;
where $\sigma_d = \sigma_{\delta 18\text{O-N2O}}; \sigma_a = \left(1 - f_{\text{O-exchange}}\right) \times \sigma_{\delta 18\text{O-NO3-}}; \sigma_b = f_{\text{O-exchange}} \times \sigma_{\delta 18\text{O-H2O}}; \sigma_c = \sigma_{\text{net 18O isotope effect}}$.

Table 7.2. A summary of selected results from the nitrification experiments conducted in Chapters 5–6.

		soil **chapter # [treatment]**	**^{15}N isotope effect (ε) or separation (Δ) measured in this thesis**	**representative δ^{15}N-NH_4^+ endmember (*in situ*)[a]**	**δ^{15}N-N_2O (modelled)**	**δ^{18}O-N_2O measured in this thesis[b]**	**δ^{18}O-N_2O observed in the literature[c]**
NITRIFICATION	forested	*upland* 5 [3–5] and 6 [3–6]	−44 ± 10‰	+5 ± 2‰	−39 ± 10‰	+18‰ to +34‰	+13‰ to +31‰
		wetland 5 [6] and 6 [7]	−16 ± 1‰		−11 ± 2‰	+23‰ to +30‰	
	agricultural	*well-drained* 5 [2] and 6 [1]	−35 ± 3‰	+6 ± 1‰	−29 ± 3‰	+19‰ to +30‰	
		poorly-drained 5 [1] and 6 [2]	−29 ± 1‰		−23 ± 1‰	+13‰ to +28‰	

[a] It is assumed that δ^{15}N-NH_4^+ is ≈ δ^{15}N-TN in these soils.

[b] The range of values measured from each soil incubated with waters at natural abundance (Chapter 5).

[c] As discussed in Chapter 5.

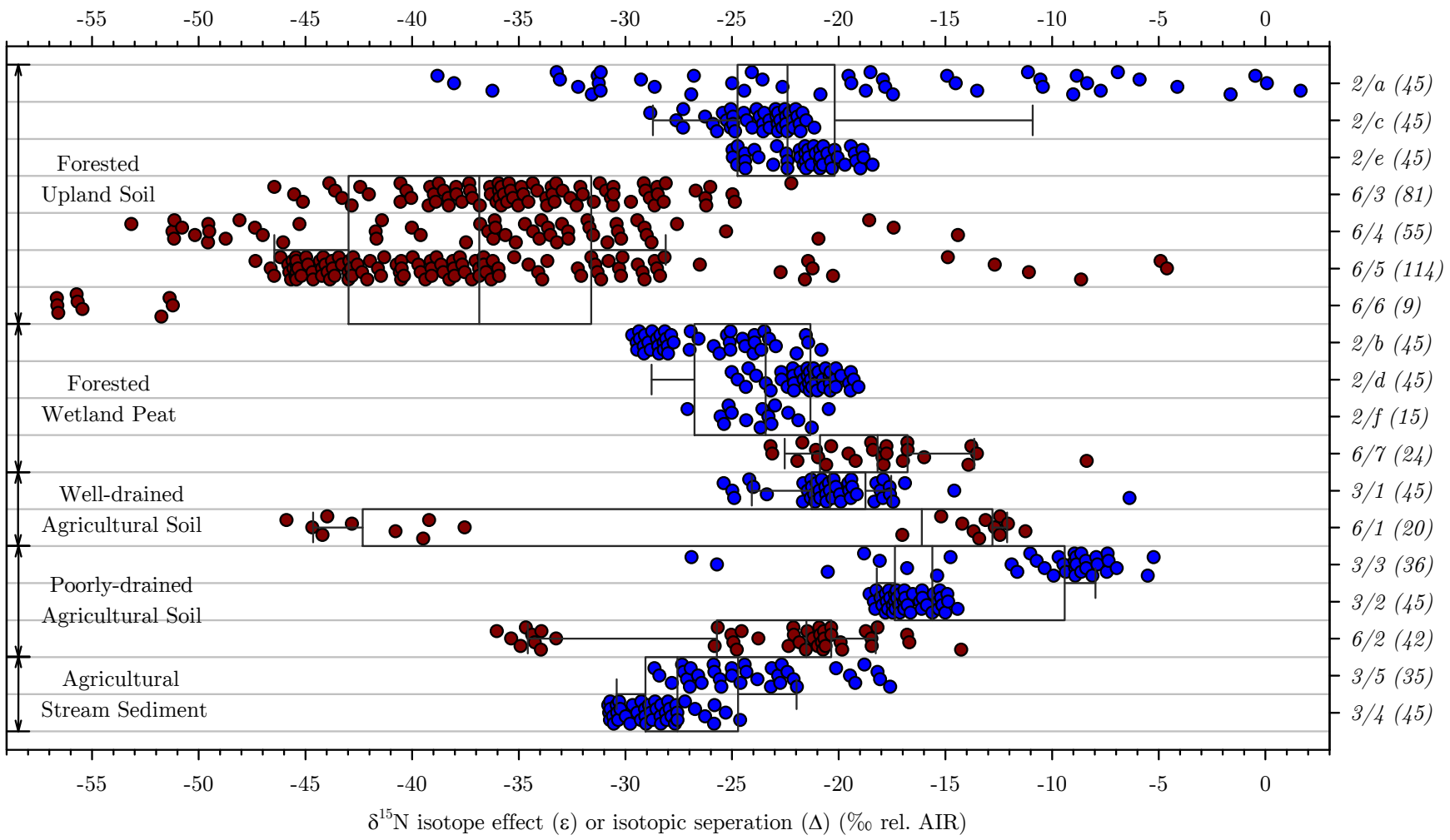


Figure 7.1a. A compilation of the ^{15}N isotope effects (ε) or separations (Δ) measured in this dissertation between N_2O and NO_3^- (denitrification - blue symbols) and between N_2O and NH_4^+ or organic-N (nitrification - red symbols). Each symbol represents an individual $\delta^{15}N$-N_2O measurement (subsequently transformed into an ε or a Δ) with an analytical precision of ± 0.2‰. *All the ^{15}N data measured in this thesis is shown here*, including early and late-time measurements when the incubations are, in some cases, obviously not at steady-state. The vertical labels (right) represent the chapter number/treatment identifier followed by the sample size (*n*) in parentheses. The box plots show the median, 25th and 75th percentiles of the data, and the whiskers represent the 10th and 90th percentiles.

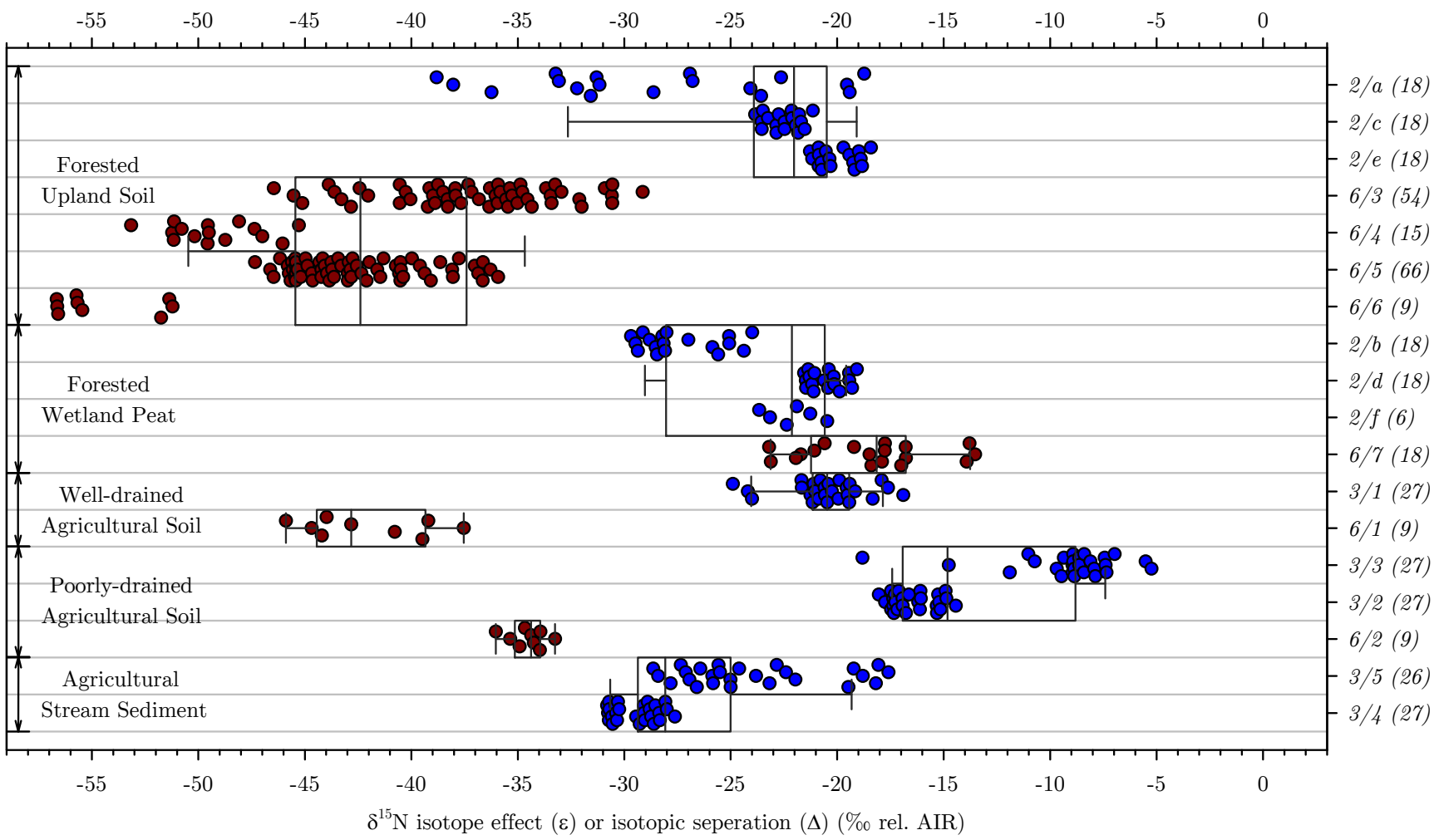


Figure 7.1b. A compilation of the ^{15}N isotope effects (ε) or separations (Δ) measured in this dissertation between N_2O and NO_3^- (denitrification - blue symbols) and between N_2O and NH_4^+ or organic-N (nitrification - red symbols). Each symbol represents an individual $\delta^{15}N$-N_2O measurement (subsequently transformed into an ε or a Δ) with an analytical precision of ± 0.2‰. *All the ^{15}N data measured in this thesis is not shown here.* In most cases, early-time measurements were excluded from this analysis (except for 6/1 and 6/2, which only includes the first sampling). Estimates of ε and Δ reported throughout this thesis are based on the data shown here.

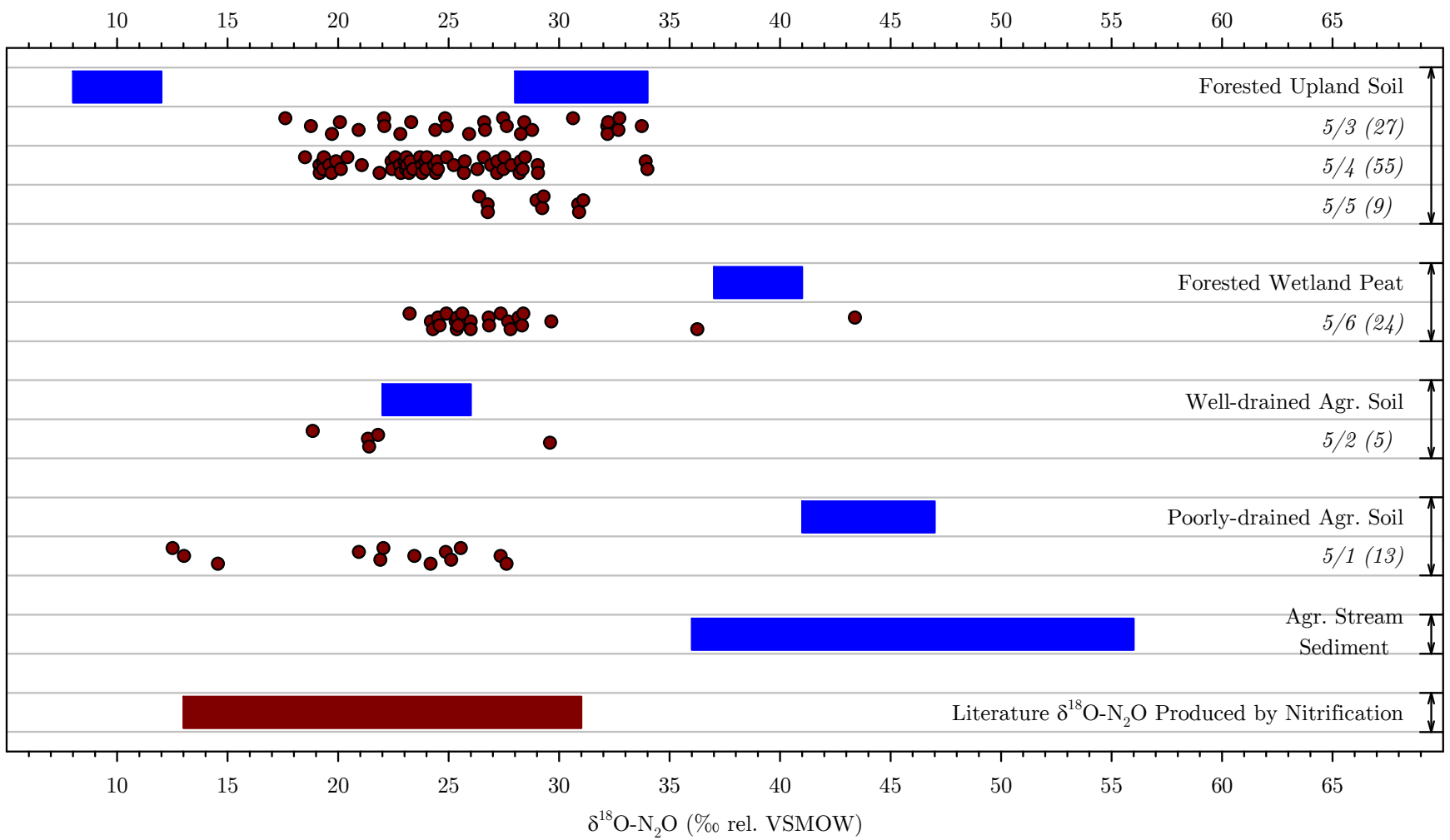


Figure 7.2. A comparison of measured δ^{18}O-N_2O data from nitrification experiments (red symbols) and modelled δ^{18}O-N_2O ranges from denitrification (blue bars). Each symbol represents an individual δ^{18}O-N_2O measurement with an analytical precision of ± 0.4‰. The modelled δ^{18}O ranges are explained in Table 7.1 and are calculated using estimates of O-exchange and ^{18}O fractionation determined for each soil, where δ^{18}O-NO_3^- = −7‰ to +9‰ and δ^{18}O-H_2O = −10‰ to −6‰. For reference, the labels represent the chapter number/treatment identifier followed by the sample size (n) in parentheses.

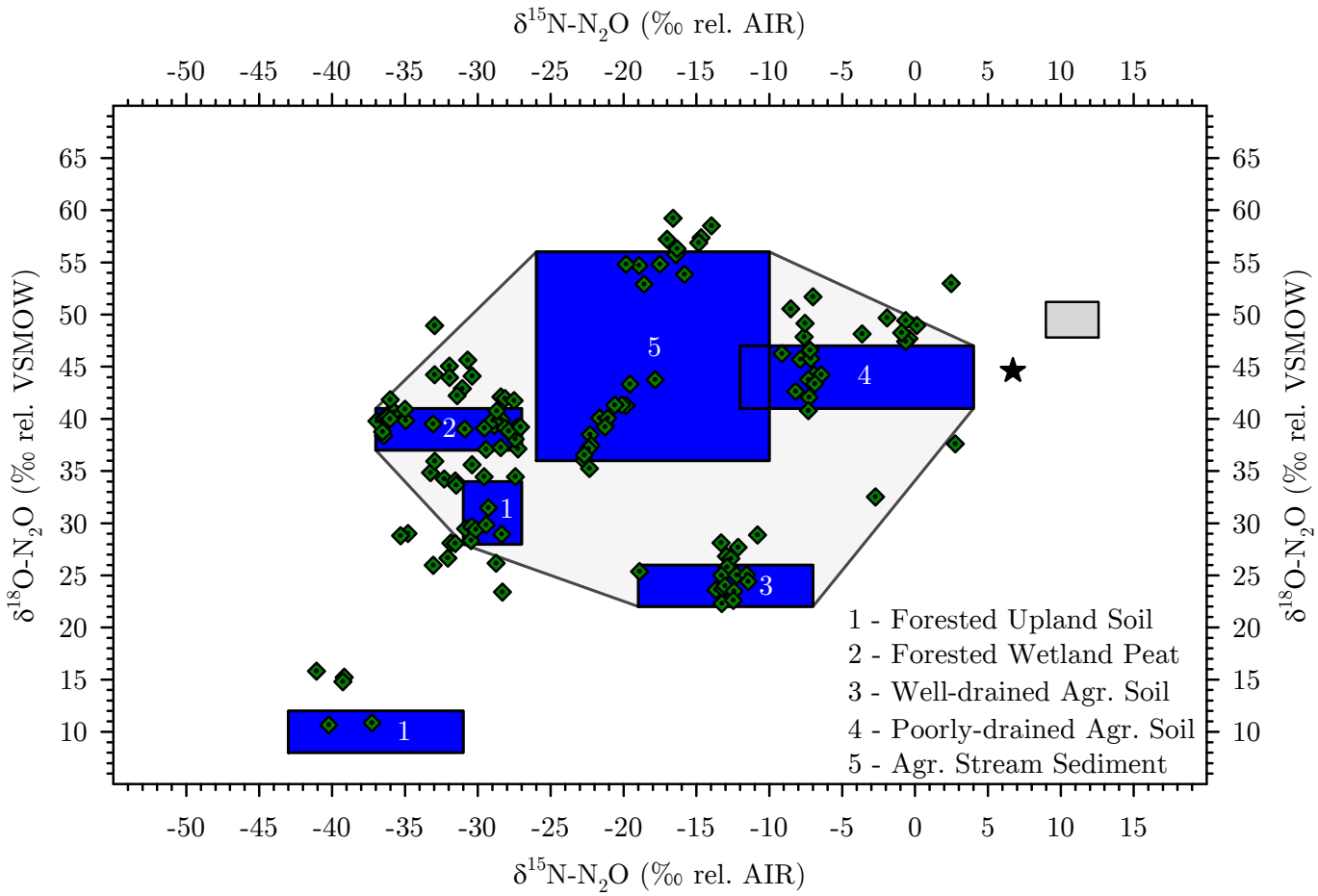


Figure 7.3. The range of $\delta^{18}O\text{-}N_2O$ and $\delta^{15}N\text{-}N_2O$ produced by denitrification in this thesis. The blue boxes correspond to the five different soil types incubated under anaerobic conditions and the boxes were drawn from the ranges tabulated in Table 7.1. The green symbols represent some of the data shown in Chapters 2-3 where $\delta^{18}O\text{-}H_2O$ was at natural abundance. This $\delta^{18}O\text{-}N_2O$ and $\delta^{15}N\text{-}N_2O$ data was normalized using representative $\delta^{18}O$ and $\delta^{15}N\text{-}NO_3^-$ endmembers and the measured ^{18}O and ^{15}N isotope effects and oxygen exchange (Table 7.1). The normalized data is shown here for illustrative purposes only to demonstrate any covariance in $\delta^{18}O$ and $\delta^{15}N$. The grey polygon that bounds most of the blue boxes is one way to depict the isotopic range in denitrifier-produced N_2O. Note that one forested upland soil treatment experienced very high oxygen exchange (90%) and a relatively low ^{18}O isotope effect (+17‰), which produced isotopically-distinct N_2O that is not bound by the polygon. The black star and the small grey rectangle represent tropospheric and stratospheric N_2O (Kaiser *et al.* 2003; Rahn & Wahlen 1997), respectively, and are labelled as such throughout the remaining figures of this chapter.

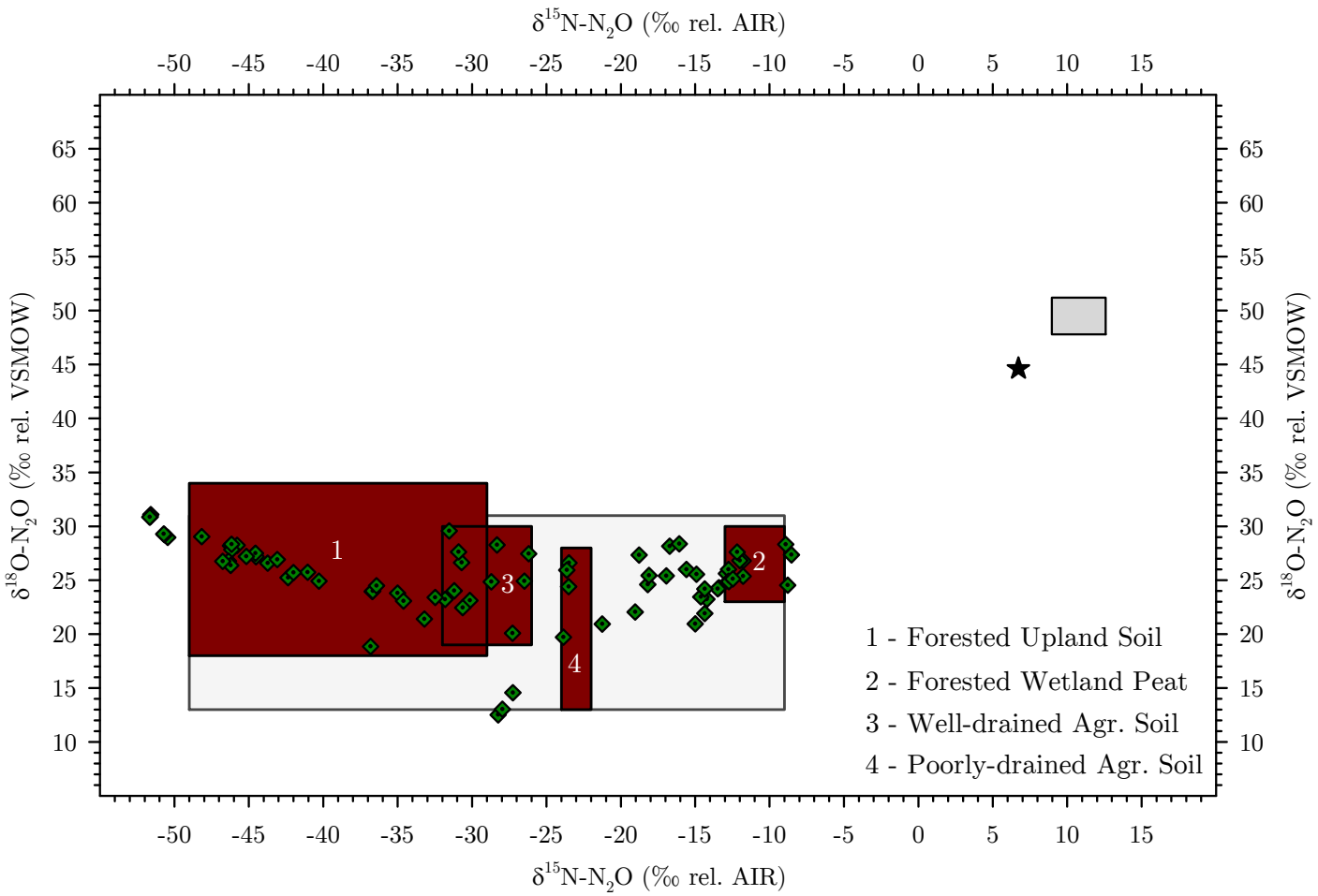


Figure 7.4. The range of δ^{18}O-N_2O and δ^{15}N-N_2O produced by nitrification in this thesis. The red boxes correspond to the four different soil types incubated under aerobic conditions and the boxes were drawn from the ranges tabulated in Table 7.2. The light-grey rectangle bounds most of the nitrifer-produced N_2O measured or modelled in this thesis. The green symbols represent some of the data shown in Chapters 5–6 (where δ^{18}O-H_2O was at natural abundance); where δ^{18}O-N_2O is measured data and δ^{15}N-N_2O is modelled data that uses representative δ^{15}N-NH_4^+ end-members and the ^{15}N isotope effect measured for each soil treatment (Table 7.2). Note that these data points (green symbols) are shown for illustrative purposes only to better describe the variability in the data. The location of each point along the δ^{15}N axis is operationally defined and the red boxes do not always capture all the data because the δ^{15}N-width of the red boxes is defined by the production-weighted ^{15}N-isotope effect.

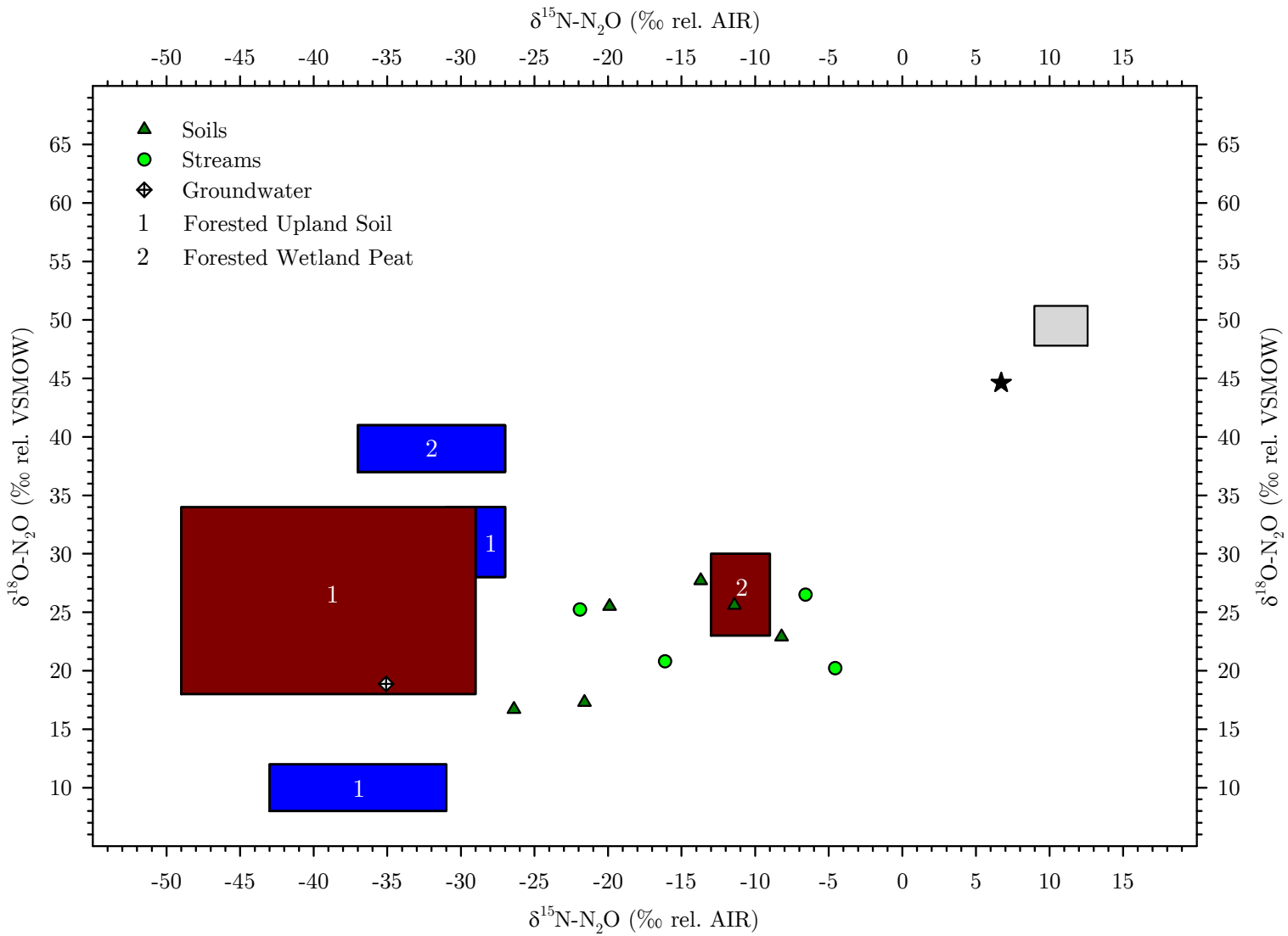


Figure 7.5. *In situ* δ^{15}N-N_2O and δ^{18}O-N_2O data collected from soils, streams and groundwater at the Turkey Lakes Watershed (unpublished results provided courtesy of J. Spoelstra) is shown alongside the range of isotopic N_2O endmembers for denitrification (blue boxes) and nitrification (red boxes) determined through soil incubations of upland and wetland TLW soils.

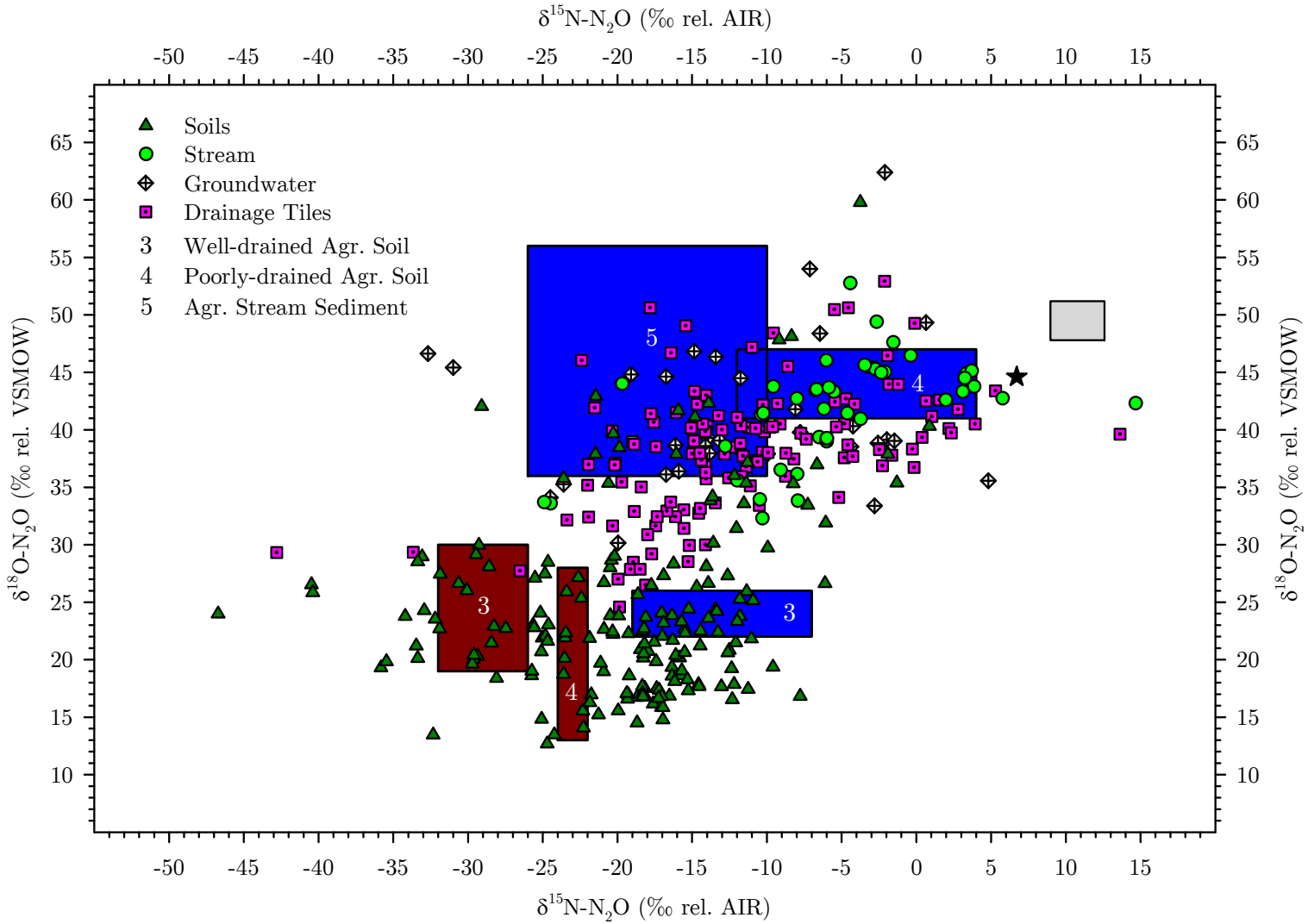


Figure 7.6. *In situ* δ^{15}N-N_2O and δ^{18}O-N_2O collected from the Strawberry Creek agricultural catchment is shown alongside the range of isotopic N_2O endmembers for denitrification (blue boxes) and nitrification (red boxes) determined through soil incubations of well-drained and poorly-drained Strawberry Creek soils and Strawberry Creek sediment. Unpublished soils data is provided courtesy of J. Spoelstra, and N_2O data collected from groundwater, agricultural drainage tiles, and the Strawberry Creek stream is provided courtesy of Rempel (2008).

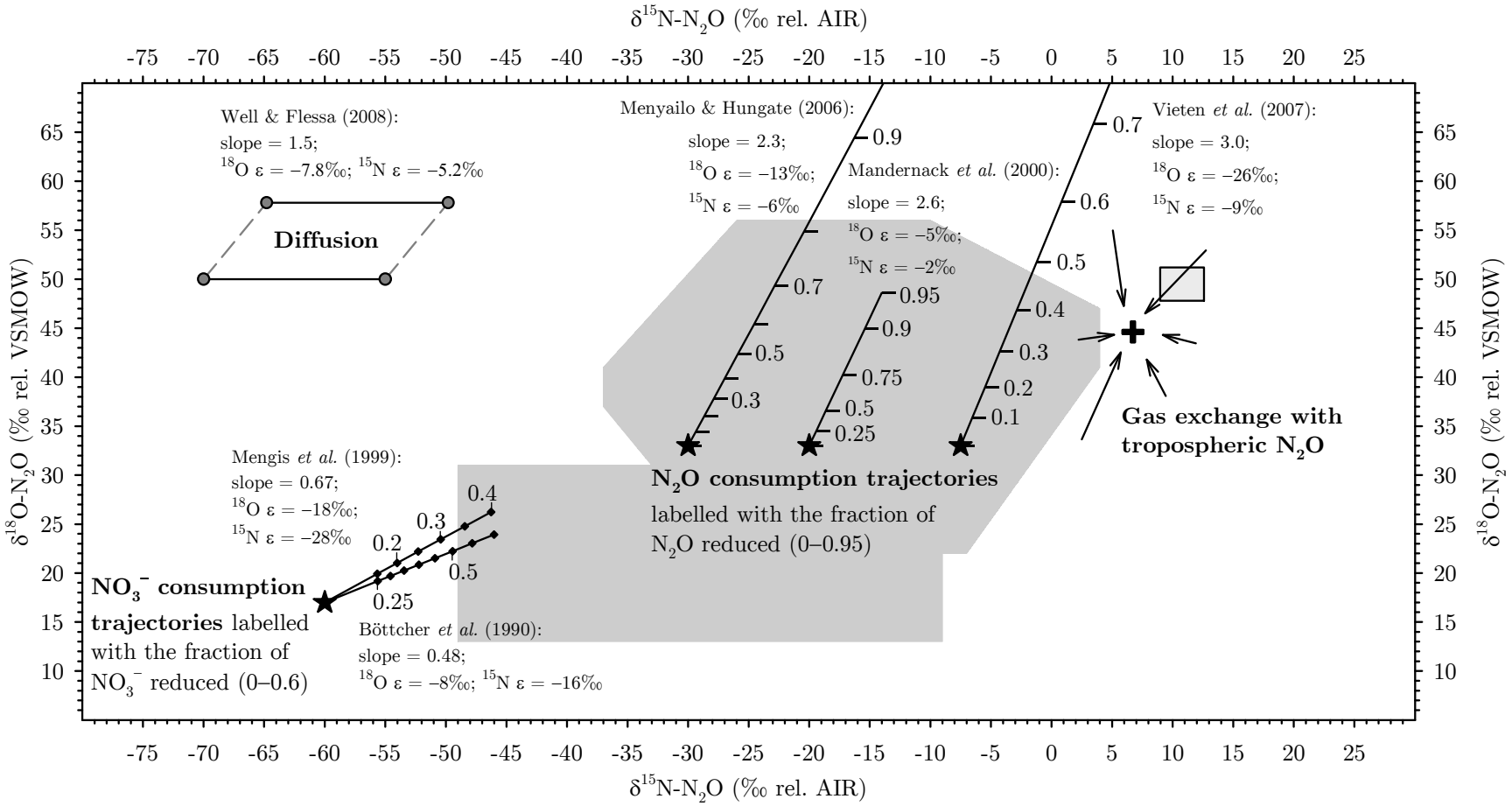


Figure 7.7. The effects of diffusion, consumption, and gas exchange on δ^{15}N and δ^{18}O-N_2O can be significant. N_2O isotope fractionation from diffusion (top-left) is not well-studied. Fractionation associated with N_2O reduction (centre) has been quantified in several studies. Only a selection of the estimates are shown here (min./max. reported estimates), illustrating how the ratio of ^{15}N and ^{18}O isotope effects is a characteristic trait (slope = 2.3–3.0) that may indicate N_2O consumption. The range of fractionation varies widely, which results in both long and short consumption trajectories depending on the fraction of N_2O reduced. NO_3^- consumption (bottom-left) by denitrifiers leaves the residual NO_3^- pool enriched in ^{18}O and ^{15}N (characteristic slope = 0.5). N_2O that is produced from NO_3^- that has been partially consumed by denitrifiers may also plot along the same trajectory. The isotopic signature of N_2O in low production/concentration environments may also be affected by gas exchange (right) with tropospheric N_2O (black cross symbol). Note: all consumption trajectories were calculated using a Rayleigh equation and assume a closed system. Additionally, the starting points of all the trajectories are randomly placed on this figure and are not representative of endmembers.

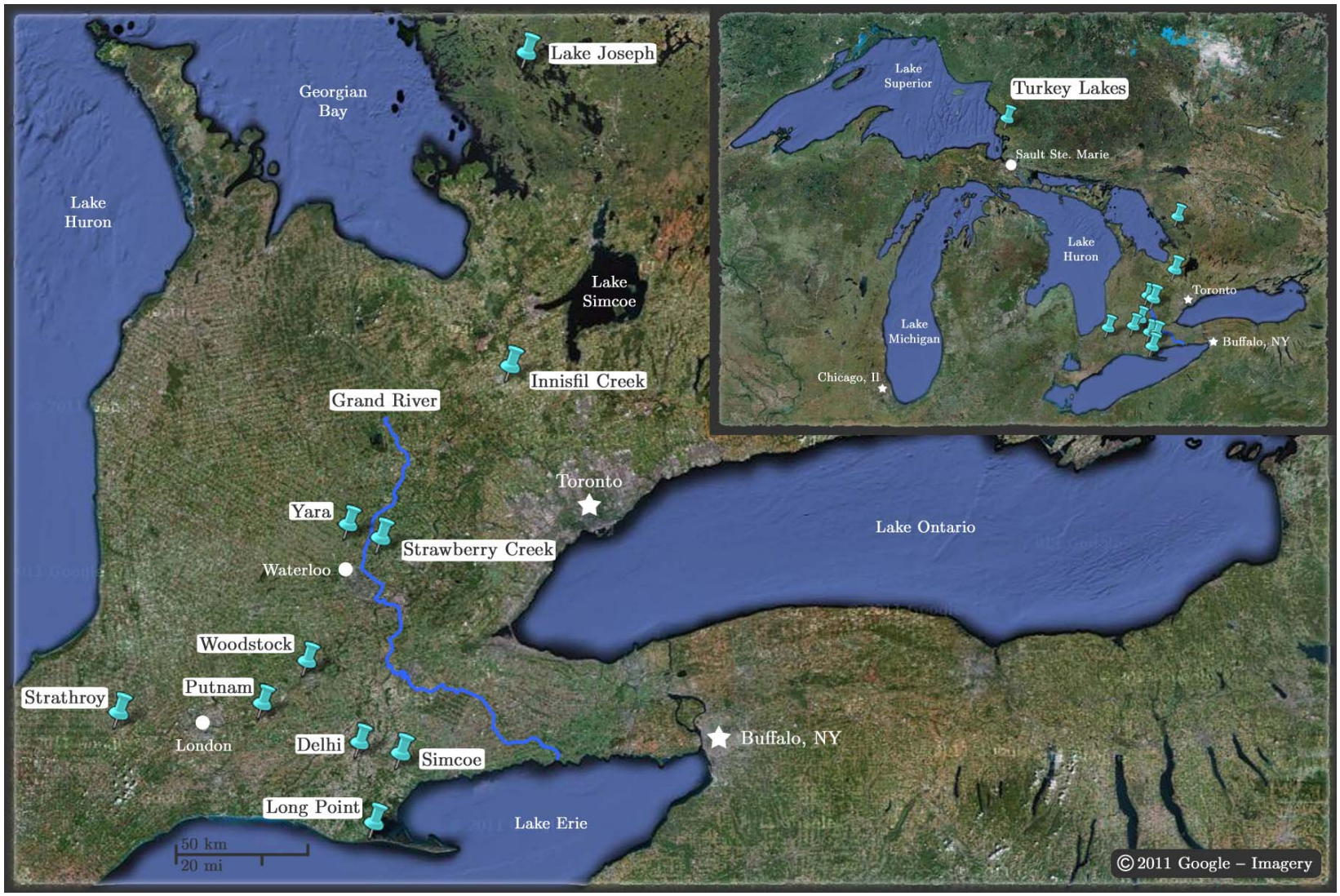


Figure 7.8a. The unpublished *in situ* data shown in this chapter was collected by University of Waterloo researchers from soils, surface waters, and groundwaters at eleven field sites throughout Ontario, Canada. The Black Brook Watershed, which is 1000 km NE of Toronto (near Grand Falls, New Brunswick) is the only site not shown on this map.

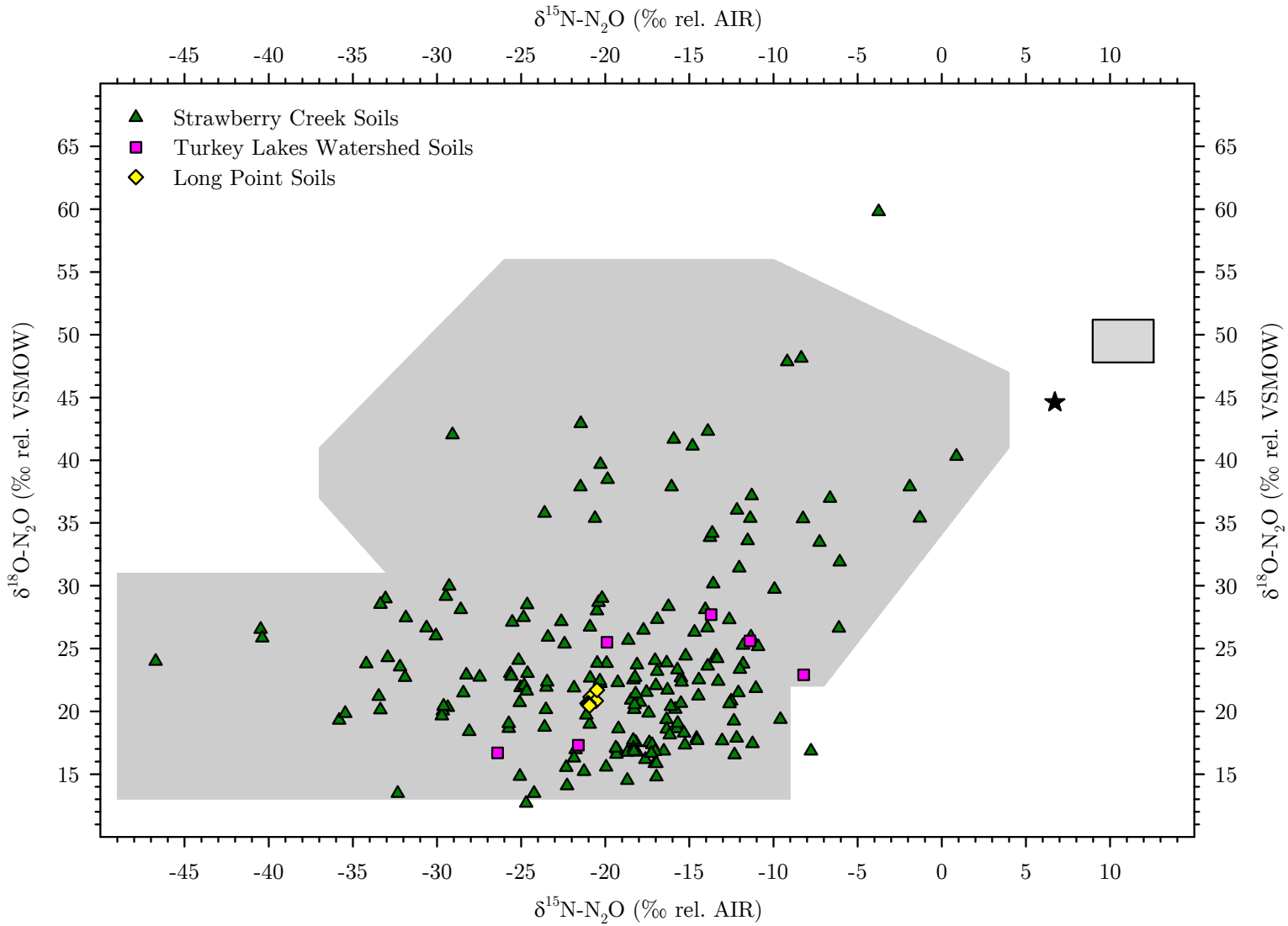


Figure 7.8b. *In situ* δ^{15}N-N_2O and δ^{18}O-N_2O from soil pore gas (n = 188) and flux collection chambers (n = 7) at Strawberry Creek, ON (Spoelstra and Schiff unpublished results), Turkey Lakes Watershed, ON (Spoelstra, unpublished results), and Long Point, ON (Li 2010). The range of isotopic N_2O endmembers for denitrification and nitrification determined in this thesis is also shown (light-grey polygon).

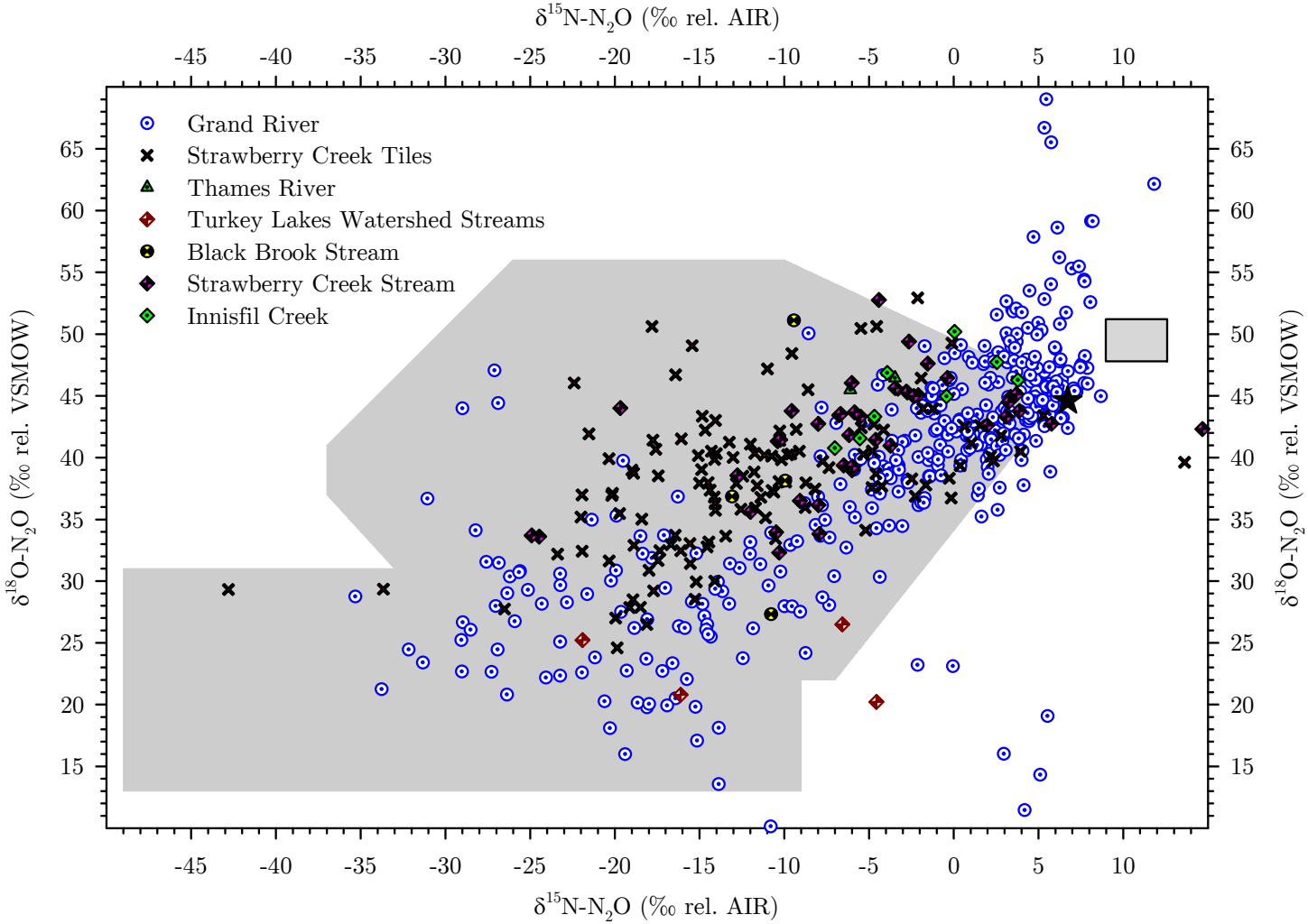


Figure 7.8c. *In situ* dissolved δ^{15}N-N_2O and δ^{18}O-N_2O collected from: creeks and streams ($n = 58$) at the Turkey Lakes Watershed, ON, Strawberry Creek, ON, Black Brook, NB, Innisfil Creek; the Grand River, ON and the Thames River ($n = 406$); and from agricultural drainage tiles at Strawberry Creek, ON ($n = 126$). Dissolved N_2O from these field sites is shown alongside the range of isotopic N_2O endmembers for denitrification and nitrification determined in this thesis (light-grey polygon). *In situ* data is provided courtesy of Rempel (2008), Thuss (2008), Flood (2010), Li (2010), and Spoelstra (unpublished).

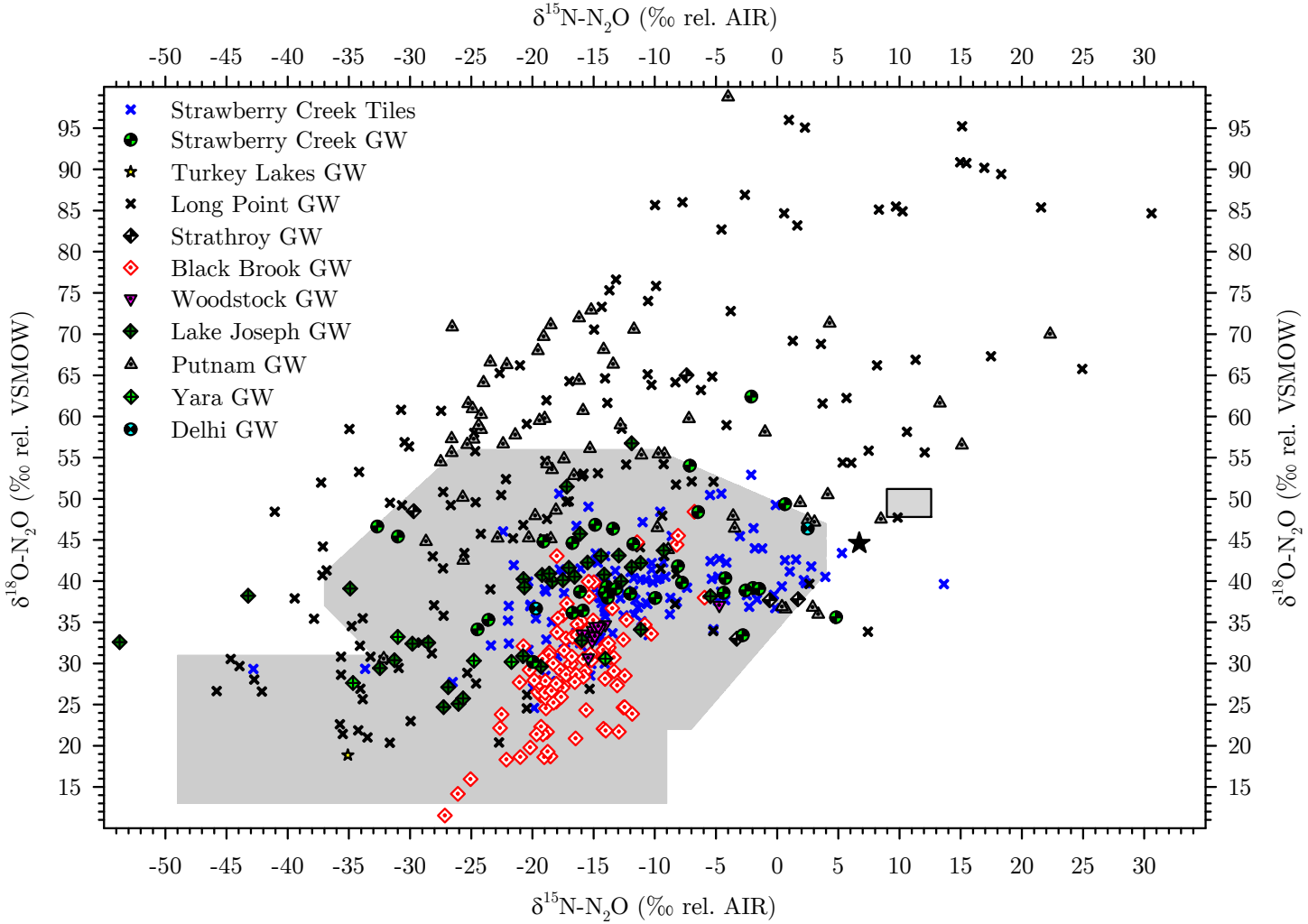


Figure 7.8d. *In situ* dissolved δ^{15}N-N_2O and δ^{18}O-N_2O collected from groundwaters at the Turkey Lakes Watershed ($n = 1$), Strawberry Creek ($n = 32$), Long Point, ON ($n = 137$), Putnam, ON ($n = 66$), Lake Joseph, ON ($n = 35$), Delhi, ON ($n = 2$), Strathroy, ON ($n = 5$), Woodstock, ON ($n = 11$), Yarra, ON ($n = 5$), and the Black Brook Watershed, NB ($n = 101$). Agricultural drainage tiles from Strawberry Creek, ON ($n = 126$) are also shown. The range of isotopic N_2O endmembers for denitrification and nitrification determined in this thesis is also shown (light-grey polygon). *In situ* data is provided courtesy of Rempel (2008), Li (2010), Spoelstra (unpublished), and Schiff (unpublished).

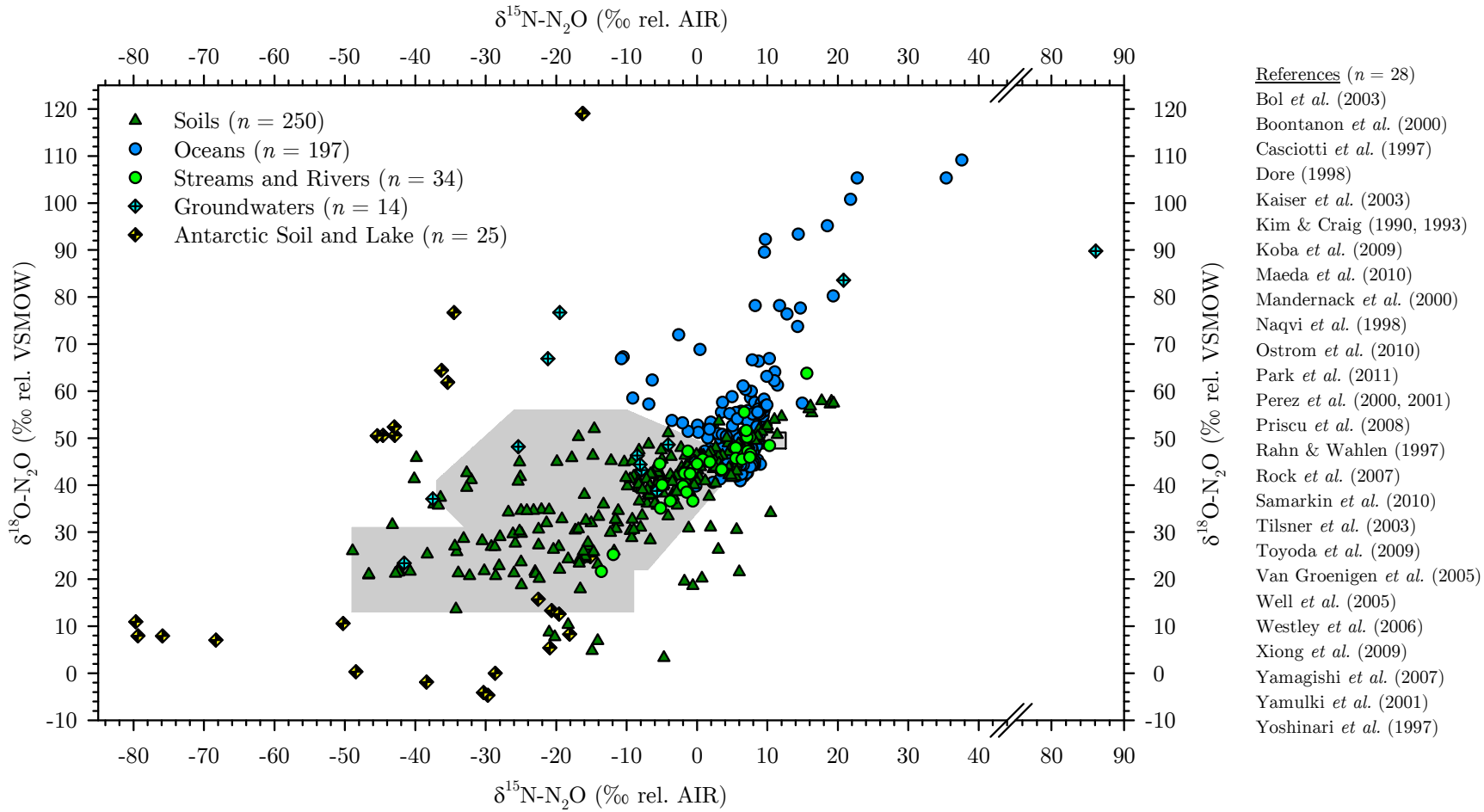


Figure 7.9a. A compilation of δ^{18}O-N_2O and δ^{15}N-N_2O data published in the peer-reviewed literature. Samples were collected globally from soils (temperate to tropical forest soils, agricultural soils, grasslands, landfill soils, and compost piles); oceans (Pacific and Indian Oceans, Arabian and Black Seas, and the Gulf of California); an agricultural stream and two rivers (Tama River, Japan and Bang Nara River, Thailand), and groundwaters. Also shown is N_2O that has accumulated underneath a permanently ice-covered lake in Antarctica, and abiotically-produced N_2O (chemodenitrification) collected from soils near a hyper-saline pond in Antarctica. The location of tropospheric N_2O is masked by a high density of data points, but the nearby dark grey box that outlines the stratospheric N_2O signal is visible. The light-grey polygon bounds the range of N_2O measured or modelled in this thesis.

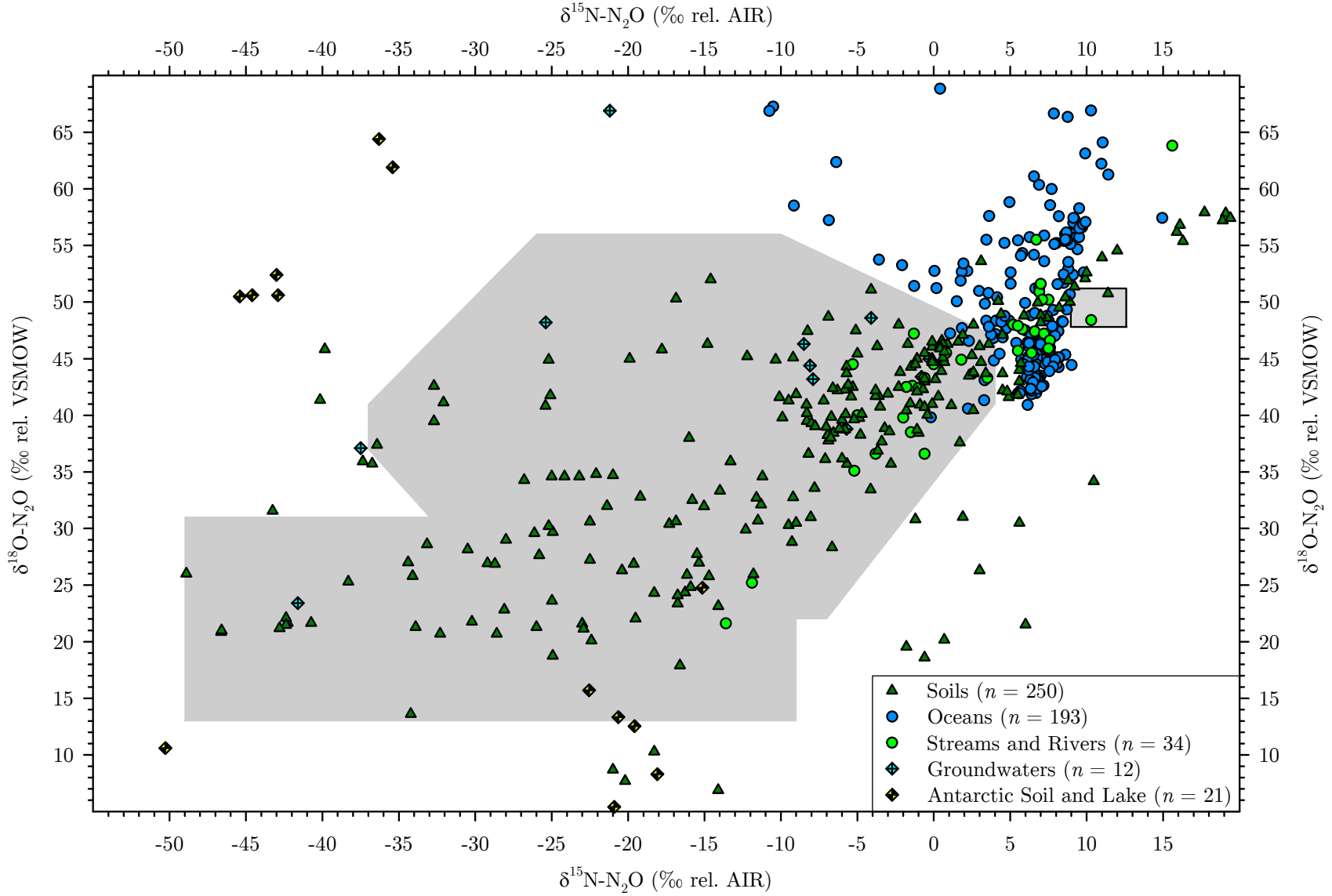


Figure 7.9b. A compilation of published δ^{18}O-N_2O and δ^{15}N-N_2O *in situ* data published in the peer-reviewed literature. This figure is identical to Figure 7.9a, except more detail can be seen because the scale on this figure is more resolved.

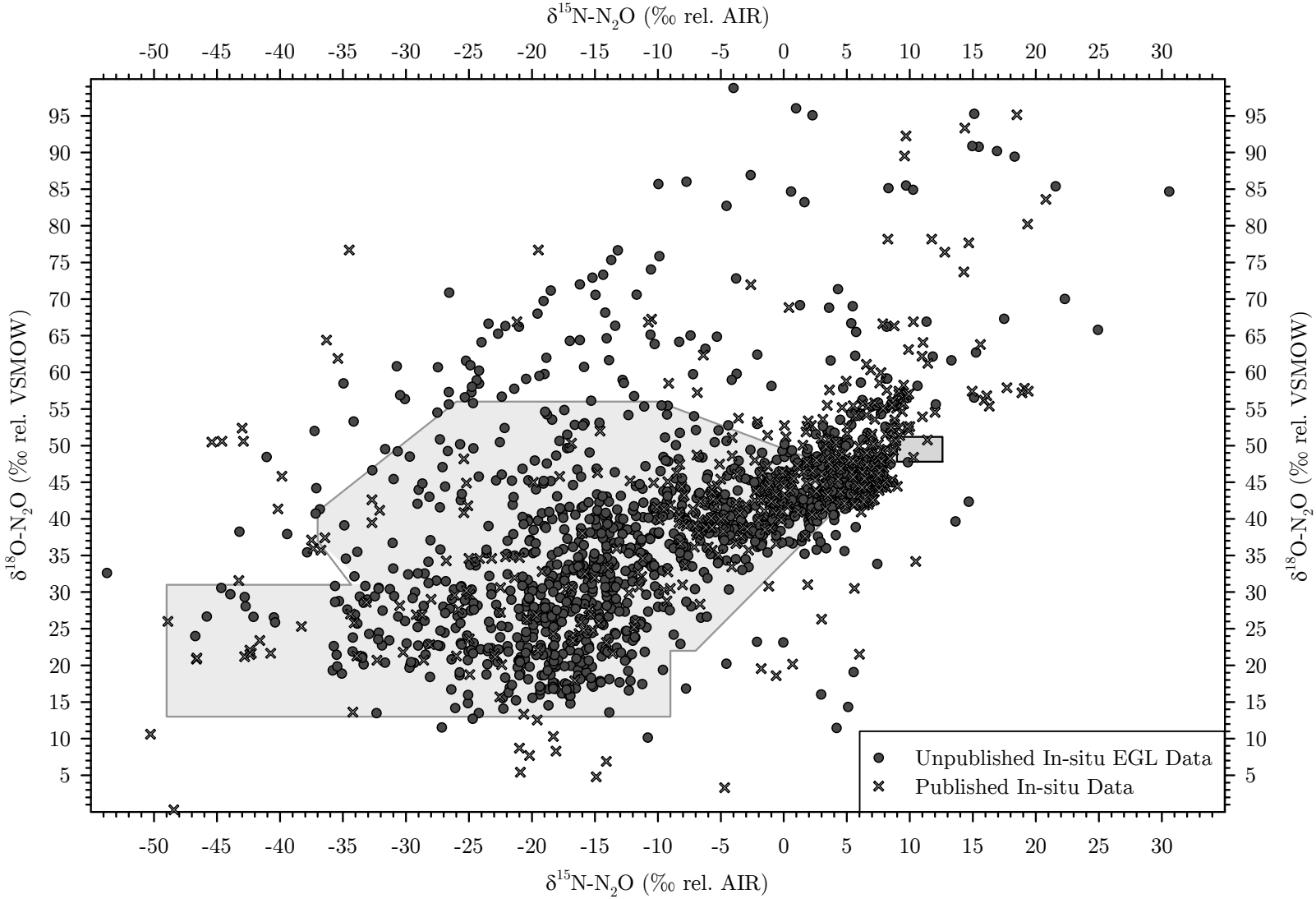


Figure 7.10a. A compilation of published and unpublished *in situ* δ^{18}O-N_2O and δ^{15}N-N_2O data shown in the peer-reviewed literature (n = 520) or collected by members of the Environmental Geochemistry Lab, University of Waterloo, Waterloo, ON (n = 1180). This figure is an assemblage of all the data shown in Figures 7.8-7.9 (n = 1700). The light-grey polygon bounds the range of N_2O measured or modelled in this thesis.

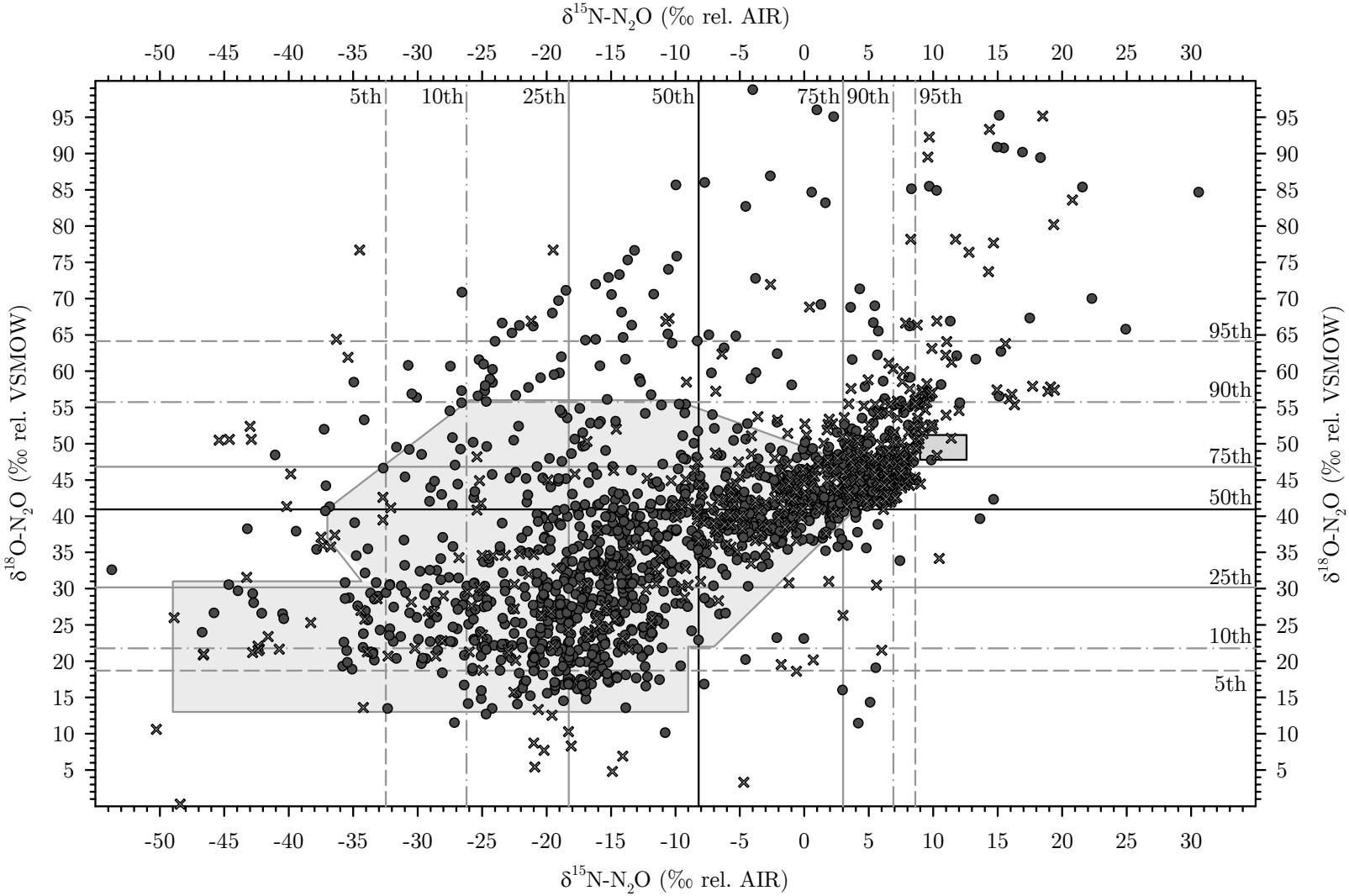


Figure 7.10b. A compilation of published ("ex"s) and unpublished (circles) *in situ* δ^{18}O-N_2O and δ^{15}N-N_2O values shown in the peer-reviewed literature ($n = 520$) or collected by members of the Environmental Geochemistry Lab, University of Waterloo, Waterloo, ON ($n = 1180$). The light-grey polygon bounds the range of N_2O measured or modelled in this thesis. The median (50^{th} percentile) δ^{15}N and δ^{18}O-N_2O values are shown as solid black lines, followed by lines that represent the $25^{th}/75^{th}$ percentiles (solid grey lines), and the $10^{th}/90^{th}$ and $5^{th}/95^{th}$ percentiles (dashed lines).

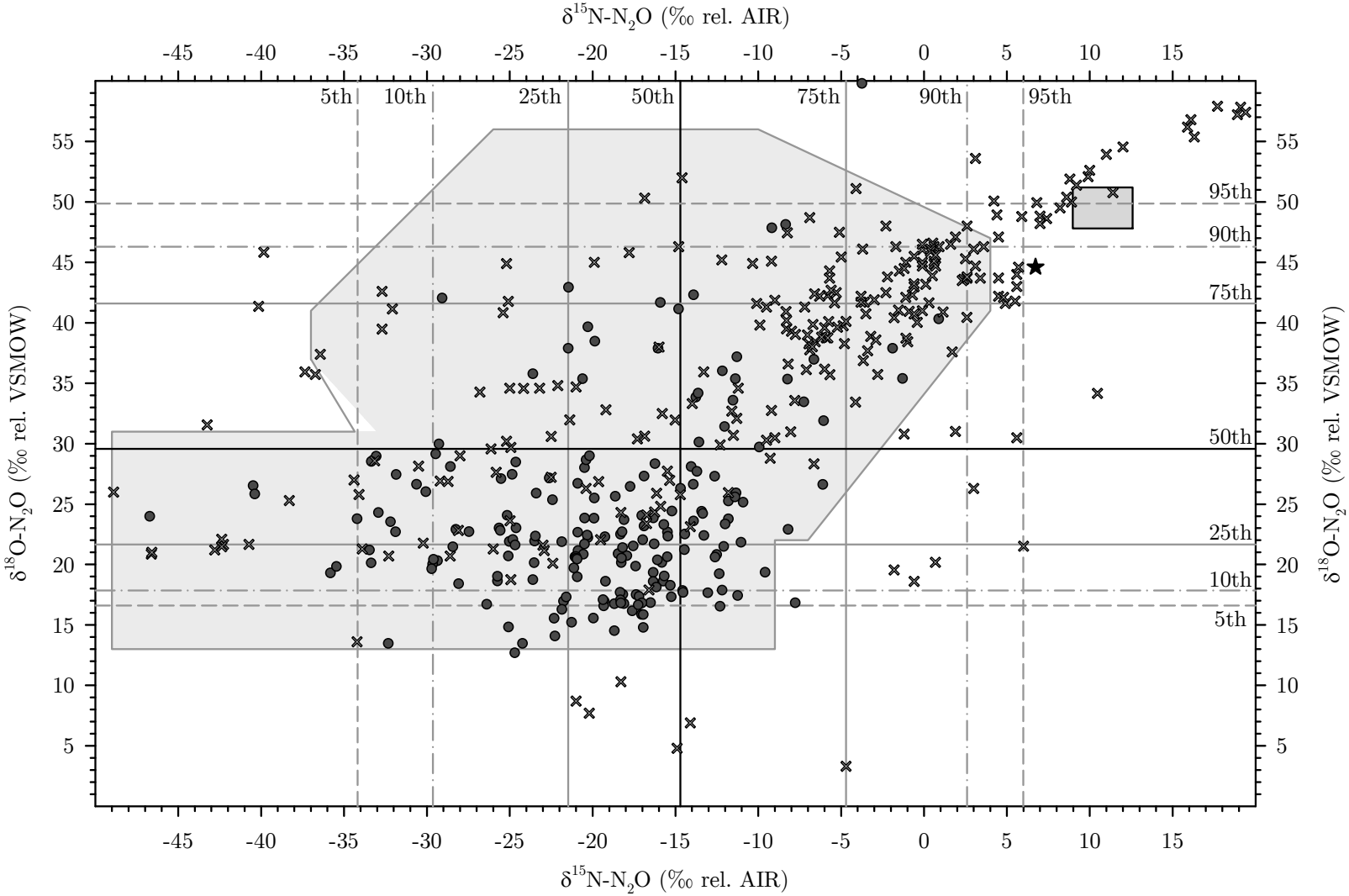


Figure 7.10c. A compilation of *in situ* soil δ^{18}O-N_2O and δ^{15}N-N_2O data shown in the peer-reviewed literature ($n = 250$; "ex"s) or collected by members of the Environmental Geochemistry Lab, University of Waterloo, Waterloo, ON ($n = 195$; circles). The light-grey polygon bounds the range of N_2O measured or modelled in this thesis. The median (50^{th} percentile) δ^{15}N and δ^{18}O-N_2O values are shown as solid black lines, followed by lines that represent the $25^{th}/75^{th}$ percentiles (solid grey lines), and the $10^{th}/90^{th}$ and $5^{th}/95^{th}$ percentiles (dashed lines).

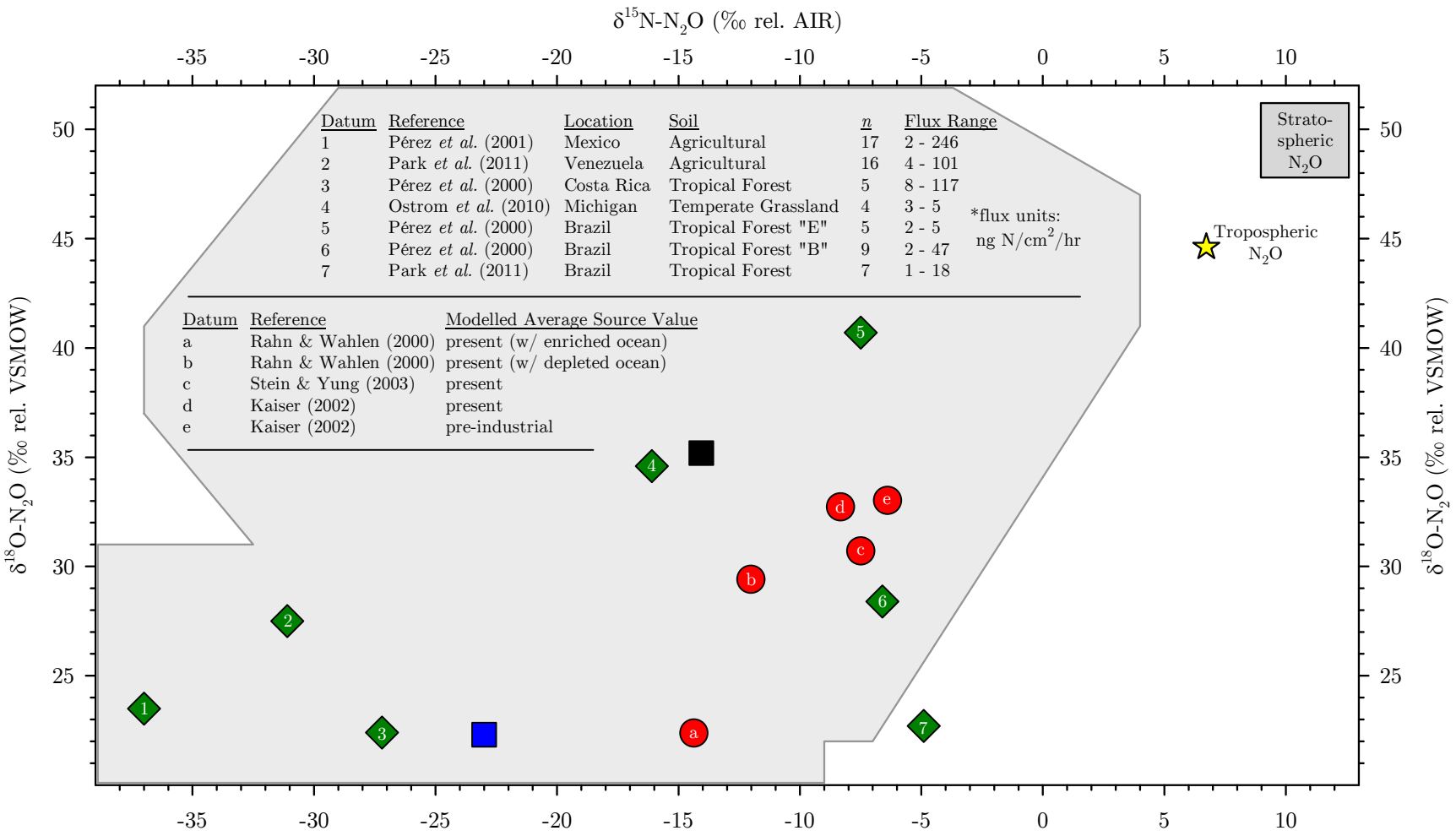


Figure 7.10d. The flux-weighted isotopic compositions of soil-emitted N_2O from several field sites throughout the Americas (green diamonds), and various modelled estimates of the average terrestrial N_2O source (red circles) derived from isotope mass-balance calculations of oceanic sources and tropospheric/stratospheric N_2O pools. The concentration-weighted average $\delta^{15}N$- and $\delta^{18}O$-N_2O of soil gas from the Strawberry Creek (blue sqaure) and of groundwater from the Black Brook Watershed (black square) is also shown for comparison (blue square). The light-grey polygon bounds the range of N_2O measured or modelled in this thesis. Note: N_2O fluxes are, by nature, highly episodic, so the flux-weighted average values are dependent on the sampling frequency and the magnitude of each flux measurement.

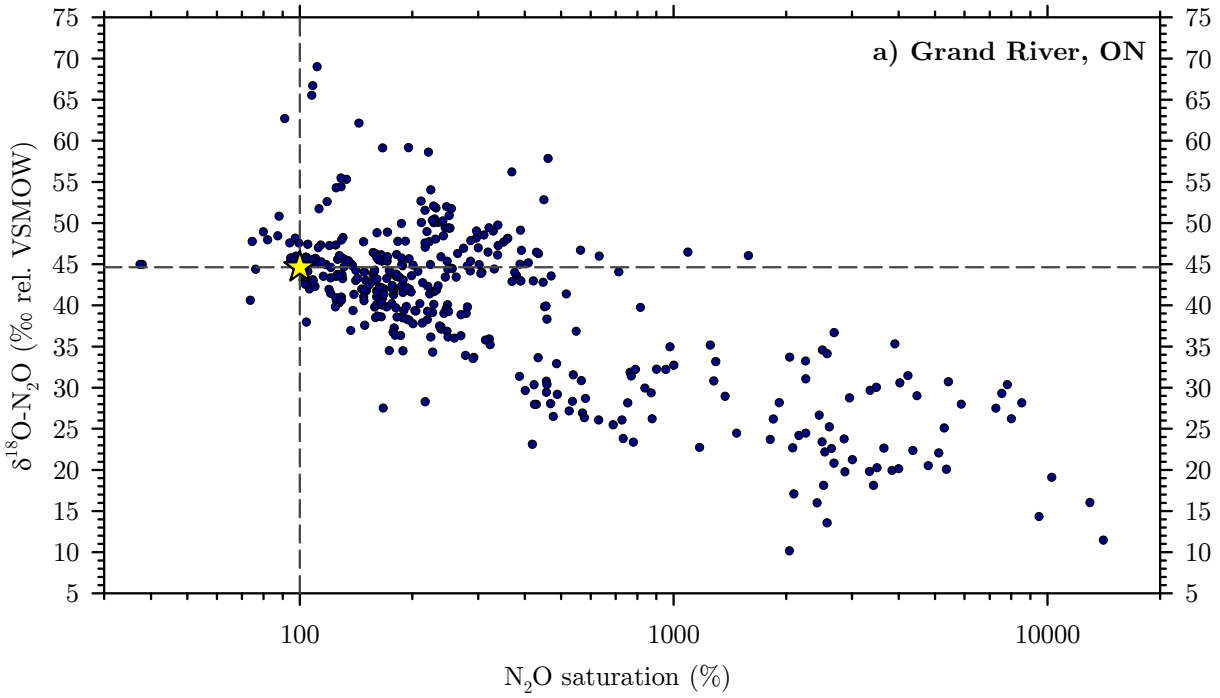


Figure 7.11a. As the concentration of N_2O in the Grand River approaches 100% atmospheric saturation, gas exchange with tropospheric N_2O (yellow star symbol; horizontal dashed line) becomes an important control, effectively masking the isotope ratios of biologically-produced N_2O. At 100% saturation they pass very close to the $\delta^{18}O$ value of tropospheric N_2O (+44.6‰; Kaiser *et al.* 2003).

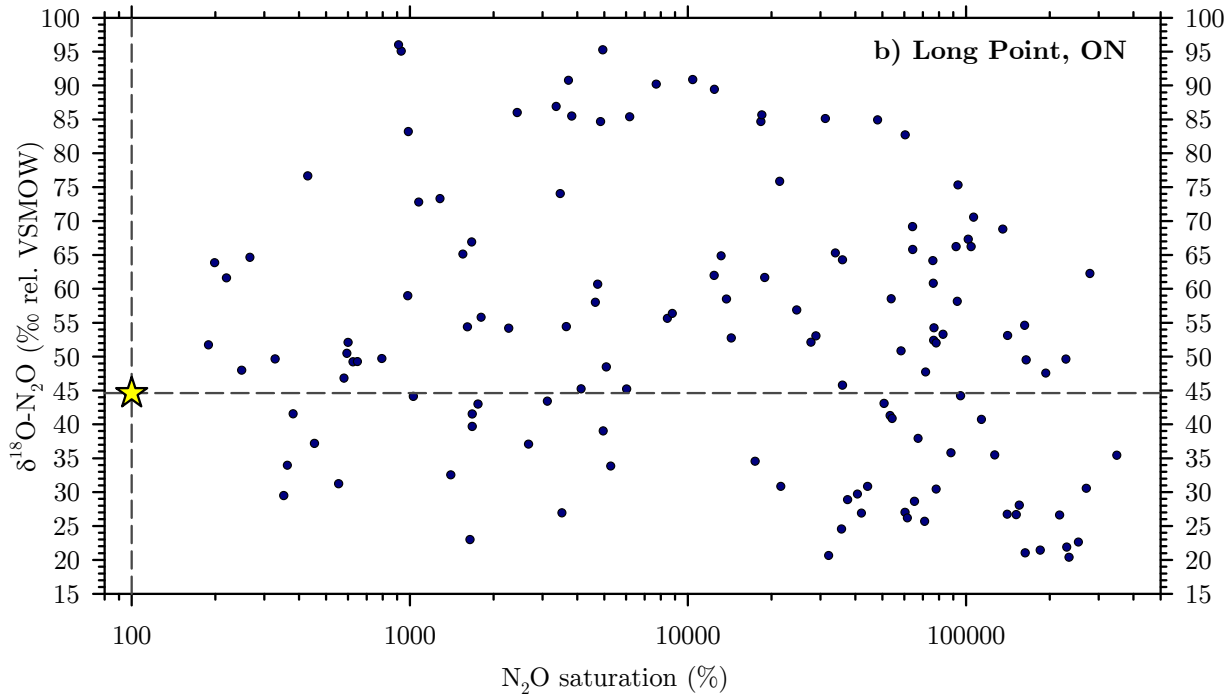


Figure 7.11b. In contrast, N_2O isotope ratios from Long Point are unaffected by gas exchange because groundwater is not in contact with the atmosphere. The N_2O isotope ratios at Long Point are controlled by nitrification, denitrification, and consumption processes.

UC PRESS AUTHORIZATION AGREEMENT (CHAPTER 1)

Subject: Re: Permission Request from website - 3/26/2011 07:34:02
From: Rebecca Wells <rebecca.wells@ucpress.edu>
Date: Mon, 28 Mar 2011 10:15:32 -0700
To: dsnider@uwaterloo.ca

28 March 2011

Dear David Snider:

Thank you for your permissions inquiry. Due to the scholarly and non-profit nature of your work, UC Press is pleased to authorize non-exclusive, one time permission for reprint rights to the material you have requested free of charge.

Permission is hereby granted to include the abstract of one article ("The Nitrogen Cascade," by James N. Galloway, John D. Aber, Jan Willem Erisman, Sybil P. Seitzinger, Robert W. Howarth, Ellis B. Cowling and B. Jack Cosby. *BioScience.* Vol. 53, No. 4 (Apr., 2003) (pp. 341-356)) in your PhD thesis, as specified in your request.

This authorization is contingent on the following terms and conditions:

1. The reproduction of this material is for the professional use cited only, and only to be used on a non-profit basis as detailed in your request.

2. The following standard acknowledgment must be included with your forthcoming work:
James N. Galloway, John D. Aber, Jan Willem Erisman, Sybil P. Seitzinger, Robert W. Howarth, Ellis B. Cowling and B. Jack Cosby, "The Nitrogen Cascade," in *BioScience* vol. 53, no. 4 (April 2003), pp. 341-356. (c) 2003 by The American Institute of Biological Sciences. Published by the University of California Press.

3. Your reproduction must not be libelous or defamatory, obscene, unlawful, or improper in any way that will invade in the proprietary or personal rights of any other person.

4. This permission is effective for a period of three (3) years.

This authorization covers your use of only the material in this book which has been copyrighted by the Regents of the University of California, University of California Press. You will need to secure additional permission for any other material, text or illustrations credited to other sources.

Use beyond the terms and conditions of this email will require a resecuring of permission.

This authorization will not be considered valid until this email is signed and returned to my attention (via post) at the address below within thirty (30) days.



AGREED AND ACCEPTED: _____

DATE: 28-March-2011

Please do not hesitate to contact me if you have any questions or concerns.

Best wishes with your project.

Sincerely,

Rebecca Wells
Permissions Administrator
University of California Press
2120 Berkeley Way
Berkeley, CA 94704
Phone: (510) 643-9795
Fax: (510) 643-7127

On Sat, Mar 26, 2011 at 7:34 AM, UC Press Web Contact Form <generalmailbox@ucpress.edu> wrote:

> Subject: Permission Request from website - 3/26/2011 07:34:02
> Name: David Snider
> Email Address: dsnider@uwaterloo.ca
> Comments:
> Dear University of California Press,
>
> I would like to reproduce the complete abstract of the following article: The Nitrogen Cascade, by James N. Galloway, John D. Aber, Jan Willem Erisman, Sybil P. Seitzinger, Robert W. Howarth, Ellis B. Cowling and B. Jack Cosby. BioScience. Vol. 53, No. 4 (Apr., 2003) (pp. 341-356).
>
> This excerpt will be included in a chapter of my PhD thesis, which will (eventually) be available electronically and in print.
>
> Do I have permission to reproduce this text if I properly cite the article and indicate that the material is copyright protected?
>
> Sincerely,
>
> David Snider
>
> University of Waterloo
> Department of Earth & Environmental Sciences
> 200 University Ave. W.
> Waterloo, Ontario N2L 3G1
> Canada
>
> ==========

ELSEVIER LICENSE
TERMS AND CONDITIONS

This is a License Agreement between David M Snider ("You") and Elsevier ("Elsevier") provided by Copyright Clearance Center ("CCC"). The license consists of your order details, the terms and conditions provided by Elsevier, and the payment terms and conditions.

Supplier	Elsevier Limited The Boulevard,Langford Lane Kidlington,Oxford,OX5 1GB,UK
Registered Company Number	1982084
Customer name	David M Snider
Customer address	University of Waterloo
	Waterloo, ON N2L 3G1
License number	2331981030124
License date	Dec 18, 2009
Licensed content publisher	Elsevier
Licensed content publication	Geochimica et Cosmochimica Acta
Licensed content title	$^{15}N/^{14}N$ and $^{18}O/^{16}O$ stable isotope ratios of nitrous oxide produced during denitrification in temperate forest soils
Licensed content author	David M. Snider, Sherry L. Schiff, John Spoelstra
Licensed content date	15 February 2009
Start Page	877
End Page	888
Type of Use	Thesis / Dissertation
Portion	Full article
Format	Both print and electronic
Are you the author of this Elsevier article?	Yes
Elsevier VAT number	GB 494 6272 12
Terms and Conditions	

INTRODUCTION

1. The publisher for this copyrighted material is Elsevier. By clicking "accept" in connection with completing this licensing transaction, you agree that the following terms and conditions apply to this transaction (along with the Billing and Payment terms and conditions established by Copyright Clearance Center, Inc. ("CCC"), at the time that you opened your Rightslink account and that are available at any time at http://myaccount.copyright.com).

GENERAL TERMS

2. Elsevier hereby grants you permission to reproduce the aforementioned material subject to the terms and conditions indicated.

3. Acknowledgement: If any part of the material to be used (for example, figures) has appeared in our publication with credit or acknowledgement to another source, permission must also be sought from that source. If such permission is not obtained then that material may not be included in your publication/copies. Suitable acknowledgement to the source must be made, either as a footnote or in a reference list at the end of your publication, as follows:

"Reprinted from Publication title, Vol /edition number, Author(s), Title of article / title of chapter, Pages No., Copyright (Year), with permission from Elsevier [OR APPLICABLE SOCIETY COPYRIGHT OWNER]." Also Lancet special credit - "Reprinted from The Lancet, Vol. number, Author(s), Title of article, Pages No.,

Copyright (Year), with permission from Elsevier."

4. Reproduction of this material is confined to the purpose and/or media for which permission is hereby given.

5. Altering/Modifying Material: Not Permitted. However figures and illustrations may be altered/adapted minimally to serve your work. Any other abbreviations, additions, deletions and/or any other alterations shall be made only with prior written authorization of Elsevier Ltd. (Please contact Elsevier at permissions@elsevier.com)

6. If the permission fee for the requested use of our material is waived in this instance, please be advised that your future requests for Elsevier materials may attract a fee.

7. Reservation of Rights: Publisher reserves all rights not specifically granted in the combination of (i) the license details provided by you and accepted in the course of this licensing transaction, (ii) these terms and conditions and (iii) CCC's Billing and Payment terms and conditions.

8. License Contingent Upon Payment: While you may exercise the rights licensed immediately upon issuance of the license at the end of the licensing process for the transaction, provided that you have disclosed complete and accurate details of your proposed use, no license is finally effective unless and until full payment is received from you (either by publisher or by CCC) as provided in CCC's Billing and Payment terms and conditions. If full payment is not received on a timely basis, then any license preliminarily granted shall be deemed automatically revoked and shall be void as if never granted. Further, in the event that you breach any of these terms and conditions or any of CCC's Billing and Payment terms and conditions, the license is automatically revoked and shall be void as if never granted. Use of materials as described in a revoked license, as well as any use of the materials beyond the scope of an unrevoked license, may constitute copyright infringement and publisher reserves the right to take any and all action to protect its copyright in the materials.

9. Warranties: Publisher makes no representations or warranties with respect to the licensed material.

10. Indemnity: You hereby indemnify and agree to hold harmless publisher and CCC, and their respective officers, directors, employees and agents, from and against any and all claims arising out of your use of the licensed material other than as specifically authorized pursuant to this license.

11. No Transfer of License: This license is personal to you and may not be sublicensed, assigned, or transferred by you to any other person without publisher's written permission.

12. No Amendment Except in Writing: This license may not be amended except in a writing signed by both parties (or, in the case of publisher, by CCC on publisher's behalf).

13. Objection to Contrary Terms: Publisher hereby objects to any terms contained in any purchase order, acknowledgment, check endorsement or other writing prepared by you, which terms are inconsistent with these terms and conditions or CCC's Billing and Payment terms and conditions. These terms and conditions, together with CCC's Billing and Payment terms and conditions (which are incorporated herein), comprise the entire agreement between you and publisher (and CCC) concerning this licensing transaction. In the event of any conflict between your obligations established by these terms and conditions and those established by CCC's Billing and Payment terms and conditions, these terms and conditions shall control.

14. Revocation: Elsevier or Copyright Clearance Center may deny the permissions described in this License at their sole discretion, for any reason or no reason, with a full refund payable to you. Notice of such denial will be made using the contact information provided by you. Failure to receive such notice will not alter or invalidate the denial. In no event will Elsevier or Copyright Clearance Center be responsible or liable for any costs, expenses or damage incurred by you as a result of a denial of your permission request, other than a refund of the amount(s) paid by you to Elsevier and/or Copyright Clearance Center for denied permissions.

LIMITED LICENSE

The following terms and conditions apply only to specific license types:

20. **Thesis/Dissertation**: If your license is for use in a thesis/dissertation your thesis may be submitted to your institution in either print or electronic form. Should your thesis be published commercially, please reapply for permission. These requirements include permission for the Library and Archives of Canada to supply single copies, on demand, of the complete thesis and include permission for UMI to supply single copies, on demand, of the complete thesis. Should your thesis be published commercially, please reapply for permission.

21. **Other Conditions**: None

COAUTHOR'S AUTHORIZATION OF USE

We, the undersigned, as coauthors of Snider *et al.* (2009) [Snider DM, Schiff SL, Spoelstra J (2009) $^{15}N/^{14}N$ and $^{18}O/^{16}O$ stable isotope ratios of nitrous oxide produced during denitrification in temperate forest soils. *Geochimica et Cosmochimica Acta*, **73(4)**, 877–888. doi:10.1016/j.gca.2008.11.004] permit David Snider to re-use this material (in its entirety or in part) in his PhD thesis ["A characterization of the controls of the nitrogen and oxygen isotope ratios of biologically-produced nitrous oxide and nitrate in soils"].

Furthermore, we acknowledge that David Snider has given Library and Archives Canada a non-exclusive, royalty-free license to use his PhD thesis for the full term of copyright protection so that Library and Archives Canada may carry out its mandate as worded in the "Theses Non-Exclusive License" (form NL/BN 59/02).

We hereby grant Library and Archives Canada the same permissions [as it relates to Snider *et al.* (2009)] to reproduce, publish, archive, preserve, conserve, communicate to the public by telecommunication or on the Internet, loan, distribute and sell David Snider's thesis worldwide, for commercial or non-commercial purposes, in microform, paper, electronic and/or any other formats.

We disclaim any responsibility for any use Library and Archives Canada makes of items owned by third parties without their permission.

Coauthor(s)		Date (dd/mm/yyyy)
Sherry L. Schiff	signatures removed for privacy purposes	20 June 2011
John Spoelstra		20-Jun-2011

AMERICAN CHEMICAL SOCIETY LICENSE TERMS AND CONDITIONS

Mar 12, 2011

This is a License Agreement between David M Snider ("You") and American Chemical Society ("American Chemical Society") provided by Copyright Clearance Center ("CCC"). The license consists of your order details, the terms and conditions provided by American Chemical Society, and the payment terms and conditions.

All payments must be made in full to CCC. For payment instructions, please see information listed at the bottom of this form.

License Number	2626671411566
License Date	Mar 12, 2011
Licensed content publisher	American Chemical Society
Licensed content publication	Environmental Science & Technology
Licensed content title	Stable Oxygen Isotope Ratios of Nitrate Produced from Nitrification: 18O-Labeled Water Incubations of Agricultural and Temperate Forest Soils
Licensed content author	David M. Snider et al.
Licensed content date	Jul 1, 2010
Volume number	44
Issue number	14
Type of Use	Thesis/Dissertation
Requestor type	Not specified
Format	Print and Electronic
Portion	50% or more of original article
Author of this ACS article	Yes
Order reference number	
Title of the thesis / dissertation	A characterization of the controls of the nitrogen and oxygen isotope ratios of biologically-produced nitrous oxide and nitrate in soils
Expected completion date	May 2011
Estimated size(pages)	300
Billing Type	Invoice
Billing Address	University of Waterloo Dept. of Earth & Environmental Sciences Waterloo, ON N2L 3G1 Canada
Customer reference info	
Total	0.00 USD
Terms and Conditions	

Thesis/Dissertation

ACS / RIGHTSLINK TERMS & CONDITIONS
THESIS/DISSERTATION

INTRODUCTION
The publisher for this copyrighted material is the American Chemical Society. By clicking "accept" in connection with completing this licensing transaction, you agree that the following terms and conditions apply to this transaction (along with the Billing and Payment terms and conditions established by Copyright Clearance Center, Inc. ("CCC"), at the time that you opened your Rightslink account and that are available at any time at <http://myaccount.copyright.com>).

LIMITED LICENSE
Publisher hereby grants to you a non-exclusive license to use this material. Licenses are for one-time use only with a maximum distribution equal to the number that you identified in the licensing process.

GEOGRAPHIC RIGHTS: SCOPE
Licenses may be exercised anywhere in the world.

RESERVATION OF RIGHTS
Publisher reserves all rights not specifically granted in the combination of (i) the license details provided by you and accepted in the course of this licensing transaction, (ii) these terms and conditions and (iii) CCC's Billing and Payment terms and conditions.

PORTION RIGHTS STATEMENT: DISCLAIMER
If you seek to reuse a portion from an ACS publication, it is your responsibility to examine each portion as published to determine whether a credit to, or copyright notice of, a third party owner was published adjacent to the item. You may only obtain permission via Rightslink to use material owned by ACS. Permission to use any material published in an ACS publication, journal, or article which is reprinted with permission of a third party must be obtained from the third party owner. ACS disclaims any responsibility for any use you make of items owned by third parties without their permission.

REVOCATION
The American Chemical Society reserves the right to revoke a license for any reason, including but not limited to advertising and promotional uses of ACS content, third party usage, and incorrect figure source attribution.

LICENSE CONTINGENT ON PAYMENT
While you may exercise the rights licensed immediately upon issuance of the license at the end of the licensing process for the transaction, provided that you have disclosed complete and accurate details of your proposed use, no license is finally effective unless and until full payment is received from you (by CCC) as provided in CCC's Billing and Payment terms and conditions. If full payment is not received on a timely basis, then any license preliminarily granted shall be deemed automatically revoked and shall be void as if never granted. Further, in the event that you breach any of these terms and conditions or any of CCC's Billing and Payment terms and conditions, the license is automatically revoked and shall be void as if never granted. Use of materials as described in a revoked license, as well as any use of the materials beyond the scope of an unrevoked license, may constitute copyright infringement and publisher reserves the right to take any and all action to protect its copyright in the materials.

COPYRIGHT NOTICE: DISCLAIMER
You must include the following copyright and permission notice in connection with any reproduction of the licensed material: "Reprinted (“Adapted” or “in part”) with permission from REFERENCE CITATION. Copyright YEAR American Chemical Society."

WARRANTIES: NONE
Publisher makes no representations or warranties with respect to the licensed material.

INDEMNITY
You hereby indemnify and agree to hold harmless publisher and CCC, and their respective officers, directors, employees and agents, from and against any and all claims arising out of your use of the licensed material other than as specifically authorized pursuant to this license.

NO TRANSFER OF LICENSE
This license is personal to you or your publisher and may not be sublicensed, assigned, or transferred by you to any other person without publisher's written permission.

NO AMENDMENT EXCEPT IN WRITING
This license may not be amended except in a writing signed by both parties (or, in the case of publisher, by CCC on publisher's behalf).

OBJECTION TO CONTRARY TERMS
Publisher hereby objects to any terms contained in any purchase order, acknowledgment, check endorsement or other writing prepared by you, which terms are inconsistent with these terms and conditions or CCC's Billing and Payment terms and conditions. These terms and conditions, together with CCC's Billing and Payment terms and conditions (which are incorporated herein), comprise the entire agreement between you and publisher (and CCC) concerning this licensing transaction. In the event of any conflict between your obligations established by these terms and conditions and those established by CCC's Billing and Payment terms and conditions, these terms and conditions shall control.

JURISDICTION
This license transaction shall be governed by and construed in accordance with the laws of the District of Columbia. You hereby agree to submit to the jurisdiction of the courts located in the District of Columbia for purposes of resolving any disputes that may arise in connection with this licensing transaction.

THESES/DISSERTATION TERMS
Regarding your request for permission to include **your** paper(s) or portions of text from **your** paper(s) in your thesis/dissertation, permission is now automatically granted; please pay special attention to the **implications** paragraph below. The Copyright Subcommittee of the Joint Board/Council Committees on Publications approved the following:

Copyright permission for published and submitted material from theses and dissertations
ACS extends blanket permission to students to include in their theses and dissertations their own articles, or portions thereof, that have been published in ACS journals or submitted to ACS journals for publication, provided that the ACS copyright credit line is noted on the appropriate page(s).

Publishing **implications** of electronic publication of theses and dissertation material
Students and their mentors should be aware that posting of theses and dissertation material on the Web prior to submission of material from that thesis or dissertation to an ACS journal may affect publication in that journal. Whether Web posting is considered prior publication may be evaluated on a case-by-case basis by the journal's editor. If an ACS journal editor considers Web posting to be "prior publication", the paper will not be accepted for publication in that journal. If you intend to submit your unpublished paper to ACS for publication, check with the appropriate editor prior to posting your manuscript electronically.

Reuse/Republication of the Entire Work in Theses or Collections: Authors may reuse all or part of the Submitted, Accepted or Published Work in a thesis or dissertation that the author writes and is required to submit to satisfy the criteria of degree-granting institutions. Such reuse is permitted subject to the ACS' "Ethical Guidelines to Publication of Chemical Research" (http://pubs.acs.org/page/policy/ethics/index.html); the author should secure written confirmation (via letter or email) from the respective ACS journal editor(s) to avoid potential conflicts with journal prior publication*/embargo policies. Appropriate citation of the Published Work must be made. If the thesis or dissertation to be published is in electronic format, a direct link to the Published Work must also be included using the ACS Articles on Request author-directed link - see http://pubs.acs.org/page/policy/articlesonrequest/index.html

* Prior publication policies of ACS journals are posted on the ACS website at http://pubs.acs.org/page/policy/prior/index.html

If your paper has not yet been published by ACS, please print the following credit line on the first page of your article: "Reproduced (or 'Reproduced in part') with permission from [JOURNAL NAME], in press (or 'submitted for publication'). Unpublished work copyright [CURRENT YEAR] American Chemical Society." Include appropriate information.

If your paper has already been published by ACS and you want to include the text or portions of the text in your thesis/dissertation in **print or microfilm formats**, please print the ACS copyright credit line on the first page of your article: "Reproduced (or 'Reproduced in part') with permission from [FULL REFERENCE CITATION.] Copyright [YEAR] American Chemical Society." Include appropriate information.

Submission to a Dissertation Distributor: If you plan to submit your thesis to UMI or to another dissertation distributor, you should not include the unpublished ACS paper in your thesis if the thesis will be disseminated electronically, until ACS has published your paper. After publication of the paper by ACS, you may release the entire thesis (**not the individual ACS article by itself**) for electronic dissemination through the distributor; ACS's copyright credit line should be printed on the first page of the ACS paper.

v1.2

COAUTHOR'S AUTHORIZATION OF USE

We, the undersigned, as coauthors of Snider *et al.* (2010) [Snider DM, Spoelstra J, Schiff SL, Venkiteswaran JJ (2010) Stable oxygen isotope ratios of nitrate produced from nitrification: ^{18}O-labeled water incubations of agricultural and temperate forest soils. *Environmental Science and Technology*, **44(14)**, 5358–5364. doi:10.1021/es1002567] permit David Snider to re-use this material (in its entirety or in part) in his PhD thesis ["A characterization of the controls of the nitrogen and oxygen isotope ratios of biologically-produced nitrous oxide and nitrate in soils"].

Furthermore, we acknowledge that David Snider has given Library and Archives Canada a non-exclusive, royalty-free license to use his PhD thesis for the full term of copyright protection so that Library and Archives Canada may carry out its mandate as worded in the "Theses Non-Exclusive License" (form NL/BN 59/02).

We hereby grant Library and Archives Canada the same permissions [as it relates to Snider *et al.* (2010)] to reproduce, publish, archive, preserve, conserve, communicate to the public by telecommunication or on the Internet, loan, distribute and sell David Snider's thesis worldwide, for commercial or non-commercial purposes, in microform, paper, electronic and/or any other formats.

We disclaim any responsibility for any use Library and Archives Canada makes of items owned by third parties without their permission.

Coauthor(s)	Date (dd/mm/yyyy)
John Spoelstra	20-Jun-2011
Sherry L. Schiff	20 Jun 2011
Jason J. Venkiteswaran	05-July-2011.

signatures removed for privacy purposes

References

Aber J, McDowell W, Nadelhoffer K, Magill A, Berntson G, Kamakea M, McNulty S, Currie W, Rustad L, Fernandez I (1998) Nitrogen saturation in temperate forest ecosystems: hypothesis revisited. *BioScience*, **48**, 921–934.

Aber JD, Nadelhoffer KJ, Steudler P, Melillo JM (1989) Nitrogen saturation in northern forest ecosystems. *BioScience*, **39**, 378–386.

Agriculture and Agri-Food Canada. The Canadian System of Soil Classification, 3rd edition. Publication 1646, 187 pp.

Aleem MIH, Hoch GE, Varner JE (1965) Water as the source of oxidant and reductant in bacterial chemosynthesis. *Biochemistry*, **54**, 869–873.

Andersson KK, Hooper AB (1983) O_2 and H_2O are each the source of one O in NO_2^- produced from NH_3 by *Nitrosomonas*: ^{15}N-NMR evidence. *FEBS Letters*, **164**, 236–240.

Andersson KK, Philson SB, Hooper AB (1982) ^{18}O isotope shift in ^{15}N NMR analysis of biological N-oxidations: H_2O-NO_2^- exchange in the ammonia-oxidizing bacterium *Nitrosomonas*. *Proceedings of the National Academy of Sciences, USA*, **79**, 5871–5875.

Anisfeld SC, Barnes RT, Altabet MA, Wu T (2007) Isotopic apportionment of atmospheric and sewage nitrogen sources in two Connecticut rivers. *Environmental Science and Technology*, **41**, 6363–6369.

Aravena R, Evans ML, Cherry JA (1993) Stable isotopes of oxygen and nitrogen in source identification of nitrate from septic systems. *Ground Water*, **31**, 180–186.

Aravena R, Mayer B (2010) Isotopes and processes in the nitrogen and sulfur cycles. *In*: Environmental Isotopes in Biodegradation and Bioremediation (eds. Aelion M, Aravena R, Hunkeler D, Höhener P). CRC Press, Taylor and Francis Group, doi:10.1201 /9781420012613.ch7

Aravena R, Robertson W (1998) Use of multiple isotope tracers to evaluate denitrification in ground water: study of nitrate from a large-flux septic system plume. Ground Water, 36, 975–982.

Arp DJ, Sayavedra-Soto LA, Hommes NG (2002) Molecular biology and biochemistry of ammonia oxidation by *Nitrosomonas europaea*. *Archives of Microbiology*, **178**, 250–255.

Arp DJ, Stein LY (2003) Metabolism of inorganic N compounds by ammonia-oxidizing bacteria. *Critical Reviews in Biochemistry and Molecular Biology*, **38**, 471–495.

ASTM International. ASTM Standard D4972-01, 2007. Standard Test Method for pH of Soils; ASTM Int.: West Conshohocken, PA, 2007. DOI: 10.1520/D4972-01R07. Available at: http://www.astm.org.

Averill BA (1996) Dissimilatory nitrite and nitric oxide reductases. *Chemical Reviews*, **96**, 2951–2964.

Barford CC, Montoya JP, Altabet MA, Mitchell R (1999) Steady-state nitrogen isotope effects of N_2 and N_2O production in *Paracoccus denitrificans*. *Applied and Environmental Microbiology*, **65**, 989–994.

Barton L, McLay CDA, Schipper LA, Smith CT (1999) Annual denitrification rates in agricultural and forest soils: a review. *Australian Journal of Soil Research*, **37**, 1073–1093.

Bauer B, Reynolds M (2008) Recovering data from scanned graphs: performance of Frantz's g3data software. *Behaviour Research Methods*, **40**, 858–868.

Bédard C, Knowles R (1989) Physiology, biochemistry, and specific inhibitors of CH_4, NH_4^+, and CO oxidation by methanotrophs and nitrifiers. *Microbiological Reviews*, **53**, 68–84.

Bedard-Haughn A, Van Groenigen J, Van Kessel C (2003) Tracing ^{15}N through landscapes: potential uses and precautions. *Journal of Hydrology*, **272**, 175–190.

Bergstermann A, Cárdenas L, Bol R, Gilliam L, Goulding K, Meijide A, Scholefield D, Vallejo A, Well R (2011) Effect of antecedent soil moisture conditions on emissions and isotopologue distribution of N_2O during denitrification. *Soil Biology and Biochemistry*, **43**, 240–250.

Birks SJ, Edwards TWD, Gibson JJ, Michel FA, Drimmie RJ, MacTavish D (2003) Canadian Network for Isotopes in Precipitation. University of Waterloo/Meteorological Service of Canada. Available at: http://www.science.uwaterloo.ca/~twdedwar/cnip/cniphome.html.

Blackmer AM, Bremner JM (1977) Nitrogen Isotope Discrimination in Denitrification of Nitrate in Soils. *Soil Biology and Biochemistry*, **9**, 73–77.

Böhlke JK, Mroczkowski SJ, Coplen TB (2003) Oxygen isotopes in nitrate: new reference materials for ^{18}O:^{17}O:^{16}O measurements and observations on nitrate-water equilibration. *Rapid Communications in Mass Spectrometry*, **17**, 1835–1846.

Bol R, Toyoda S, Yamulki S, Hawkins JMB, Cardenas LM, Yoshida N (2003) Dual isotope and isotopomer ratios of N_2O emitted from a temperate grassland soil after fertiliser application. *Rapid Communications in Mass Spectrometry*, **17**, 2550–2556.

Bollman A, Conrad R (1997a) Enhancement by acetylene of the decomposition of nitric oxide in soil. *Soil Biology and Biochemistry*, **29**, 1057–1066.

Bollman A, Conrad R (1997b) Acetylene blockage technique leads to underestimation of denitrification rates in oxic soils due to scavenging of intermediate nitric oxide. *Soil Biology and Biochemistry*, **29**, 1067–1077.

Boontanon N, Ueda S, Kanatharana P, Wada E (2000) Intramolecular stable isotope ratios of N_2O in the tropical swamp forest in Thailand. *Naturwissenschaften*, **87**, 188–192.

Bothe H, Jost G, Schloter M, Ward BB, Witzel, K-P (2000) Molecular analysis of ammonia oxidation and denitrification in natural environments. *FEMS Microbiology Reviews*, **24**, 673–690.

Böttcher J, Strebel O, Voerkelius S, Schmidt H-L (1990) Using isotope fractionation of nitrate-nitrogen and nitrate-oxygen for evaluation of microbial denitrification in a sandy aquifer. *Journal of Hydrology*, **114**, 413–424.

Bremner JM (1997) Sources of nitrous oxide in soils. *Nutrient Cycling in Agroecosystems*, **49**, 7–16.

Brumme R (1995) Mechanisms of carbon and nutrient release and retention in beech forest gaps. III. Environmental regulation of soil respiration and nitrous oxide emissions along a microclimatic gradient. *Plant and Soil*, **169**, 593–600.

Buchwald C, Casciotti KL (2010) Oxygen isotopic fractionation and exchange during bacterial nitrite oxidation. *Limnology and Oceanography*, **55**, 1064–1074.

Burns DA, Kendall C (2002) Analysis of $\delta^{15}N$ and $\delta^{18}O$ to differentiate NO_3^- sources in runoff at two watersheds in the Catskill Mountains of New York. *Water Resourses Research*, **38 (1051)**, doi:10.1029/2001WR000292.

Butterbach-Bahl K, Willibald G, Papen H (2002) Soil core method for direct simultaneous determination of N_2 and N_2O emissions from forest soils. *Plant and Soil*, **240**, 105–116.

Canada Soil Survey Committee, Sub-Committee On Soil Classification (1978) *The Canadian system of soil classification.* Canadian Department of Agriculture Publication; 1646. p.164.

Cantera JJL, Stein LY (2007) Molecular diversity of nitrite reductase genes (*nirK*) in nitrifying bacteria. *Environmental Microbiology*, **9**, 765–776.

Casciotti K, Rahn T, Wahlen M (1997) Stable isotopes of N and O in nitrous oxide emissions from fertilized soil (abstract), *Eos, Transactions, American Geophysical Union*, 78(46), fall meeting supplement, F58.

Casciotti KL (2009) Inverse kinetic isotope fractionation during bacterial nitrite oxidation. *Geochimica et Cosmochimica Acta*, **73**, 2061–2076.

Casciotti KL, Böhlke JK, McIlvin MR, Mroczkowski SJ, Hannon JE (2007) Oxygen isotopes in nitrite: analysis, calibration, and equilibration. *Analytical Chemistry*, **79**, 2427–2436.

Casciotti KL, McIlvin M, Buchwald C (2010) Oxygen isotopic exchange and fractionation during bacterial ammonia oxidation. *Limnology and Oceanography*, **55**, 753–762.

Casciotti KL, Sigman DM, Galanter Hastings M, Böhlke JK, Hilkert A (2002) Measurement of the oxygen isotopic composition of nitrate in seawater and freshwater using the denitrifier method. *Analytical Chemistry*, **74**, 4905–4912.

Casciotti KL, Sigman DM, Ward BB (2003) Linking diversity and stable isotope fractionation in ammonia-oxidizing bacteria. *Geomicrobiology Journal*, **20**, 335–353.

Casciotti KL, Ward BB (2001) Dissimilatory nitrite reductase genes from autotrophic ammonia-oxidizing bacteria. *Applied and Environmental Microbiology*, **67**, 2213–2221.

Cerling TE, Solomon DK, Quade J, Bowman JR (1991) On the isotopic composition of carbon in soil carbon dioxide. Geochimica et Cosmochimica Acta, 55, 3403–3405.

Chang CY, Langston J, Riggs M, Campbell DH, Silva SR, Kendall C (1999) A method for nitrate collection for $\delta^{15}N$ and $\delta^{18}O$ analysis from waters with low nitrate concentrations. *Canadian Journal of Fisheries and Aquatic Sciences*, **56**, 1856–1864.

Chapuis-Lardy L, Wrage N, Metay A, Chotte JL, Bernoux M (2006) Soils, a sink for N_2O? A review. *Global Change Biology*, **12**, 1–17.

Chen D, Li Y, Grace P, Mosier AR (2008) N_2O emissions from agricultural lands: a synthesis of simulation approaches. *Plant and Soil*, **309**, 169–189.

Chipperfield M (2009) Nitrous oxide delays ozone recovery. *Nature Geoscience*, **2**, 742–743.

Clark I, Fritz P (1997) Environmental Isotopes in Hydrogeology. Chapter 1: The Environmental Isotopes. Lewis Publishers, Boca Raton

Colliver BB, Stephenson T (2000) Production of nitrogen oxide and dinitrogen oxide by autotrophic nitrifiers. *Biotechnology Advances*, **18**, 219–232.

Coplen TB, Böhlke JK, De Bievre P, Ding T, Holden NE, Hopple JA, Krouse HR, Lamberty A, Peiser HS, Revesz K, Rieder SE, Rosman KJR, Roth E, Taylor PDP, Vocke RD Jr., Xiao YK (2002) Isotope-abundance variations of selected elements. IUPAC Technical Report. *Pure and Applied Chemistry*, **74,** 1987–2017.

Cowell DW, Wickware GM (1983) Preliminary analysis of soil chemical and physical properties, Turkey Lakes Watershed, Algoma, Ontario. Turkey Lakes Watershed Unpublished Report No. 83–08, pp. 25.

Davidson EA (1992) Sources of nitric oxide and nitrous oxide following wetting of dry soil. *Soil Science Society of America Journal*, **56**, 95–102.

Davidson EA (1993) Soil water content and the ratio of nitrous oxide and nitric oxide emitted from soil. *In*: The Biogeochemistry of Global Change: Radiative Trace Gases (ed. Oremland RS). Chapman and Hall, New York.

De Boer W, Kowalchuk GA (2001) Nitrification in acid soils: micro-organisms and mechanisms. *Soil Biology and Biochemistry*, **33**, 853–866.

De Laeter JR, Böhlke JK, De Bièvre P, Hidaka H, Peiser HS, Rosman KJR, Taylor PDP (2003) Atomic weights of the elements: review 2000 (IUPAC Technical Report). *Pure and Applied Chemistry*, **75**, 683–800.

Delaune RD, Lindau CW, Sulaeman E, Jugsujinda A (1998) Nitrification and denitrification estimates in a Louisiana swamp forest soil as assessed by ^{15}N isotope dilution and direct gaseous measurements. *Water, Air, and Soil Pollution*, **106**, 149–161.

Delwiche CC, Steyn PL (1970) Nitrogen isotope fractionation in soils and microbial reactions. *Environmental Science and Technology*, **4**, 929–935.

Denman KL, Brasseur G, Chidthaisong A, Ciais P, Cox PM, Dickinson RE, Hauglustaine D, Heinze C, Holland E, Jacob D, Lohmann U, Ramachandran S, da Silva Dias PL, Wofsy SC, Zhang X (2007) Couplings between changes in the climate system and biogeochemistry. *In*: Climate Change 2007: The Physical Science Basis. Contribution of Working Group I to the Fourth Assessment Report of the Intergovernmental Panel on Climate Change (eds. Solomon S, Qin D, Manning M, Chen Z, Marquis M, Averyt KB, Tignor M, Miller HL). Cambridge University Press, Cambridge and New York.

DiSpirito AA, Hooper AB (1986) Oxygen exchange between nitrate molecules during nitrite oxidation by *Nitrobacter*. *The Journal of Biological Chemistry*, **261**, 10,534–10,537.

Dore JE, Popp BN, Karl DM, Sansone FJ (1998) A large source of atmospheric nitrous oxide from subtropical North Pacific surface waters. *Nature*, **396**, 63–66.

Epstein S, Mayeda T (1953) Variation of O^{18} content of waters from natural sources. *Geochimica et Cosmochimica Acta*, **4**, 213–224.

Firestone MK, Davidson EA (1989) Microbial basis of NO and N_2O production and consumption in soils. *In*: Exchange of Trace Gases Between Terrestrial Ecosystems and the Atmosphere (eds. Andreae MO, Schimel DS). John Wiley and Sons, New York.

Firestone MK, Firestone RB, Tiedje JM (1980) Nitrous oxide from soil denitrification: Factors controlling its biological production. *Science*, **208**, 749–751.

Flood K (2010) Investigating nitrate in the Innisfil Creek subwatershed. BSc honours thesis, University of Waterloo, Waterloo, Ontario, Canada.

Flückiger J, Blunier T, Stauffer B, Chappellaz J, Spahni R, Kawamura K, Schwander J, Stocker TF, Dahl-Jensen D (2004a) N_2O and CH_4 variations during the last glacial epoch: insight into global processes. *Global Biogeochemical Cycles*, **18 (GB1020)**, doi:10-1029/2003GB002122.

Flückiger J, Dällenbach A, Blunier T, Stauffer B, Stocker TF, Raynaud D, Barnola JM (1999a) Variations in atmospheric N_2O concentration during abrupt climatic changes. *Science*, **285**, 227–230.

Flückiger J, Dällenbach A, Stauffer B (1999b) N_2O data covering abrupt climatic changes. IGBP Pages/World Data Center-A for Paleoclimatology. Data Contribution Series #1999-057. NOAA/NGDC Paleoclimatology Program, Boulder CO, USA.

Flückiger J, Spahni R, Blunier T, Stauffer B (2004b) Grip N_2O and CH_4 data for Dansgaard-Oeschger Events 18 and 20, IGBP Pages/World Data Centre for Paleoclimatology. Data

Contribution Series #2004-005. NOAA/NGDC Paleoclimatology Program, Boulder CO, USA.

Fogel ML, Cifuentes LA (1993) Isotopic fractionation during primary production. *In*: Organic Geochemistry (eds. Engel MH, Macko SA). Plenum Press, New York.

Forster P, Ramaswamy V, Artaxo P, Berntsen T, Betts R, Fahey DW, Haywood J, Lean J, Lowe DC, Myhre G, Nganga J, Prinn R, Raga G, Schulz M, van Dorland R (2007) Changes in atmospheric constituents and in radiative forcing. *In*: Climate Change 2007: The Physical Science Basis. Contribution of Working Group I to the Fourth Assessment Report of the Intergovernmental Panel on Climate Change (eds. Solomon S, Qin D, Manning M, Chen Z, Marquis M, Averyt KB, Tignor M, Miller HL). Cambridge University Press, Cambridge and New York.

Foster NW, Hazlett PW, Nicolson JA, Morrison IK (1989) Ion leaching from a sugar maple forest in response to acidic deposition and nitrification. *Water, Air, and Soil Pollution*, **48**, 251–261.

Foster NW, Morrison IK, Nicolson JA (1986) Acid deposition and ion leaching from a podzolic soil under hardwood forest. *Water, Air, and Soil Pollution*, **31**, 879–889.

Frame CH, Casciotti KL (2010) Biogeochemical controls and isotopic signatures of nitrous oxide production by a marine ammonia-oxidizing bacterium. *Biogeosciences*, **7**, 2695–2709.

Francis CA, Breman JM, Kuypers MMM (2007) New processes and players in the nitrogen cycle: the microbial ecology of anaerobic and archaeal ammonia oxidation. *The ISME Journal*, **1**, 19–27.

Fry, B (2006) Stable Isotope Ecology, Springer, New York.

Galloway JN, Aber JD, Erisman JW, Seitzinger SP, Howarth RW, Cowling EB, Cosby BJ (2003) The nitrogen cascade. *BioScience*, **53**, 341–356.

Galloway JN, Dentener FJ, Capone DG, Boyer EW, Howarth RW, Seitzinger SP, Asner GP, Cleveland CC, Green PA, Holland EA, Karl DM, Michaels AF, Porter JH, Townsend AR, Vörösmarty CJ (2004) Nitrogen Cycles: Past, Present, and Future. *Biogeochemistry*, **70**, 153–226.

Galloway JN, Townsend AR, Erisman JW, Bekunda M, Cai Z, Freney JR, Martinelli LA, Seitzinger SP, Sutton MA (2008) Transformation of the nitrogen cycle: recent trends, questions, and potential solutions. *Science*, **320**, 889–892.

Garbeva P, Baggs EM, Prosser JI (2007) Phylogeny of nitrite reductase (*nirK*) and nitric oxide reductase (*norB*) genes from *Nitrosospira* species isolated from soil. *FEMS Microbiology Letters*, **266**, 83–89.

Gat J (1996) Oxygen and hydrogen isotopes in the hydrologic cycle. *Annual Review of Earth and Planetary Sciences*, **24**, 225–262.

Granger J, Sigman DM, Prokopenko MG, Lehmann MF, Tortell PD (2006) A method for nitrite removal in nitrate N and O isotope analyses. *Limnology and Oceanography-Methods*, **4**, 205–212.

Granger J, Sigman DM, Lehmann MF, Tortell PD (2008) Nitrogen and oxygen isotope fractionation during dissimilatory nitrate reduction by denitrifying bacteria. *Limnology and Oceanography*, **53**, 2533–2545.

Groffman PM, Altabet MA, Böhlke JK, Butterback-Bahl K, David MB, Firestone MK, Giblin AE, Kana TM, Nielsen LP, Voytek MA (2006) Methods for measuring denitrification: Diverse approaches to a difficult problem. *Ecological Applications*, **16**, 2091–2122.

Hales HC, Ross DS (2008) Drastic short-term changes in the isotopic composition of soil nitrate in forest soil samples. *Soil Science Society of America Journal*, **72**, 1645–1652.

Hayatsu M, Tago K, Saito M (2008) Various players in the nitrogen cycle: diversity and functions of the microorganisms involved in nitrification and denitrification. *Soil Science and Plant Nutrition*, **54**, 33–45.

Högberg P (1997) Tansley Review No. 95: ^{15}N natural abundance in soil-plant systems. *New Phytologist*, **137**, 179–203.

Hollingham M (2011) Groundwater nitrate and nitrous oxide in the Long Point region: insights from stable isotopes. BSc honours thesis, University of Waterloo, Waterloo, Ontario, Canada.

Hollocher TC (1984) Source of the oxygen atoms of nitrate in the oxidation of nitrite by *Nitrobacter agilis* and evidence against a P-O-N anhydride mechanism in oxidative phosphorylation. *Archives of Biochemistry and Biophysics*, **233**, 721–727.

Hollocher TC, Tate ME, Nicholas DJD (1981) Oxidation of ammonia by *Nitrosomonas europaea*. *The Journal of Biological Chemistry*, **256**, 10,834–10,836.

Hübner H (1986) Chapter 9: Isotope effects of nitrogen in the soil and biosphere. *In*: Handbook of Environmental Isotope Geochemistry, Volume 2, The Terrestrial Environment (eds. Fritz P, Fontes JCh). Elsevier, Amsterdam, Oxford, New York, Tokyo.

Intergovernmental Panel on Climate Change (2001) Climate Change 2001: The Scientific Basis.

Intergovernmental Panel on Climate Change (2007) Climate Change 2007: The Physical Science Basis – Summary for Policymakers.

IUSS Working Group WRB (2006) World reference base for soil resources 2006. 2nd edition. World Soil Resources Reports No. 103. FAO, Rome.

Jamieson TS (2010) Quantification of oxygen dynamics in the Grand River using a stable isotope approach. PhD thesis, University of Waterloo, Waterloo, Ontario, Canada.

Jeffries DS, Kelso JRM, Morrison IK (1988) Physical, chemical and biological characteristics of the Turkey Lakes Watershed, central Ontario, Canada. *Canadian Journal of Fisheries and Aquatic Sciences*, **45 (Supp.1)**, 3–12.

Jensen HL (1929) On the influence of the carbon: nitrogen ratios of organic material on the mineralisation of nitrogen. *Journal of Agricultural Sciences*, **19**, 71–82.

Jetten MSM, van Niftrik L, Strous M, Kartal B, Keltjens JT, Op den Camp HJM (2009) Biochemistry and molecular biology of anammox bacteria. *Critical Reviews in Biochemistry and Molecular Biology*, **44**, 65–84.

Jia Z, Conrad R (2009) Bacteria rather than Archaea dominate microbial ammonia oxidation in an agricultural soil. *Environmental Microbiology*, **11**, 1658–1671.

Jinuntuya-Nortman M, Sutka RL, Ostrom PH, Gandhi H, Ostrom NE (2008) Isotopologue fractionation during microbial reduction of N_2O within soil mesocosms as a function of water-filled pore space. *Soil Biology and Biochemistry*, **40**, 2273–2280.

Kaiser J (2002) Stable isotope investigations of atmospheric nitrous oxide. Doctoral Dissertation. Johannes Guttenberg University.

Kaiser J, Rockmann T, Brenninkmeijer C (2003) Complete and accurate mass spectrometric isotope analysis of tropospheric nitrous oxide. *Journal of Geophysical Research*, **108(D15)**, 4476, doi:10.1029/2003JD003613.

Kendall C (1998) Chapter 16: Tracing nitrogen sources and cycling in catchments. *In*: Isotope Tracers in Catchment Hydrology (eds. Kendall C, McDonnell JJ). Elsevier Science, Amsterdam.

Kendall C, Caldwell EA (1998) Chapter 2: Fundamentals of isotope geochemistry. *In*: Isotope Tracers in Catchment Hydrology (eds. Kendall C, McDonnell JJ). Elsevier Science, Amsterdam.

Kendall C, Doctor DH (2003) Vol. 5.11: Stable isotope applications in hydrologic studies. *In*: Treatise on Geochemistry, Volume 5 (eds. Holland HD, Turekian KK). Elsevier Science, Oxford.

Kim K-R, Craig H (1990) Two-isotope characterization of N_2O in the Pacific Ocean and constraints on its origin in deep water. *Nature*, **347**, 58–61.

Kim KR, Craig H (1993) Nitrogen-15 and oxygen-18 characteristics of nitrous oxide: A global perspective. *Science*, **262**, 1855–1857.

Knowles R (1982) Denitrification. *Microbiological Reviews*, **46**, 43–70.

Koba K, Osaka K, Tobari Y, Toyoda S, Ohte N, Katsuyama M, Suzuki N, Itoh M, Yamagishi H, Kawasaki M (2009) Biogeochemistry of nitrous oxide in groundwater in a forested ecosystem elucidated by nitrous oxide isotopomer measurements. *Geochimica et Cosmochimica Acta*, **73**, 3115–3133.

Könneke M, Bernhard AE, de la Torre, JR, Walker CB, Waterbury JB, Stahl DA (2005) Isolation of an autotrophic ammonia-oxidizing marine archaeon. *Nature*, **437**, 543–546.

Kool DM, Dolfing J, Wrage N, Willem Van Groenigen JW (2011) Nitrifier denitrification as a distinct and significant source of nitrous oxide from soil. *Soil Biology and Biochemistry*, **43**, 174–178.

Kool DM, Müller C, Wrage N, Oenema O, Van Groenigen JW (2009b) Oxygen exchange between nitrogen oxides and H_2O can occur during nitrifier pathways. *Soil Biology and Biochemistry*, **41**, 1632–1641.

Kool DM, Wrage N, Oenema O, Dolfing J, Van Groenigen JW (2007) Oxygen exchange between (de)nitrification intermediates and H_2O and its implications for source determination of NO_3^- and N_2O: a review. *Rapid Communications in Mass Spectrometry*, **21**, 3569–3578.

Kool DM, Wrage N, Oenema O, Harris D, Van Groenigen JW (2009a) The ^{18}O signature of biogenic nitrous oxide is determined by O exchange with water. *Rapid Communications in Mass Spectrometry*, **23**, 104–108.

Kool DM, Wrage N, Zechmeister-Boltenstern S, Pfeffer M, Brus D, Oenema O, Van Groenigen J-W (2010) Nitrifier denitrification can be a source of N_2O from soil: a revised approach to the dual-isotope labelling method. *European Journal of Soil Science*, **61**, 759–772.

Kowalchuk GA, Stephen JR (2001) Ammonia-oxidizing bacteria: a model for molecular microbial ecology. *Annual Review of Microbiology*, **55**, 485–529.

Kroopnick P, Craig H (1972) Atmospheric oxygen: isotopic composition and solubility fractionation. *Science*, **175**, 54–55.

Kuenen JG (2008) Anammox bacteria: from discovery to application. *Nature reviews. Microbiology*, **6**, 320–326.

Lane GA, Dole M (1956) Fractionation of oxygen isotopes during respiration. *Science*, **123**, 574–576.

Lee K-S, Bong Y-S, Lee D, Kim Y, Kim K (2008) Tracing the sources of nitrate in the Han River watershed in Korea, using $\delta^{15}N\text{-}NO_3^-$ and $\delta^{18}O\text{-}NO_3^-$ values. *Science of the Total Environment*, **395**, 117–124.

Lees H (1952) Hydroxylamine as an intermediate in nitrification. *Nature*, **169**, 156–157.

Legendre P (2001) Model II regression – User's guide. Département de sciences biologiques, Université de Montréal. 23 pp. Available at: http://www.fas.umontreal.ca/biol/legendre/.

Leininger S, Urich T, Schloter M, Schwark L, Qi J, Nicol GW, Prosser JI, Schuster SC, Schleper C (2006) Archaea predominate among ammonia-oxidizing prokaryotes in soils. *Nature*, **442**, 806–809.

Li C, Aber J, Stange F, Butterbach-Bahl K, Papen H (2000) A process-oriented model of N_2O and NO emissions from forest soils: 1. Model development. *Journal of Geophysical Research*, **105(D4)**, 4369–4384.

Li L (2010) Use of N_2O and its isotopic composition to investigate nitrogen processes in groundwater. MSc thesis, University of Waterloo, Waterloo, Ontario, Canada.

Lide DR (ed.) (2010) Dissociation constants of inorganic acids and bases. *In*: CRC Handbook of Chemistry and Physics, 90^{th} Edition (Internet Version). CRC Press/Taylor and Francis, Boca Raton.

Machida T, Nakazawa T, Fujii Y, Aoki S, Watanabe O (1995) Increase in the atmospheric nitrous oxide concentration during the last 250 years. *Geophysical Research Letters*, **22**, 2921–2924.

Maeda K, Toyoda S, Shimojima R, Osada T, Hanajima D, Morioka R, Yoshida N (2010) Source of nitrous oxide emissions during the cow manure composting process as revealed by isotopomer analysis of and *amoA* abundance in Betaproteobacterial ammonia-oxidizing bacteria. *Applied and Environmental Microbiology*, **76**, 1555–1562.

Maier RM, Pepper IL, Gerba CP (2009) Environmental Microbiology, 2^{nd} edition. Academic Press, Oxford.

Maljanen M, Liikanen A, Silvola J, Martikainen PJ (2003) Nitrous oxide emissions from boreal organic soil under different land-use. Soil Biology and Biochemistry, 35, 689–700.

Mandernack KW, Mills CT, Johnson CA, Rahn T, Kinney C (2009) The $\delta^{15}N$ and $\delta^{18}O$ values of N_2O produced during the co-oxidation of ammonia by methanotrophic bacteria. *Chemical Geology*, **267**, 96–107.

Mandernack KW, Rahn T, Kinney C, Wahlen M (2000) The biogeochemical controls of the $\delta^{15}N$ and $\delta^{18}O$ of N_2O produced in landfill cover soils. *Journal of Geophysical Research*, **105(D14)**, 17,709–17,720.

Mariotti A, Germon JC, Hubert P, Kaiser P, Letolle R, Tardieux A, Tardieux P (1981) Experimental determination of nitrogen kinetic isotope fractionation: Some principles; illustrations for the denitrification and nitrification processes. *Plant and Soil*, **62**, 413–430.

Mariotti A, Germon JC, Leclerc A (1982) Nitrogen isotope fractionation associated with the $NO_2^- \rightarrow N_2O$ step of denitrification in soils. *Canadian Journal of Soil Science*, **62**, 227–241.

Mayer B, Bollwerk SM, Mansfeldt T, Hutter B, Veizer J (2001) The oxygen isotope composition of nitrate generated by nitrification in acid forest floors. *Geochimica et Cosmochimica Acta*, **65**, 2743–2756.

Mayer B, Boyer EW, Goodale C, Jaworski NA, van Breemen N, Howarth RW, Seitzinger S, Billen G, Lajtha K, Nadelhoffer K, van Dam D, Hetling LJ, Nosal M, Paustian K (2002)

Sources of nitrate in rivers draining sixteen watersheds in the northeastern U.S.: isotopic constraints. *Biogeochemistry*, **57/58**, 171–197.

McIlvin MR, Altabet MA (2005) Chemical conversion of nitrate and nitrite to nitrous oxide for nitrogen and oxygen isotopic analysis in freshwater and seawater. *Analytical Chemistry*, **77**, 5589–5595.

McIlvin MR, Casciotti KL (2006) Method for the analysis of $\delta^{18}O$ in water. *Analytical Chemistry*, **78**, 2377–2381.

Megonigal JP, Hines ME, Visscher PT (2003) Chapter 8.08: Anaerobic metabolism: linkages to trace gases and aerobic processes. *In*: Treatise on Geochemistry, Volume 8 (eds. Holland HD, Turekian KK). Elsevier Science, Oxford.

Meijide A, Cardenas LM, Bol R, Bergstermann A, Goulding K, Well R, Vallejo A, Scholefield D (2010) Dual isotope and isotopomer measurements for the understanding of N_2O production and consumption during denitrification in an arable soil. *European Journal of Soil Science*, **61**, 364–374.

Mengis M, Schiff S, Harris M, English M, Aravena R, Elgood R, MacLean A (1999) Multiple geochemical and isotopic approaches for assessing ground water NO_3^- elimination in a riparian zone. *Ground water*, **37**, 448–457.

Menyailo OV, Hungate BA (2006) Stable isotope discrimination during soil denitrification: production and consumption of nitrous oxide. *Global Biogeochemical Cycles*, **20**, GB3025.

Mitchell MJ, Foster NW, Shepard JP, Morrison IK (1992) Nutrient cycling in Huntington Forest and Turkey Lakes deciduous stands: nitrogen and sulphur. *Canadian Journal of Forest Research*, **22**, 457–464.

Mitchell MJ, Piatek KB, Christopher S, Mayer B, Kendall C, McHale P (2006) Solute sources in stream water during consecutive fall storms in a northern hardwood forest watershed: a combined hydrological, chemical and isotopic approach. *Biogeochemistry*, **78**, 217–246.

Moir JWB, Crossman LC, Spiro S, Richardson DJ (1996) The purification of ammonia monooxygenase from *Paracoccus denitrficans*. *FEBS letters*, **387**, 71–74.

Mook WG (2000) Volume I. Introduction: theory, methods, review. *In*: Environmental isotopes in the hydrological cycle, principles and applications. (ed. Mook WG). UNESCO and IAEA. Technical documents in hydrology, No. 39, vol. 1.

Nadelhoffer KF, Fry B (1988) Controls on natural N-15 and C-13 abundances in forest soil organic-matter. *Soil Science Society of America Journal*, **52**, 1633–1640.

Naqvi SWA, Yoshinari T, Jayakumar DA, Altabet MA, Narvekar PV, Devol AH, Brandes JA, Codispoti LA (1998) Budgetary and biogeochemical implications of N_2O isotope signatures in the Arabian Sea. *Nature*, **394**, 462–464.

Nicolson JA (1988) Water and chemical budgets for terrestrial basins at the Turkey Lakes Watershed. *Canadian Journal of Fisheries and Aquatic Sciences*, **45(Suppl. 1)**, 88–95.

Opdyke MR, Ostrom NE, Ostrom PH (2009) Evidence for the predominance of denitrification as a source of N_2O in temperate agricultural soils based on isotopologue measurements. *Global Biogeochemical Cycles*, **23 GB4018**, doi:10.1029/2009GB003523.

Ostrom NE, Pitt A, Sutka R, Ostrom PH, Grandy AS, Huizinga KM, Robertson GP (2007) Isotopologue effects during N_2O reduction in soils and in pure cultures of denitrifiers. *Journal of Geophysical Research*, **112**, G02005, doi:10.1029/2006JG000287.

Ostrom NE, Russ ME, Popp B, Rust TM, Karl DM (2000) Mechanisms of nitrous oxide production in the subtropical North Pacific based on determinations of the isotopic abundances of nitrous oxide and di-oxygen. *Chemosphere–Global Change Science*, **2**, 281–290.

Ostrom NE, Sutka R, Ostrom PH, Grandy AS, Huizinga KM, Gandhi H, vonFischer JC, Robertson GP (2010) Isotopologue data reveal bacterial denitrification as the primary source of N_2O during a high flux event following cultivation of a native temperate grassland. *Soil Biology and Biochemistry*, **42**, 499–506.

Otte S, Schalk J, Kuenen JG, Jetten MSM (1999) Hydroxylamine oxidation and subsequent nitrous oxide production by the heterotrophic ammonia oxidizer *Alcaligenes faecalis*. *Applied Microbiology and Biotechnology*, **51**, 255–261.

Pardo LH, Kendall C, Pett-Ridge J, Chang CCY (2004) Evaluating the source of streamwater nitrate using $\delta^{15}N$ and $\delta^{18}O$ in nitrate in two watersheds in New Hampshire, USA. *Hydrological Processes*, **18**, 2699–2712.

Park S, Pérez T, Boering KA, Trumbore SE, Gil J, Marquina S, Tyler SC (2011) Can N_2O stable isotopes and isotopomers be useful tools to characterize sources and microbial pathways of N_2O production and consumption in tropical soils? *Global Biogeochemical Cycles*, **25 (GB1001)**.

Parkin TB (1987) Soil microsites as a source of denitrification variability. *Soil Science Society of America Journal*, **51**, 1194–1199.

Pérez T (2005) Factors that control the isotopic composition of N_2O from soil emissions. *In*: Stable Isotopes and Biosphere-Atmosphere Interactions: Processes and Biological Controls (eds. Flanagan LB, Ehleringer JR, Pataki DE). Elsevier, San Diego

Pérez T, Garcia-Montiel D, Trumbore S, Tyler S, De Camargo P, Moreira M, Piccolo M, Cerri C (2006) Nitrous oxide nitrification and denitrification ^{15}N enrichment factors from Amazon forest soils. *Ecological Applications*, **16**, 2153–2167.

Pérez T, Trumbore S, Tyler S, Matson P, Ortiz-Monasterio I, Rahn T, Griffith D (2001) Identifying the agricultural imprint on the global N_2O budget using stable isotopes. *Journal of Geophysical Research-Atmospheres*, **106**, 9869–9878.

Pérez T, Trumbore SE, Tyler SC, Davidson EA, Keller M, de Camargo PB (2000) Isotopic variability of N_2O emissions from tropical forest soils. *Global Biogeochemical Cycles*, **14**, 525–535.

Petrone RM, Smith C, Macrae ML, English MC (2006) Riparian zone equilibrium and actual evapotranspiration in a first order agricultural catchment in Southern Ontario, Canada. *Agricultural Water Management*, **86**, 240–248.

Poth M (1986) Dinitrogen production from nitrite by a *Nitrosomonas* isolate. *Applied and Environmental Microbiology*, **52**, 957–959.

Prinn RG, Cunnold D, Rasmussen R, Simmonds P, Alyea F, Crawford A, Fraser P, Rosen R (1990) Atmospheric emissions and trends of nitrous oxide deduced from ten years of ALE/GAGE data. *Journal of Geophysical Research*, **95(D11)**, 18,369–18,385.

Prinn RG, Weiss RF, Fraser PJ, Simmonds PG, Cunnold DM, Alyea FN, O'Doherty S, Salameh P, Miller BR, Huang J, Wang RHJ, Hartley DE, Harth C, Steele LP, Sturrock G, Midgley PM, McCulloch A (2000) A history of chemically and radiatively important gases in air deduced from ALE/GAGE/AGAGE. *Journal of Geophysical Research*, **105(D14)**, 17,751–17,792.

Priscu JC, Christner BC, Dore JE, Westley MB, Popp BN, Casciotti KL, Lyons WB (2008) Supersaturated N_2O in a perennially ice-covered Antarctic lake: molecular and stable isotopic evidence for a biogeochemical relict. *Polar Research*, **53**, 2439–2450.

Prosser JI (1990) Autotrophic nitrification in bacteria. *In*: Advances in Microbial Physiology, Vol. 30 (eds. Rose AH, Tempest DW), Academic Press, New York.

Prosser JI, Nicol GW (2008) Relative contributions of archaea and bacteria to aerobic ammonia oxidation in the environment. *Environmental Microbiology*, **10**, 2931–2941.

Rahn T, Wahlen M (1997) Stable isotope enrichment in stratospheric nitrous oxide. *Science*, 278, 1776–1778.

Rahn T, Wahlen M (2000) A reassessment of the global isotopic budget of atmospheric nitrous oxide. *Global Biogeochemical Cycles*, **14**, 537–543.

Rempel M (2008) NO_3^- and N_2O at the Strawberry Creek catchment: tracing sources and processes using stable isotopes. MSc thesis, University of Waterloo, Waterloo, Ontario, Canada.

Revesz K, Woods PH (1990) A method to extract soil water for stable isotope analysis. *Journal of Hydrology*, **115**, 397–406.

Ritchie GAF, Nicholas DJD (1972) Identification of the sources of nitrous oxide produced by oxidative and reductive processes in *Nitrosomonas europaea*. Biochemical Journal, 126, 1181–1191.

Robertson GP, Groffman PM (2006) Chapter 13: Nitrogen transformations. *In*: Soil Microbiology, Ecology and Biochemistry (ed. Paul EA). Academic Press, Oxford.

Robertson LA, Dalsgaard T, Revsbech N-P, Kuenen JG (1995) Confirmation of 'aerobic denitrification' in batch cultures, using gas chromatography and ^{15}N mass spectrometry. *FEMS Microbiology Ecology*, **18**, 113–120.

Robertson WD, Schiff SL (2008) Persistent elevated nitrate in a riparian zone aquifer. *Journal of Environmental Quality*, **37**, 669–679.

Rock L, Ellert BH, Mayer B, Norman AL (2007) Isotopic composition of tropospheric and soil N_2O from successive depths of agricultural plots with contrasting crops and nitrogen amendments. *Journal of Geophysical Research*, **112 (D18303)**.

Rodhe H (1990) A comparison of the contribution of various gases to the greenhouse-effect. *Science*, **248**, 1217–1219.

Rosamond M (in progress) Nitrogen cycling in the Grand River, Ontario, Canada, with a focus on nitrous oxide. PhD thesis, University of Waterloo, Waterloo, Ontario, Canada.

Rossi A (2010) Nitrification and denitrification processes in groundwater studied by nitrate isotopes in Lake Joseph (ON), Canada. MSc thesis, La Sapienza University of Rome, Rome, Italy.

Samarkin VA, Madigan MT, Bowles MW, Casciotti KL, Priscu JC, McKay CP, Joye SB (2010) Abiotic nitrous oxide emission from the hypersaline Don Juan Pond in Antarctica. *Nature Geoscience*, **3**, 341–344.

Schmidt HL, Voerkelius S (1989) Origin and isotope effects of oxygen in compounds of the nitrogen cycle. Proceedings of the 5^{th} Working Meeting on Isotopes in Nautre, Leipzich. pp. 613–624.

Schmidt I, Look C, Bock E, Jetten MSM (2004) Ammonium and hydroxylamine uptake and accumulation in *Nitrosomonas*. *Microbiology*, **150**, 1405–1412.

Scholefield D, Hawkins JMB, Jackson SM (1997) Development of a helium atmosphere soil incubation technique for direct measurement of nitrous oxide and dinitrogen fluxes during denitrification. *Soil Biology and Biochemistry*, **29**, 1345–1352.

Seitzinger S, Harrison JA, Böhlke JK, Bouwman AF, Lowrance R, Peterson B, Tobias C, Van Drecht G (2006) Denitrification across landscapes and waterscapes: a synthesis. *Ecological Applications*, **16**, 2064–2090.

Senger N (in progress) Trends in NO_3^- in groundwater in the Nottawasaga Valley watershed. MSc thesis, University of Waterloo, Waterloo, Ontario, Canada.

Sharp Z (2007) Principles of stable isotope geochemistry. Pearson Prentice Hall, New Jersey.

Shearer G, Kohl DH (1988) Nitrogen isotopic fractionation and ^{18}O exchange in relation to the mechanism of denitrification of nitrite by *Pseudomonas stutzeri*. *The Journal of Biological Chemistry*, **263**, 13,231–13,245.

Shrestha NK, Hadano S, Kamachi T, Okura I (2002) Dinitrogen production from ammonia by *Nitrosomonas europaea*. *Applied Catalysis*, **237**, 33–39.

Silva SR, Kendall C, Wilkison DH, Ziegler AC, Chang CY, Avanzino RJ (2000) A new method for collection of nitrate from fresh water and the analysis of nitrogen and oxygen isotope ratios. *Journal of Hydrology*, **228**, 22–36.

Smith KA, Ball T, Conen F, Dobbie KE, Massheder J, Rey A (2003) Exchange of greenhouse gases between soil and atmosphere: interactions of soil physical factors and biological processes. *European Journal of Soil Science*, **54**, 779–791.

Smith RV, Burns LC, Doyle RM, Lennox SD, Kelso BHL, Foy RH, Stevens RJ (1997) Free ammonia inhibition of nitrification in river sediments leading to nitrite accumulation. *Journal of Environmental Quality*, **26**, 1049–1055.

Snider DM, Schiff SL, Spoelstra J (2009) $^{15}N/^{14}N$ and $^{18}O/^{16}O$ stable isotope ratios of nitrous oxide produced during denitrification in temperate forest soils. *Geochimica et Cosmochimica Acta*, **73**, 877–888.

Snider DM, Spoelstra J, Schiff SL, Venkiteswaran JJ (2010) Stable oxygen isotope ratios of nitrate produced from nitrification: ^{18}O-labeled water incubations of agricultural and temperate forest soils. *Environmental Science and Technology*, **44**, 5358–5364.

Soil Classification Working Group (1998) The Canadian System of Soil Classification, 3rd edition. Agriculture and Agri-Food Canada Publication 1646, NRC Press, 187 pp.

Spalding RF, Exner ME (1993) Occurrence of nitrate in groundwater–a review. *Journal of Environmental Quality*, **22**, 392–402.

Spoelstra J, Schiff SL, Elgood RJ, Semkin RG, Jeffries DS (2001) Tracing the sources of exported nitrate in the Turkey Lakes Watershed using $^{15}N/^{14}N$ and $^{18}O/^{16}O$ isotopic ratios. *Ecosystems*, **4**, 536–544.

Spoelstra J, Schiff SL, Hazlett PW, Jeffries DS, Semkin RG (2007) The isotopic composition of nitrate produced from nitrification in a hardwood forest floor. *Geochimica et Cosmochimica Acta*, **71**, 3757–3771.

Spoelstra J, Schiff SL, Jeffries DS, Semkin RG (2004) Effect of storage on the isotopic composition of nitrate in bulk precipitation. *Environmental Science and Technology*, **38**, 4723–4727.

Stein LY, Yung YL (2003) Production, isotopic composition, and atmospheric fate of biologically produced nitrous oxide. *Annual Review of Earth and Planetary Sciences*, **31**, 329–356.

Sutka RL, Adams GC, Ostrom NE, Ostrom PH (2008) Isotopologue fractionation during N_2O production by fungal denitrification. *Rapid Communications in Mass Spectrometry*, **22**, 3989–3996.

Sutka RL, Ostrom NE, Ostrom PH, Breznak JA, Gandhi H, Pitt AJ, Li F (2006) Distinguishing nitrous oxide production from nitrification and denitrification on the basis of isotopomer abundances. *Applied Environmental Microbiology*, **72**, 638–644.

Sutka RL, Ostrom NE, Ostrom PH, Gandhi H, Breznak JA (2003) Nitrogen isotopomer site preference of N_2O produced by *Nitrosomonas europaea* and *Methylococcus capsulatus* Bath. *Rapid Communications in Mass Spectrometry*, **17**, 738–745.

Sutka RL, Ostrom NE, Ostrom PH, Gandhi H, Breznak JA (2004) Erratum. Nitrogen isotopomer site preference of N_2O produced by *Nitrosomonas europaea* and *Methylococcus capsulatus* Bath. *Rapid Communications in Mass Spectrometry*, **18**, 1411–1412.

Tappe W, Laverman A, Bohland M, Braster M, Rittershaus S, Groeneweg J, van Verseveld HW (1999) Maintenance energy demand and starvation recovery dynamics of *Nitrosomonas europaea* and *Nitrobacter winogradskyi* cultivated in a retentostat with complete biomass retention. *Applied Environmental Microbiology*, **65**, 2471–2477.

Thamdrup B, Dalsgaard T (2002) Production of N_2 through anaerobic ammonium oxidation coupled to nitrate reduction in marine sediments. *Applied Environmental Microbiology*, **60**, 1312–1318.

Thuss SJ (2008) Nitrous oxide production in the Grand River, Ontario, Canada: new insights from stable isotope analysis of dissolved nitrous oxide. MSc thesis, University of Waterloo, Waterloo, Ontario, Canada.

Tiedje JM (1988) Ecology of denitrification and dissimilatory nitrate reduction to ammonium. *In*: Biology of Anaerobic Microorganisms (ed. Zehnder JBA). John Wiley and Sons, Inc., New York.

Tiedje JM, Sexstone AJ, Myrold DD, Robinson JA (1982) Denitrification: ecological niches, competition and survival. *Antonie van Leeuwenhoek Journal of Microbiology*, **48**, 569–583.

Tilsner J, Wrage N, Lauf J, Gebauer G (2003) Emissions of gaseous nitrogen oxides from an extensively managed grassland in NE Bavaria, Germany II. Stable isotope natural abundance of N_2O. *Biogeochemistry*, **63**, 249–267.

Toyoda S, Iwai H, Koba K, Yoshida N (2009) Isotopomeric analysis of N_2O dissolved in a river in the Tokyo metropolitan area. *Rapid Communications in Mass Spectrometry*, **23**, 809–821.

Toyoda S, Mutobe H, Yamagishi H, Yoshida N, Tanji Y (2005) Fractionation of N_2O isotopomers during production by denitrifier. *Soil Biology and Biochemistry*, **37**, 1535–1545.

Toyoda S, Yoshida N (1999) Determination of nitrogen isotopomers of nitrous oxide on a modified isotope ratio mass spectrometer. *Analytical Chemistry*, **71**, 4711–4718.

Treusch AH, Leininger S, Kletzin A, Schuster SC, Klenk H-P, Schleper C (2005) Novel genes for nitrite reductase and Amo-related proteins indicate a role of uncultivated mesophilic crenarchaeota in nitrogen cycling. *Environmental Microbiology*, **7**, 1985–1995.

UNEP and WHRC (2007) Reactive nitrogen in the environment: too much or too little of a good thing. United Nations Environment Programme, Paris.

United Nations Population Division (1999). The World at six billion. United Nations Population Division, Department of Economic and Social Affairs, United Nations Secretariat. ESA/P/WP.154, 12 October 1999.

US-EPA (2006) Global anthropogenic non-CO_2 greenhouse gas emissions: 1990–2020. United States Environmental Protection Agency, EPA 430-R-06-003, June 2006. Washington, D.C., http://www.epa.gov/nonco2/econ-inv/downloads/GlobalAnthroEmissionsReport.pdf

Van Groenigen JW, Zwart KB, Harris D, van Kessel C (2005) Vertical gradients of $\delta^{15}N$ and $\delta^{18}O$ in soil atmospheric N_2O–temporal dynamics in a sandy soil. *Rapid communications in mass spectrometry*, **19**, 1289–1295.

Vandenhoff A (2007) Extreme N_2O production in a riparian zone with a low organic carbon content aquifer. BSc honours thesis, University of Waterloo, Waterloo, Ontario, Canada.

Venkiteswaran JJ (2008) Greenhouse gas cycling in experimental boreal reservoirs. PhD Thesis, University of Waterloo, ON, Canada. Available at: http://uwspace.uwaterloo.ca /handle/10012/4168

Venter JC, Remington K, Heidelberg JF, Halpern AL, Rusch D, Eisen JA, Wu D, Paulsen I, Nelson KE, Nelson W, Fouts DE, Levy S, Knap AH, Lomas MW, Nealson K, White O, Peterson J, Hoffman J, Parsons R, Baden-Tillson H, Pfannkoch C, Rogers YH, Smith HO (2004) Environmental genome shotgun sequencing of the Sargasso Sea. *Science*, **304**, 66–74.

Vieten B, Blunier T, Neftel A, Alewell C, Conen F (2007) Fractionation factors for stable isotopes of N and O during N_2O reduction in soil depend on reaction rate constant. *Rapid Communications in Mass Spectrometry*, **21**, 846–850.

Vitousek PM, Aber JD, Howarth RW, Likens GE, Matson PA, Schindler DW, Schlesinger WH, Tilman DG (1997) Human alteration of the global nitrogen cycle: sources and consequences. *Ecological Applications*, **7**, 737–750.

Wada E, Ueda S (1996) Carbon, nitrogen and oxygen isotope ratios of CH_4 and N_2O on soil ecosystems. *In*: Mass Spectrometry of Soils (eds. T. W. Boutton and S. Yamasaki). Marcel Dekker, New York.

Wada E, Yoshida N, Yoshioka T, Yoh M, Kabaya Y (1991) ^{15}N abundance of N_2O in aquatic ecosystems with emphasis on denitrification. *In*: Cycling of Reduced Gases in the Hydrosphere (eds. D. D. Adams, S. P. Seitzinger and P. M. Crill). E. Schweizerbart, Stuttgart. 115–124.

Wahlen M, Yoshinari T (1985) Oxygen isotope ratios in N_2O from different environments. *Nature*, **313**, 780–782.

Ward MH, deKok TM, Levallois P, Brender J, Gulis G, Nolan BT, VanDerslice J (2005) Workgroup Report: Drinking-Water Nitrate and Health–Recent Findings and Research Needs. *Environmental Health Perspectives*, **113**, 1607–1614.

Wassenaar LI (1995) Evaluation of the origin and fate of nitrate in the Abbotsford Aquifer using the isotopes of ^{15}N and ^{18}O in NO_3^-. *Applied Geochemistry*, **10**, 391–405.

Wassenaar LI, Koehler G (1999) An on-line technique for the determination of the $\delta^{18}O$ and $\delta^{17}O$ of gaseous and dissolved oxygen. *Analytical Chemistry*, **71**, 4965–4968.

Wassenaar LI, Venkiteswaran JJ, Schiff SL, Koehler G (2010) Aquatic community metabolism response to municipal effluent inputs in rivers quantified using diel $\delta^{18}O$ values of dissolved oxygen. *Canadian Journal of Fisheries and Aquatic Sciences*, **67**, 1232–1246.

Webster EA, Hopkins DW (1996) Nitrogen and oxygen isotope ratios of nitrous oxide emitted from soil and produced by nitrifying and denitrifying bacteria. *Biology and Fertility of Soils*, **22**, 326–330.

Wehrfritz J-M, Reilly A, Spiro S, Richardson DJ (1993) Purification of hydroxylamine oxidase from *Thiosphaera pantotropha*. Identification of electron acceptors that couple heterotrophic nitrification to aerobic denitrification. *FEBS Letters*, **335**, 246–250.

Well R, Flessa H (2008) Isotope fractionation factors of N_2O diffusion. *Rapid Communications in Mass Spectrometry*, **22**, 2621–2628.

Well R, Flessa H (2009a) Isotopologue signatures of N_2O produced by denitrification in soils. *Journal of Geophysical Research*, **114 (G02020)**.

Well R, Flessa H (2009b) Isotopologue enrichment factors of N_2O reduction in soils. *Rapid Communications in Mass Spectrometry*, **23**, 2996–3002.

Well R, Flessa H, Jaradat F, Toyoda S, Yoshida N (2005) Measurement of isotopomer signatures of N_2O in groundwater. *Journal of Geophysical Research*, **110 G02006**.

Well R, Flessa H, Xing L, Xiaotang J, Römheld V (2008) Isotopologue ratios of N_2O emitted from microcosms with NH_4^+ fertilized arable soils under conditions favouring nitrification. *Soil Biology and Biochemistry*, **40**, 2416–2426.

Westley M, Yamagishi H, Popp B, Yoshida N (2006) Nitrous oxide cycling in the Black Sea inferred from stable isotope and isotopomer distributions. *Deep Sea Research Part II: Topical Studies in Oceanography*, **53**, 1802–1816.

Williard KWJ, DeWalle DR, Edwards PJ, Sharpe WE (2001) ^{18}O isotopic separation of stream nitrate sources in mid-Appalachian forested watersheds. *Journal of Hydrology*, **252**, 174–188.

Winogradsky S (1890). 2nd memoire. Recherches sur les organismes de la nitrification. *Annales De L'Institut Pasteur*, **4**, 257–275.

Wrage N, van Groenigen JW, Oenema O, Baggs EM (2005) A novel duel-isotope labelling method for distinguishing between soil sources of N_2O. *Rapid Communications in Mass Spectrometry*, **19**, 3298–3306.

Wrage N, Velthof GL, Oenema O, Laanbroek HJ (2004) Acetylene and oxygen as inhibitors of nitrous oxide production in *Nitrosomonas europaea* and *Nitrosospira briensis*: a cautionary tale. *FEMS Microbiology Ecology*, **47**, 13–18.

Wrage N, Velthof GL, van Beusichem ML, Oenema O (2001) Role of nitrifier denitrification in the production of nitrous oxide. *Soil Biology and Biochemistry*, **33**, 1723–1732.

Xiong ZQ, Khalil MAK, Xing G, Shearer MJ, Butenhoff C (2009) Isotopic signatures and concentration profiles of nitrous oxide in a rice-based ecosystem during the drained crop-growing season. *Journal of Geophysical Research*, **114 (G02012)**.

Xue D, Botte J, De Baets B, Accoe F, Nestler A, Taylor P, van Cleemput O, Berglund M, Boeckx P (2009) Present limitations and future prospects of stable isotope methods for nitrate source identification in surface- and groundwater. *Water Research*, **43**, 1159–1170.

Yamagishi H, Westley MB, Popp BN, Toyoda S, Yoshida N, Watanabe S, Koba K, Yamanaka Y (2007) Role of nitrification and denitrification on the nitrous oxide cycle in the eastern tropical North Pacific and Gulf of California. *Journal of Geophysical Research*, **112 (G02015)**, doi: 10.1029/2006JG000227

Yamulki S, Toyoda S, Yoshida N, Veldkamp E, Grant B, Bol R (2001) Diurnal fluxes and the isotopomer ratios of N_2O in a temperate grassland following urine amendment. *Rapid Communications in Mass Spectrometry*, **15**, 1263–1269.

Yamulki S, Wolf I, Bol R, Grant B, Brumme R, Veldkamp E, Jarvis SC (2000) Effects of dung and urine amendments on the isotopic content of N_2O released from grasslands. *Rapid Communications in Mass Spectrometry*, **14**, 1356–1360.

Ye RW, Averill BA, Tiedje JM (1994) Denitrification: production and consumption of nitric oxide. *Applied and environmental microbiology*, **60**, 1053–1058.

Ye RW, Fries MR, Bezborodnikov SG, Averill BA, Tiedje JM (1993) Characterization of the structural gene encoding a copper-containing nitrite reductase and homology of this gene to DNA of other denitrifiers. *Applied Environmental Microbiology*, **59**, 250–254.

Ye RW, Toro-Suarez I, Tiedje JM, Averill BA (1991) $H_2{}^{18}O$ isotope exchange studies on the mechanism of reduction of nitric oxide and nitrite to nitrous oxide by denitrifying bacteria. *The Journal of Biological Chemistry*, **266**, 12,848–12,851.

Yoshida N (1984) Nitrogen isotope studies on the geochemical cycle of nitrous oxide. Ph. D thesis, Tokyo Institute of Technology.

Yoshida N (1988) ^{15}N-depleted N_2O as a product of nitrification. *Nature*, **335**, 528–529.

Yoshida N, Toyoda S (2000) Constraining the atmospheric N_2O budget from intramolecular site preference in N_2O isotopomers. *Nature*, **405**, 330–334.

Yoshida T, Alexander M (1970) Nitrous oxide formation by *Nitrosomonas europaea* and heterotrophic microorganisms. *Soil Science Society of America Proceedings*, **34**, 880–882.

Yoshinari T, Altabet M, Naqvi S, Codispoti L, Jayakumar A, Kuhland M, Devol A (1997) Nitrogen and oxygen isotopic composition of N_2O from suboxic waters of the eastern tropical North Pacific and the Arabian Sea–measurement by continuous-flow isotope-ratio monitoring. Marine Chemistry, 56, 253–264.

Yoshinari T, Wahlen M (1985) Oxygen isotope ratios in N_2O from nitrification at a wastewater treatment facility. *Nature*, **317**, 349–350.

Zumft WG (1997) Cell biology and molecular basis of denitrification. *Microbiology and Molecular Biology Reviews*, **61**, 533–616.